# A Hybrid Core-Shell rhOP-1 Nanoparticulate Delivery System for Enhanced New Bone Regeneration in Distraction Osteogenesis

**Ziyad Samir Haidar, D.D.S.**

Faculty of Dentistry
McGill University
Montréal, Canada

**August 2009**

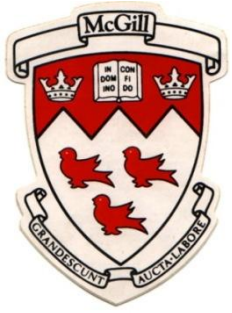


A thesis submitted to the Faculty of Graduate and Postdoctoral Studies of McGill University in partial fulfillment of the degree of doctor of philosophy in dental sciences and research

# ABSTRACT

Distraction osteogenesis (DO) is a prevalent surgical technique for the correction of congenital orthopaedic deformities and craniofacial developmental conditions. Yet, clinical benefits continue to be limited by a number of complications mainly as a result of the protracted treatment time during which the fixator has to be kept *in situ* until the newly-formed bone in the distracted zone consolidates (or hardens), thus exacerbating significant medical, psychological and socio-economical problems on patients, their families and caregivers. On the other hand, protein therapy particularly with the use of potent osteoinductive cytokines from the TGF-β superfamily has been hailed as the most promising alternative to conventional bone grafts. Currently, rhBMP-2 and rhBMP-7/OP-1 have been approved for their "restricted" clinical use in long bone healing and spinal fusion. Prospective clinical trials have reported variability in results ranging from full bone bridging to no bone union and to optimize the therapeutical outcome, the incorporated high and unsafe dosages of the growth factors (mainly due to their very short half-life), timing of release and their application systems necessitate further development. Thus far, loading the protein solution into collagen sponges prior to surgical implantation has shown poor retention and rapid clearance of BMPs within a much shorter period than bone healing requires, especially in humans. Also, such carriers do not provide controlled or customizable release and can comprise outcome by foreign body reactions due to their nature, composition and incomplete degradation. Hence, biocompatible delivery systems that release the bioactive load locally and continuously over proper periods of time for the regeneration of native bone using lower and safer *drug* concentrations are needed.

This doctoral dissertation describes the development and evaluation of a novel hybrid nanoparticulate rhOP-1 delivery system demonstrating characteristics suitable for enhancing de novo bone regeneration and accelerating consolidation in DO. The work is divided into two main phases: (**1**) Formulating biocompatible, biodegradable, monodisperse, physically-stable and cytocompatible cationic core-shell nanoparticles with good protein encapsulation efficiency to provide sustained release over prolonged periods of time. The resulting suspension of nanoparticles also exhibited an extended shelf-life with leeway for drug

loading via simple rehydration immediately prior to use thus preventing degradation or loss of the encapsulant. (**2**) Evaluating the effect of a single injection of the hybrid nanoparticles loaded with low dosages of rhOP–1 on new bone regeneration and consolidation in a rabbit model of long bone distraction osteogenesis. Findings demonstrate the potential of the core-shell nanoparticles in minimizing the therapeutic protein dosage for DO via their localized, release-controlled, osteogenic and naturally-biocompatible polymeric properties without causing any clinical side effects or pre-mature ossification that often requires repeat osteotomies with considerable morbidity. Furthermore, results suggested that the released bioactive load from the delivery system as well as any resulting effects were restricted or confined to the site of administration in the muscle tissue of young rats with no complications from any degradation by-products. Consequently, a novel, safe and promising injectable delivery system for the administration of exogenous growth factors is presented. In a clinical setting, it can be expected to shorten the treatment period of DO and improve the functional outcome in patients via the earlier removal of the fixator. With the continually increasing understanding of morphogens, future studies might exploit the therapeutic potential and cost-effectiveness of the hybrid nanoparticles incorporated with combinations of BMPs, other morphogens and/or biomolecules in pathologies and conditions beyond DO or bone defects and fracture healing.

# RÉSUMÉ

L'ostéogenèse par distraction osseuse (OD) est une technique chirurgicale répandue pour la correction de difformités orthopédiques congénitales et craniofaciales. Pourtant, les avantages cliniques continuent d'être limités par un certain nombre de complications comme à la suite d'un traitement de longue durée pendant lequel le fixateur doit être gardé *in situ* jusqu'à ce que l'os nouvellement formé dans la zone distraite se consolide; pouvant significativement engendrer voire aggraver certains problèmes médicaux, psychologiques et socio-économiques pour les patients, leur famille et le personnel médical. D'un autre côté, la thérapie à base de protéine et plus particulièrement l'utilisation de puissantes cytokines de la superfamille TGF-β a été considérée comme l'alternative la plus prometteuse à la greffe conventionnelle d'os. Actuellement, BMP-2 et BMP-7/OP-1 ont été approuvés pour leur utilisation clinique "restreinte" dans la longue guérison osseuse et la fusion spinale. Pourtant, certaines études ont rapporté une certaine variabilité dans les résultats, allant du pontage osseux complet jusqu'à l'absence d'unification osseuse. Et pour optimiser le résultat thérapeutique, le haut dosage incertain des facteurs de croissance (principalement dû à leur très courte demi-vie), le choix du temps de relargage et de leurs systèmes d'application requièrent des développements supplémentaires et approfondis. Jusqu'à présent, le chargement de protéines dans les éponges à collagène, avant l'implantation chirurgicale, a résulté en une pauvre rétention et une clairance rapide de BMPs durant une période plus brève que ce que nécessite la guérison osseuse surtout dans le cas des humains. De plus, de tels vecteurs ne permettent pas un relargage contrôlé ou a façon et peuvent aboutir à des réactions à des corps étrangers, en raison de leur nature, de leur composition et de leur dégradation incomplète. Donc, le développement d'un système de délivrance qui relargue le chargement bioactif localement et continuellement sur des périodes de temps appropriées pour faciliter la régénération de l'os natif à des concentrations plus basses et moins dangereuses est nécessaire. Cette thèse de doctorat décrit le développement et l'évaluation d'un système de délivrance hybride, combinant nanoparticules et rhOP-1, qui démontre des caractéristiques convenables pour l'accélération d'OD. Le travail présenté dans cette thèse est divisé en deux phases principales : (**1**) La formulation de nanoparticules à structure cœur-coquille biocompatible, biodégradable, monodisperse, physiquement stable, non-toxique et

chargée positivement a été évaluée, notamment à travers l'amélioration de l'efficacité d'encapsulation de protéines. De plus, la délivrance constante linéaire multi-étapes de protéines sur des périodes de temps prolongées peut être modulée. La suspension de nanoparticules ainsi obtenue a une durée de conservation prolongée tout en maintenant à façon le simple chargement de protéines. (**2)** L'effet d'une injection simple de ces nanoparticules faiblement chargées en rhOP-1 sur la régénération et la consolidation osseuse a été évalué avec un modèle de lapin d'OD. Les résultats obtenus suggèrent que la structure cœur-coquille de ces nanoparticules injectables, grâce au contrôle de relargage localisé, ainsi que les propriétés biocompatible et ostéogéniques des polymères formant la coquille, maintient la bioactivité. Par conséquent, cela a pour effet de minimiser les doses thérapeutiques nécessaires de rhOP-1 en vue d'améliorer la nouvelle régénération osseuse et d'accélérer la consolidation dans une OD tibiale, sans causer ni effet indésirable clinique ni ossification prématurée, exigeant souvent des ostéotomies répétées à morbidité considérable. De plus, les résultats ont montré que la charge bioactive relarguée par le vecteur, ainsi que tout effet induit, ont été restreints ou confinés au site d'administration dans le tissu musculaire de jeunes rats, sans complication considérable par tout sous-produit de dégradation.

Par conséquent, un vecteur hybride injectable à base de nanoparticules, à structure cœur-coquille, prometteur a été présenté et évalué en vue de l'administration localisée et à relargage contrôlé de facteurs de croissance exogéniques. D'un point de vue clinique, ce système pourrait raccourcir la durée de traitement d'OD et améliorer le résultat fonctionnel chez les patients grâce à l'enlèvement précoce du dispositif de fixation. De futures études pourraient impliquer l'exploitation de ses propriétés thérapeutiques à moindre coût sur des modèles animaux avec des pathologies ou conditions autres que l'OD ou liées à des défauts osseux.

# ACKNOWLEDGMENTS

I must say that the content of this doctoral dissertation fills my senses with pride and joy where from the inception of the program almost 5 years ago, I have justly dedicated all of my heart, intellect, vivacity and personal life to at last witness it come to fruition. Given my academic background, it was a definite challenge to pull my self away from the familiarity and perhaps ease of clinical work and evidence-based dentistry and into a laboratory setting seldom experienced possibly since my high school years prior to 1994. All along, this endeavor was confronted with countless doubtful faces and speculations. Therefore, no words can truly and fully express my respect, gratitude, admiration and appreciation to the focal role that my supervisor and mentor, **Professor Maryam Tabrizian**, has had throughout this journey. Without any doubt, Maryam holds every credit to whom I grew up to be today. From day one, Maryam always drove me forwards, motivated me when I was in a down fall, shared valuable advice and guidance when I was lost and offered significant feedback on my performance and progress, with a smile and may be more often with a frown (when such was well-deserved or felt needed), which now as I look back, the mere memory brings me a smile. Thank you Maryam for your passion, dedication, command, advice, generosity and friendship; I am forever indebted. On top, I would like to take this opportunity and express my admiration for the exceptional multidisciplinary pool of hand-picked graduate students, committed research assistants and devoted technicians that you have assembled with a brilliant vision. Thus, I sincerely acknowledge with appreciation **all members of Biomed, CBB and Biomat'X Laboratory** and in no particular order these incredible individuals: Mrs. Line Mongeon, for her shared time and expertise in AFM, SEM and TEM; Dr. Fereshteh Azari, for her huge help in cell biology, the release assays, cryo-TEM as well as her amity; Dr. Marinella Sandros, for sharing her passion for chemistry and hilarity; Dr. Julien Fatisson, for dedicating his physico-chemical expertise and his unconditional friendship; and last but certainly not least, my desk-neighbor in the Genome Lab, Sania Mansouri for entertaining the often silent and lonely space we both inhabited throughout the last years. Thank you for the tips on basic chemistry skills that I lacked and mostly for sharing the morning news, stories and your cherished camaraderie during the 2006 Lebanon War.

This project would not have been possible without the support of my co-supervisor, **Dr. Reggie Hamdy**. I am fortunate and proud to be one of your trainees. Despite how busy, hectic, long and strenuous the day would be, Dr. Hamdy will always ensure creating a window to share his invaluable insights, practical solutions and guidance. Perhaps this is what most supervisors are expected to provide when they agree to mentor you. Yet, as students we tend to forget that they do have many

more responsibilities, other tasks, buzzing phones, vibrating pagers, demanding secretaries and ongoing thoughts in their minds and most importantly, that they are human beings as well. I realize today, although both of my advisers are indeed super-humans; I might have been at times ignorant, selfish and irritating; adding more to their tiring. Thus, I would like to take this opportunity and share my sincere apologies and gratitude for all. As well, deserving my heartfelt gratitude is a remarkable member of Dr. Hamdy's staff at the Montreal Shriners Hospital who also was of unforgettable support and assistance to me and this project: **Madame Josée Perron**; for her infinite care, encouragement, reviving jokes and palliative hugs. Praise also goes to Mrs. Tasima Haque, Miss Norine Alam, Mrs. Dominique Lauzier and Mrs. Mary Kotsiopriftis and Mr. Guy Charette for their help and gravity in obtaining and analyzing the results of the in vivo studies, in spite of their tremendously busy schedules.

To this end, I need to recognize once more the generosity of my supervisors in providing all of the facilities, equipment, materials, training and supporting staff necessary for my work, from which I have gained experience in numerous analytical methods and technical skills, I never thought achievable. I have also benefited greatly from the opportunities I was provided to participate in various national and international biomaterial and bone tissue engineering conferences. Hence, I would like to acknowledge the funding sources, scholarships and travel awards that made the past years possible without major financial restraints: the Canadian Institutes for Health Research, Center for Bone & Periodontal Diseases, National Science & Engineering Research Council, Shriners of North America, International Bone & Mineral Society, Faculty of Dentistry and McGill University.

I will be forever grateful to my beloved parents, my idolized sister, my two precious brothers and my treasured friends who blessed me throughout my life-time and offered their absolute compassion, encouragement and unconditional benevolence, especially when I decided to pursue my higher studies. Finally, I dedicate this ripe fruit to my mother homeland, Lebanon, land of dignity, perseverance, hope and courage, yearning that someday, I would be a servant and a contributor to her amelioration and prosperity.

# TABLE OF CONTENTS

ABSTRACT ..... 2
RÉSUMÉ ..... 4
ACKNOWLEDGMENTS ..... 6
TABLE OF CONTENTS ..... 8
LIST OF FIGURES ..... 12
LIST OF TABLES ..... 13
GLOSSARY OF ACRONYMS ..... 14
CONTRIBUTIONS OF AUTHORS ..... 15

**SECTION I: GENERAL INTRODUCTION**

**CHAPTER 1 INTRODUCTION ..... 16**

**1.1.** STATE OF THE FIELD OF BONE TISSUE ENGINEERING ..... 16
1.1.1. 2000–2010: The Bone and Joint Decade ..... 16
1.1.2. Protein Therapy: BMPs – a brief history and state of art ..... 17
1.1.3. Distraction Osteogenesis (DO): a bone regeneration and repair model ..... 20
**1.2.** THESIS OUTLINE ..... 22

**CHAPTER 2 RATIONALE, OBJECTIVES AND ORIGINAL CONTRIBUTIONS ..... 26**

**2.1.** RATIONALE ..... 26
**2.2.** HYPOTHESIS ..... 27
**2.3.** AIM AND DESIGN ..... 27
**2.4.** OBJECTIVES ..... 28
**2.5.** JUSTIFICATION ..... 30
2.5.1. Nanoparticulate Drug Delivery Systems (DDSs) ..... 30
2.5.2. Polymeric Drug Carriers and Delivery Systems (DSs) ..... 30
2.5.3. Phospholipid vesicles (LIPOSOMES) ..... 31
2.5.4. Natural Polymers (ALGINATE and CHITOSAN) ..... 32
2.5.5. BMP-7/OP-1 – the DRUG/PROTEIN of choice ..... 34
2.5.6. Core-Shell Nanoparticulate rhOP-1 DS For DO ..... 35
**2.6.** SUMMARY OF ORIGINAL CONTRIBUTIONS ..... 37

**SECTION II: BACKGROUND AND LITERATURE REVIEW**

**CHAPTER 3 CURRENT CHALLENGES IN BMP DELIVERY ..... 39**

**3.1.** ABSTRACT ..... 41
**3.2.** INTRODUCTION: rhBMPs IN BONE REGENERATION AND REPAIR ..... 42
**3.3.** CHALLENGES IN rhBMP DELIVERY ..... 43
**3.4.** DELIVERY SYSTEMS PARAMETERS AND REQUIREMENTS ..... 45
3.4.1. Release Kinetics and Retention at defect site ..... 46
3.4.2. Dose and Concentration ..... 47
3.4.3. Localized and release-controlled delivery ..... 48
3.4.4. Injectable and Multiple Growth Factor Delivery ..... 50
**3.5.** FUTURE PROSPECTS ..... 51
**3.6.** ACKNOWLEDGMENTS ..... 52

**CHAPTER 4 DELIVERY MATERIALS AND CARRIER TYPES FOR BMPs ..... 54**

**4.1.** ABSTRACT ..... 55
**4.2.** INTRODUCTION ..... 56

**4.3.** rhBMP DELIVERY SYSTEMS ..... 56
**4.4.** rhBMP-SPECIFIC CARRIER TYPES AND DEIVERY MATERIALS ..... 57
**4.5.** NATURAL-ORIGIN POLYMERIC CARRIERS ..... 58
4.5.1. Collagen ..... 58
4.5.2. Alginate and Chitosan ..... 60
4.5.3. Hyaluronic acid ..... 61
**4.6.** INORGANIC MATERIALS ..... 61
4.6.1. Hydroxyapatite ..... 62
4.6.2. Calcium phosphates and Bioactive glasses ..... 62
**4.7.** SYNTHETIC BIODEGRADABLE POLYMERIC CARRIERS ..... 63
**4.8.** COMPOSITES ..... 64
**4.9.** FUTURE PROSPECTS ..... 67
**4.10.** ACKNOWLEDGMENTS ..... 67
**4.11.** SUPPLEMENTARY INFORMATION ..... 68

**CHAPTER 5 DISTRACTION OSTEOGENESIS (DO) ..... 69**

**5.1.** ABSTRACT ..... 71
**5.2.** DEFINITION ..... 72
**5.3.** HISTORICAL BACKGROUND ..... 72
**5.4.** BIOLOGICAL BASIS OF NEW BONE FORMATION IN DO ..... 75
5.4.1. Principles of DO ..... 75
5.4.2. Histological Features of DO ..... 76
5.4.3. Type(s) of Bone Formation in DO ..... 78
**5.5.** CLINICAL APPLICATIONS OF DO ..... 79
5.5.1. Clinical Problems and Limitations of DO ..... 81
5.5.2. Attempts to Accelerate Bone Formation in DO ..... 81
5.5.3. BMPs and BMP Signaling Pathways in Bone Formation and DO ..... 82
**5.6.** CONCLUSIONS ..... 88

**SECTION III: IN VITRO WORK**

**CHAPTER 6 FORMULATION OF HYBRID CORE-SHELL NANOPARTICLES ..... 90**

**6.1.** ABSTRACT ..... 92
**6.2.** INTRODUCTION ..... 93
**6.3.** MATERIALS AND METHODS ..... 94
6.3.1. Formulation of Liposomes ..... 94
6.3.2. Preparation of Nanoparticles ..... 95
6.3.3. Characterization of Nanoparticles ..... 95
6.3.3.1. Particle Size, Surface Charge and Stability ..... 95
6.3.3.2. Morphology (AFM) ..... 96
6.3.3.3. Entrapment Efficiency and Loading Capacity (BSA) ..... 96
6.3.3.4. Protein Release Study (BSA) ..... 97
6.3.3.5. Modeling of Release Kinetics ..... 97
6.3.4. Statistical Analysis ..... 98
**6.4.** RESULTS AND DISCUSSION ..... 99
6.4.1. Particle Size and Size Distribution ..... 99
6.4.2. Surface Charge and Physical Stability ..... 101
6.4.3. Morphology ..... 103
6.4.4. Protein Entrapment Efficiency and Loading Capacity ..... 104
6.4.5. Protein Release Profile ..... 106
6.4.6. Release Kinetics ..... 107
**6.5.** CONCLUSIONS ..... 109
**6.6.** ACKNOWLEDGMENTS ..... 110

**CHAPTER 7 MODULATED RELEASE OF BIOACTIVE rhOP-1 ..... 111**
**7.1.** ABSTRACT ..... 113
**7.2.** INTRODUCTION ..... 114
**7.3.** MATERIALS AND METHODS ..... 117
7.3.1. Materials ..... 117
7.3.2. Preparation of Nanoparticles ..... 117
7.3.3. Characterization of Nanoparticles ..... 118
7.3.3.1. Particle Size, Surface Charge and Stability ..... 118
7.3.3.2. Cell Culture ..... 118
7.3.3.3. Cytotoxicity Assay ..... 118
7.3.3.4. Stability in Fetal Bovine Serum ..... 119
7.3.3.5. Entrapment Efficiency and Loading Capacity ..... 119
7.3.3.6. Protein Release Study ..... 119
7.3.3.7. Measurement of ALP Activity ..... 120
7.3.3.8. Modeling Release Kinetics ..... 120
7.3.4. Statistical Analysis ..... 121
**7.4.** RESULTS AND DISCUSSION ..... 121
7.4.1. Preparation and Characterization of Core-Shell Nanoparticles ..... 121
7.4.2. Stability in Serum ..... 122
7.4.3. Cytotoxicity ..... 122
7.4.4. OP-1 loading Capacity and Entrapment Efficiency ..... 123
7.4.5. OP-1 Release Profile ..... 124
7.4.6. ALP Activity ..... 126
7.4.7. OP-1 Release Kinetics ..... 128
**7.5.** CONCLUSIONS ..... 130
**7.6.** ACKNOWLEDGMENTS ..... 130

**SECTION IV: IN VIVO WORK**

**CHAPTER 8 BIOCOMPATIBILITY AND SAFETY IN WISTAR RATS ..... 131**

**8.1.** ABSTRACT ..... 134
**8.2.** INTRODUCTION ..... 136
**8.3.** MATERALS AND METHODS ..... 138
8.3.1. Nanoparticles and Evaluation of rhOP-1 Encapsulation ..... 138
8.3.2. Animals ..... 139
8.3.3. Experimental Study Design and Analysis ..... 139
8.3.3.1. Study Protocol ..... 139
8.3.3.2. Biochemical and Hematological Analysis ..... 140
8.3.3.3. Histopathological Analysis ..... 140
8.3.3.4. Immunohistochemistry ..... 141
8.3.3.5. Quantitative Grading of Immunostaining ..... 141
8.3.3.6. Statistical Analysis ..... 142
**8.4.** RESULTS AND DISCUSSION ..... 143
8.4.1. Clinical Signs and Body Weight Changes ..... 145
8.4.2. Serum Biochemical and Hematological Findings ..... 145
8.4.3. Organ Weights ..... 148
8.4.4. Histopathalogical Findings ..... 148
8.4.5. Molecular Changes Post-injections in Muscle ..... 150
**8.5.** CONCLUSION ..... 155
**8.6.** LIMITATIONS AND FUTURE STUDIES ..... 155
**8.7.** ACKNOWLEDGMENTS ..... 156

**CHAPTER 9 EVALUATION OF NEW BONE FORMATION IN RABBIT DO ..... 157**

**9.1.** ABSTRACT ..... 159
**9.2.** INTRODUCTION ..... 160
**9.3.** MATERIALS AND METHODS ..... 162

9.3.1. Animals ..... 162
9.3.2. Operative Protocol ..... 162
9.3.3. Formulation of rhOP-1/Core-Shell Nanoparticles ..... 164
9.3.4. Evaluation of rhOP-1 Encapsulation ..... 165
9.3.5. Study Protocol ..... 165
9.3.6. Radiology ..... 166
9.3.7. Bone Histomorphometry ..... 166
9.3.8. Immunohistochemistry ..... 167
9.3.9. Qualitative and Quantitative Immunostaining ..... 168
**9.4.** RESULTS ..... 168
9.4.1. Cellular Changes Post-injections ..... 169
9.4.1.1. Radiology ..... 169
9.4.1.2. Bone Densitometry ..... 170
9.4.1.3. Bone Architecture ..... 171
9.4.1.4. Histomorphometry of Regenerate ..... 173
9.4.2. Molecular Changes Post-injections ..... 174
**9.5.** DISCUSSION ..... 176
**9.6.** ACKNOWLEDGMENTS ..... 179
**9.7.** SUPPLEMENTARY DATA ..... 180

**SECTION V : THESIS CONCLUSIONS AND FUTURE PROJECT DIRECTIONS**

**CHAPTER 10 CONCLUSIONS AND FUTURE PERSPECTIVES ..... 181**

**10.1.** CONCLUSIONS TO DATE ..... 181
**10.2.** SUMMARY OF ACCOMPLISHMENTS ..... 182
**10.3.** FUTURE PERSPECTIVES AND DIRECTIONS FOR THE PROJECT ..... 187
**10.4.** ONGOING STUDIES ..... 188
10.4.1. Wild-Type (WT) Mouse Model of Tibial DO (TDO) – The Protocol ..... 190
10.4.2. A Dose-Response Curve for rhOP-1 in WT ♂ Mice TDO ..... 192
10.4.3. The Effect of rhOP-1/NPs in WT ♂ Mice TDO ..... 194

**CHAPTER 11 CUMULATIVE BIBLIOGRAPHY LISTING ..... 196**

**SECTION VI: APPENDICES**

**APPENDIX A - CONVENTIONS IN NANOPARTICLE CHARACTERIZATION ..... 221**
**A.1.** AVERAGE SIZE MEASURMENT (DLS) ..... 221
**A.2.** SURFACE CHARGE MEASURMENT (ZETA POTENTIAL) ..... 222
**A.3.** MTT ASSAY ..... 223
**A.4.** HUMAN BMP-7/OP-1 ELISA CONSTRUCTION KIT ..... 223
**A.5.** RELEASE KINETICS AND THE HIGUCHI MODEL ..... 224
**A.6.** MICROSCOPIC IMAGING: AFM AND TEM ..... 226
**A.7.** IN VIVO MODELS IN BONE TISSUE ENGINEERING ..... 228

**APPENDIX B - SUPLLIMENTARY IN VITRO EXPERIMENTS ..... 231**
**B.1.** EFFECT OF SUCROSE AS A CRYOPROTECTANT ..... 231
**B.2.** EFFECT OF INCUBATION TIME ..... 232
**B.3.** EFFECT OF POLYMER CONCENTRATION ..... 233
**B.4.** EFFECT OF PBS ..... 234
**B.5.** EFFECT OF CENTRIFUGATION/WASHING AND MOLECULAR WEIGHT ..... 235
**B.6.** EFFECT OF EXTRUSION AND FILTRATION ..... 235

**APPENDIX C - ARTICLE REPRINTS ..... 237**

**APPENDIX D - CANDIDATE CURRICULUM VITAE ..... 275**

# LIST OF FIGURES

**FIGURE 1.1.** Bone Tissue Engineering using BMPs ..... 17
**FIGURE 1.2.** Schematic of the Illizarov ring fixator used in long bone DO ..... 20

**FIGURE 2.1.** Schematic presentation of liposomes (L) ..... 31
**FIGURE 2.2.** Molecular structure of sodium alginate (AL) ..... 32
**FIGURE 2.3.** Molecular structure of chitin and chitosan (CH) ..... 33
**FIGURE 2.4.** Schematic presentation of the layer-by-layer (LbL) technique ..... 36

**FIGURE 3.1.** Tissue engineering approaches and combinations ..... 42
**FIGURE 3.2.** In vitro release profile for rhOP-1 from core-shell NPs ..... 49

**FIGURE 4.1.** Selected electron microscopy of various BMP carriers ..... 64

**FIGURE 5.1.** Hippocrates' (460-370 BC) fracture technique & fixation ..... 73
**FIGURE 5.2.** Historical evolution of the DO principles & technique ..... 73
**FIGURE 5.3.** Gavriel A. Illizarov – Father of DO ..... 74
**FIGURE 5.4.** Histology of the structure of an osteoregenerate in DO ..... 77
**FIGURE 5.5.** Craniomaxillofacial distraction systems (internal & external) ..... 80
**FIGURE 5.6.** Crystal structure of human BMP-2 and BMPRII ..... 83
**FIGURE 5.7.** The BMP Signaling pathway ..... 85

**FIGURE 6.1.** Particle size change with the polymeric shell build-up ..... 100
**FIGURE 6.2.** PI distribution and stability over time at room temperature ..... 101
**FIGURE 6.3.** Surface charge alternation with the shell build-up ..... 102
**FIGURE 6.4.** Nanoparticle stability pre- and post-lyophilization ..... 103
**FIGURE 6.5.** AFM micrographs of un-coated and coated liposomes ..... 104
**FIGURE 6.6.** In vitro loading capacity & encapsulation efficiency of BSA ..... 105
**FIGURE 6.7.** In vitro cumulative & absolute BSA release profiles/30d ..... 106
**FIGURE 6.8.** Modeling of in vitro BSA release kinetics ..... 108

**FIGURE 7.1.** Stability of un-coated and coated liposomes in FBS ..... 122
**FIGURE 7.2.** In vitro cytotoxicity (viability of mouse pre-osteoblasts) ..... 122
**FIGURE 7.3.** In vitro loading capacity & encapsulation efficiency of OP-1 ..... 123
**FIGURE 7.4.** In vitro cumulative & absolute OP-1 release profiles/45d ..... 126
**FIGURE 7.5.** ALP activity (differentiation of pre-osteoblasts) assay ..... 127
**FIGURE 7.6.** Modeling of in vitro OP-1 release kinetics ..... 129

**FIGURE 8.1.** Timeline schematic for the biocompatibility study in rats ..... 139
**FIGURE 8.2.** Cryo-TEM of 3-bi-layered core-shell nanoparticles ..... 143
**FIGURE 8.3.** Body weight changes (in g) pre- and post-IM injections ..... 145
**FIGURE 8.4.** Blood serum biochemical and hematological data ..... 146
**FIGURE 8.5.** Histological images of the harvested rat organs ..... 149
**FIGURE 8.6.** Histological and immunostained images of hind muscle ..... 151

**FIGURE 9.1.** Timeline schematic for the rabbit DO study model ..... 163
**FIGURE 9.2.** Cryo-TEM of un-coated and coated liposomes ..... 164
**FIGURE 9.3.** Radiology images of rabbit tibiae post-injections ..... 169
**FIGURE 9.4.** BMD of the regenerate in the distraction gap ..... 171

**FIGURE 9.5.** µCT images of tibiae at 3 weeks post-injections .....172
**FIGURE 9.6.** Histological of the center of the distracted zone.....173
**FIGURE 9.7.** Immunohistochemistry at 3 weeks post-injections.....174
**FIGURE 9.8.** Supplementary immunohistochemistry images.....180

**FIGURE 10.1.** Schematic of the ring fixator made for the WT mice.....190
**FIGURE 10.2.** Summary of the long bone DO protocol in WT mice .....191
**FIGURE 10.3.** Preliminary data/rhOP-1 dose-response in ♂ WT mice.....193

**FIGURE A.1.** A simulated in vitro tri-phasic drug release profile/model.....224

**FIGURE B.1.** Optimum cryoprotectant (sucrose) concentration study.....231
**FIGURE B.2.** Effect of incubation time on NP size & surface charge .....232
**FIGURE B.3.** Effect of polymer concentration on NP surface charge.....233
**FIGURE B.4.** Effect of PBS on NP size and surface charge .....234
**FIGURE B.5.** Effect of centrifugation/washing and MW on NP size .....235
**FIGURE B.6.** Effect of filtration on liposome size and dispersion.....236

## LIST OF TABLES

**TABLE 1.1.** Growth Factors.....18
**TABLE 1.2.** The Bone Morphogenetic Protein subfamily.....19

**TABLE 3.1.** General requirements for BMP delivery systems.....45

**TABLE 4.1.** Overview of FDA-approved rhBMP devices .....56
**TABLE 4.2.** Major classes of BMP carrier materials .....57
**TABLE 4.3.** rhBMP-2 and rhBMP-7/rhOP-1 use in clinical studies.....59
**TABLE 4.4.** rhBMP-2 and rhBMP-7/rhOP-1 in animal studies .....68

**TABLE 6.1.** In vitro parametric characterization of un-coated liposomes .....99
**TABLE 6.2.** In vitro BSA release rate and correlation coefficients.....109

**TABLE 7.1.** In vitro OP-1 release rate and correlation coefficients .....130

**TABLE 8.1.** Parametric changes pre- and post- rhOP-1 loading.....144
**TABLE 8.2.** Organ weights of injected rats sacrificed on day 70.....148
**TABLE 8.3.** Immunolocalization in the harvested muscle of rats.....154

**TABLE 9.1.** Summary of µCT analysis of rabbit DO regenerate .....171
**TABLE 9.2.** Histomorphometry analysis of rabbit DO regenerate .....173
**TABLE 9.3.** Immunolocalization in the center of the distraction gap .....175
**TABLE 9.4.** Immunolocalization in the callus of the distraction gap .....175

| | |
|---|---|
| **rh** | recombinant human |
| **µCT** | micro-Computed Tomography |
| **AFM** | Atomic Force Microscopy |
| **AL** | Alginate |
| **ALP** | Alkaline Phosphatase |
| **ALT** | Alanine Transaminase |
| **AST** | Aspartate Transaminase |
| **BHM** | Bone Histomorphometry |
| **BMD** | Bone Mineral Density |
| **BMP** | Bone Morphogenetic Protein |
| **BMPR** | Bone Morphogenetic Protein Receptor |
| **BSA** | Bovine Serum Albumin |
| **BUN** | Blood Urea Nitrogen |
| **BV/TV** | Bone Volume/Tissue Volume |
| **CH** | Chitosan |
| **DDAB** | dimethyldioctadecyl-ammonium bromide |
| **DDSs or DS** | Drug Delivery System(s) or Delivery System or *carrier* |
| **DO** | Distraction Osteogenesis |
| **DPPC** | 1, 2-Dipalmitoyl-sn-glycero-3-phosphocholine |
| **ELISA** | enzyme-linked immunosorbent assay |
| **FBS** | Fetal Bovine Serum |
| **GF** | Growth Factor |
| **H** | Higuchi ideal |
| **HMW** | High Molecular Weight |
| **IM** | Intra-muscular |
| **kDa** | kilodalton (atomic or molecular mass unit) |
| **LbL, L-b-L or LBL** | layer-by-layer |
| **Lipo, LUV or L** | Liposome(s) or Large Uni-lamellar Vesicles |
| **LMW** | Low Molecular Weight |
| **M** | Molar |
| **MTT** | 3-(4,5-dimethylthiazol-2-yl)-2,5-diphenyltetrazolium bromide |
| **ml or mL** | milliliter |
| **mV** | millivolt |
| **MW** | Molecular Weight |
| **nm** | nanometer |
| **NP or NPs** | Nanoparticle or Nanoparticles |
| **NZW and WT** | New Zealand White (rabbits) and Wild-Type (mice) |
| **OP-1 or BMP-7** | Osteogenic Protein-1 or Bone Morphogenetic Protein-7 |
| **PBS** | Phosphate Buffered Saline |
| **PI** | Polydispersity Index |
| **RBCs** | Red Blood Cells |
| **RT** | Room Temperature: $20^{o}$C ($68^{o}$F) – $25^{o}$C ($77^{o}$F) |
| **RT$^{2}$PCR** | Real Time Reverse Transcription Polymerase Chain Reaction |
| **Smad `** | Homologue of MAD (Mothers against Decapentalegic) |
| **TEM** | Transmission Electron Microscopy |
| **UPW or HPW** | Ultra-pure Water or Highly-pure Water |
| **WBCs** | White Blood Cells |
| **WT** | Wild-Type (mice) |

# CONTRIBUTIONS OF AUTHORS

This dissertation is presented as a compilation of published, in press, submitted and incomplete (on thesis submission date: August 31st of 2009) manuscripts written by the candidate under the supervision of the Ph.D. program supervisors. The works are mainly based on theoretical and experimental data generated from the literature, in vitro and in vivo studies designed and conducted by the candidate, who was responsible for experimental design, data collection, analysis and interpretation. **Prof. Maryam Tabrizian** and **Dr. Reggie Charles Hamdy** are the co-supervisors appearing on all manuscripts to reflect their supervisory roles during the execution of the presented studies. Other contributors, colleagues and co-authors appear on some of the manuscripts to reflect their involvement in technical aspect(s) of the presented works and/or manuscript preparation. These efforts were recognized and acknowledged when and where deemed necessary.

# CHAPTER 1
# General Introduction to Thesis

## 1.1. Bone Tissue Engineering

### 1.1.1. 2000-2010: The Bone and Joint Decade

Bone is one of the tissues with the most regenerative capabilities in the human body. Yet, healing of bone fractures and reconstruction of large or critical-sized bone defects continue to present a significant challenge for orthopedists, traumatologists, craniofacial as well as oral and maxillofacial surgeons (Einhorn 1995). To address the need for increased awareness and research into musculoskeletal injuries and disorders, the United Nations and the World Health Organization declared the years 2000-2010 as the Bone and Joint Decade (Weinstein 2000). For example, in the United States alone, over 8 million long bone fractures are sustained with at least 500,000 bone grafting procedures performed annually (Bishop and Einhorn 2007). Although autologous cancellous bone grafts are still routinely used to heal bone defects due to possessing all the important qualities of osteoinduction, osteoconduction, osteointegration and osteogenesis, they are plagued with problems of limited supply, donor site morbidity including pain, infection, hematoma formation and increased costs as well as variability in fusion success rate. The use of processed allografts and xenografts is also limited due to potential rejection of foreign tissue and disease transmission as well as poor osteogenic capacity of the transplanted bone. In addition, free bone transfer is associated with donor site morbidity as well as limited quality and quantity (Finkemeier 2002). Hence, **bone graft substitutes** mainly ceramics, metals and plastics have received great interest in the last decades although seldom result in complete bony integration and are often toxic due to wear (Salgado et al. 2004). Therefore, developing **alternative solutions for bone tissue engineering** that would replace the conventional grafting procedures remains crucial (Rose et al. 2004); with the goal being to regenerate *native* bone to completely fill such defects, not only in terms of quantity but quality as well (Einhorn 2003; Haidar et al. 2009 a, b, c). The state of the field of bone tissue engineering in regenerative medicine uses growth factors incorporated into biomaterials, alone or in combination with precursor or stem cells, possibly

from the patient him/herself. Thus far, three *new* strategies for osteogenesis are currently undergoing vigorous investigation: the transduction of genes encoding osteogenic cytokines into cells at repair sites (gene therapy); the transplantation of cultured osteogenic cells derived from host bone marrow (stem cell therapy) and the application of biologically-active osteoinductive morphogens in combination with the appropriate carriers and/or other biomaterials at the target site (protein therapy). Gene- and stem cell therapies for bone healing will probably represent the next major advance however are still in their infancy requiring considerable resources and investigation regarding safety and efficacy in humans (Kimelman et al. 2007). **Protein therapy** (Figure 1.1) in contrast, has revealed the most practical promise for the near future, predominantly with the use of potent bone cytokines from the Transforming Growth Factor-β Family (TGF-β), despite some limitations (Li and Wozney 2001; Uludag et al. 2001; Nakashima and Reddi 2003; Einhorn 2003; Rose et al. 2004; Termaat et al. 2005; Gautschi et al. 2007).

### 1.1.2. Protein Therapy: BMPs – *a brief historical synopsis and state-of-art overview*

Modern recombinant DNA technology has made it possible to identify several growth factors as displayed in Table 1.1. However, it dates back to as early as 1889 when decalcified bone was noticed to induce healing of bone defects (Senn 1889). Lavender (Levander 1938)

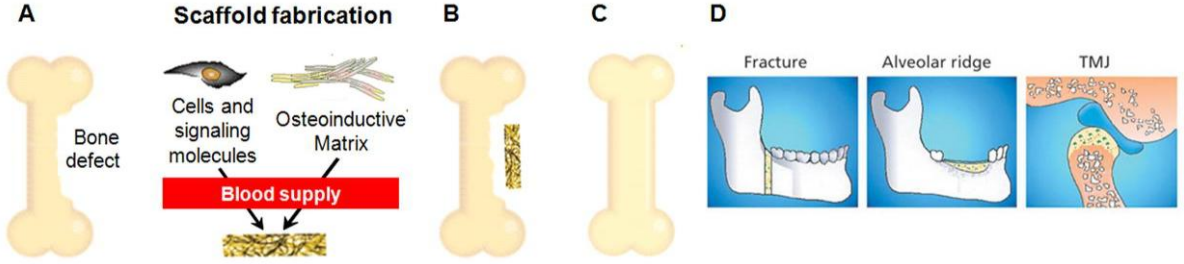


**FIG 1.1. Tissue engineering (osteoinduction for osteoregeneration and repair)**. BMPs have been demonstrated to have the potential for tissue engineering and regeneration of long bones **(A-C)** as well as other craniofacial structures and related indications such as: mandibular bone, alveolar ridge augmentation, cartilage repair in the temporomandibular joint (TMJ), oral implants, endodontic treatment and regeneration of periodontal tissues **(D)**. Modified from Nakashima and Reddi 2003.

provided the first evidence of ectopic bone formation and later on by Lacroix (Lacroix 1945) following injecting bone crude extracts 'osteogenin' into muscle tissue. Yet, the pioneering work of Marshall R. Urist in 1965 (Urist 1965) was what marked a landmark on research in

the bone field; discovering that the active compound responsible for bone regeneration was thus a *mix* of proteins that he then named - **Bone Morphogenetic Proteins (BMPs).**

**TABLE 1.1. Growth Factors**

| *Growth Factor* | *Abbreviation* | *Source* | *Molecular Weight (kDa)* | *Activity* | *Reference(s)* |
|---|---|---|---|---|---|
| **Transforming Growth Factor-β** | TGF-β | Platelets, bone extracellular matrix | 25.0 – 44.0 | Proliferation of mesenchymal cells | Na 2007 |
| **Bone Morphogenetic Proteins** | BMP-2<br>BMP-7/OP-1 | Osteoprogenitors, osteoblasts, bone extracellular matrix | ~ 26.0<br>31.5 – 49.0 | Differentiation and migration of bone-forming cells (osteocytes and osteoblasts) | Govender 2002<br>Ripamonti 2001<br>Haidar 2008b |
| **Fibroblast Growth Factors** | FGF-1 / bFGF | Macrophages, chondrocytes and osteoblasts | 17.2 – 24.0 | Mitogenic for mesenchymal cells, chondrocytes and osteoblasts | Mizuno 2003 |
| **Insulin-like Growth Factors** | IGFs<br>IGF-I / IGF-II | Liver cells, pancreas and brain (*possibly*) | < 25.0 – 34.0 | Proliferation and differentiation of osteoprogenitor cells | Chen 2006 |
| **Platelet-derived Growth Factors** | PDGFs | Platelets and osteoblasts | 24.0 – 29.0 | Proliferation of mesenchymal cells and osteoblasts | Lee 2002 |

In the years that followed, Urist's students, Sampath and Reddi created a crude but highly reproducible bioassay for BMPs in ectopic bone formation (Sampath and Reddi 1981). The assay was based on the activity of the alkaline phosphatase enzyme and the content of calcium in the newly formed bone. Reddi then proposed that BMPs were responsible for the initiation of a cascade of developmental events; in which progenitor cells in the bone marrow were induced or stimulated to produce bone cells leading to bone regeneration (Reddi and Huggins 1972; Reddi 1987). During the 80s and 90s, BMP genes were cloned and recombinant proteins were shown to be biologically potent (Wozney et al. 1988). Much work followed with the availability of large amounts of recombinant human (rh) BMPs (rhBMPs) mainly in their evaluation for clinical applications such as spinal fusion, fracture healing and oro-dental tissue engineering (Nakashima and Reddi 2003; Seeherman and Wozney 2005; Bessa et al. 2008 a) as summarized in Table 1.2. Today, BMPs are considered peptide signaling molecules that play *diverse* roles in development, growth, repair and regeneration. There are 18 distinct BMPs, 15 of which occur in humans. In a recent review, Reddi further proposed naming BMPs: ***body*** *morphogenetic proteins*, due to their extensive roles as inductive signals for the development of tissues and organs beyond bone including the nervous system, heart, kidney, liver, gut, skin, eyes as well as teeth (Reddi 2001; Reddi 2005). Yet, the human application of these biologically-active osteoinductive growth factors

(protein therapy) is still rather far from optimal. To obtain approximately one microgram of a BMP, one kilogram of human bone is required. Therefore, the need to use milligram quantities of either of these proteins in order to produce a therapeutic effect suggests that optimized clinical application of BMP has not yet been achieved. Furthermore, it is well established today that the clinical **safety** and **efficacy** of rhBMPs will depend critically on the delivery strategy and carrier used where when administered in solution; they are rapidly cleared, resulting in suboptimal healing (associated largely with collagen-based carriers). Hence, the delivery of specific rhBMPs (proper dose and concentration) at the pertinent duration of time efficient for bone regeneration and repair using a biocompatible, biodegradable and bioresorbable delivery vehicle that stabilizes and prevents the rapid diffusion or dispersal of the growth factor(s) and promotes localized osteogenesis at the defect site is consequently essential (Li and Wozney 2001; Mont et al. 2004; Gautschi et al. 2007, Bessa et al. 2008 a, b).

**TABLE 1.2. Bone Morphogenetic Protein (BMP) Family**

| *BMP subfamily* | *BMP Molecule* | *Generic name* | *Function* | *Reference(s)* |
|---|---|---|---|---|
| **BMP-2/4** | BMP-2 | BMP-2A | Osteoinduction, osteoblast differentiation, cartilage morphogenesis and lung, eye, kidney and cardiac development | Wozney et al. 1988 |
| | BMP-4 | BMP-2B | | Bessa et al. 2008a |
| **BMP-3** | BMP-3 | Osteogenin | Most abundant BMP in bone: inhibit morphogenesis and osteogenesis | Reddi1987; Reddi 2005 |
| | BMP-3B | GDF-10 | | |
| **BMP-7** | BMP-5 | BMP-5 | Chondrogenesis, limb development and bone morphogenesis | |
| | BMP-6 | Vgr-1 | Chondrogenesis, bone morphogenesis and estrogen mediation | Reddi 2001 |
| | BMP-7 | OP-1 | Osteoinduction, cartilage and bone morphogenesis, kidney and eye development | Simic and Vukicevic 2005 |
| | BMP-8 | OP-2 | Osteoinduction and spermatogenesis | Reddi 2005 |
| | BMP-8B | OP-3 | Spermatogenesis | |
| **BMP-9** | BMP-9 | GDF-2 | Hepatogenesis, glucose metabolism and bone morphogenesis | Chen et al. 2004 |
| **BMP-10** | BMP-10 | BMP-10 | Cardiac development and morphogenesis | |
| **BMP-11** | BMP-11 | GDF-8, myostatin | Patterning mesodermal and neuronal tissues, eye, pancreas and kidney development | Reddi 2003 |
| **BMP-12** | BMP-12 | GDF-7, CDMP-3 | Tendon and ligament development | |
| **BMP-13** | BMP-13 | GDF-6, CDMP-2 | Induces tendon and ligament-like tissue formation (hypertrophy) | Reddi 2005 |
| **BMP-14** | BMP-14 | GDF-5, CDMP-1 | Chondrogenesis, angiogenesis, tendon healing and bone formation | |
| **BMP-15** | BMP-15 | GDF-9B | Follicle-stimulating hormone activity modification | Knight and Glister 2006 |
| **BMP-16** | BMP-16 | Nodal | Embryonic patterning | Zeng et al. 2007 |
| **BMP-17** | BMP-17 | Lefty | Embryonic patterning | |
| **BMP-18** | BMP-18 | Lefty | Embryonic patterning | |

BMP-1 is not a BMP family member. GDF: growth/differentiation factor, Vgr: vegetal related, OP: osteogenic protein, and CDMP: cartilage-derived morphogenetic protein

The ultimate goal for protein therapy today is **to develop safe**, **proficient**, **predictable**, **user-friendly** and **cost-effective** BMP delivery systems that would completely replace conventional bone grafting procedures. For a clinically beneficial outcome, cytokines such as BMPs require a **localized** and **release-controlled delivery system** to guide tissue regeneration and prevent the rapid dispersal of the growth factors from sites of regeneration and repair. The role of rhBMPs, particularly BMP-2, -6, -7 and -9 in de novo bone formation

and the involved signaling pathways have received great interest in the past years and are currently ongoing as there is still much that needs to be understood regarding the potency of individual BMPs, BMP combinations and their use in clinical settings. (Rosen 2006). The current state of knowledge is reviewed in Chapters 3, 4 and 5 of this thesis when the clinical application (in vivo model of bone healing and repair); distraction osteogenesis is presented in detail. It is introduced briefly next.

### 1.1.3. Distraction Osteogenesis (DO) – *a bone regeneration and repair model*

DO is a prevailing surgical technique widely used for bone lengthening. It includes performing an osteotomy followed by gradually distracting the two bone segments resulting in de novo bone formation within the distracted gap as is displayed in Figure 1.2 (Ilizarov 1989 a, b). However, a main limitation is the **long period of time required for the newly formed bone to consolidate** entailing prolonged fixation with considerable morbidity (Paley 1990). BMP-7, also known as osteogenic protein-1 or OP-1 has been shown to be involved in cellular recruitment and in the proliferation and differentiation of osteoprogenitor cells into bone-forming cells, thus accelerating the formation of new bone in numerous preclinical (Cook and Rueger 1996; Ripamonti et al. 2000; Hamdy et al. 2003) and clinical studies (Cook 1999; Friedlaender et al. 2001; Vaccaro et al. 2008). Nonetheless, **supra-physiological** and expensive dosages of rhOP-1 in the **milligram range** for satisfactory bone healing continue to be required. As mentioned earlier, the clinical efficacy of rhBMPs will *almost* always depend on the carrier used. The foremost limitations include the rapid diffusion of rhOP-1 away from the site and loss of its bioactivity, resulting in ectopic bone formation or suboptimal local induction and hence failure of bone regeneration. For example, 28.5 mg rhOP-1 with a Type I collagen carrier were evaluated in a rabbit model of long bone DO. The poor results reported in comparison to control animals were explained by the relatively large bulk of the solid carrier used therefore mechanically

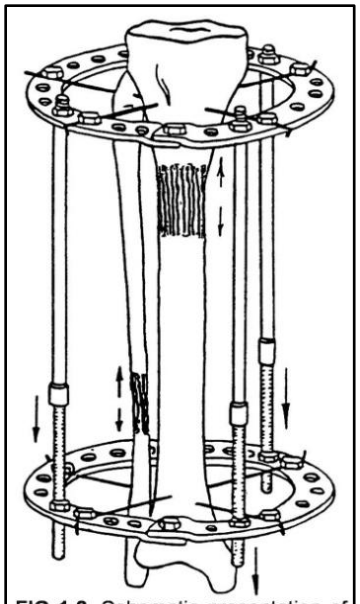

**FIG 1.2.** Schematic presentation of the DO bone lengthening procedure displaying the Illizarov external ring fixator used in limbs (1951).

obstructing the osteoregeneration process (Sailhan et al. 2006) in addition to the typical initial *large* burst protein release. Several materials for the delivery of rhBMP-2 and rhOP-1 have been developed in recent years however with limited and/or restricted clinical use and the **ideal drug delivery system** is still to be developed. Consequently, developing an *appropriate* and *adequate* delivery system that would improve the efficacy and maintain the bioactivity of the incorporated rhBMP(s), other growth factors and biomolecules (and perhaps allow for the use of much lower, safer and less expensive dosages) would be largely beneficial in the overall enhancement of a procedure such as long bone DO if not in conditions beyond the regeneration and repair of osseous tissue. This is today an investigative focus of many research groups around the globe as is the motivation behind the work presented in this doctoral dissertation.

## 1.2. Thesis Outline

The research work outlined herein aims at developing a novel biocompatible and potentially clinically-effective **nanosized rhBMP-7/rhOP-1 delivery system** in an attempt to provide a solution to the limitations currently hindering the practical application of protein therapy in bone tissue engineering, specifically in cases of bone lengthening. This project is comprised of two major components: in vitro and in vivo. Accordingly, the thesis was divided into **VI main sections**, as follows: general introduction; literature review; in vitro work; in vivo work; conclusions and future perspectives with a look into some of the ongoing works (uncompleted/unpublished works by the date of thesis submission) and finally an appendices section providing supplementary information as per McGill University thesis preparation guidelines. In the following chapter (Chapter 2), the rationale, hypothesis, design and justification for the formulated hybrid core-shell nanoparticulate delivery system and overall project objectives are outlined followed with a presentation of original contributions. **Section II** commences this thesis with a **review of published literature** that was initially undertaken to determine the current state of protein therapy as well as the clinical application model; distraction osteogenesis, to establish the criteria for developing an *ideal* delivery system, if possible. Chapters 3 through 5 present this background review in three parts. The first part discusses the general requirements for growth factor delivery systems emphasizing the distinction between carriers and delivery systems and localized and release-controlled delivery strategies in clinical bone tissue engineering (Chapter 3). Then, the various formulations of rhBMP-2 and rhBMP-7 carrier materials and delivery systems ranging from simple nano/microparticles to complex 3-D scaffolds, particularly with the use of natural polymers and their composites in sites of orthopaedic and craniofacial bone regeneration and repair are examined (Chapter 4). Finally, the historical development, current status and BMP signaling involvement during DO are highlighted to provide an understanding of the limitations impeding the procedure and the potential of protein therapy therein. During this background review, it was noted that injectable delivery systems have been gaining interest as a less invasive method for the repair of osseous defects, avoiding extensive/secondary surgery. More significantly, BMP therapy via the currently clinically-available collagen carriers has been shown to result in great response variability ranging from full bone

bridging within weeks to no bony union, mainly due to their poor BMP retention properties, unpredictable and uncontrolled protein release kinetics. Hence, our approach needed to constitute a novel biocompatible, biodegradable, stable, safe and effective drug delivery system with localized and release-controlled properties that is injectable as is preferable by surgeons to provide a malleable alternative to conventional bone grafting procedures, collagen sponges and possibly beyond. It is noteworthy that the first two reviews (Chapters 3 and 4) have been submitted and accepted recently as invited articles and for that reason will include some of the results from the experimental manuscripts published at an *earlier* stage. The third review discussing DO (Chapter 5) is *part* of a more comprehensive review article focusing on the most recent attempts for accelerating the consolidation phase of the DO procedure in preclinical and clinical studies. It is undergoing writing and is scheduled to be submitted for peer-review in September of 2009. The **in vitro component** of the project is presented *mainly* in **Section III** and illustrates the initial challenge of incorporating a liposomal core in a shell of alternating self-assembled layers of natural polymers; alginate and chitosan to develop a non-toxic, biocompatible, biodegradable, stable and release-controlled protein delivery system at the nanoscale. It first discusses the feasibility of formulating and characterizing spherical and stable core-shell nanoparticles ($\leq$ 400 nm in size) with the desirable surface charge characteristics, dispersion homogeneity and release kinetics (using a model protein) under mild conditions in water as a proof of concept. This parametric study was published in and is presented in Chapter 6 with a reprint in Appendix C. In Chapter 7, the physico-chemical characterization and optimization of the nanoparticles is presented with further set of experiments following the loading of a range of rhBMP-7/rhOP-1 concentrations in terms of encapsulation efficiency, loading capacity and release kinetics demonstrating the effect of the layer-by-layer electrostatically self-assembled core-shell design on maintaining the bioavailability of the released morphogen. It provides more information on the stability of the nanoparticles in simulated physiological media as well as their potential cytocompatibility, in vitro. This manuscript was published and a reprint is included in Appendix C as well. Following the successful development and characterization of the nanoparticles in vitro, their **in vivo assessment** initiated. **Section IV** provides a detailed presentation of the application of unloaded and loaded nanoparticles with rhBMP-7/rhOP-1 and findings in two animal species; rats and rabbits. In Chapter 8, the in vivo

biocompatibility and safety of the nanoparticles was evaluated in young normal rats upon intramuscular administration. This was followed by analysis of blood serum biochemistry and comparative histopathology for signs of toxicity and/or adverse effects. The included manuscript has been submitted for publication consideration in August of 2009. It also contains further parametric data that were not reported in the earlier in vitro works; the stability of the nanoparticles post-lyophilization/loading with rhOP-1 in addition to a microscopic (cryo-TEM) image revealing the presence of the polymeric shell around the liposomal core providing further evidence on its supportive role in maintaining the spherical morphology and integrity of the system under harsh preparatory conditions. The evaluation of the unloaded and rhOP-1 loaded nanoparticulate system in a rabbit model of long bone DO is presented next in Chapter 9 as a manuscript just accepted for publication. The regenerate was analyzed radiographically, histomorphometrically and immunohistochemically for cellular and molecular changes following the administration of different formulations of the nanoparticles. **Section V** ends this dissertation with a discussion of the overall **conclusions** to date, future perspectives and research directions for the project; presented in Chapter 10. A brief look into some of the other (ongoing/unpublished) manuscripts is included herein in order to shed light on part of the proposed project outlook. In a wild-type mouse DO model, two studies were planned and executed principally under the objective of enhancing and accelerating the consolidation phase in DO. Primarily, the aim was to develop a rhBMP-7/rhOP-1 dose-response curve as this was not done before in mice undergoing tibial bone lengthening (Chapter 10.4.2). Then, the rhBMP-7/rhOP-1 loaded delivery system was re-evaluated in the same animal DO model looking at effects on other aspects of bone regeneration such as the biomechanical characteristics of the regenerate (Chapter 10.4.3). These studies have all concluded experimentally (total sample size = 160 mice); however the full manuscripts were not included as they are on hold *pending final results*. Nevertheless, the protocol followed (Chapter 10.4.1) and preliminary data are described briefly in this section. The **cumulative thesis bibliography** is listed in Chapter 11. The **Appendices** available in **Section VI** provide: supplementary information on some of the techniques, methods, materials used generally in the field of drug delivery and more specifically in the evaluation and characterization of the formulated nanoparticles reported herein (Appendix A); other unpublished experimental in vitro data to complement

the findings reported in Section III as well as the suggestions for the future directions of this project outlined in Section V (Appendix B); reprints for the published articles and copyright waivers (Appendix C); in vivo protocols and research compliance certificates (Appendix D) and finally the curriculum vitae of the doctoral degree candidate (Appendix E).

# CHAPTER 2
# Rationale, Hypothesis, Objectives and Contributions

## 2.1. Rationale

It is well-recognized today that the full clinical safety and efficacy of various drugs, growth factors and in particular BMPs will *almost* always depend on the availability of a delivery system providing a sustained and prolonged release of adequate bioactive protein concentrations to the desired defect site. In the absence of such systems, bolus delivery is unpredictable and has been shown over the years to have a limited effect due to the rapid diffusion (and clearance) of exogenous proteins away from the application site and loss of their bioavailability. Consequently, supra-physiological and expensive dosages of BMPs in the milligram range (several orders of magnitude above the natural occurrence in bone) continue to be required for satisfactory bone healing. Such large dosages could have adverse and unknown long-term drawbacks (immunological reactions, development of antibodies and carcinogenic effects). Therefore, it becomes imperative to attempt to decrease the BMP dosages required in humans through maintaining their osteogenic efficiency perhaps via localizing and controlling the release kinetics of BMP delivery systems. However, adjustment of BMP release kinetics from the FDA-approved carriers (mostly collagen-based) is difficult and has not been accomplished thus far. Protein release from these BMP-soaked collagen sponges tends to be rapid where 70-90% of the load is depleted by the first week while bone healing is often a much longer process requiring weeks or months, especially in higher mammals with less responsive pools of cells. An optimal BMP release profile will also vary with animal species, anatomic site, defect size and vascularity among other key factors.

Thus, a *novel* ideal delivery system must (***i***) maintain the bioactivity and bioavailability of the encapsulated/entrapped growth factor(s), (***ii***) prevent rapid protein diffusion/clearance; (***iii***) release the BMP(s) in a predictable, metered and sustained manner, in terms of efficient dosage and duration of stimuli to target cells while allowing for profile modulation according to application site needs; (***iv***) provide an attractive environment for bone cells to

migrate as large volumes of bone might be required to form; (***v***) be biocompatible, non-toxic, stable (shelf-life), easy-to-manufacture, user-friendly (simple loading and preferably injectable) and cost-effective (lower yet therapeutic levels of recombinant BMPs).

The presence of BMPs over the entire duration of regeneration and repair might eventually reduce the variation in response observed among the clinical human trials themselves as well as with pre-clinical studies. Furthermore, an injectable system with customizable release, which current collagen sponges cannot accomplish, may also augment the bone healing response and overall therapeutic outcome without causing any unnecessary tissue distress from invasive surgeries.

## 2.2. Hypothesis

The efficiency of exogenous rhBMP-7/rhOP-1 will increase when applied locally via a custom-made, release-controlled and injectable nanosized delivery system; permitting the use of lower and safer dosages of the growth factor to enhance new bone formation and accelerate consolidation in long bone distraction osteogenesis.

## 2.3. Aim and Design

The *global* **aim** of this research project is to develop a tunable *drug* delivery system that preserves the biological activity of the encapsulant and provide low-burst, linear, sustained (over long periods of time) and localized release following a *single* administration (injectable solution). In cases of distraction osteogenesis, *specifically*, this would offer a patient-friendly alternative through ensuring high compliance rates post-operatively and the possible earlier removal of the fixator. In addition, it would also allow flexibility in achieving different release rates among other characteristics for other therapeutic proteins and biomolecules, host species, anatomic sites and thus a broader range of possible clinical applications.

The **design** constitutes an injectable suspension of biocompatible, biodegradable, stable and non-toxic nanoparticles composed of a cationic liposomal core and a *customizable* shell constructed via the electrostatic-based self-assembly of natural polymers; anionic alginate and cationic chitosan providing several compartments within it that would efficiently

accommodate a range of encapsulant concentrations and provide constant and bioactive delivery at the application site.

## 2.4. Objectives

After identifying the clinical application of interest (enhancing and accelerating the consolidation phase in distraction osteogenesis), the protein of choice (BMP-7/OP-1) and the properties of the *ideal* delivery system required (Chapters 2.1, 3, 4 and 5), the following objectives were established and are presented step-by-step:

**1.** (**a**) Prepare cationic, stable and monodisperse submicron uni-lamellar phospholipid vesicles and determine/optimize their in vitro characteristics with reproducibility; (**b**) coat the liposomes with alternating self-assembled layers of natural polymers to formulate discrete and well-defined cationic core-shell hybrid particles and (**c**) characterize and optimize the formulated nanoparticles for hydrodynamic size, morphology, surface charge, dispersion homogeneity, stability, drug encapsulation efficiency, drug loading capacity and drug release kinetics with a model protein for initial proof of concept, in vitro (Chapter 6);

**2.** Fulfill Objective **1** for the nanoparticles with a range of rhBMP-7/rhOP-1 concentrations and determine their stability in simulated physiological media, effect on alkaline phosphatase activity and in vitro cytocompatibility (Chapter 7);

**3.** Assess the in vivo biocompatibility and safety of the rhBMP-7/rhOP-1 nanoparticulate delivery system following intramuscular administration. For this purpose, a protocol was developed in young male normal Wistar rats (Chapter 8);

**4.** (**a**) Optimize a previously developed bone lengthening protocol in terms of animal handling, operative procedure, post-operative care and the study timeline and (**b**) evaluate the cellular and molecular changes following the administration of the hybrid delivery system (unloaded compared to loaded with *low* rhBMP-7/rhOP-1 dosages) in the rabbit DO model through radiographical verification, bone densitometry and quantitative computed

tomography, histomorphometry and immunohistochemistry analysis of the regenerate in the distracted gap (Chapter 9);

**5.** Others (*planned and initiated at later stages, in a wild-type mouse DO model*): develop a rhOP-1 dose-response curve and re-evaluate $H_o$ (Objective 4) in a larger sample size and using much lower protein concentrations (Chapter 10).

These objectives were established bearing in mind that developing a *single* delivery system effective for *all* regenerative medicine or drug delivery applications is not *realistically* likely. Rather, physico-chemical characterization and optimization will definitely be necessary to fulfill the criterion relative to each particular therapeutic purpose, nevertheless with feasibility and ease.

## 2.5. Justification

### 2.5.1. Nanoparticulate Drug Delivery Systems (DDSs)

Today, controlled drug delivery technology represents one of the revolutionary areas of science involving a multidisciplinary experimental approach contributory to human health management. Compared to conventional dosage forms, these delivery systems provide improved efficacy (through improved release profiles and drug targeting), reduced toxicity and improved patient compliance and convenience. Macromolecules are often used as drug carriers in these systems. Nanoparticles, first developed around 1970, are defined as particulate dispersions or solid particles with a size in the range of 10-1000 nm (Mohanraj and Chen 2006). They were initially devised as carriers for vaccines and anticancer drugs. Nano- and micro-particles are the dosage forms that have consummated much attention due to their attractive tendency to amass in sites of inflammation (RaviKumar 2000). Compared to microparticles, nanosized delivery systems have demonstrated superiority in terms of longer residencies in general circulation, consequently extending the macromolecule biological activity (Vinogradov et al. 2002). They are dependant on the biomaterials(s) used of which there is an abundance to choose from. In addition, the preparative conditions (such as temperature, aqueous media and pH) involved in the design and formulation of nanoparticulate delivery systems are of crucial importance for the incorporation of biomolecules in order for the structure and bioactivity of the load to be preserved.

### 2.5.2. Polymeric Drug Carriers

Recently, polymeric-based drug carriers have attracted increasing attention and while numerous immobilization techniques have been described, physical entrapment within naturally-occurring polymers remains among the most popular today. That is due to ease and simplicity of preparation, low cost and gentle formulation conditions; guaranteeing elevated preservation of protein viability (Li et al. 2005). Natural polymers offer biocompatibility, biodegradability, hydrophilicity in addition to protection of the encapsulated protein. Alginate and chitosan are introduced below however phospholipid vesicles are described first.

### 2.5.3. Liposomes (Core)

Liposomes were discovered about 50 years ago by A. Bangham and since then they became very versatile tools in biology and medicine. They are the smallest artificial spherically-shaped vesicles with a lipid bi-layer membrane (Figure 2.1) that can be produced through the spontaneous organization of phospholipids and cholesterol in an aqueous medium (Charrois et al. 2003). Since the 1990s, liposomes have been extensively investigated and are considered the most studied drug delivery systems (Chaize et al. 2004), due to their exceptional biocompatibility and appealing ability to carry both hydrophobic and hydrophilic drugs provided that there is a net ionic charge. Cationic (positively-charged) liposomes have been considered to have favorable characteristics in facilitating electrostatic interactions with anionic (negatively-charged) biomolecules and with cellular membranes which are also anionic. Nonetheless, one main challenge remains. Stability in vivo is an obstacle, as liposomes are cleared rapidly from systemic circulation by cellular uptake via the reticulo-endothelial system (RES).

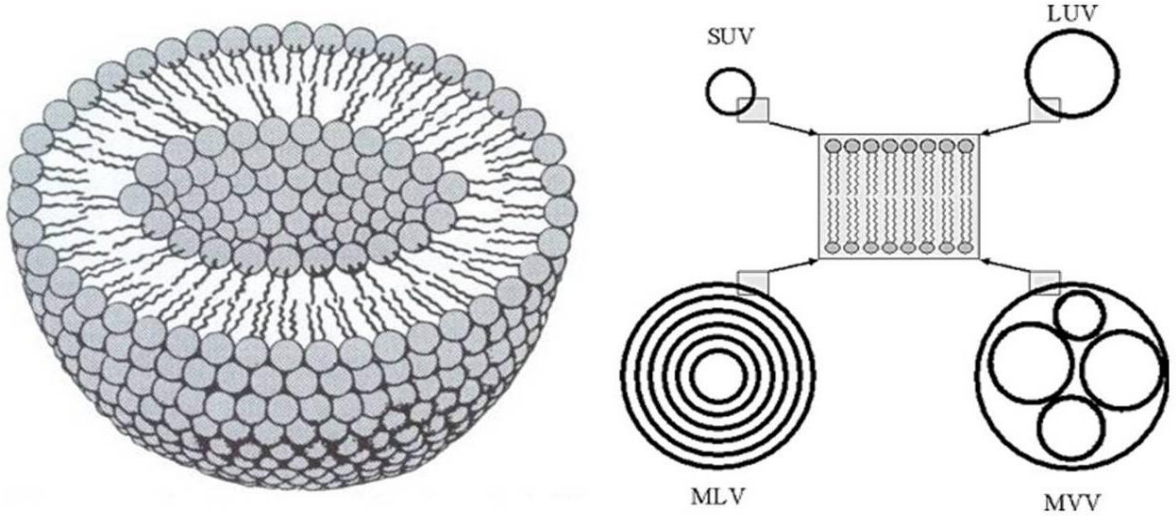


**FIG 2.1.** Liposome structure formed by phospholipids. Schematic shows different formats of liposomes: Small Uni-lamellar Vesicles (SUV); Large Uni-lamellar Vesicles (LUV); Multi-lamellar Vesicles (MLV); and Multi-vesicular Vesicles (MVV).

Attempts to overcome this have been made via (i) liposomal size variation (< 200 nm – nanosized) or (ii) liposomal surface modification by coating it with *one* layer of hydrophilic

polymers (Takeuchi et al. 2000). Stealth® (referring to the expectation that these particles would travel through the bloodstream virtually un-noticed by the immune system thus avoiding adsorption of blood proteins, uptake by the mono-nuclear phagocystic system and clearance by the RES resulting in long circulation life-times) liposomes, is a good example (Charrois et al. 2003). Other limitations are associated with cytotoxicity and aggregation; hence *most* attention in recent years has turned *away* and towards the use of polymeric nanoparticles for drug (protein, gene, etc …) delivery (Mohanraj and Chen 2006).

### 2.5.4. Alginate and Chitosan (Shell)

Alginate and chitosan are examples of hydrophilic polyionic polysaccharides that have been widely investigated and described as the most interesting polymers for use in systems formulated with drug or gene delivery purposes where the inclusion of targeting ligands is feasible (Shu and Zhu 2002; Prabaharan 2008).

**Alginates** (Bregni et al. 2000) are linear un-branched anionic polymers (marine sources, algae) containing β-(1→4)-linked $_{D}$-mannuronic acid and α-(1→4)-linked $_{L}$-guluronic acid residues (Figure 2.2). They are haemocompatible and

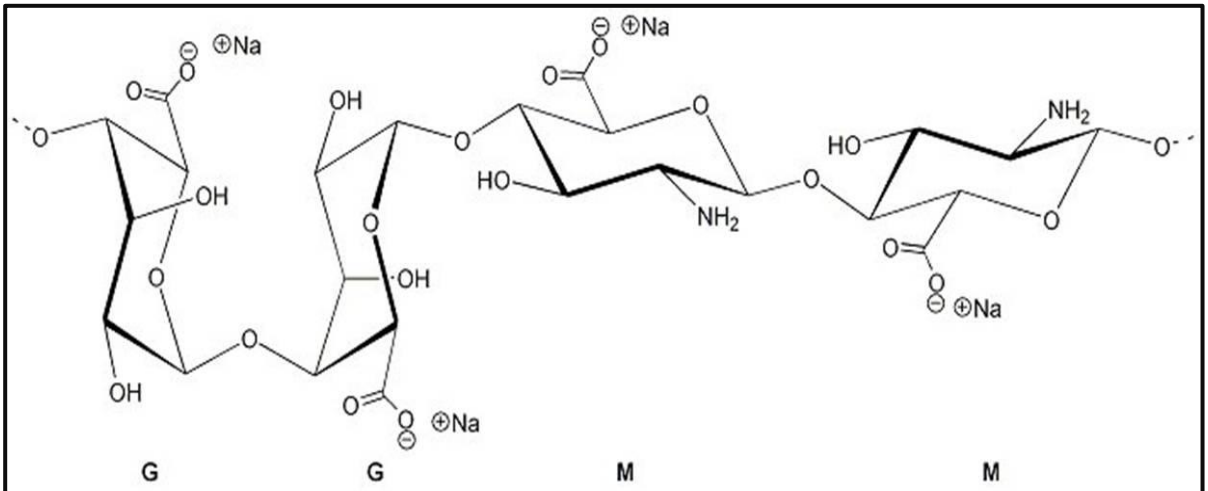

FIG 2.2. Structure of sodium alginate.

have not been found to accumulate in any major organs, thus demonstrating sufficient evidence of biocompatibility and biodegradability, in vitro and in vivo.

**Chitosan** (Vila et al. 2002) is the second most abundant natural polymer. It is a linear cationic polysaccharide (Figure 2.3) with interspersed *D*-glucosamine, and acetyl-*D*-glucosamine units (derived by the *N*-deacetylation of chitin, a biopolymeric product found in the shells of crustaceans). It is a biocompatible, non-toxic, non-immunogenic and biodegradable polymer with bioadhesive, wound healing, antimicrobial as well as *osteogenic* properties; making it favorable for biomedical applications (Prabaharan 2008; Haidar et al. 2009 a, b,c).

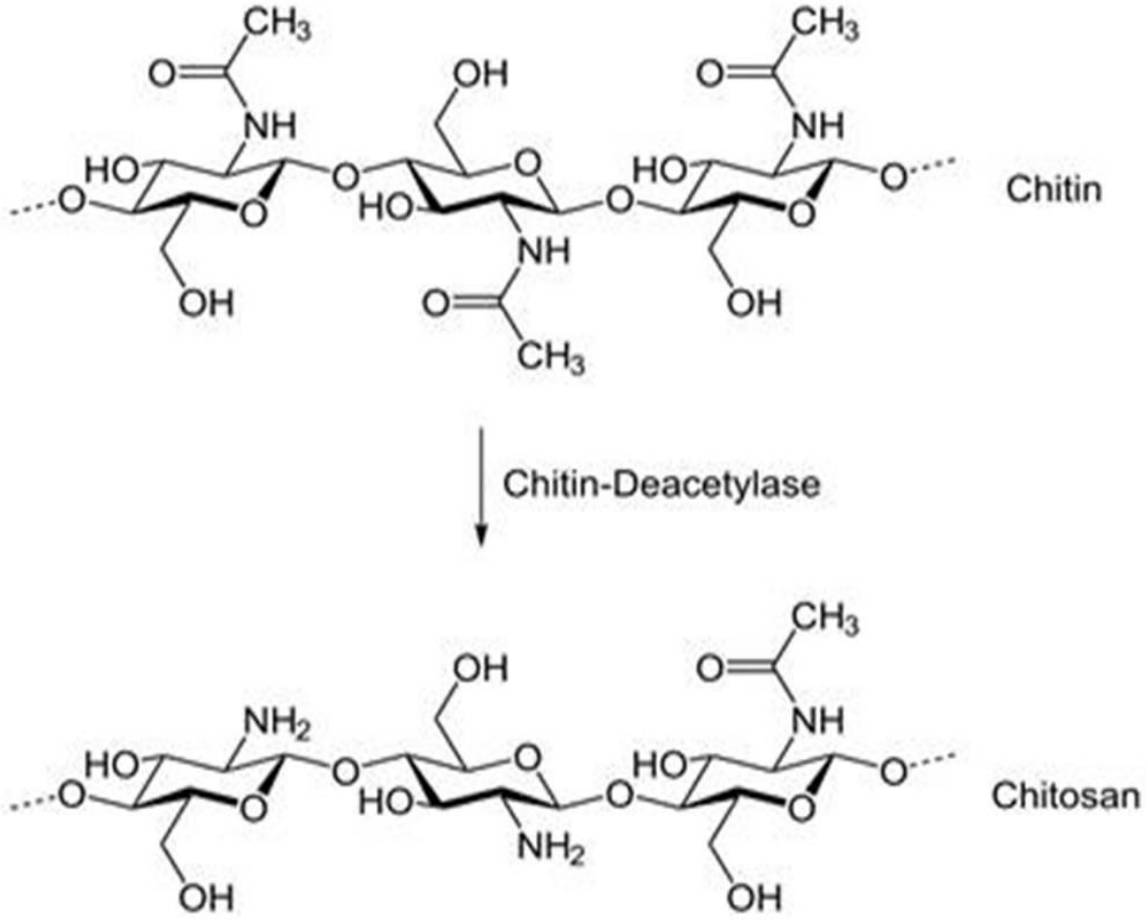


**FIG 2.3.** Structure of chitin and chitosan. The ratio of *D*-glucosamine and *N*-acetyl-*D*-glucosamine units in chitosan is referred to as the ***degree of deacetylation***.

In addition, chitosan have demonstrated exceptional abilities in crossing mucosal barriers, passing through the tight junctions of the intestinal epithelium and binding to and

transversing cellular membranes; showing enhanced and prolonged systemic absorption of the encapsulant (Prabaharan 2008; Haidar et al. 2009 a, b).

Both, alginate and chitosan have been extensively studied for drug delivery in different forms, such as microcapsules (Gaserod et al. 1998), beads (Shu and Zhu 2002) or even wound dressing membranes (Wang et al. 2002) to name a few. **Alginate-chitosan polyionic complexes** form through *ionic gelation* via electrostatic interactions between the *carboxyl* groups of alginate and the *amine* groups of chitosan. For example, hollow capsules of sodium alginate and chitosan were layer-by-layer (l-b-l) engineered for controlled drug release applications (Shenoy et al. 2003) and very much recently, our group (Douglas and Tabrizian 2005) designed and evaluated chitosan and alginate nanoparticles for potential gene therapy applications. Such polyelectrolyte complexes fulfill the requirements for most delivery systems including being biocompatible, biodegradable, bioadhesive (and osteogenic) and non-toxic while protecting and limiting the release of associated biomolecules more effectively than either biopolymer alone (Qiu et al. 2008, Issa et al 2008 a, b). Furthermore, these natural polyelectrolytes, being extensively used in our laboratory for many years and in an array of applications are consequently well-characterized, chemically and enzymatically.

### 2.5.5. BMP-7/OP-1: the Drug / Protein of Choice (in Long Bone DO)

Over 15 distinct BMPs have been isolated so far and BMP-2, -4, -6 and -7 (and -9) have been reported to have osteoinductive potentials (Abe 2006). The exogenous application of BMPs, specifically BMP-2 and BMP-7/OP-1 has been shown to accelerate bone formation in numerous clinical and pre-clinical reports (Ripamonti et al. 2000; Einhorn 2003; Termaat et al. 2005) with no significant differences between them (when used alone). In a rat model of DO, OP-1 application immediately after surgery accelerated bone formation (Mizumoto et al. 2003). In contrast, our own experiments in rabbits showed that OP-1 injected at the *end* of the distraction period did not have a marked effect on bone consolidation (Hamdy et al. 2003). Subsequent studies revealed that this lack of effectiveness could be due to that only **very low amounts of OP-1 receptor proteins were present** at that time (Hamdy et al. 2003). Consequently it was projected that better results could be obtained when OP-1 was

injected into the distraction gap **early** during the distraction phase, when OP-1 receptors are abundantly expressed. Indeed, we found that injecting OP-1 in a rabbit model of distraction osteogenesis accelerated bone consolidation (Mandu-Hrit et al. 2006). However, in order to be effective, **large dosages of exogenous BMPs** have to be administered. As mentioned earlier, such supra-physiological dosages may have many short- and long-term drawbacks including the unknown effect on the growth plate in the skeletally immature patient, developing embryos, possibility of formation of antibodies and developing malignancies, and the associated huge cost of the proteins (Rengachary 2007). Furthermore, proteins generally experience short half-lives in the order of minutes or hours (< 12 hrs) due to enzymatic degradation, evisceration through the RES and immunological inactivation once applied in vivo. Hence, we then hypothesized that developing a way to intrinsically stimulate BMP expression with lower, safer and cost-effective bioactive dosages may be an attractive alternative mode of treatment (Haque et al. 2005; Mandu-Hrit et al. 2006; Haidar et al. 2008 b; Haidar et al. 2009 a, c).

### 2.5.6. Core-Shell Hybrid Nanoparticulate rhOP-1 DS for Tibial DO

Combining the advantages of liposomes and natural polymers with those of core-shell nanosized particles and hydrogels (formed by spontaneous ionic gelation), a novel injectable drug delivery system that entraps the water-soluble and readily diffusible positively-charged OP-1 molecules within a core composed of cationic uni-lamellar liposomes and a surrounding shell composed of alternating and self-assembled matrices of negatively-charged alginate and positively-charged chitosan polymers formulated using the l-b-l technology (Quinn and Caruso 2004) was developed as is displayed in Figure 2.4. The l-b-l self-assembly allows for evaluating the step-by-step build-up and monitoring any changes with each deposited layer. Also, preparation of the involved biomaterials in mild conditions suitable for fragile biomolecules with short half-lives is feasible. This idea of drug entrapment within the layers of the liposomal core and the coatings of the polymeric shell should allow efficient loading capacity (in the several compartments including the aqueous core, the lipid bi-layer and the polyelectrolyte film), stability and more importantly, a reduced and possibly controlled (by controlling the number of layers) release of OP-1 to the

site of interest. The system was evaluated in long bone DO; yet, it might be appropriate for craniofacial indications, as well as other applications; cardiovascular perhaps.

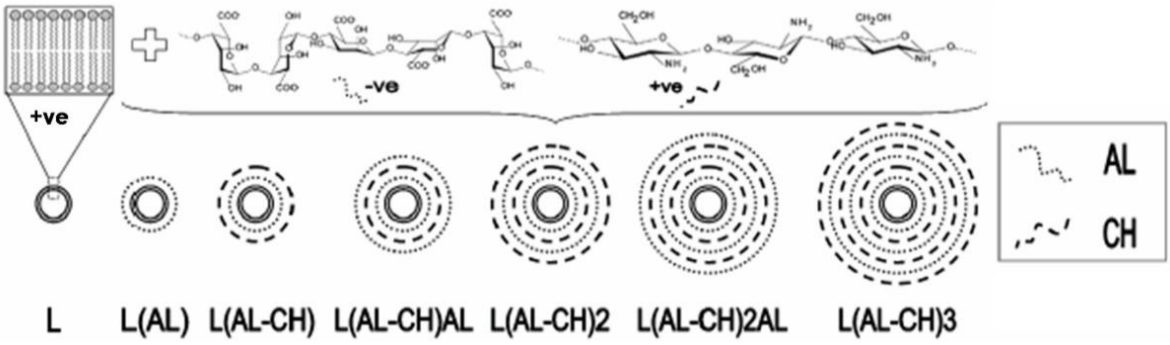


**FIG 2.4.** Schematic presentation of the layer-by-layer (LbL or l-b-l) self-assembly of Alginate (**AL**) and Chitosan (**CH**) on LUVs or Liposomes (**L**) with up to six layers shown. rhOP-1 would be encapsulated within the core, the shell and the surrounding surface of the nanoparticles (NPs).

## 2.6. Summary of Original Contributions

This dissertation contains mainly two published in vitro manuscripts, two published review articles, an accepted in vivo manuscript (in press) and another in vivo manuscript currently under peer review. In addition, parts from three incomplete manuscripts (a review and two in vivo studies) undergoing writing have been included. Chronologically, the first publication (Chapter 6) was printed in the peer-reviewed *Biomaterials*. It presents the formulation and characterization of novel core-shell nanoparticles through the study of parameters such as average size, surface charge, physical stability, microscopic morphology as well as the encapsulation efficiency, loading capacity and release kinetics of a model protein, bovine serum albumin. The second publication (Chapter 7) was printed in the peer-reviewed *Journal of Biomedical Materials Research Part A*. It first presents the in vitro cytocompatibility of the nanoparticles assayed with mouse preosteoblast cells and the cell viability determined by colorimetry. Then the release profiles of a range of OP-1 concentrations were obtained and the release kinetics identified. Finally, the alkaline phosphatase activity of preosteoblasts was evaluated using a micro-BCA assay. The third and fourth publications (Chapters 3 and 4, respectively) were invited review articles accepted in the peer-reviewed *Biotechnology Letters* and are available online, titled: Recombinant BMP Delivery for Bone Regeneration and Repair and divided into 2 parts; *A*: Current Challenges in BMP Delivery and *B*: Delivery Systems for BMPs in Orthopaedic and Craniofacial Tissue Engineering. Those works focused on the related literature published mainly between the years 2000 and 2009. The fifth manuscript (Chapter 9), accepted very much recently (August 2009) in the peer-reviewed *Growth Factors*, presents the evaluation of the nanoparticulate rhOP-1 delivery system in a rabbit model of long bone distraction osteogenesis (DO). The sixth manuscript (Chapter 8), submitted (August 2009) to the peer-reviewed *Biomaterials*, presents the biocompatibility and safety of the unloaded and OP-1 loaded nanoparticles injected intramuscularly in rats. All of these 6 manuscripts have been included in this thesis in full and as submitted for publication. The seventh manuscript (Chapter 5) is a review article updating knowledge on the attempts for accelerating distraction osteogenesis, emphasizing on the role of protein therapy and BMPs. Upon completion, it will be submitted to the *Journal of Orthopaedic Surgery and Research*. Here in, only a shortened portion presenting

an overview on the procedure, principles, applications and limitations of distraction osteogenesis was included. The remaining 2 manuscripts were not entirely incorporated in this thesis (Chapter 10) as well and include: an eighth manuscript presenting the first study on developing a rhOP-1 dose-response curve in a mouse long bone DO model and a ninth manuscript evaluating the OP-1 loaded nanoparticles in the same model. Final results are pending. Upon completion, these manuscripts will be submitted for peer-review in *Bone*, shortly.

# CHAPTER 3
# rhBMP Therapy – Current Challenges in BMP Delivery

Bone Morphogenetic Proteins (BMPs) form a unique group of proteins within the Transforming Growth Factor (TGF-β) superfamily with pivotal roles in the regulation of bone induction, maintenance and repair as highlighted in Section I of this thesis (Chapter 1.1.2). The application of BMP-2 and BMP-7 with embryonic rat calvarial cells, rat osteosarcoma cells and/or mouse fibroblasts resulted in enhanced osteoblastic differentiation and elevated expression of bone mineralization proteins. The stimulation of new bone formation and healing of different bone fractures including critical-sized defects and long bone non-unions (which do not heal spontaneously) following the application of BMP-2 or BMP-7 was also demonstrated in models ranging from rodents to rabbits to dogs to sheep to non-human primates. Consequently, these pre-clinical studies have validated their safety and efficacy in promoting bone regeneration and repair. However, results from the three major randomized clinical trials in humans (BMP-2 in open tibial fractures and spinal fusion and BMP-7 in long bone non-unions) have shown significant discrepancy. A literature review was initially carried out to identify the state-of-art and current limitations in bone tissue engineering and regenerative medicine focusing on the pre-clinical and clinical application of protein or BMP-therapy. This work was *motivated* primarily by the problems related to the delivery aspect(s) of BMP-therapy. Hence, the research discrepancies and slower response in humans that may be attributed to the presence of a smaller population of multipotent cells less responsive than in smaller animals or to the complex signaling pathways of the BMPs themselves and their antagonists were not the central focus here in. In this chapter, the promises and problems of rhBMP therapy are discussed in the context of findings from in vitro, pre-clinical and clinical studies; thus emphasizing the rationale behind the **current need for developing novel carrier systems to deliver bioactive BMPs** to sites of bone regeneration and repair. The universal characteristics necessary for an *ideal* carrier are identified. Bone healing by recombinant BMPs will predominantly depend on the parameters of a *combined* localized and release-controlled delivery system including: protein release kinetics and retention, protein dose/concentration, mechanism(s) of release and

nature of the vehicle used. Such key factors hindering the development of a safe and stable rhBMP delivery system appropriate for use in humans with dependable success and reproducibility in different defect sites and sizes are examined next.

This work has been in published in Biotechnology Letters and is reprinted with permission; DOI 10.1007/s10529-009-0099-x; Wednesday August 19th 2009; ISSN 0141-5492 (Print); ISSN 1573-6776 (Online) 

Manuscript submitted to *Biotechnol. Letters* (June 8th 09) and published online (Aug 19th 09).

# Review: Delivery of Recombinant Bone Morphogenetic Proteins for Bone Regeneration and Repair

## Part A: Current Challenges in BMP Delivery

**Ziyad S. Haidar[a-d], Reggie C. Hamdy[b, d], Maryam Tabrizian[a-c]**

[a] *Faculty of Dentistry, McGill University, Montréal (QC) Canada*
[b] *Center for Biorecognition and Biosensors, McGill University, Montréal (QC) Canada*
[c] *Department of Biomedical Engineering, Faculty of Medicine, McGill University, Montréal (QC) Canada*
[d] *Shriners Hospital for Children and Division of Orthopaedics, McGill University, Montréal (QC) Canada*

## 3.1. ABSTRACT

Recombinant human bone morphogenetic proteins (rhBMPs) have been extensively investigated for developing therapeutic strategies aimed at the restoration and treatment of orthopaedic as well as craniofacial conditions. In this first part of the review, we discuss the rationale for the necessary use of carrier systems to deliver rhBMP-2 and rhBMP-7 to sites of bone tissue regeneration and repair. General requirements for growth factor delivery systems emphasizing the distinction between localized and release-controlled delivery strategies are presented highlighting the current limitations in the development of an effective rhBMP-specific delivery system applicable in clinical bone tissue engineering.

**Keywords:** *Bone morphogenetic proteins; bone regeneration; bone repair; delivery systems; controlled-release; growth factors; orthopaedics; craniofacial surgery*

## 3.2. Introduction: rhBMPs in Bone Regeneration & Repair

Healing of bone fractures and reconstruction of critical-sized bone defects continue to present a significant challenge for orthopedists, traumatologists and maxillofacial surgeons. To address this need, the United Nations and the World Health Organization declared the years 2000-2010 as the Bone and Joint Decade (Weinstein 2000). Although autologous bone grafts are routinely used, limited graft accessibility and donor site morbidity as well as increased costs continue to drive the development of alternative methods for bone regeneration and repair (Geiger et al. 2003; Bishop and Einhorn 2007). Thus far, three new strategies (Rose et al. 2004) are currently undergoing vigorous investigation: the transduction of genes encoding cytokines with osteogenic capacity into cells at repair sites (gene therapy); the transplantation of cultured osteogenic cells derived from host bone marrow (stem cell therapy) and the application of osteoinductive growth factors (protein therapy), as shown below in Figure 3.1.

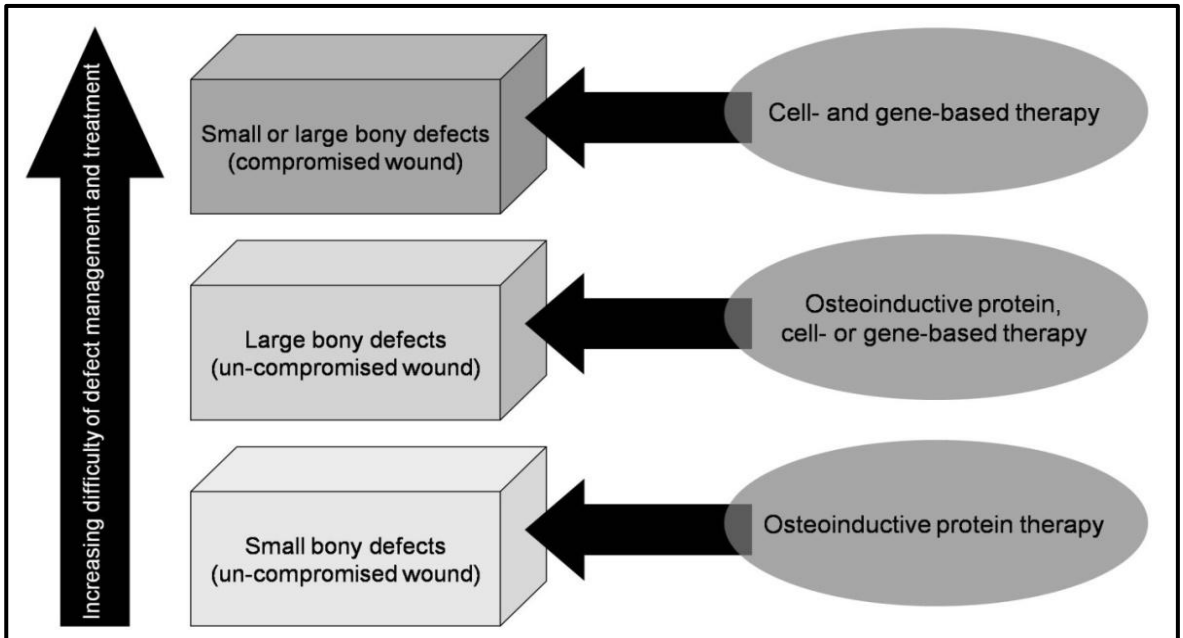


**FIG 3.1.** Tissue engineering therapeutic approaches and combinations according to defect complexity and difficulty. Adopted from Nussenbaum and Krebsbach 2006.

Gene- and stem cell-based therapy will probably represent the next major advance however presently are still in their infancy regarding safety and efficacy in humans (Kimelman et al. 2007). Protein therapy, on the other hand, has demonstrated the most practical promise,

mainly incorporating osteoinductive morphogens such as bone morphogenetic proteins (BMPs) even so with some limitations. BMPs are among the most potent cytokines in tissues and organs even beyond bone (Reddi 2005). The role of BMPs in bone development and repair has been extensively reviewed by numerous authors (Termaat et al. 2005; Bessa et al. 2008a). BMP-2, -4, -7 and -9 may be the most potent osteoblastic differentiation inducers of mesenchymal progenitor cells into osteoblasts. For example, BMP-7, also known as osteogenic protein-1 or OP-1 has been shown to enhance the formation of new bone in numerous preclinical (Ripamonti et al. 2000; Hamdy et al. 2003) and clinical studies (Friedlaender et al. 2001; Vaccaro et al. 2008). BMPs are known to act locally; yet, the exact cellular and molecular mechanisms are not fully understood (Gautschi et al. 2007). Small amounts induce cellular responses in vitro, however, when administered in vivo, rapid degradation and consequently insufficient and improper tissue regeneration occurred (Engstrand et al. 2008). It was suggested that the clinical efficacy of recombinant human (rh) forms of BMPs will depend on the carrier system used to ensure an effective delivery of adequate protein concentrations to the desired site (Mont et al. 2004). Thus far, several materials for the delivery of rhBMP-2 and rhOP-1 have been developed however with restricted clinical use (Termaat et al. 2005). This review aims at addressing the current challenges in BMP delivery strategies emphasizing the differences between *'localized'* and *'release-controlled'* systems commonly and mistakenly used interchangeably in an attempt to further understand the requirements for an effective protein therapy in clinical bone tissue engineering (where the 'carriers' such as collagen-based if can be considered localized given their application by implantation in defect sites, they are not release-controlled).

## 3.3. Challenges in rhBMP Delivery

For osteoregeneration to yield proper healing, mechanical stability in the defect site, osteogenic cells and osteoinductive growth factors in combination with a suitable carrier or delivery system, conceptualized as the "Diamond Concept" (Giannoudis et al. 2007) are necessary. The main role of the delivery system consequently is to retain the growth factor at the defect site for the bone regeneration and repair pertinent duration of time according to defect anatomical site, size and vascularity in order to allow the regenerative tissue forming

cells to migrate to the defect area, proliferate and differentiate (Issa et al. 2008 a, b, c). BMPs are soluble and if delivered in a buffer solution, their clearance is rapid. Less than 5% of the BMP dose remains at the application site whereas combinations of the proteins with gelatin foam or collagen showed increased retention ranging from 15% to 55% (Hollinger et al. 1998). The use of biomaterials that can retain and sequester BMPs at the site of interest have been shown to greatly enhance efficacy and reduce protein dose by localizing the morphogenetic stimulus (Chen and Mooney 2003). Hence, the pharmacokinetics of rhBMP therefore can be influenced by the carrier used. Moreover, other challenges are related to individual proteins - regulation of effects and dose-response ratio. BMPs are currently being used in supra-physiologic concentrations and expensive dosages in the milligram range for satisfactory bone healing (Luginbuehl et al. 2004). The resulting tissue effects are occasionally overwhelming when viewed from a clinical point of view. Soft tissue edema, erythema, local inflammation, heterotopic ossification and immune response are the most remarkable although rarely reported. Osteoclastic activation has been noted in some cases as well where applied in large doses; bone resorption occurred (Gautschi et al. 2007). Additionally, currently used rhBMP-2 and rhBMP-7 are produced lacking a heparin-binding domain, hence probably reducing their clinical bioactivity (Saito et al. 2008). Recently, the osteoinductive effects of rhBMP-2 in combination with a complex of heparin and chitosan in a gel formulation were shown to be superior when compared to rhBMP-2 implanted with type-I collagen in a rat model (Engstrand et al. 2008). Chemically-modified BMPs with enhanced affinity to their carriers showing altered stability, solubility, surface binding, bioactivity and biospecificity have been reported (Gautschi et al. 2007). Therefore, despite the ample evidence of the benefit of BMPs in bone regeneration and repair from preclinical and clinical studies, conclusive knowledge about BMP dosage, time-course, release dynamics and carriers remains to be determined. It is unclear why the impressive and convincing results seen in vitro and in animal models are difficult to reproduce in humans (Einhorn 2003). Unfavorable release kinetics, insufficient mechanical stability and porosity to allow cell and blood vessel infiltration into the carrier and inflammatory tissue reactions are few reasons. The effects of BMPs must therefore be *localized* as well as *regulated*. BMP delivery will also depend on the anatomic location where the treatment is required, the

vitality of the soft tissue envelope and the mechanical strain environment provided by the surgical procedure (Einhorn 2003).

## 3.4. Delivery Systems Parameters & Requirements

Delivery systems should have the ability to provoke optimal inflammatory responses, be biocompatible and are often required to be bioresorbable. Processing conditions need to prevent protein aggregation or denaturation. Also, they have to be easily and cost-effectively manufactured for large-scale production. Appropriate storage, stability, handling and sterilization conditions are favored as well. Finally, all these processes need to be approved by regulatory agencies for the desired indication and application (Rose et

**TABLE 3.1. GENERAL REQUIREMENTS FOR BMP DELIVERY SYSTEMS**

- Biocompatibility
- Predictable biodegradability
- Low immunogenicity and antigenicity
- Enhancement of cellular vascularization and attachment
- Affinity to BMPs and bone (defect)
- Maintenance and enhancement of BMP bioactivity
- Controlled and metered/tailored protein release at an effective dose for the appropriate period of time according to defect anatomical site, size and vascularity
- Malleability and ease of manufacture
- Safety, stability, sterility, availability and cost-effectiveness
- Regulatory agencies approval for the desired clinical indication and application

Adopted and updated from Geiger et al. 2003.

al. 2004; Seeherman and Wozney 2005). It has become clear that there is probably not one single desirable pharmacokinetic profile that is predictive of success (Geiger et al. 2003) where various carrier and delivery materials have been examined in vitro, in vivo as well as in humans. These include demineralized collagenous bone matrix, collagen products, gelatin hydrogels, natural polymers and combinations of these materials and others (Lee and Shin 2007; Haidar et al. 2008 a, b). Table 3.1 summarizes the desirable qualities of an ideal bone

morphogenetic protein delivery system or carrier. Clearly, there is no ideal carrier or delivery system for all growth factors, pathologies, indications or clinical applications. Immediately after administration or implantation, BMPs are subject to the presence of fluid, protein competition, enzymatic activity, temperature, pH influence and salt concentrations (Dard et al. 2000). Each of these factors could lead to the release of a totally denatured growth factor in an uncontrolled manner and thus appends to the limited success of clinical BMP therapies. It is important thereby to emphasize that the enhancement of bone healing by BMPs is predominantly dependant on the parameters of a *combined* localized and release-controlled carrier/delivery system including: protein release kinetics and retention, protein dose size/ concentration, mechanism of release and nature of the vehicle used in terms of biomaterial(s) and design/geometry.

### 3.4.1. Release Kinetics & Retention at Defect Site

In physiologic bone repair some growth factors such as BMP-2 are predominantly expressed during the early inflammatory phase. Others are up-regulated during the chondrogenic and osteogenic phases and have a biphasic expression pattern or are constitutively present. Furthermore, the cell pool present in the defect zone is dynamic by nature and different stimuli can attract different cell types to invade the compromised area (Cho and Nuttall 2002). Therefore, the impact of localized release kinetics for the therapeutic enhancement of skeletal repair becomes evident. Furthermore, recent evidence has suggested that cementogenesis and osteogenesis occur at different rates during BMP-stimulated regeneration (Issa et al. 2008 a, b, c). However, very few have investigated the influence of release kinetics on bone regeneration. The effect of BMP-2 release from slow and fast degrading gelatin carriers was not significantly different in a rat model of periodontal defects (Talwar et al. 2001). Higher retention times for BMP-2 were more osteoinductive in a rat ectopic assay (Uludag et al. 2001) and the prolonged delivery of BMP-2 enhanced the in vivo osteogenic efficacy of the protein compared to short-term delivery at equivalent dosage in another recent study (Jeon et al. 2008). Furthermore, retention of BMPs depends on whether the protein is immobilized within the carrier, adsorbed onto the surface or covalently-bonded during its formulation (Luginbuehl et al. 2004). Release should preferably

be sustained over time (Haidar et al. 2008 a, b). In designing a delivery system for differentiation factor release, it is apparent that the extremes of release (bolus injections or prolonged low level release) are not beneficial to bone induction (Geiger et al. 2003). While timing of the protein release is important, the dynamic nature of the healing zone makes it difficult to assess the state of the defect. It is certainly dependant on the type of defect, its location and appearance, the patient's age, gender, hormone and nutritional status, illness and other parameters (Li and Wozney 2001). Other factors (Kirker-Head 2000) influencing release rates include protein size and conformational changes, solubility, polymer/scaffold composition/geometry and molecular weight. Also, different animal species, ages and sizes may have varying optimum release profiles.

### 3.4.2. Dose & Concentration

Maintaining a critical threshold concentration of the rhBMP at the defect site for the necessary period of time (temporal distribution) is crucial. Such supra-physiological dosages range from 0.01 mg/ml in small animal models such as rats to 0.4 mg/ml in rabbits to more than 1.5 mg/ml in non-human primates. Different anatomical sites require different therapeutic doses depending on the degree of vascularization, defect size and the number of resident responding cells. Ranges vary from fusion site to fusion site as well. In humans, for anterior inter-body fusion a total dose of 4.2–12 mg of rhBMP-2 at a concentration of 1.5mg/ml is recommended. For inter transverse arthrodesis, the suggested dose of rhBMP-2 (based on pilot clinical trials) is 20 mg on each side at a concentration of 2.0 mg/ml delivered in a 60% hydroxyapatite and 40% tricalcium phosphate (granules) carrier (Boden et al. 2002). The recommended dose of rhBMP-7 for recalcitrant long bone non-unions is 7mg or 2 vials (each containing 3.5 mg reconstituted with 1 g of type I bovine collagen) and implanted at the non-union site. New delivery systems with optimized and controlled release profiles may decrease or even alleviate the need for excessive and expensive concentrations of BMPs. Our own work with rhBMP-7 encapsulated in a core-shell nanoparticulate delivery system showed that a dose as low as 100 ng/ml was significantly sufficient to enhance preosteoblast differentiation noted by an increased alkaline phosphatase activity over 7 days, *in vitro* (Haidar et al. 2008 a, b). The formation of ectopic bone is also a potential concern

that is substantially under-investigated. Paramore et al. implanted BMP-7 into the epidural space of dogs after laminectomy and posterolateral fusion. Animals demonstrated bone formation adjacent to their spinal cords causing mild spinal cord compression (Paramore et al. 1999). Novel carriers need to contain the BMP, prevent ectopic and heterotopic bone formation and utilize lower, safe and cost-effective dosages.

### 3.4.3. Mechanisms of Localized & Release-controlled BMP Delivery

Growth factors release from a localized and release-controlled delivery system can either be (i) diffusion-controlled, (ii) chemical and/or enzymatic reaction-controlled, (iii) solvent-controlled, or (iv) controlled by combinations of these mechanisms (Luginbuehl et al. 2004; Haidar et al. 2008 a, b).

Diffusion-controlled release is governed by the solubility and diffusion coefficient of the protein in the aqueous medium, protein partitioning between the aqueous medium and material of the delivery system, the protein loading and the diffusional distance (Li and Wozney 2001). An example of diffusion-controlled release is BMP-2 release from porous scaffolds that was regulated via adjustment of pore size (Whang et al. 2000). In our own studies, TGF-β1 release from coral particles was modulated through modification of adsorption conditions and particle size (Demers et al. 2002). BMP-7 release from core-shell nanoparticles was controlled via the layer-by-layer build-up of natural polymers on liposomes (Haidar et al. 2008 a, b) as displayed in Figure 3.2.

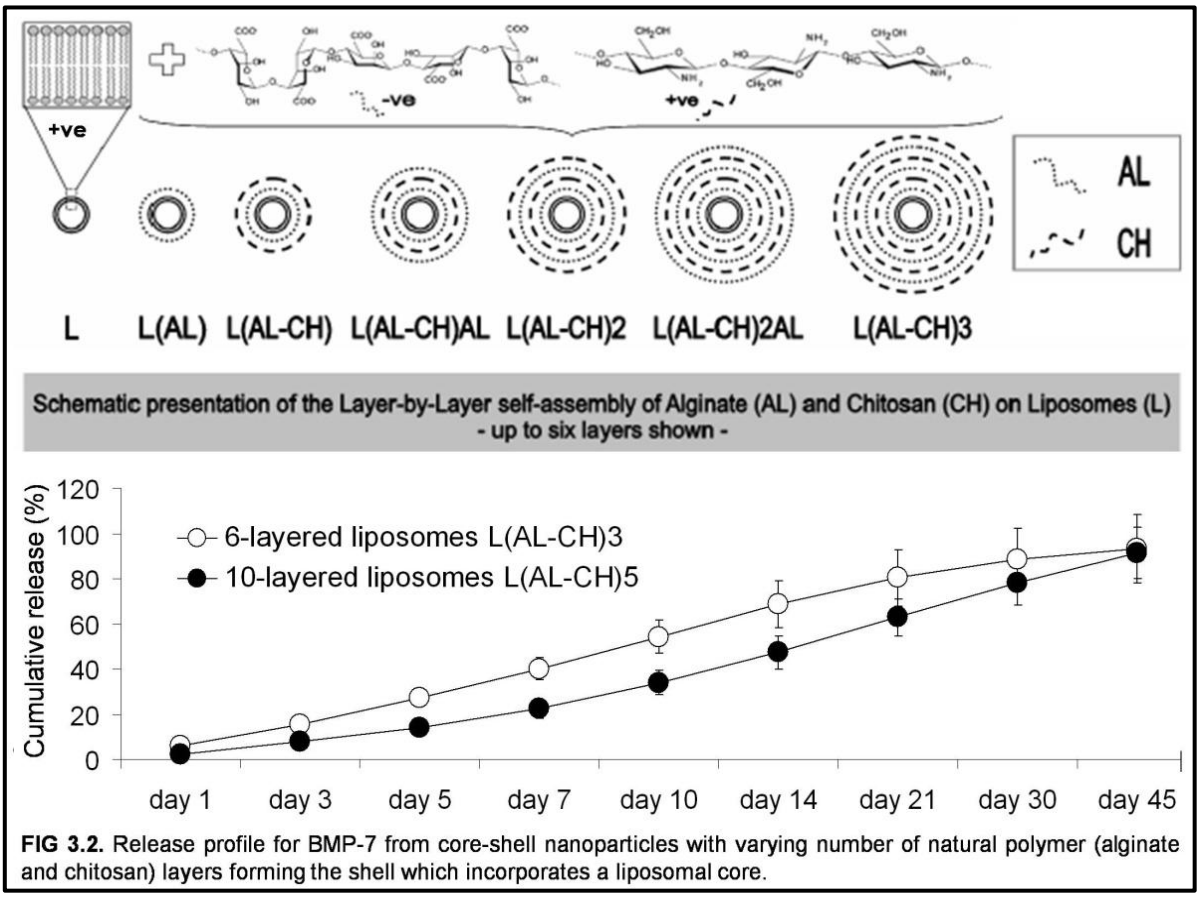


**FIG 3.2.** Release profile for BMP-7 from core-shell nanoparticles with varying number of natural polymer (alginate and chitosan) layers forming the shell which incorporates a liposomal core.

The combination of the polymeric electrostatic-based assembly technique and nanoscaled liposomes yielded a stable and non-toxic delivery system consisting of a suspension of monodisperse nanoparticles suitable for the potential administration of growth factors via a parental injection as is preferable by surgeons. The nanoparticles tolerate extended shelf storage and allow for protein loading immediately preceding administration, preventing degradation or loss of the encapsulant. Controlled linear and multistep release of bioactive BMP-7 over an extended period of 45 days was evident. The increase in shell thickness slowed the rate of protein release where BMP-7 release from uncoated liposomes was clearly faster than from coated liposomes. BMP-7 release from this physically dispersed polymeric system may be described by several possible mechanisms: diffusion, polymer degradation, ion complexation, and interactions among the protein and the polymers, although it is primarily governed by a diffusion-based or affinity-based mechanism.

Chemical and/or enzymatic reaction-controlled systems include erodible systems, where the protein is physically immobilized in the carrier matrix and released by degradation or dissolution of the carrier, or systems, where the protein is chemically bound to the polymer backbone and released upon hydrolytic or enzymatic cleavage of the bond. TGF-β1 release from cross-linked collagen sponges depended on the extent of cross-linking, as observed post-subcutaneous implantation into skull defects in rabbits (Ueda et al. 2002), for example. In solvent- or swelling-controlled systems, the protein is embedded in a carrier matrix and diffusional release occurs as a consequence of the rate-controlled penetration of solvent (water) into the system. Hence, to mimic the space- and time-restricted physiologic pattern of growth factor kinetics by the release kinetics of a vehicle, different strategies of controlling growth factor delivery are available (Luginbuehl et al. 2004).

### 3.4.4. Injectable & Multiple Growth Factor Delivery

Injectable delivery systems are gaining much interest as they could provide a less invasive method for the regeneration and repair of osseous defects with clinical indications including fresh fractures, non-union or delayed union, large bone defects associated with osseous tumor resection as well as the acceleration of periodontal therapy hence avoiding extensive/secondary surgery (Einhorn et al. 2003; Bishop and Einhorn 2007).

A single, local, percutaneous injection of 80 ug rhBMP-2 in 25 uL buffer vehicle was shown to accelerate healing in femoral fracture rat model (Einhorn et al. 2003). Our group demonstrated earlier that a single bolus injection of rhBMP-7 (75 ug in acetate buffer) accelerated bone formation during long bone distraction osteogenesis in rabbits (Hamdy et al. 2003; Mandu-Hrit et al. 2006). Furthermore, preliminary results from our most recent in vivo assays in the same model have demonstrated that osteogenesis and consolidation were accelerated via a single localized injection of the core-shell delivery system loaded with a dose of no more than 1.0 ug rhBMP-7 (Haidar et al. 2009 c) accentuating the role of local and release-controlled nanoparticles. Also, we have demonstrated how the injected unloaded delivery system did not interfere with the osteoregenerative process mainly due to its biocompatible and biodegradable nature. Moreover, the natural polymers used to formulate the nanoparticles especially chitosan has been shown to promote osteogenesis and enhance

the bioactivity of the encapsulated protein via controlling the release profile (Prabaharan 2008). The use of this novel cost-effective delivery system has the potential to shorten the treatment period of long bone distraction osteogenesis and thus could diminish the morbidity and improve the functional outcome in patients via the earlier removal of the external fixator.

Injectable scaffolds for bone tissue engineering are consisted of a mixture of bioactive molecules and solidifiable precursors which are injected into the defect site to form a 3-D structure in situ (Hou et al. 2004). Hosseinkhani et al. fabricated injectable transparent 3-D networks (hydrogel) of self-assembled peptide-amphiphile and BMP-2 and showed significant homogenous ectopic bone formation in the back subcutis of rats (Hosseinkhani et al. 2007).

Since growth factors act in a coordinated cascade of events to restore bone, delivering combinations of growth factors may have a great potential. However, the choice of growth factor combinations has to be with great care. The sequential release of BMP-2 in combination with IGF-1 has already been explored by Raiche and Puleo, nevertheless with commercialization-related difficulties (Raiche and Puleo 2004; Westerhuis et al. 2005). In another example, rhBMP-2 and bFGF absorbed to a collagen sponge resulted in decreased bone formation in a rabbit model of tibial fracture (Vonau et al. 2001).

In conclusion, the delivery of the appropriate biologically-active growth factor(s) at the proper dose and concentration for the intended application using a biocompatible, biodegradable and bioresorbable delivery vehicle that will stabilize and prevent the rapid diffusion or dispersal of the encapsulant and promote localized osteogenesis at the defect site is essential.

## 3.5. Future Prospects

Bone regeneration and repair with BMPs are leading a new era in orthopaedic and craniofacial reconstruction. Their ability to substantially enhance bone formation and facilitate healing will likely be optimized by the simultaneous use with other growth and

differentiation factors and/or with an expanded responsive cell population. The challenge for researchers today remains to deliver these osteoinductive factors in ways that would ensure consistent clinical success in humans. Currently, delivery of BMPs is still attempted through the direct local application of rhBMP to the regeneration or repair site with (primarily with the use of collagen carriers) or without a release-controlled carrier. Future studies will need to focus on the development of customizable, localized and release-controlled delivery materials and systems with the surgical practicality (mainly injectable) and adjustable growth factor(s) release profiles, according to defect site, size and vascularity. Intelligent delivery systems would provide BMPs and other growth factors in response to physiological requirements, having the capacity to sense changes of the bone defect's microenvironment and accordingly, alter protein release. Such systems may represent a step towards individualizing protein release kinetics. Given the complex nature of osseoregeneration, it is possible that multiple growth factor delivery exhibiting both stimulatory and inhibitory responses (for noggin, for instance) on bone formation with different release characteristics be the most desirable approach clinically, with caution to the choice of combinations. Other issues such as biosafety, cost-effectiveness, user-friendliness and optimum delivery time need to be addressed as well. Advances in biotechnology and biomaterials will certainly expand the number of tissue-engineering approaches with the use of BMPs assuring a promising future beyond the present Bone and Joint decade for millions of patients worldwide.

## 3.6. Acknowledgments

The authors wish to thank grants from the Shriners of North America, Fonds de la Recherche en Santé du Québec, the National Science and Engineering Research Council, the Canadian Institutes of Health Research (CIHR) - Regenerative Medicine/Nanomedicine and the Center for Biorecognition and Biosensors (CBB), McGill University, Montréal, Québec, Canada. Dr. Haidar acknowledges scholarships from the Center for Bone and Periodontal Diseases Research and the Shriners Hospital, Montréal, Québec, Canada.

# CHAPTER 4
# rhBMP Therapy – BMP Delivery Systems

The main role of a delivery system is to retain the bioactive growth factor(s) at the site of interest for a prolonged time frame, providing an initial support to which cells attach and form regenerated tissue. The type of tissue is of vital importance, as different mechanical requirements apply for the repair of bone, cartilage or tendon. For the highly vascularized nature of bone, a delivery system should permit or even enhance vascular ingrowth, for instance. Several **materials for the delivery of BMPs** have been investigated and developed in recent years with only some collagen-based formulations (mostly absorbable collagen sponges) for rhBMP-2 and rhBMP-7/rhOP-1 obtaining regulatory approval for their *restricted* clinical use in humans. Furthermore, those carriers, devices or products are not considered delivery systems (mainly injectable in the context of this thesis) as they are simply graft materials requiring implantation and surgical site preparation similar to conventional bone grafting procedures.

The recent advances in biomaterial science have certainly boosted the number of tissue-engineering approaches and strategies available for bone healing with the use of several BMPs. The major categories of carrier biomaterials include: natural polymers such as collagen, alginates and chitosan; inorganic materials such as hydroxyapatite; synthetic polymers such as poly(lactic acid) and poly D,L-lactide-co-gycolic acid (PLGA); in addition to composites or material combinations used to optimize the benefits and get through the shortcomings of the other classes of biomaterials. Therefore, the literature is extensive and the number of publications is constantly multiplying with the development of new materials and composites.

Those are spread over a very broad range of potential applications and intentions of use. In this chapter representing the second part of the background review, the advantages and disadvantages of some of these delivery materials are highlighted.

An examination of a representative selection of pre-clinical and clinical (orthopaedic and craniofacial) studies incorporating rhBMP-2 and rhBMP-7 delivery systems is presented to further recognize the requirements, approaches, advancements and shortcomings investigated to date. The need and potential for designing localized and release-controlled *injectable* delivery systems based on natural polymers and formulated at the nano-scale, to overcome the limitations from the use of synthetic polymers and diminish the risks of disease transmission from the use of bovine collagen are thereby rationalized; providing the context for the global aim, design and the works carried out in this project.

This work has been in published in Biotechnology Letters and is reprinted with permission; DOI 10.1007/s10529-009-0100-8; Wednesday August 19th 2009; ISSN 0141-5492 (Print); ISSN 1573-6776 (Online) 

Appendix C contains a copy of the publication where the tables are perhaps clearer for the reader.

Manuscript submitted to *Biotechnol. Letters* (June 8th 09) and published online (Aug 19th 09).

# Review: Delivery of Recombinant Bone Morphogenetic Proteins for Bone Regeneration and Repair

## Part B: Delivery Systems for BMPs in Orthopaedic and Craniofacial Tissue Engineering

**Ziyad S. Haidar[a-d], Reggie C. Hamdy[b, d], Maryam Tabrizian[a-c]**

[a] *Faculty of Dentistry, McGill University, Montréal (QC) Canada*
[b] *Center for Biorecognition and Biosensors, McGill University, Montréal (QC) Canada*
[c] *Department of Biomedical Engineering, Faculty of Medicine, McGill University, Montréal (QC) Canada*
[d] *Shriners Hospital for Children and Division of Orthopaedics, McGill University, Montréal (QC) Canada*

## 4.1. ABSTRACT

Localized and release-controlled delivery systems for the sustained expression of the biologic potency of rhBMPs are essential. A substantial number of biomaterials have been investigated thus far. Most fail after implantation or administration mainly due to either being too soft, difficult to control and/or stabilize mechanically. In this second part, we review a representative selection of rhBMP-2 and rhBMP-7 carrier materials and delivery systems ranging from simple nano/microparticles to complex 3-D scaffolds in sites of orthopaedic and craniofacial bone regeneration and repair.

**Keywords:** *Bone morphogenetic proteins; biomaterials; microparticles; nanoparticles; delivery systems; controlled-release; growth factors; bone regeneration; synthetic polymers*

## 4.2. Introduction

Attempts to induce de novo bone formation for bridging defects using bone grafting procedures, segmental bone transport, distraction osteogenesis or biomaterials have been applied to a great extent (Kneser et al. 2006; Mussano et al. 2007). Several materials for the delivery of recombinant human (rh) forms of bone morphogenetic proteins (BMPs) have been developed in recent years with only specific collagen-based formulations for rhBMP-2 and rhBMP-7/rhOP-1 obtaining FDA approval for their restricted clinical use in humans, namely in orthopaedic and spinal fusion applications (Table 4.1). The ultimate goal would be to develop safe, proficient, user-friendly and cost-effective rhBMP delivery systems that would completely replace traditional grafting procedures in a number of diverse applications (Moioli et al. 2007; Schmidmaier et al. 2008).

In this review, we classify and discuss the carrier biomaterials, particularly natural and synthetic polymers and their combinations in different formats for the delivery of rhBMP-2 and rhBMP-7 to preclinical and clinical sites of bone regeneration and repair.

TABLE 4.1. OVERVIEW OF FDA-APPROVED rhBMP-2 AND rhBMP-7/rhOP-1 DEVICES

| *Protein* | *FDA approval year* | *Indications* | *Delivery system* | *Type of FDA approval* |
|---|---|---|---|---|
| rhBMP-2 | 2002 | Single-level anterior lumbar interbody fusion | Medtronic INFUSE® Bone Graft + LT-CAGE® | Full |
| | | Acute, open tibial shaft fractures | Medtronic INFUSE® Bone Graft + intramedullary nail | |
| rhBMP-7/rhOP-1 | 2002 | Posterolateral (intertransverse) lumbar spinal fusion | Stryker® OP-1 putty | HDE program |
| | | Recalcitrant long bone non-unions | Stryker® OP-1 implant | |

ACS: absorbable collagen sponge; LT-CAGE®: lumbar tapered fusion device; HDE: humanitarian device exemption; OP-1 putty: rhOP-1 + Type I bovine bone collagen matrix + carboxymethylcellulose as an additive; OP-1 implant: rhOP-1 + purified bone-derived collagen particles as a scaffold

## 4.3. rhBMP Delivery Systems

Challenges in BMP delivery were discussed in part A (Chapter 3). It has been for long suggested that to induce osteogenesis, a suitable delivery system is required for new bone to form due to the very short half-life (1-4 hours) of these cytokines (Takaoka et al. 1991), thus requiring large single doses or multiple smaller applications (Talwar et al. 2001). Also, given that BMPs are not bony tissue-specific (Okubo et al. 2000), their localized (vs. systemic) and release-controlled (vs. un-controlled) delivery is necessary to prevent any un-desired and un-controlled ectopic bone formation in non-bony tissues of the body (Schmidmaier et al. 2008).

The FDA approved bovine collagen-based delivery devices for rhBMP-2 and rhBMP-7 have limited indications in spinal interbody fusion and open tibial non-unions, respectively, mainly due to the large doses required to achieve the desired osteogenic effect where there is more exogenous BMP in a single dose than is present in 1000 humans, hence raising serious concerns regarding safety and cost (Kwon and Jenis 2005). Supra-physiological concentrations resulting from imperfect release kinetics of BMPs where 30%

TABLE 4.2. MAJOR CLASSES OF CARRIER MATERIALS AND SELECTIVE EXPERIMENTAL STUDIES OF BMP-INCORPORATED DELIVERY SYSTEMS

| *Carrier material* | *Advantages* | *Disadvantages* | *Types* | BMP/material type/animal model/site | Selected references |
|---|---|---|---|---|---|
| Natural polymers | Biocompatible, biodegradable, soluble in physiologic fluids with natural affinity for BMPs | Immunogenicity, pathogen transmission processing and sterilization difficulties | Collagen (gel, nanofibres, scaffolds and films), fibrin glue, alginate and chitosan | BMP-2/gelatin hydrogel/rabbit ulna<br>BMP-2/chitosan/rat mandible | Yamamoto et al. 2006<br>Issa et al. 2008a,b |
| Inorganic materials | Similar to bone, degradable/non-degradable, osteoconductive, self-setting ability in vivo and have affinity for BMPs | Brittle, difficult to mold and some calcium phosphate cements (CPC) are exothermic | CPC, bioactive glasses, Hydroxyapatite, hyaluronic acid, , tri-calcium phosphates, metals, ceramics and calcium sulfate | BMP-2/ Hyaluronic acid/in vitro/spine<br>BMP-2/CPC in ACS/monkey/spine<br>BMP-2/CPC putty/rabbit cranium | Kim and Valentini 2002<br>Barnes et al. 2005<br>Haddad et al. 2006 |
| Synthetic polymers | Excellent chemical and mechanical properties, easy to process and sterilize, flexible to tailor and reproducible | Inflammatory response, localized pH drop due to by-product s acidity and limited biological function | Polymers of α- hydroxy esters such as PLA, PGA and copolymers of these two monomers (PLGA) | BMP-2/PLGA microparticle/rat cranium<br>BMP-2/PLA-DX-PEG<br>Injectable PLA-PEG/mouse/orthotropic | Woo et al. 2001<br>Saito et al. 2003<br>Saito et al. 2005 |
| Composites | According to combination from different material (and biomolecule) classes | Complex manufacturing processes | Collagen-HA and titanium-PLLA | BMP-2/Collagen-PLG-alginate/rat calvaria<br>BMP-7/PLGA- PLLA scaffold/rat s.c.<br>BMP-7/liposomes coated with alginate and chitosan (layer-by-layer)/rabbit/tibia | Kenley et al. 1994<br>Wei et al. 2007<br>Haidar et al. 2008a,b<br>Haidar et al. 2009 |

*Modified and updated from Li and Wozney 2001; Lee and Shin 2007*

of the encapsulate is lost in the initial bust phase (Geiger et al. 2003) are additionally being related to severe clinical complications including generalized hematomas in soft tissue and para-implant bone resorption (Gautschi et al. 2007; Robinson et al. 2008).

## 4.4. rhBMP-specific Carrier Types and Delivery Materials

Researchers have commonly explored biomaterials with demonstrated osteoconductive properties. However, an *ideal* BMP carrier material needs to be osteoconductive, osteoinductive and osteogenic (Seeherman and Wozney 2005; De Long et al 2007; Schmidmaier et al. 2008). Although intensively evaluated in animal studies (please see supplementary Table 4.4) as well as in clinical trials with satisfactory results, bovine collagen has also demonstrated some safety issues mainly owing to its xenogenic origin. Polymeric matrices have attracted attention over the last years to achieve the localized and controlled release of proteins over long periods of time and overcome limitations in enzymatic susceptibility, stability during storage and efficacy upon administration (Termaat et al. 2005; Moioli et al. 2007; Schmidmaier et al. 2008).

Generally, the major categories of carrier materials (Table 4.2) include: **(1)** *natural-origin polymers* such as collagen, hyaluronans, soy- and alga-derived materials, and poly(hydroxyalkanoates); **(2)** *inorganic materials and ceramics/cements* such as hydroxyapatite, tri-calcium phosphates and -sulphates as well as bioglasses and metals; **(3)** *synthetic biodegradable polymers* such as poly(lactic acid) (PLA), polyglycolide (PLG) and their copolymers, poly L-lactic acid (PLLA), poly D,L-lactide-co-gycolic acid (PLGA) and poly ε-caprolactone (PCL); and **(4)** *composites* which are combinations that take advantage of each material class as well as other biomolecules (Fei et al. 2008).

## 4.5. Natural-origin Polymeric Carriers

### 4.5.1. Collagen

***Collagen*** is the most abundant protein in connective tissues of mammals and the major non-mineral component of bone with a well established role in cellular infiltration and wound healing (Geiger et al. 2003). It has been prepared in powders, membrane films and implantable absorbable sponges as well as in aqueous forms (Geiger et al. 2003; Lee and Yuk 2007). Despite known for versatility and ease of manipulation, manufacturing collagen carriers is highly sensitive to several factors including mass, soaking time, protein concentrations, sterilization methods, buffer composition as well as pH and ionic strength (between collagen and the encapsulant) that directly affects the binding of rhBMPs (Goa and Uludag 2001; Lee and Yuk 2007). Absorbable collagen sponges (ACS) have been evaluated in numerous in vivo models and clinical trials. In the healing of a critical-sized radial defect stabilized by an external fixator, Sciadini and Johnson compared the efficacy of various dosages of rhBMP-2 delivered in an ACS to autogenous bone grafts in 27 dogs. Defects treated with rhBMP-2 showed better healing than those treated with the ACS alone or autogenous bone grafts (Sciadini and Johnson 2000). Paramount evidence, nonetheless, is derived from well-designed clinical trials. Table 4.3 lists selected examples of randomized clinical trials and clinical case series. The BESTT study investigated low (0.75 mg/mL) and high (1.5 mg/mL) doses of rhBMP-2 impregnated in an ACS. At 12 months, patients in the latter group had statistically significant accelerated healing, fewer invasive interventions and

a lower rate of non-union than the control group (Govender et al. 2002). In patients requiring staged maxillary sinus floor augmentation, rhBMP-2/ACS safely induced adequate bone formation for the placement and functional loading of endosseous dental implants (Boyne et al 2005). The use of rhBMP-2/ACS without concomitant bone grafting materials in critical-sized mandibular defects produced excellent regeneration in a very recent case review of 14 patients (Herford and Boyne 2008).

**TABLE 4.3. rhBMP-2 AND rhBMP-7/rhOP-1 USE IN CLINICAL STUDIES**

| *Protein* | *Carrier* | *Application* | *Total # of patients* | *Reference* |
|---|---|---|---|---|
| | Absorbable collagen sponge (ACS) | Anterior lumbar interbody arthrodesis | 46 and 279 (2 trials) | Burkus et al. 2002 a,b |
| | Bovine ACS | Open tibial shaft intermedullary fixation | 450 | Govender et al. 2002 |
| | Bovine ACS | Cervical anterior arthrodesis | 33 | Baskin et al. 2003 |
| **rhBMP-2** | Xenogenic bone (Bio-Oss) | Maxillary implant placement | 11 | Jung et al. 2003 |
| | ACS | Anterior lumbar interbody arthrodesis | 131 | Burkus et al. 2005 |
| | ACS | Maxillary sinus floor augmentation | 48 | Boyne et al. 2005 |
| | ACS | Mandibular continuity defects | 14 | Herford and Boyne 2008 |
| | Type I collagen | Fibular osteotomy (critical-sized defects) | 24 | Geesink et al. 1999 |
| | Type I collagen | Maxillary sinus floor elevation | 3 | Van der Bergh et al. 2000 |
| | Type I collagen | Tibial intramedullary fixation (non-union) | 122 | Friedlaender et al. 2001 |
| **rhBMP-7/rhOP-1** | Type I collagen | Posterolateral lumbar arthrodesis (non-instrumented) | 20 | Johnsson et al. 2002 |
| | ACS | Fresh tibial fracture (external fixation) | 14 | Maniscalco et al. 2002 |
| | OP-1 putty* | Posterolateral lumbar fusions | 36 | Vaccaro et al. 2005 |
| | OP-1 putty | Posterolateral lumbar arthrodesis (instrumented) | 19 | Kanayama et al. 2006 |
| | OP-1 putty | Posterolateral lumbar arthrodesis | 24 | Vaccaro et al. 2008 |

*OP-1 putty consists of rhOP-1, Type I bovine bone collagen matrix and an additive; carboxymethylcellulose sodium

On the other hand, no differences using rhBMP-7 incorporated in type I collagen carriers over a period of 24 months were detected in a prospective clinical trial (Friedlaender et al. 2001). It was concluded to be similar to autografts in the management of non-unions except for the pain factor associated with the donor site. Although eliminating the need to harvest autologous bone and alleviating the associated pain, animal-derived collagens are limited by their xenogenic nature (mostly bovine and porcine skin) where anti-type I collagen antibodies developed in almost 20% of patients treated with rhBMP-2/ACS (Sciadini and Johnson 2000, Geiger et al. 2003; Bessa et al. 2008 b). Also, sterilization is usually using ethylene oxide prior to soaking the sponge in the BMP solution; hence, with an effect on the release kinetics or the bioactivity of the protein within (Gittens and Uludag 2001). Furthermore, without delivery *in situ*, BMPs rapidly diffuse away from defect site (Sciadini and Johnson 2000) probably explaining some of the discrepancies noted in preclinical and clinical outcomes (Chen and Mooney 2003). Therefore, other sources of collagen

(recombinant perhaps) and biomaterials are currently being evaluated for rhBMP delivery, though still at the preclinical stages.

### 4.5.2. Alginate and Chitosan

***Alginate*** (AL) is a non-immunogenic polysaccharide abundantly found in the surface of seaweeds used in a wide range of tissue engineering applications due to its gel-forming properties (Tönnesen and Karlsen 2002). Injectable in situ-forming AL gels were prepared then loaded with an osteoinductive growth factor (IGF-I), for example. Significantly accelerated proliferation of osteoblast-like MG-63 cells favorable for the conformal filling of bone defects was demonstrated (Luginbuehl et al. 2005). Furthermore, encapsulant release from AL matrices can be modulated by different parameters such as particle size, viscosity and chemical composition. Liew et al. in a recent investigation found that particle size affected the extent of burst release and the higher the viscosity the slower the encapsulant release. (Liew et al. 2006).

***Chitosan*** (CH) is a cationic copolymer of *N*-acetyl-D-glucosamine and glucosamine prepared by *N*-deacetylation of chitin well-known for its biological, chelating and adsorbing properties (Kumar et al. 2004; Lee and Yuk 2007). Practical use of CH has been mainly confined to un-modified forms as they have solely demonstrated favorable biodegradation kinetics slower than polymers such as collagen. However, the chemical-modification and graft co-polymerization onto CH further improved controlling the release profile of bioactive molecules and some have been described as osteoinductive materials (Prabaharan 2008). Novel chemically-modified CHs with controllable photo-curability showed enhanced biocompatibility and bone tissue repair in athymic rats (Qiu et al. 2008). Furthermore, rhBMP-2/CH accelerated osteogenesis in a rat critical-sized mandibular defect. CH adapted well to the defect and had favorable release kinetics as revealed by the amount of new bone tissue (Issa et al. 2008 a, b).

### 4.5.3. Hyaluronic Acid

***Hyaluronic acid*** (HA) is another naturally-occurring biopolymer, which plays a significant role in wound healing. HA and its derivatives have been largely studied in biomedical and tissue engineering applications as gels, sponges and pads and as a viscous gel injected percutaneously in ophthalmic surgery (O'Regan et al. 1994, Bessa et al. 2008 b). HA also has an osteoinductive action itself where it has been shown to result in improved bone formation in mandibular defects in comparison to collagen sponges when both carriers were used to deliver BMP-2 in rats as well as in a human clinical trial (Arosarena and Collins 2005). That is probably due to that HA-based delivery vehicles might posses the capacity to retain more BMPs than collagen (Kim and Valentini 2002). In addition, hyaluronans seem to stimulate the proliferation of bone marrow stromal cells, expression of osteocalcin, enhance ALP activity and interact positively with BMPs to generate direct and specific cellular effects. This increased affinity is attributed to HA being anionic thus forming ionic bonds with the cationic BMPs significant for potential future clinical applications (Peng et al. 2008).

Other less common natural polymers in BMP delivery include gelatin, dextran and fibrin as they are limited by their mechanical strength and fusion with other biomolecules or biomaterials seems necessary, nonetheless with promising applications in angiogenesis (Young et al. 2005).

## 4.6. Inorganic Materials

### 4.6.1. Hydroxyapatite

***Hydroxyapatite*** (HAP) is well known for its osteoconductivity and has been widely used as a bone-substitute material clinically since the 1970s due of its ability to bond directly with bone (Li and Wozney 2001). Synthetic HAP comes in ceramic (porous and non-porous) or non-ceramic, cementable form (Moore et al. 2001) with only porous HAP being evaluated as a scaffold and a controlled release carrier (particles, powder, granules, disks or blocks) of

BMPs for bone regeneration (Bessa et al. 2008 b). However, lack of bone induction due to the high affinity between the material and the BMPs in addition to the lack of resorption of the HAP and dependence on the geometry of the substratum was evident (Noshi et al. 2001). Therefore, HAP has been often combined with tri-calcium phosphates, collagen, other natural and synthetic polymers to form a more rigid, resorbable and porous BMP carrier. Generally, such composites have demonstrated better local BMP delivery and bone formation than HAP alone in various bone defects in vivo (Schopper et al. 2008; Kim et al. 2008).

### 4.6.2. Calcium Phosphates and Bioactive Glasses

Inorganic materials such as ***calcium phosphate-based cements***, ***ceramics*** and ***coatings*** (CPCs) have proven to be versatile carriers that can be formulated as implantable and injectable cements. They harden in vivo and can be used to deliver bioactive growth factors (in low temperature forms to prevent protein denaturation) with established prominent bone formation (Moore et al. 2001; Ginebra et al. 2006). Ceramics are known to mimic natural bony structure when implanted (Schmidmaier et al. 2008). Furthermore, overall, lower dosages of BMPs are required with the use of CPCs compared to other carriers (Ginebra et al. 2006). However, phase separation during injection, lack of intrinsic macroporosity to allow cell infiltration, intrinsic radiopaque nature and decreased mechanical tensile and shear properties compared to bone and other materials are among the main disadvantages of CPCs (Seeherman and Wozney 2005). Modifications to increase injectability and macroporosity in vivo have been recently reported (Bohner and Baroud 2005). Also, CPCs have been used as a bulking agent to improve the osteogenicity of ACS loaded with rhBMP-2 where it helped lowering the BMP dose (> 3-fold) in a spinal fusion model in the non-human primate model (Barnes et al. 2005).

***Bioactive glasses*** (BG) are a group of hard and non-porous silica-based bioactive compounds which are known to bond directly to bone due to their good osteointegrative and osteoconductive properties. They have different resorption rates depending on their chemical

compositions where solubility is proportional to the sodium oxide content (Välimäki and Aro 2006). BG such as 45S5 Bioglass® are commonly used as filler material for fractured bone, augmentation of the alveolar ridge and vertebral implants. Recent studies have shown that BG induce a high local bone turnover in vitro and in vivo where they increase the BMP effect, support osteoblast growth and favor osteoblast differentiation by stimulating the synthesis of phenotypic markers like alkaline phosphatase, collagen Type I and osteocalcin (Moore et al. 2001; Välimäki and Aro 2006).

## 4.7. Synthetic Biodegradable Polymeric Carriers

Unlike collagen, ***synthetic biodegradable polymers*** pose no danger of immunogenicity or possibility of disease transmission. A number of synthetic biodegradable polymeric delivery systems for BMP-2 were discussed in two recent reviews (Saito et al. 2003; Saito et al. 2005). The most commonly used polymers herein are PLLA and PLGA. Their degradation is primarily via hydrolysis and different proportional combinations of PGA and PLA, for example, demonstrate various material properties which in turn affect biodegradability. Material crystallinity and scaffold morphology (pore size/number) also play an important role in biodegradability where a more porous scaffold degrades faster as will that comprised of low molecular weight polymers. Synthetic polymers can be processed into highly porous 3-D scaffolds, fibers, sheets, blocks or microspheres (Seeherman and Wozney 2005). BMP release is by means of diffusion, polymer swelling followed by fast diffusion-controlled release, and polymer erosion (Engstrand et al. 2008). Bioresorbable PLA/PGA beads were found to be superior to collagen when used to deliver rhBMP-2 to transosseous rat mandibular defects (Zellin and Linde 1997). PLGA was evaluated successfully in several canine defect models such as for BMP-2-induced periodontal regeneration, maxillary alveolar cleft repair, and segmental ulnar long-bone defects (Sigurdsson et al. 1996; Mayer et al. 1996; Itoh et al. 1998). Nonetheless, the main limitation is their acidic breakdown by-products and the associated risk of inflammatory response if not cleared quickly which is detrimental to the stability of the encapsulated BMPs and the overall therapeutic outcome

(Saito et al. 2005). As a result, a continuous supply of osteoinductive factors would be crucial to compensate for polymer degradation (Schliephake et al. 2008).

## 4.8. Composites

Combinations of different material classes (Table 4.2) have been used to optimize the benefits and overcome the limitations of many of the above materials. Examples of recent ***composites*** include glycidyl methacrylated dextran (Dex-GMA)/gelatin scaffolds containing microspheres loaded with rhBMP-2 and implanted into the periodontal defects of dogs (Chen et al. 2007), PLGA-gelatin composites for the delivery of rhBMP-2 to vertical alveolar ridge augmentation in dogs (Kawakatsu et al. 2008), HAP-coated porous

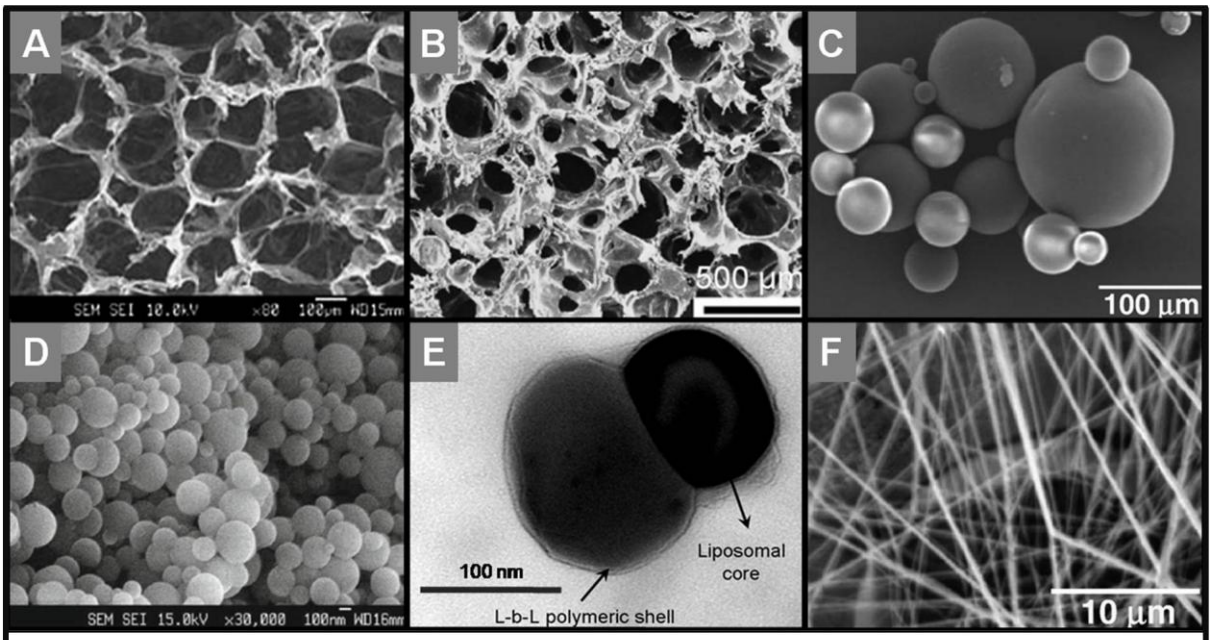


**FIG 4.1.** Selected electron microscopy images representing various delivery systems and carrier biomaterials evaluated for BMPs. (**A**) Porous collagen sponge, bar = 100µm (**B**) PLGA-coated gelatin sponge (**C**) PLGA microspheres (**D**) Heparin-conjugated PLGA nanoparticles, bar = 100nm (**E**) core-shell nanoparticles constituting liposomes, alginate and chitosan (**F**) PLGA nanofibres. Adopted from Moioli et al. 2007; Lee and Shin 2007; Kim et al. 2008; Haidar et al. 2009.

titanium/rhBMP-2/HA in the metaphysic of the distal femur of rabbits (Peng et al. 2008) and PEG hydrogel/rhBMP-2/HAP/TCP granules in the rabbit calvarial bones (Jung et al. 2008). A 3-D highly porous PLA/HAP/collagen scaffold was prepared for use in healing of canine

segmental bone defects. The HAP/collagen portion was to mimic the natural extracellular matrix of bone, with the collagen serving as a template for apatite formation. All defects healed satisfactorily (Hu et al. 2003). Fu et al. recently combined rabbit mesenchymal stem cells (MSCs) with AL/BMP-2 and implanted the composite in a posterolateral intertransverse fusion model in 24 rabbits. Results demonstrated that MSCs delivered with rhBMP-2 (2.5 mg) are more osteoinductive than MSCs without rhBMP-2 and that the composite material enhanced bone formation and spine fusion success (Fu et al. 2008).

Nano- and micro-particles from synthetic polymers and natural polymers (Figure 4.1) are other dosage forms that have consummated much attention for the localized and release-controlled delivery of growth factors due to their attractive tendency to amass in sites of inflammation (Lee and Shin 2007). Enhanced in vivo tissue regeneration using PLGA and gelatin microparticles for growth factor release was reported (Park et al. 2005).

Compared to microparticles, **nanoparticle** and nanofiber delivery systems have demonstrated superiority in terms of longer residencies in general circulation, consequently extending the bioactivity of the entrapped molecule (Nair and Laurencin 2008). In a recent example of a combined localized and release-controlled delivery system, PLGA nanospheres (NS) immobilized onto prefabricated nanofibrous PLLA scaffolds were used to load and deliver rhBMP-7 (Wei et al. 2007; Ma 2008). BMP-7 delivered from NS-scaffolds induced significant ectopic bone formation while passive adsorption of the protein into the scaffold resulted in failure of bone induction either due to the loss of protein bioactivity or its rapid release from the scaffolds upon implantation in vivo. We have successfully encapsulated a model protein, bovine serum albumin in monodisperse and non-toxic nanoparticles constituting a core of cationic liposomes and a shell constructed through the layer-by-layer electrostatic-based self-assembly of alternating layers of anionic AL and cationic CH. The release profile was characterized by an initial burst followed by sustained albumin release, highly desirable for growth factor delivery; particularly in large bony defects (Haidar et al. 2008 a).

In a subsequent work, the ability of the core-shell nanoparticulate delivery system to encapsulate a range of concentrations of BMP-7 was evaluated. The system exhibited high

physical stability in simulated physiological media as well as an extended shelf-life allowing for immediate protein loading prior to administration, preventing degradation or loss of the encapsulant. A sustained triphasic linear release of BMP-7 was evident for an extended period of 45 days with the bioactivity of the protein maintained via enhancing pre-osteoblast differentiation (Haidar et al. 2008 b).

In a rabbit model of tibial distraction osteogenesis, accelerated osteogenesis and consolidation was evident following a single injection of the nanoparticles loaded with a dose of no more than 1.0 µg rhBMP-7 (Haidar et al. 2009c) in comparison to earlier results from a single injection of rhBMP-7 (75 µg in saline), accentuating the role of the injectable localized and release-controlled nanoparticles (Mandu-Hrit et al. 2006).

Other groups investigated injectable scaffolds and matrices for drug delivery in bone tissue engineering (Kretlow et al. 2007). A recent example is the work of Hosseinkhani et al. where an injectable hydrogel of self-assembled peptide-amphiphile and BMP-2 was fabricated. Significant homogenous ectopic bone formation in the back subcutis of rats was demonstrated (Hosseinkhani et al. 2007). A 3-D scaffold for the sequential delivery of BMP-2 and BMP-7 was recently developed (Basmanav et al. 2008). The system consisted of microspheres of polyelectrolyte complexes of poly(4-vinyl pyridine) and AL loaded with both proteins and incorporated in PLGA scaffolds. Neither BMP-2 nor BMP-7 delivery had any direct effect on cellular proliferation; however, their co-administration enhanced osteogenic differentiation to a higher degree than with their single administration. This was suggested to be due to the physical properties (pore size and distribution) of the foams. In conclusion, no single clinically-effective delivery system for rhBMP-2, rhBMP-7 or any other bone growth factors has been developed to date.

## 4.9. Future Prospects

The use of delivery systems is crucial for reliable bone formation and economic application of BMPs. Many carrier materials have been investigated. Collagen matrices have been clinically successful nevertheless with shortcomings including biodegradability, local retention and controlling release kinetics of BMPs. A limited number of other potential delivery systems have been developed and are still at the preclinical stage. Nonetheless, advances in the field will eventually lead to novel customized and optimized BMP-specific carrier materials. Better, safer and more integrated minimally-invasive drug delivery systems that utilize smaller amounts of BMPs effectively are needed. They will be insoluble under physiological conditions in order to retain the BMP yet absorbable by host tissue after implantation/administration so that be replaced by the regenerating bone, preferably following single application. Controlled prospective clinical trials should follow. The use of BMPs and other less understood morphogens will extend into much broader range of orthopaedic as well as craniofacial and oro-dental indications including bone, cartilage and tendon/ligament (and periodontal) tissue regeneration and repair.

## 4.10. Acknowledgments

The authors wish to thank grants from the Shriners of North America, Fonds de la Recherche en Santé du Québec, the National Science and Engineering Research Council, the Canadian Institutes of Health Research (CIHR) - Regenerative Medicine/Nanomedicine and the Center for Biorecognition and Biosensors (CBB), McGill University, Montréal, Québec, Canada. Dr. Haidar acknowledges scholarships from the Center for Bone and Periodontal Diseases Research and the Shriners Hospital, Montréal, Québec, Canada.

## 4.11. Supplementary Information

**TABLE 4.4. BMP-2 AND BMP-7/OP-1 APPLICATION IN ANIMAL STUDIES (past the year 2000)**

| *Protein* | *Carrier* | *Animal Model (site)* | *Reference* |
|---|---|---|---|
| BMP-2 | Absorbable collagen sponge (ACS) | Monkey (mandible) | Boyne 2001 |
| | ACS (w/o hydroxyapatite) | Dog (alveolar ridge) | Barboza et al. 2000 |
| | Hydroxyapatite/collagen | Dog (long bone) | Itoh et al. 2002 |
| | Poly-lactic acid (PLLA) composite Scaffold | Rat (ectopic model) | Chang et al. 2007 |
| | Injectable 3-D nano-scaffolld | Rat (ectopic model) | Hosseinkhani et al. 2007 |
| BMP-7/OP-1 | Bovine collagenous matrix | Baboon (calvaria) | Ripamonti et al. 2000 |
| | Porous hydroxyapatite | Monkey (craniofacial bone) | Ripamonti et al. 2001 |
| | Hydroxyapatite | Sheep (spine) | Blattert et al. 2002 |
| | Hydrochloric acid | Rat (femur) | Mizumoto et al. 2003 |
| | Acetate buffer | Rabbit (tibia) | Hamdy et al. 2003 |
| | Acetate buffer | Rabbit (tibia) | Mandu-Hrit et al. 2006 |
| | Acetic acid | Rat (femur) | Hak et al. 2006 |
| | OP-1 putty w/o carboxymethylcellulose | Sheep (tibia) | Pluhar et al. 2006 |
| | poly-L-glycolic acid (PLGA) biospheres | Sheep (spine) | Phillips et al. 2006 |
| | PLGA nanospheres in PLLA scaffolds | Rat (ectopic) | Wei et al. 2007 |

# CHAPTER 5
## Distraction Osteogenesis (DO) – A Bone Regeneration Model

Bone is a highly specialized tissue that differs from all other non-mineralized connective tissues in that it is hard, attributable to the mineralized extracellular matrices. Although the human body possesses an enormous regenerative capacity, bone healing continues to be limited in an array of defects and clinical indications involving the implantation of bone grafts. In an attempt to improve the correction of severe bony anomalies, distraction osteogenesis (DO) has been introduced as an early alternative to traditional orthopaedic, craniofacial or orthognathic surgery. DO can be considered a very special, altered form of fracture healing that takes advantage of the regenerative potential of bone tissue in addition to mechanical force to induce and direct bone formation as well as the remodeling of cartilage, nerve, muscle, blood vessel and skin. DO creates a controlled fracture in a bony structure and then separates the two viable bone segments in a controlled and gradual manner. This process induces the formation of new bone in between the distracted segments. DO can be performed using internal or external devices. Today, it is a well-established and widespread surgical technique for the correction of congenital orthopaedic deformities such as limb-length discrepancies, transporting bone to bridge and fill segmental bone defects and treating fracture non-unions following trauma as well as for the correction of craniofacial developmental conditions and TMJ growth disturbances including obstructive sleep apnea and upper airway obstruction in addition to alveolar ridge reconstruction prior to the placement of dental implants. Despite the success of DO standardizing its world-wide application for limb lengthening, clinical benefits continue to be limited by a number of complications mainly as a result of the protracted treatment time during which the external fixator has to be kept in situ until the newly-formed bone in the distracted zone consolidates (or hardens); which can last *longer* than 12 months. In turn, this can exacerbate significant medical, psychological and socio-economical problems on patients, their families as well as caregivers. Complications specific to the distraction process include: device failure; pin-site infection with external or semi-buried devices, nonunion and premature fusion. Others related to the osteotomy include neurovascular injuries and to psychosocial well-being and

recovery such as the length of treatment time and the physical appearance of patients; mostly clear in children. Numerous studies have attempted several approaches to accelerate bone regeneration and consolidation in DO; however protein therapy particularly with the use of rhBMPs seems to be the most promising to date. In the following pages, the aim is to provide an understanding of the procedure and its limitations. It is a part of a more comprehensive review article motivated by the lack in the available literature for a current update on the attempts explored to enhance DO.

Unpublished Manuscript. To be submitted to the *Journal of Orthopaedic Surgery and Research*.

# Accelerating New Bone Regeneration and Consolidation during Distraction Osteogenesis – an Update

**Ziyad S. Haidar**[a-d], **Reggie C. Hamdy**[b, d], **Maryam Tabrizian**[a-c]

[a] *Faculty of Dentistry, McGill University, Montréal (QC) Canada*
[b] *Center for Biorecognition and Biosensors, McGill University, Montréal (QC) Canada*
[c] *Department of Biomedical Engineering, Faculty of Medicine, McGill University, Montréal (QC) Canada*
[d] *Shriners Hospital for Children and Division of Orthopaedics, McGill University, Montréal (QC) Canada*



## 5.1. ABSTRACT

Distraction osteogenesis (DO) is a prevailing surgical technique widely used for bone lengthening and includes performing an osteotomy followed by gradually distracting the two viable bone segments resulting in de novo bone formation within the distracted gap. However, a main limitation is the long period of time required for the newly formed bone to consolidate. Therefore, accelerating DO and specifically distraction and consolidation by enhancing the quantity and quality of bone formation would shorten the length of time the fixator has to be kept in situ, thus improving patient comfort, compliance and the overall outcome of the treatment, especially in children. Over the last decades, several approaches have been explored although none have yet shown any efficiency in humans. The most recent attempts at accelerating the consolidation phase have been focusing on the application of certain growth factors in combination with delivery systems.

**Keywords:** *Angiogenesis; Bone morphogenetic proteins; bone regeneration; biomaterials; consolidation; delivery systems; distraction osteogenesis; polymers; growth factors; mechanical stimulation; nanoparticles; rhythm of distraction*

## 5.2. Definition

Benefiting greatly from the regenerative potential of the human body and bone tissue, DO is a surgical procedure primarily used for limb-lengthening purposes where large quantities of bone are produced by means of stimulating local host tissues via mechanical *gradual* distraction forces. DO is a form of biologic in vivo tissue engineering whereby viable new bone is generated as a result of regularly separating the two viable osteomized bone edges, at the molecular level. It also allows for the simultaneous expansion of the functional soft tissue matrix; blood vessels, nerves, mucosa, fascia, skin, muscles, ligaments and/or periosteum in cases of craniofacial and mandibular DO in a process collectively referred to as ***distraction histiogenesis*** (Murray and Fitch 1996; Lauterburg et al. 2006).

## 5.3. Historical Background

Mechanical tension is one of the key signals required for embryological bone formation and growth during morphogenesis. Endochondral bone lengthening was first documented in ancient times when Hippocrates described the application of external traction forces on broken bones using two leather rings connected to four slightly bent rods made from the elastic cornel tree in order to provide tension as displayed in Figure 5.1. The tension applied to the separated bone segments was controlled by the amount of rod bending (Samchukov et al. 1998). However, the first to introduce the concept of limb lengthening was de Chauliac in the 14$^{th}$ century using a pulley system consisting of a weight attached to the leg by a cord so that to exert continuous traction on long bone fractures (Peltier 1968). The first osteotomy or surgical division of bone was performed by Barton in 1826 (Codivilla 1994) and the first external skeletal fixator device utilizing two double hooks connected by a screw and inserted through the skin was developed later on towards the middle of the 19$^{th}$ century (Malgaigne 1847).

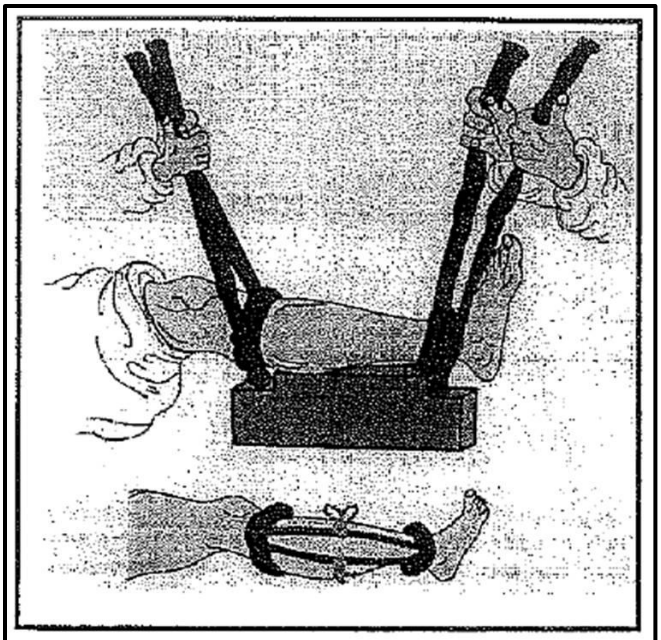

**FIG 5.1.** Hippocrates' (460 - 370 BC) fracture technique and external fixation apparatus (Samchukov et al. 1998).

Considerable evolution of external fixation (Figure 5.2) has took place since then where the first limb lengthening procedure applied on a femur by creating an oblique osteotomy followed by placing external skeletal traction onto the osteomized bone segments was performed by Alessandro Codivilla in 1905.

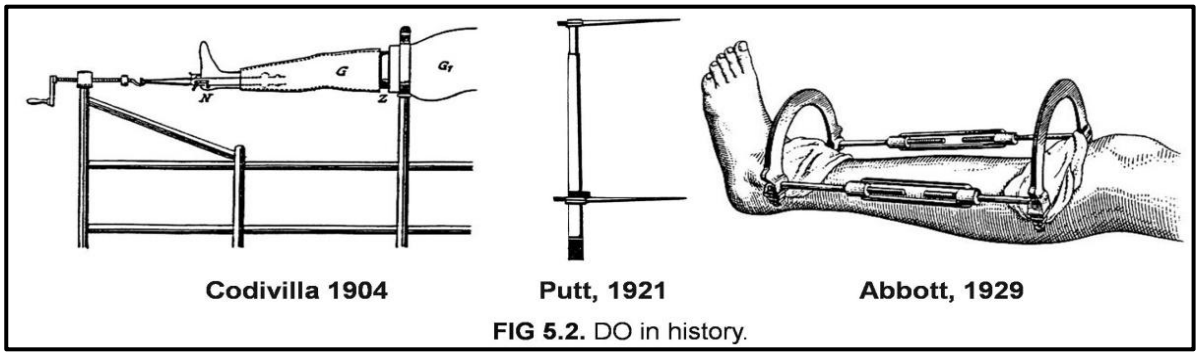


**FIG 5.2.** DO in history.

Nonetheless, wound infection, tissue necrosis and unreliable and controlled bone formation were common drawbacks back then (Codivilla 1994; Samchukov et al. 1998; Lauterburg et al. 2006; Codivilla 2008).

The work of the Russian orthopaedic surgeon Gavriel A. Illizarov is considered the most significant contribution to the improvement of DO where he was the one who developed the modern principles and phases of bone lengthening earning him the title; *Father of DO*. In 1951, while treating a patient with a short amputation stump in the small Siberian community of Kurgan, Illizarov performed an osteotomy and applied external fixation to lengthen the stump with the intention of placing a bone graft.

The new apparatus consisted of two metal rings joined together with threaded rods as displayed in Figure 5.3. After a delay of few days post-osteotomy, Illizarov noticed that bone as well as soft tissue regenerated when subjected to slow and gradual distraction and therefore eliminating the need for the graft. He later developed a low-energy, subperiosteal osteotomy technique (corticotomy) and a unique protocol for limb lengthening: 5-7 days latency period followed by distraction at a rate of 1 mm per day performed in four increments of 0.25mm (Illizarov 1989 a, b). Thousands of patients with different orthopaedic problems were then treated by Illizarov where mechanical tension which is one of the key signals of morphogenesis during embryological bone formation and growth was utilized by him as a foundation for his DO technique.

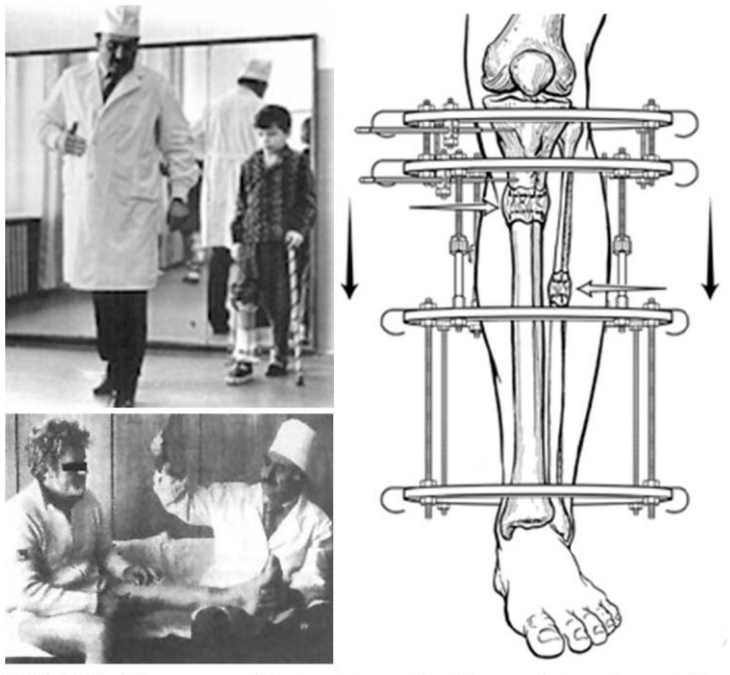

**FIG 5.3.** Illizarov with some patients and a schematic presentation of his external ring fixation method.

Today, DO is a prevailing surgical technique for the minimally-invasive correction of limb length discrepancies, severe bone loss (critical-sized bone defects) as well as the reconstruction of many craniofacial deformities as will be discussed later on in this chapter.

## 5.4. Biological Basis of New Bone Formation in DO

### 5.4.1. Principles of DO

In human patients, the treatment protocol of DO consists of a surgical osteotomy of the bone followed by three sequential periods or phases: (1) **latency phase**, the duration from bone division to the onset of traction where the patient is left to recover from surgery for 5-7 days, the wound is allowed to reduce swelling and most importantly the reparative callus develops ; (2) **distraction phase**, the time when gradual distraction is applied and new bone (or regenerate) at the desired or maximum possible length is formed (5 cm would require 50 days of distraction, at 1 mm/day for example); and (3) **consolidation phase**, the period where the newly-formed bone is allowed to mature, mineralize and corticalize after distraction has discontinued with the fixator left in situ (Illizarov 1989 a, b; Samchukov et al. 2001). It is noteworthy that distraction rate cannot exceed 1.5 mm/day as it might cause delayed ossification, pseudoarthrosis and/or soft tissue, nerve and muscle damage. Also, it cannot be less than 0.5 mm/day as regenerate bone might consolidate prematurely. The consolidation phase is the lengthiest of all 3 periods of DO where almost 1 month is required for every 1 cm of lengthened bone. The goal is for the regenerate bone to be indistinguishable from the surrounding native bone and to be biomechanically strong enough to withstand the stresses exerted during mechanical usage (Hamdy et al. 1997; Welch et al. 1998; Haidar et al. 2009 c). Besides the involved biological principle known as the 'Tension-Stress effect' for the genesis and growth of tissues, it has been a long held belief in the fields of bone tissue engineering and orthopaedics that the influence of blood supply and loading of bones and joints are of crucial significance for the successful outcome of a treatment procedure. Similarly in DO, blood supply and angiogenesis are closely associated and necessary to support the mechanical loading of bones and joints where if inadequate, atrophic or degenerative changes can result (Ilizarov, 1992; Ohashi et al. 2007).

### 5.4.2. Histological Features of DO

At the histological level, DO bone is very similar to that of fracture healing (McKibbin 1989; Campisi et al. 2002). The de novo bone formation is initiated when the callus is subjected to a controlled traction force thereby interrupting the fracture healing process. DO, therefore can be considered as a bony fracture that is subjected to a specific mechanical environment requiring sufficient blood supply, rigid fixation and stabilization in addition to an adequately precise distraction rate and rhythm for the bone to continue to grow in length. Briefly, the histological pattern typically observed is mainly as *follows*:

Hematoma formation as a result of vascular disruption between and around the bone segments occurs immediately after performing the osteotomy. It is subsequently converted into a clot with bony necrosis occurring at the end of the fractured bone segments. The clot is then replaced with granulation tissue consisting of inflammatory cells, fibroblasts, collagen and invading capillaries (Iranov 1996). This soft callus stage is marked by a continuous capillary ingrowth and the conversion of the granulation tissue into a fibrous tissue by fibroblasts. Also, cartilage replaces the granulation tissue more towards the periphery of the intersegmentary gap than in the central region of the callus (Komuro et al. 1994). During normal fracture healing, the fibrocartilaginous tissue of the soft callus is replaced by bone by osteoblasts. During DO, this *normal* process is interrupted by the application of gradual traction to the soft callus where a fibrous interzone develops in the gap formed between the separated bone segments. Fibroblasts secrete collagen fibers along the orientation and direction of the distraction force. This fibrous tissue is transformed later into bone tissue, as early as two weeks after the start of distraction. The new bone is formed from the periosteum, the cortex at the site of the osteotomy and the spongiosa.

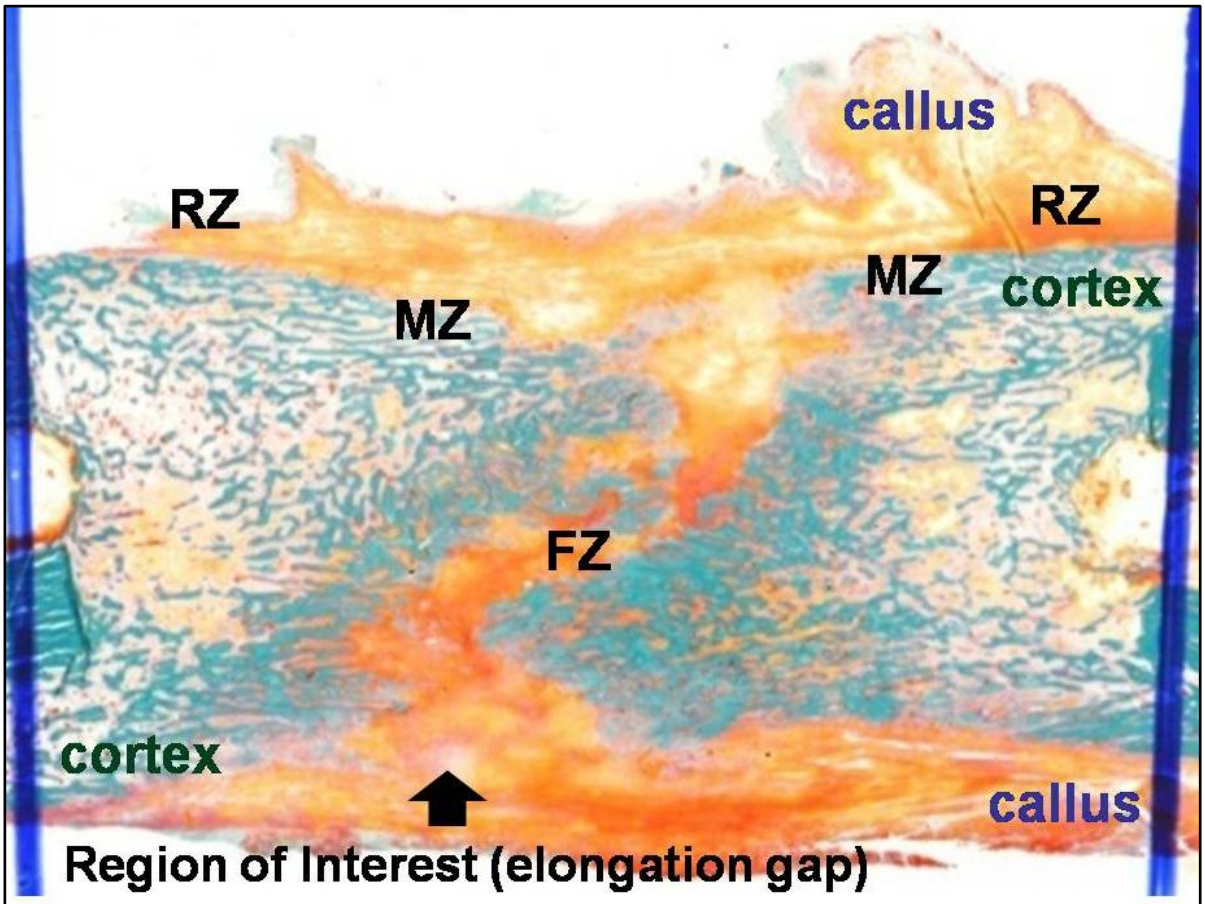


**FIG 5.4.** Histological illustration of the three-zone structure of a distraction osteo-regenerate. **FZ**: Fibrous interzone; **MZ**: Mineralization zone and **RZ**: Remodeling zone. Section was prepared from the Rabbit DO model (See **Chapter 9**: Control group; distraction only + 0.2 mL saline injection) study using Trichrome Goldner staining showing mineralized tissue (trabecular bone and cartilage) in greenish blue, and un-mineralized cartilage in orange .

It proceeds from the osteotomy cuts towards the center almost always creating a fibrous radiolucent interzone between the two advancing edges of the mineralization front with the fibers and the new bone trabeculae oriented parallel to the distraction force as illustrated in Figure 5.4 (Shearer et al. 1992; Aronson et al. 1997). Besides, several histological studies have demonstrated the significance of the osteotomy, stability of the fixator in situ, use of the proper rate and rhythm of distraction and presence of adequate vascularization and local blood supply between the newly-formed columns/margins of bone to prevent delayed or failed bone healing in DO (Choi et al. 2000; Ohashi et al. 2007).

After distraction ends, the fibrous interzone gradually ossifies and one distinct zone of bone *completely* bridges the gap. Although the regenerate forms predominantly by membranous ossification, isolated islands of cartilage may also be observed, suggesting endochondral bone formation. The types of bone formation in DO are exemplified below. As the regenerate matures, the zone of primary trabeculae significantly decreases and later fully resorbs (Komuro et al. 1994). The consolidation phase is affected by several factors including the amount of distraction and the age of the patient (Yasui et al. 1993). The reported consolidation period for mandibular DO is 1-4 weeks in children and 6-12 weeks in adults. This can extend to 6 months for other craniofacial bones and even more in long bones (Chin and Toth 1996).

### 5.4.3. Type(s) of Bone Formation in DO

Bone formation is an intricately balanced development that is coordinated by a complex network of signaling pathways. Although bone formation in DO is mostly intramembranous (Aronson 1997; Farhadieh et al. 2000; Campisi et al. 2003), endochondral bone is also present (Windhager et al. 1995). Our own previous works, though, have shown that endochondral ossification occurred rather *significantly* in DO (Walsh et al. 1994; Hamdy et al. 1997). The major difference between those two types of bone formation is the presence or absence of an intermediate cartilaginous phase (Zelzer and Olsen 2003). During **intramembranous bone formation**, mesenchymal precursor cells proliferate and differentiate directly into osteoblasts that produce a collagen matrix known as osteoid. The osteoblasts then begin to mineralize this osteoid forming a primary immature bone tissue called woven bone which slowly matures into lamellar bone (Zelzer and Olsen 2003). On the other hand, **endochondral bone formation** involves mesenchymal cells that condense and differentiate into chondrocytes that secrete an avascular cartilaginous matrix containing type II (Col2) and type X (Col10) collagen. The hypertrophic, differentiated chondrocytes proceed to mineralize the surrounding cartilaginous matrix. This calcified matrix is then infiltrated by vascular tissue and the process of angiogenesis attracts osteoclast precursors to the new bone. The osteoclasts excavate the hematopoietic bone marrow cavity while new osteoblasts are recruited to replace the cartilage scaffold with bone matrix (Zelzer and Olsen

2003). A third mechanism of bone formation in DO has also been described and is referred to as **transchondroid ossification** (Yasui et al. 1997). Herein, cartilage forms except it is *directly* transformed into bone rather than by the traditionally accepted endochondral pathway (Li et al. 1999).

It is generally accepted that perhaps either ossification process or a combination of more than one process occur in the same time. The percentage of new bone formation in DO will therefore, vary from one specimen to another, from one species to another and will depend on numerous factors, particularly the osteotomy, the stability of the fixation and both the timing and rate of distraction (Farhadieh et al. 2000; Li et al. 2000; Kusec et al. 2003) possibly explaining some of the discrepancies noted in the literature.

## 5.5. Clinical Applications of DO

As portrayed earlier, DO is a well-established and widespread surgical technique largely practiced in the orthopaedic field with applications in bone lengthening and correction of limb length discrepancies, filling segmental bone defects, treating angular deformities and fracture non-unions following trauma, debridement after severe cases of osteomyelitis and resections of malignant bone tumors. Nevertheless, the application of DO is also common in the field of reconstructive surgery particularly in the craniofacial complex where patients with cranio-maxillofacial anomalies/deficiencies benefit from mandibular, maxillary and alveolar DO (Batra et al. 2006; Yamauchi and Takahashi 2006).

It is worth mentioning that in 1973, Snyder first described the use of the Illizarov technique to lengthen a surgical osteotomy in a canine model (Costantino et al. 1993) while the first human mandibular DO was performed by McCarthy in 1989 and reported in 1992 (McCarthy et al. 1992). Today, patients undergo DO for the treatment of craniofacial microsomia, craniosynostoses, Nager's syndrome, Treacher Collins syndrome, Pierre Robin sequence, post-traumatic temporomandibular joint (TMJ) or TMJ growth disturbances, bone transport of the jaw and a variety of other sporadic developmental anomalies in the lower jaw including mandibular lengthening and widening for the correction of obstructive sleep apnea and upper airway obstruction (in cases of bilateral mandibular hypoplasia and children

dependant on tracheostomy) and alveolar reconstruction for the placement of dental implants (Swennen et al. 2001; Cascone et al. 2005; Smith and Senders 2005; Chiapasco et al. 2006). Hence, a variety of internal, external and miniature distraction devices have been developed in recent years as displayed in Figure 5.5.

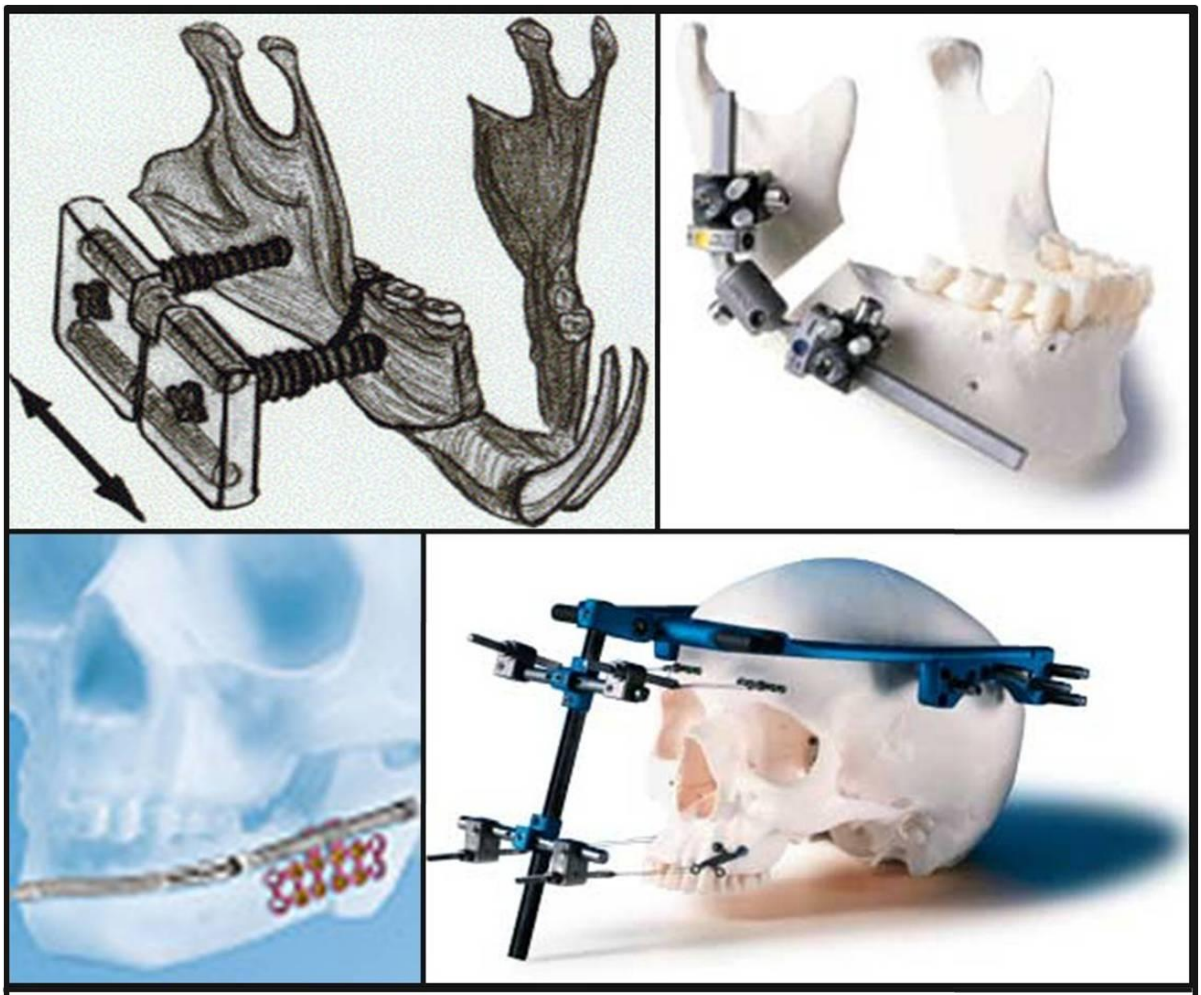

**FIG 5.5.** Examples of craniomaxillofacial distraction systems (external and internal distraction devices) that are used to gradually lengthen the mandible body and ramus. The top left schematic is for Snyder's work in a canine model (Costantino et al. 1993). The other images are available online at www.us.synthes.com

### 5.5.1. Clinical Problems and Limitations of DO

The **main problem** of DO today whether in orthopaedics or craniofacial applications remains to be the protracted time required for the newly-formed bone in the distracted zone to consolidate during which the external (*usually*) fixator needs to remain in place, as highlighted throughout this thesis. This often results in several side effects, medical and socio-economic problems for the patient and his/her family; especially when the treatment period can last as long as 12 months if not more in some cases. A number of the clinical drawbacks from the *extended* external fixation include pin tract infections, cutaneous scars, bone infections, soft tissue swelling, pain, the necessity of a secondary procedure for removal of *internal* devices as well as psychological effects (Paley 1990). Other issues are related to the patient's age and the surgical specifics of the osteotomies including neurovascular and dental injuries. Therefore, **accelerating DO** and specifically distraction and consolidation by enhancing the quantity and quality of bone formation would shorten the length of time the fixator has to be kept *in situ*, thus improving patient comfort, compliance and the overall outcome of the treatment, especially in children.

### 5.5.2. Attempts to Accelerate Bone Formation in DO

Over the last decades, several approaches have been explored to accelerate osteogenesis, including mechanical (Walsh et al. 1994; Meyer et al. 2001), electrical and electromagnetic stimulation (Hamanishi et al. 1995), low-velocity ultrasound (Shimazaki et al. 2000), the use of growth hormones (Mosekilde and Bak 1993), Prostaglandin E2 (Keller et al. 1993), bone marrow extracts (Hamanishi et al. 1994), demineralized bone matrix (Hagino and Hamada 1999), osteoblast-like cells transplantation (Tsubota et al. 1999), mesenchymal stem cells (Kitoh et al. 2004) and bisphosphonates (Little et al. 2003). Although some approaches have shown potential, none have yet shown any efficiency in human trials.

Thus far, *low-intensity pulsed ultrasound* (LIPUS) is one of the most successful attempts investigated. It has shown effectiveness in fracture repair (Leung et al. 2004). In DO, it has been used in animal models (Mayr et al. 2001; Chan et al. 2006) and in humans (El-Mowafi and Mohsen 2005; Gebauer et al. 2005). However, these studies have shown **no** significant

differences in bone mineral density or biomechanical strength between the treated and untreated calluses. Moreover, it is still unclear which mechanism translates the mechanical forces generated by the LIPUS into new bone formation (Claes et al. 2005). In another example, it was suggested that the external mechanical tension exerted during DO is what determines differentiation between chondrocytes and osteoblasts. And so, the type of new bone formation involved might be directly related to the magnitude of the strain or stimulus applied (Meyer et al. 2001).

### 5.5.3. Protein Therapy and BMPs in DO

#### 5.5.3.1. BMPs in Bone Formation

Bone contains a cocktail of morphogens including transforming growth factor beta (TGF-β), platelet-derived growth factor (PDGF), bone morphogenetic proteins (BMPs), insulin-like growth factors I and II (IGF-I and IGF-II) and fibroblast growth factors (FGFs). Generally, bone formation by BMPs is an orderly sequence involving the recruitment of undifferentiated mesenchymal progenitor cells and driving osteogenic precursors down the osteoblasts, osteoclasts and chondroblasts differentiation pathways, consequently stimulating bone formation in vivo (Urist 1965). Many cell types synthesize BMPs as large precursor molecules (Figure 5.6) with a region containing seven cysteine residues at their carboxy-terminal ends, common among all members of the TGF-β superfamily. BMPs are composed of an amino acid terminal sequence of 15 to 25 amino acids, a poorly conserved pro-domain that varies from 20 to 375 amino acids and a carboxyl terminal domain of 110 to 140 amino acids (Kingsley 1994). Proteolytic cleavage releases the mature carboxyl terminal domain from the pro-domain and following folding and dimerization possible also with other BMPs, it becomes biologically active (Wozney 1992). For example, mature BMP-2 is a homodimer of two 114-peptides subunits. Dimeric molecules can be either homodimers (when both subunits are the same) or heterodimers (two different subunits) resulting in structural and chemical differences.

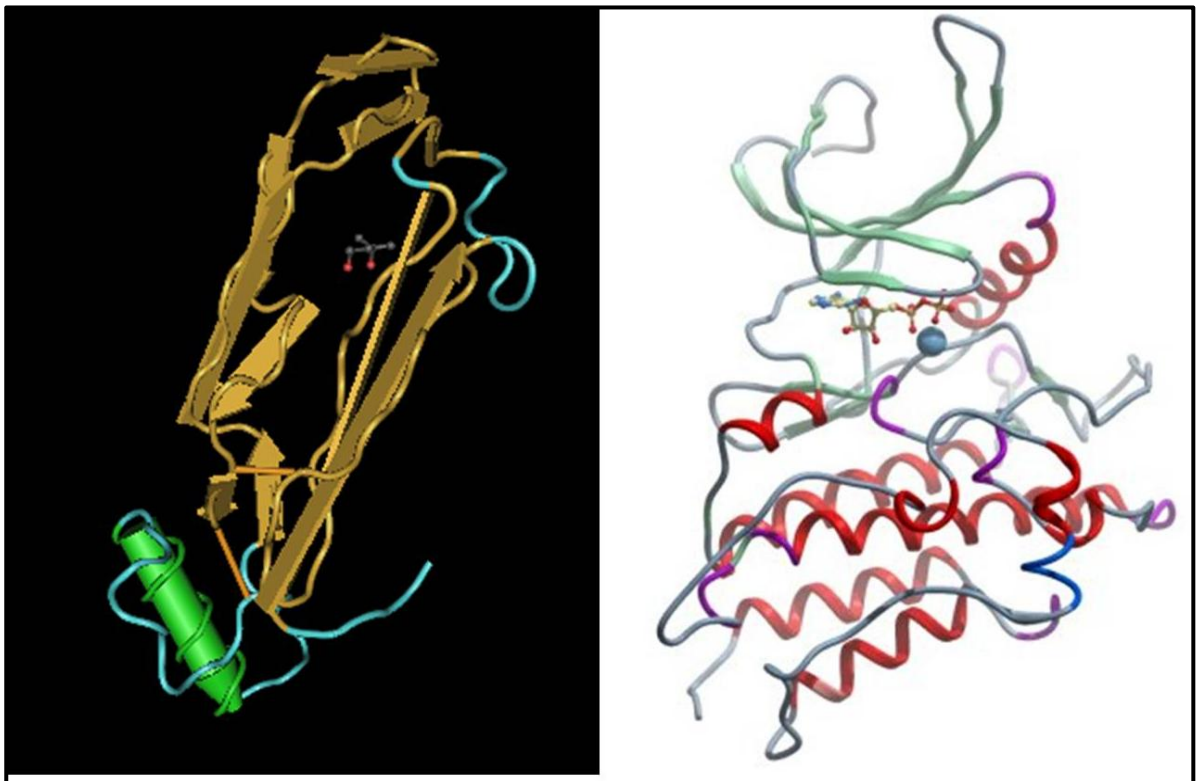

**FIG 5.6. LEFT:** Crystal structure of human BMP-2 at 2.7A resolution. **RIGHT:** BMP Receptor, type II (serine/threonine kinase) isoform1 precursor (Scheufler et al. 1999).

These differences have been suggested to explain the variations in their biologic potential and binding characteristics where heterodimer (synergy) forms of BMP-2 and OP-1 have shown greater (up to ten-fold) osteogenic potency in cartilage and bone formation when compared to BMP-2 alone (Rosen et al. 1996; Sykaras and Opperman 2003). Hence, the past speculation that BMPs act in concert in such that the induction of one BMP leads to the modulation and expression of other BMPs and subsequent chemotaxis, cellular proliferation and differentiation is valid. However, the biologic functions of individual BMPs have been reported in the literature with variance in different cell lines, culture conditions as well as anatomic sites. This was perhaps due to the differences in the protein concentrations, extraction methods and preparatory/examination conditions in addition to the specifics of targeted tissues. Also, BMPs are highly resistant to heat, denaturants and pH extremes (Wozney et al. 1988; Rosen 2006).

### 5.5.3.2. BMP Signaling Pathways in Bone Formation and during DO

Upon secretion from cells, BMPs have one of several described fates: immediately exert their actions locally, bound up by extracellular antagonists present at the site of their secretion, or enhance their biologic activities by anchoring with other proteins and receptors and become more available to target cells (Rosen 2006). Two types of receptors have been characterized and cloned, types I (high affinity) and II (low affinity). In mammalian species, type I receptors have been further divided into 7 subtypes and similarly, type II receptors to 5 subtypes (Demers and Hamdy 1999). All receptors possess intrinsic serine-threonine kinase activity (Figure 5.6). However, it is noteworthy that receptor subtypes IA (BMPR-IA) and IB (BMPR-IB) have demonstrated the greatest affinity for BMPs (than BMPR-II) and so both are required for signaling (Rosen 2006). So, two downstream signaling pathways have been identified. The first is known as the Smad cascade. Smads are intracellular proteins and are considered the major cytoplasmic signal transducers for the serine/threonine kinase receptors (Miyazono et al. 2000). The other pathway involves two mitogen-activated protein cascades (MAPK). In either case, regulation of gene transcription, results. The gene transcription mediated by BMP receptors serves to promote osteogenesis via promoting differentiation of pluripotent stem cells to differentiate into bone-forming cells in addition to cartilage-forming cells (Rosen et al. 1996; Demers and Hamdy 1999; Miyazono et al. 2000; Rosen 2006).

BMP binding (Figure 5.7.) to pre-formed BMP type I and type II heteromeric complexes activates (***S***imilar to) ***m***others ***a***gainst ***d***ecapentaplegic or Smad signaling. Eight different Smads have been identified (Smads 1 through 8) in mammals and are classified into three subclasses according to structure and mechanism of action; i.e. receptor-regulated Smads (R-Smads such as Smads 1, 5 and 8 that are BMP-activated and Smads 2 and 3 that are activated by TGF-β); common-partner Smads (Co-Smads such as Smads 4 and 3 which are common BMP and TGF-β mediated Smads) and inhibitory Smads (I-Smads such as Smads 6 and 7). The Smad signaling cascade is initiated by type II receptors where they associate with and phosphorylate type I receptors which in turn phosphorylate and activate the R-Smad proteins.

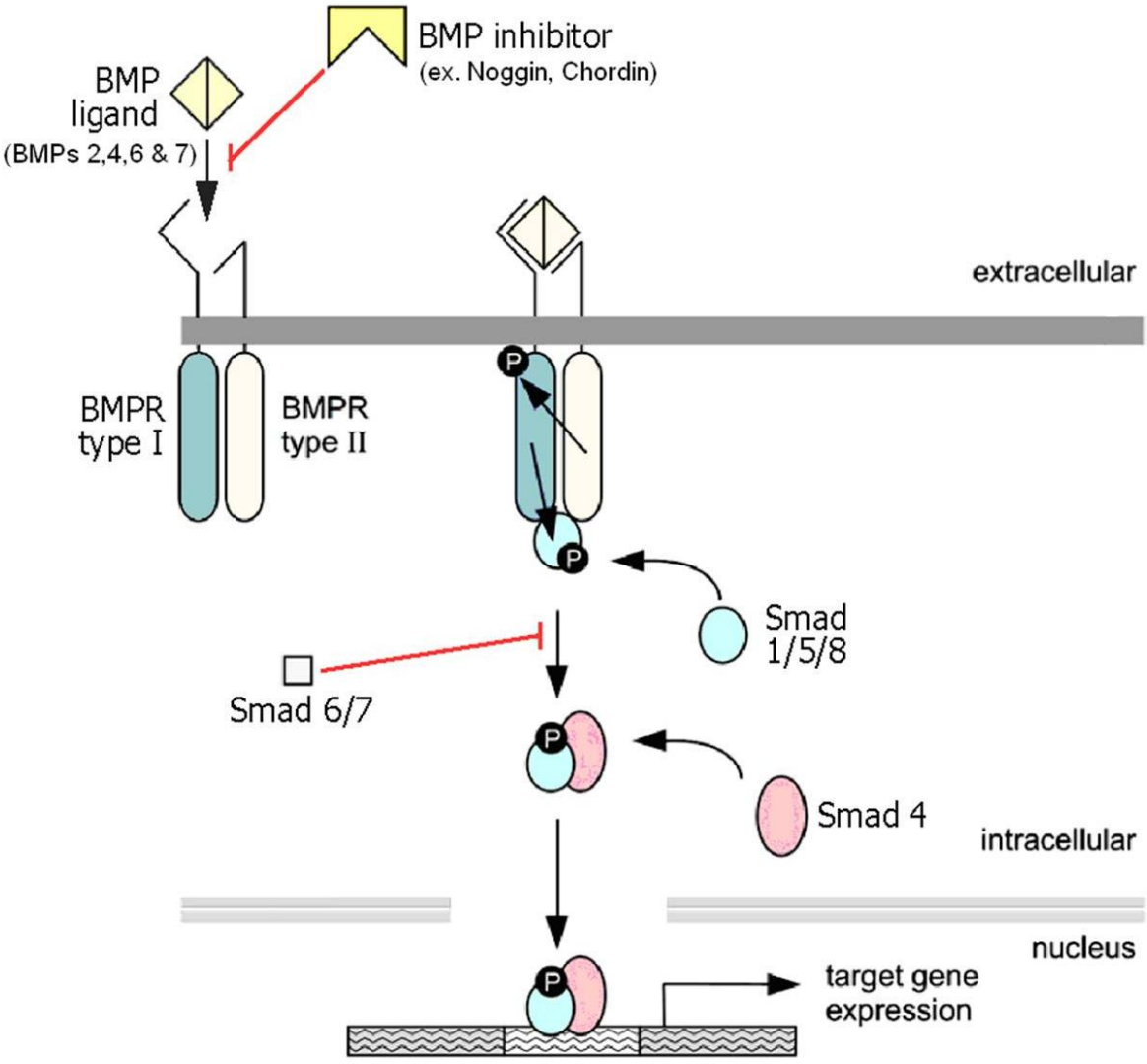


**FIG 5.7.** The BMP Signaling Pathway. Adapted from Balesman et al. 2002.

This is then translocated into the nucleus where the transcriptional activity of specific target genes (osteopontin, for example) is modified. Conversely, I-Smads negatively regulate BMP signaling by competing with the R-Smads for interactions with the other Smad subtypes and by targeting them to initiate degradation via the ubiquitin-mediated proteasomal pathway in either a ligand-independent and/or -dependant fashion (Miyazono et al. 2000; Shi and Massagué 2003). Smad-ubiquitin regulatory factor (Smurf); Smurfs 1 and 2 have been shown to specifically interact with Smads 1, 5, 6 and 7. Smurf 1 which binds to ubiquitin

through a conserved cysteine located at the carboxyl terminus of the molecule is located in the nucleus before exportation to the cell membrane and cytoplasm to induce the proteasomal degradation of type I receptors and Smads 1 and 5. Hence, Smurfs are implicated in this ubiquitin-mediated degradation process of different components of the BMP signaling pathway (Miyazono et al. 2000) where receptor turnover is enhanced (Shi and Massagué 2003; Deregowski et al. 2006). However, how the specificity of BMP-receptor signaling is determined and what regulates cell-specific production of BMPs or their receptors remain to be established, according to Rosen (Rosen 2006) where many ligands bind to the same receptors and many receptors bind the same ligands suggesting that ligand-receptor pairing is inadequate to generate a specific signal within the TGF-β superfamily. Additionally, the physiological role of BMP antagonists (interact directly with BMP ligands to restrict their biological activities extracellularly by preventing intracellular signaling and concomitantly decrease the mineralization potential; especially noted with BMP-2, -4, -6 and -7) and their interplay with their BMPs within the bone environment that has been proposed to represent a negative feedback mechanism to limit BMP action and was shown to be constantly changing with aging/illness still entail further understanding.

#### 5.5.3.3. BMPs in DO

In DO, TGF-β expression was stimulated in osteoblasts and fibroblasts within the distraction callus in humans (Holbein et al. 1995). The most recent attempts at accelerating the **consolidation phase** have been focusing on the application of certain growth factors. Okazaki et al. investigated the effects of a single local injection of rhFGF-2 into the center of the callus in a rabbit model of DO on the *final* day of distraction. An increased rate of bone formation was demonstrated evident by an increase in bone mineral content in the distraction gap (Okazaki et al. 1999). In another example, IGF-1 infusion enhanced osteoblast activity at the distraction gap in a rabbit mandible resulting in bony union (Stewart et al. 1999). It has been also shown to potentiate the osteoinductive activities of other factors although that the overall osteoinductive capacity of TGF-β was reported to be much weaker when compared to that of BMPs (Rosier et al. 1998); where among all cytokines proposed to be involved in the regulation of bone synthesis and turnover, BMPs were reported to be the only

differentiation factors able to *singularly* induce de novo bone formation in vitro as well as in vivo (Urist 1965), as discussed earlier in Chapters 3 and 4 (Haidar et al. 2009 a, b). In DO specifically, BMPs have shown great potential, BMP-2 and more often BMP-7/OP-1, suggesting to be ideal candidates for the acceleration of bone regeneration. They have both been evaluated in animal DO models of both long and flat bones with *promising* results (Hamdy et al. 2003; Zakhary et al. 2005), with also very little known about their roles and signaling pathways during the DO phases. This is again largely attributed to complexity of the molecular mechanism of bone formation as is during DO and the *unnatural* presence of distraction forces. Nonetheless, it is evident today that several different signaling pathways as well as other transcription factors (such as Runx2, Sox-9 or osterix that interact with Smads and modulate gene expression) are involved as described in the earlier paragraph. Our group is amongst those who have been focusing on this aspect for several years where for instance the optimal time for the local application of OP-1 (Mandu-Hrit et al. 2006), the expression patterns of BMPs, BMP-signaling Smads and Smad ubiquitin regulatory factors known as Smurfs (Haque et al. 2006), the role of a key markers of vascularization such as vascular endothelial growth factor and its receptors and the platelet endothelial cell adhesion molecule (Mandu-Hrit et al. 2008), the temporal and spatial profile of FGFs, IGFs and TGF-β (Haque et al. 2007), the role of BMP antagonists such as Noggin, Chordin, Gremlin and Inhibin (Haque et al. 2008) in addition to characterizing the signaling pathway of Wnts (Alsalmi et al. 2009) during DO were hitherto be determined with most not previously reported in the literature available on distraction osteogenesis or fracture healing.

It has been shown that BMPs act at the earliest stage of osteoinduction via influencing gene transcription of pluripotent stem cells to promote differentiation into osteoprogenitor cells (Croteau et al. 1999). Our group has previously characterized the temporal and spatial expression of BMPs in membranous bone formation in a rabbit mandibular DO model (Campisi et al. 2003). Interestingly, an intense OP-1 signal was detected in the vascularized connective tissue and was expressed in osteoblasts, chondrocytes and fibroblasts during the first 2 weeks of distraction. *These signals decreased significantly or were even absent during the consolidation period*. This lead to suggesting that exogenous OP-1 administered during the consolidation period when endogenous OP-1 production abruptly tapers might enhance bone formation (Hamdy et al. 2003); however was only modestly successful. Later findings

in a rabbit model of long bone DO revealed that the acceleration of new bone formation can be rather attained after the administration of OP-1 **early** (vs. at the end) during the distraction period when OP-1 receptors are abundantly expressed (Mandu-Hrit et al. 2006) and was also found to be most likely depending on a non-vascular mechanism (Mandu Hrit et al. 2008).

Findings from such studies along with the well-established call for a biocompatible, biodegradable, safe, customizable, localized and release-controlled injectable protein delivery system gave birth to the research work presented in herein as well as other ongoing studies conferred towards the end of this dissertation. Mostly, these investigations are motivated to find a way to intrinsically stimulate BMP expression as an alternative mode of treatment minimizing if not diminishing the need and associated drawbacks of supra-physiological and expensive dosages of exogenous BMPs.

## 5.6. Conclusions

DO today is a prevailing surgical technique widely used for bone lengthening and the reconstruction of and array of bone-related defects and conditions. It is not a new concept. Over the years, researchers determined that soft tissue must be kept from invading any bone-to-bone interface in order for the free bone edges to heal. Studies are underway to determine what impact genetics, growth factors and signaling pathways may further have on bone repair, how to decrease bone morbidity and to identify improvements in this surgical intervention. It has been determined that a greater distance in movement can be achieved using DO, with less disruption to surrounding tissues. Nevertheless, DO does not eliminate the underlying disease process that led to the initial bone deficiency and when performed at an early age, additional surgery may become necessary. A main limitation, however, is the long period of time required for the newly formed bone to consolidate entailing prolonged external fixation with considerable morbidity. Through genetically-modified cell lines, recombinant BMPs are being produced as singular molecular species in unlimited quantities (although still very expensive to obtain and use). On top, rhBMPs do not cause a host-versus-graft immune response and are free of infectious agents or contaminants. BMP-7/

OP-1 have been shown to accelerate the formation of new bone in numerous preclinical and clinical studies. Nonetheless, the clinical efficacy of rhOP-1 will depend on the carrier used to ensure a sustained, multi-step, and prolonged delivery of adequate protein concentrations to the desired site of tissue regeneration and repair, the distraction callus and its surrounding, herein. Our previous studies have shown that several BMPs and their receptors are upregulated during the distraction period and gradually disappearing during the consolidation phase. Also, it was noted that the expression of inhibitory Smads was high during the consolidation phase suggesting that the BMP-related osteogenic activity is controlled through a negative feedback mechanism. This means that endogenous BMP production, especially OP-1, declines in osteoblasts in the consolidation phase. In addition, the BMP signaling pathway was suggested to be upregulated by the mechanical forces exerted during distraction and downregulated once these forces cease in the consolidation phase. Therefore, it was concluded that the osteogenic potential of BMPs (whether endogenous or exogenous) might be limited by the upregulation of the inhibitory Smads and Smurfs when the activity of the BMPs is at its maximum. This further provided information about the optimal time for exogenous administration of BMPs, early in the distraction period.

Based on these findings, the aim of the work (presented in Section IV; Chapter 9) was to evaluate the effect of an **early**, **single** and **localized** injection of the release-controlled core-shell nanoparticles loaded with a range of OP-1 concentrations in a rabbit DO model on new bone formation and consolidation to investigate the pursuit possibilities of (a) reducing the often necessary large, unpredictable and costly OP-1 dosages and (b) the earlier removal of the external fixation device or apparatus; for a favorable and steady therapeutic outcome.

# CHAPTER 6
# Core-Shell NPs – Formulation and Characterization

Most drug delivery systems must be biocompatible, biodegradable (at a proper rate and with no by-products), non-immunogenic, non-toxic and stable at the least. For those proteins with short biological half-lives, such delivery systems should also permit their immobilization at therapeutically-effective levels and provide their release in a predictable or metered manner over apt periods of time with the possibility of modulating or calibrating the release kinetics according to the specific requirements of a certain application (concentration, anatomical site and size among others factors), as discussed earlier.

Therefore, the *main objective* of this phase of the project was to develop a novel delivery system suitable for bioactive proteins directed by these requirements. In the present parametric study representing the first set of in vitro experiments, the formulation and physico-chemical characterization of the liposomes and the natural polymers resulting in the core-shell nanoparticles introduced and justified in Chapter 2 are reported. For the physical characteristics of the majority of drug delivery systems, particle size and surface charge are considered of paramount significance to their role in efficiently associating with biomolecules and proteins, cellular uptake in addition to systemic particle distribution, fate and stability.

Guided by these basic necessities, the initial challenge was to formulate with reproducibility, stable cationic liposomes suitable for the later build-up of alginate and chitosan. It was also deemed favorable to have the ability to produce these liposomes in a time-effective manner. Therefore, the cationic surfactant used was explored in a range of molar concentrations (4% to 19%), cholesterol was incorporated to strengthen the lipid bi-layer and extrusion/filtration of the vesicles was optimized to yield small, monodisperse and stable lipid vesicles in approximately 60 minutes per 8-9 mL. For the polymers and the subsequent layer-by-layer self-assembly forming the shell around the liposomal core, the pH, volume ratio, incubation and centrifugation times were optimized to finally result in cationic, spherical, monodisperse

and stable nanoparticles (even upon freeze-drying/rehydration) as small as 350 nm. For the proof of concept, bovine serum albumin was incorporated as a model protein and the encapsulation efficiency, loading capacity and release kinetics from both, uncoated and coated liposomes determined.

The results of most of these experiments were reported in a manuscript published in the peer-reviewed *Biomaterials* and are reproduced next. A reprint is included in Appendix C. Relevant information regarding some of the materials, methods and analytical techniques applied in this work are further described in Appendix A. Supplementary experiments not reported herein are included in Appendix B.

# Protein release kinetics for core-shell hybrid nanoparticles based on the layer-by-layer assembly of alginate and chitosan on liposomes

**Ziyad S. Haidar[a-d], Reggie C. Hamdy[b,d], Maryam Tabrizian[a-c]**

[a] *Faculty of Dentistry, McGill University, Montréal (QC) Canada*
[b] *Center for Biorecognition and Biosensors, McGill University, Montréal (QC) Canada*
[c] *Department of Biomedical Engineering, Faculty of Medicine, McGill University, Montréal (QC) Canada*
[d] *Shriners Hospital for Children and Division of Orthopaedics, McGill University, Montréal (QC) Canada*

Received 10 September 2007; Accepted 6 November 2007, Available online 10 December 2007

## 6.1. ABSTRACT

The present work is focused on the formulation of core-shell nanoparticles via the layer-by-layer (L-b-L) self-assembly technique for delivery of biomacromolecules; such as bone growth factors. The drug encapsulation efficiency of liposomes are enhanced with the increased stability of polyelectrolyte systems achieved through the alternate adsorption of several layers of natural polymers; anionic alginate and cationic chitosan on cationic nanosized phospholipids vesicles. The resulting particles were characterized for their size, surface charge, morphology, encapsulation efficiency, loading capacity and release kinetics over an extended period of 30 days. The L-b-L deposition technique succeeded in building a spherical, monodisperse and stable hybrid nanoparticulate protein delivery system with a cumulative size of 383 ± 11.5 nm and zeta potential surface charge of 44.61 ± 3.31 mV for 5 bi-layered liposomes. The system offers numerous compartments for encapsulation including the aqueous core and within the polyelectrolyte shell demonstrating good entrapment and sustained linear release of a model protein, bovine serum albumin, *in vitro*. Our results demonstrate that this delivery system features an extended shelf-life and can be loaded immediately prior to administration, thus preventing any loss of the protein.

**Keywords:** *Controlled drug release; Liposome; Polysaccharide; Self-assembly*

## 6.2. Introduction

The recent advancements in the field of biotechnology have led to the development of abundant recombinant protein-based drugs such as vaccines, enzymes and hormones. Yet, since their isolation and purification, optimizing a delivery mechanism continues to be the primary obstacle for the clinical introduction of many protein-based drugs (Solheim 1998; Li and Wozney 2001). Predominantly due to their short biological half-life, lack of long-term stability, tissue-selectivity, potential toxicity and risk of carcinogenic activity (Luginbuehl et al. 2004). Hence, repetitive highly-dosed injections are often required to obtain the intended therapeutic efficiency, without causing any toxicity or other side effects. The optimal carrier would preserve the biological activity and viability of the protein, prevent its rapid clearance, and, preferably release it in a predictable or metered manner. Accordingly, the development of such new protein-based drugs coincides with the development of custom-made and release-controlled delivery systems (Li and Wozney 2001; Luginbuehl et al. 2004; Crommelin et al. 2003; Davis and Illum 1998; Richardson et al. 2001).

Liposomes are the commonly investigated vehicles for delivery of therapeutic compounds, such as enzymes (Illum and Davis 1991; Chaize et al. 2004) because of their biocompatibility and appealing ability to carry hydrophobic and hydrophilic drugs. Nonetheless, stability *in vivo* remains a setback, due to their high tendency to degrade or aggregate and fuse leading to leakage of the entrapped drug during storage or after administration. Additionally, they are rapidly cleared from the circulation via uptake by the cells of the reticulo-endothelial system (Takeuchi et al. 2000). To overcome those problems, varying the size of the liposome (Takeuchi et al. 1998; Takeuchi et al. 2001) or modifying the liposomal surface via coating with a single layer of hydrophilic polymers have been investigated (Charrois and Allen 2003). Accordingly, the idea of polyelectrolyte coatings obtained by the alternate deposition of polyanions and polycations emerged as a novel way to functionalize surfaces (Thierry et al. 2003; Quinn and Caruso 2004). This was quickly applied to the drug delivery field where the layer-by-layer (L-b-L) technique extended from the build-up of multi-layered polyelectrolytic films on macroscopic flat substrates (Decher 1997) to the construction of core-shell particles on various spherical templates and colloidal particles (Walker and Grant 1998; Bogdanovic et al. 2002; Yap et al. 2005). However,

particle flocculation or aggregation was difficult to overcome and thus far, the adsorption of only a single layer of biopolymer, such as polyvinyl alcohol (PVA) (Takeuchi et al. 1998) or chitosan (Galovic et al. 2002) on a charged liposomal surface has been reported. In previous work, we have been successful with the L-b-L assembly of polyelectrolytes on 2- and 3-dimensional artificial and biological systems. In addition to being non-toxic, biocompatible, biodegradable and hydrophilic, we have shown that biomolecules could be assembled and entrapped within polyelectrolyte layers, hence maintaining their bioactivity (Thierry et al. 2003; Hillberg and Tabrizian 2006). We also designed alginate-chitosan nanosized polyionic complexes for gene therapy (Douglas and Tabrizian 2005). Besides the known advantages including the size property, longer shelf-life and ability to entrap more drugs (Gref et al. 1994), nanosized systems reside longer in circulation, and therefore greatly extend the macromolecular biological activity when compared to microparticles (Desai et al. 1996).

Combining the advantages of liposomes with those of L-b-L assembly systems, we report in this work a novel core-shell release-controlled delivery system. The core is composed of charged large unilamellar liposomes (LUVs) and the shell is constructed through the L-b-L self-assembly of alternating layers of sodium alginate and chitosan. The system was characterized and loaded with a model protein, bovine serum albumin (BSA) to evaluate its encapsulation efficiency, loading capacity and release profile over an extended period. The BSA release kinetics were finally analyzed with the renowned Higuchi model (Higuchi 1961).

## 6.3. Materials and Methods

### 6.3.1. Formulation of Liposomes

LUVs were formulated via the thin-film hydration technique. A lipid phase was prepared by dissolving 1, 2-Dipalmitoyl-sn-glycero-3-phosphocholine (DPPC: Genzyme Pharmaceuticals, Switzerland), cholesterol (Sigma-Aldrich Chemical) and a cationic surfactant; dimethyldioctadecyl-ammonium bromide (DDAB: Sigma-Aldrich Chemical) in a chloroform-methanol (Fisher Scientific) mixture (4:1, v/v). DDAB was used in a 4% molar

concentration to tailor the surface charge of the liposomes. The solvent mixture was removed from the lipid phase by rotary evaporation under vacuum resulting in the deposition of a homogenous dry lipid film. The film was hydrated with highly-pure water (HPW), vortexed to obtain a suspension of positively-charged multi-lamellar vesicles and transferred into a mini extruder (Avanti® Polar Lipids, Inc.) with two 200 nm pore size 19 mm polycarbonate filters (GE Osmonics).

### 6.3.2. Preparation of Nanoparticles

Fresh alginate (AL) and chitosan (CH) 1mg/mL solutions were prepared in HPW (18.2 MΩ $cm^{-1}$). Alginic acid (low viscosity; 12 kDa molecular weight) and chitosan (85% deacetylated; 91.11 kDa molecular weight) were purchased from Sigma-Aldrich Chemical. CH solution was prepared in 1% (v/v) acetic acid aqueous solution and the final pH adjusted with 1M NaOH to 5.5. Overnight stirring and filtration followed. For the L-b-L build-up, the cationic liposomes were coated with alternating layers of negatively charged AL and positively charged CH (volume ratio of 1:2 respectively) until the desired number of polyelectrolyte layers was achieved. With the deposition of each polymeric layer, the solution was incubated at room temperature for 60 minutes under gentle stirring. Centrifugation at 1600*g* for 15 minutes in order to eliminate aggregates that may form upon the mixture of liposomes and polymeric material (washing) followed.

### 6.3.3. Characterization of Nanoparticles

#### 6.3.3.1. Particle Size, Surface Charge and Physical Stability

Average hydrodynamic diameter (size), size distribution (polydispersity index; PI) and mean count rate (MCR) of all un-coated and coated liposomes were assessed at 25°C by a particle sizer using a low-angle laser light-scattering device (HPPS, Malvern Instruments). The net surface charge was determined by zeta (ζ) potential with a ZetaPlus analyzer using laser Doppler anemometry (Brookhaven Instruments, USA). Using sucrose as a cryoprotectant, aliquots of particle suspensions were freeze-dried at -54ºC for 48 hours (Thermo Savant,

Modulyo D-115). Physical stability upon rehydration of lyophilized powders in HPW to the original volume was evaluated.

#### 6.3.3.2. Morphology

Morphological analysis was performed by atomic force microscopy (AFM). Samples were deposited onto alginate-coated silica (Si) wafers. Slides were scanned with a Nanoscope® IIIa Scanning Probe Microscope (Digital Instruments, USA) in a liquid cell at room temperature in contact mode using a silicon nitride ($Si_3N_4$) cantilever at a scan rate of 1.850 Hz.

#### 6.3.3.3. Protein Encapsulation Efficiency and Loading Capacity

Accurately weighed lyophilized nanoparticles were re-hydrated to the original volume with different concentrations of BSA (66 kDa molecular weight, Pierce Biotechnologies) solution (0 to 2.0 mg/ml). The BSA-loaded particles were separated from the un-adsorbed protein by ultracentrifugation for 30 minutes at 180000*g* and 25°C (Beckman TL-100 Ultracentrifuge). Un-adsorbed BSA in the supernatant was quantified using a colorimetric method (Micro BCA protein assay, Pierce Biotechnologies) by reading the absorbance at 562 nm (µQuant, Bio-Tek Instruments). The loading capacity (LC) and encapsulation efficiency (EE) of the nanoparticles were calculated using equations (1 and 2) (Calvo et al. 1997; Douglas and Tabrizian 2005):

$$LC = \frac{BSA_{total} - BSA_{super}}{Mass_{part}} \times 100 \quad (1)$$

$$EE = \frac{BSA_{total} - BSA_{super}}{BSA_{total}} \times 100 \quad (2)$$

where $BSA_{total}$ is the initial amount of BSA; $BSA_{super}$ is the amount of un-adsorbed albumin measured in the supernatant, and $Mass_{part}$ is the mass of the initial nanoparticles powder lyophilized.

#### 6.3.3.4. Protein Release Study

Aliquots of nanoparticle suspensions loaded with albumin were maintained at 37°C. Suspensions were then ultracentrifuged for 20 minutes at 180000*g* and 25°C to separate the nanoparticles from the supernatant containing released protein for quantitative analysis. The pellet was re-suspended in 3 ml of HPW and the procedure repeated similarly over a period of 30 days at pre-determined time points. The amount of released BSA was analyzed spectrophotometrically by measuring the protein concentration in the supernatant using the micro-BCA method and reading the absorbance at 562 nm. The cumulative amount of BSA released over the time period were calculated using the following equation (3) (Dhoot and Wheatley 2003; Kim et al. 2003):

$$\text{Cumulative protein released (\%)} = \frac{BSA_{super}}{BSA_{total}} \times 100 \qquad (3)$$

where $BSA_{super}$ is the cumulative amount of protein released at each time point and $BSA_{total}$ is the actual loading of the protein determined earlier.

#### 6.3.3.5. Modeling of Release Kinetics

To describe the release rate and characteristics of BSA from this delivery system as the square root of a time-dependant process based on diffusion, the Higuchi model (Higuchi 1961) was applied. The basic equation (4) is:

$$Q_t = \left[2DS\varepsilon\left(A - 0.5S\varepsilon\right)\right]^{0.5} \times t^{0.5} = k_H\sqrt{t} \qquad (4)$$

where $Q_t$ is the amount of drug released in time $t$, $D$ is the diffusion coefficient, $S$ is the solubility of drug in the dissolution medium, $\varepsilon$ is the porosity, $A$ is the drug content per cubic centimeter of matrix and $k_H$ is the Higuchi constant. Equation (4) can be further simplified and expressed as:

$$\frac{M_t}{M_\infty} = k_H \times \sqrt{t} \qquad (5)$$

where $M_t$ is the cumulative absolute amount of drug released at time $t$, $M_\infty$ is the absolute cumulative amount of drug released at infinite time (which should be equal to the absolute amount of drug incorporated within the system at time t = 0). Thus, the fraction of drug released is proportional to the square root of time. Alternatively, the drug release rate is proportional to the reciprocal of the square root of time.

### 6.3.4. Statistical Analysis

All experiments were done in triplicate. The results are reported as means ± standard deviations. Unpaired or paired *t*-tests were performed for all comparisons to assess for statistical significance at the 95% confidence level.

## 6.4. Results and Discussion

### 6.4.1. Particle Size and Size Distribution

The relevant size, PI, MCR and ζ-potential surface charge for bare liposomes (L; 4% DDAB) are displayed in Table 6.1. This concentration was previously investigated proving to yield stable, monodisperse vesicles where DDAB concentrations of less than 4% or more than 19% were reported to alter the colloidal stability of the liposome suspension (Crispin et al. 2002). The buildup of multi-layers on LUVs was accompanied by an increase in particle size, as determined by HPPS.

**TABLE 6.1.** Average size, polydispersity (PI), mean count rate (MCR in kcps) and zeta (ζ) potential surface charge of bare liposomes with 4% DDAB concentration

| Size (nm)* | SE | PI* | SE | MCR* | SE | Zeta (mV)* | SE |
|---|---|---|---|---|---|---|---|
| 180 | 10.5 | 0.227 | 0.015 | 257 | 1.64 | +35.48 | 2.159 |

Values are reported as mean (*) ± standard error (SE) of the mean.

The mean particle diameter of initial LUVs is 180 ± 10.5 nm versus 345 ± 10.9 nm for liposomes coated with six polyelectrolyte layers (Figure 6.1). It is noteworthy that the adsorption of the first chitosan layer [L(AL-CH)] on a previously adsorbed alginate layer [L(AL)] causes a decrease of the mean particle size; especially noticeable with the first two layers stabilizing afterwards. This behavior might be explained by the ability of the shorter polymer chains of alginate to easily diffuse between the longer polymer chains of chitosan due to the strong ionic electrostatic interactions and complexation of the polymers forming a denser network (Calvo et al. 1997). As we reported in a previous work (Douglas and Tabrizian 2005), low-molecular weight chitosan favored the creation of smaller chitosan-alginate nanoparticles, as compared to high-molecular weight chitosan. These results are displayed in the insert of Figure 6.1. Moreover, the PI is a measure of dispersion homogeneity, ranging from 0 to 1. Values between 0 and 0.3 indicate a relatively homogeneous dispersion (Chu et al. 1991). As shown in Figure 6.2a, the PI tends to decrease

with the addition of polymers nevertheless it remained in the range that indicates dispersion homogeneity (< 0.24).

The literature provides evidence that particles (< 500 nm) cross membranes of epithelial cells through endocytosis while larger particles (> 5µm) would be taken up via lymphatics (Savic et al. 2003; Zhang and Feng 2006). Dong and Feng (Dong and Feng 2004) reported

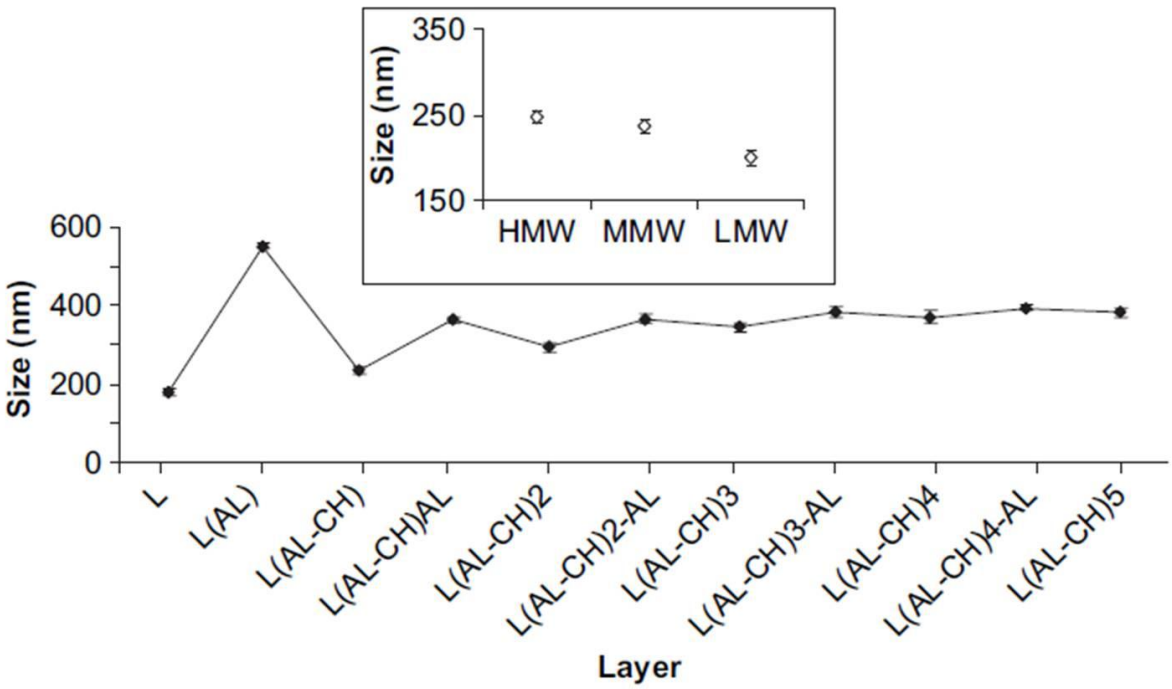


**FIG 6.1.** Average particle size change with the adsorption of each polyelectrolyte layer. The first value is for bare liposomes and continues up to the fifth bi-layer; L(AL-CH)5. **Insert:** displays change with different molecular masses of chitosan adsorbed to liposomes coated with a single layer of alginate; L(AL). Difference between the HMW (232.6 kDa) and LMW (62.53 kDa) groups is significant with $\rho$<0.05. MMW chitosan: 91.11 kDa. Values are reported as mean ± standard error of the mean.

that nanoparticles have greater ease of targeting tumors and delivering anti-cancer drugs reason being that they have higher surface area/volume ratio making it easier for the entrapped drug to be released in addition to having the advantage in permeating through the physiological drug barriers. Additionally, we monitored particle size change stored at room temperature over a period of 12 months. Figure 6.2b reveals no significant difference indicating the effect of the L-b-L self-assembly in stabilizing these nanoparticles and enhancing their shelf-life.

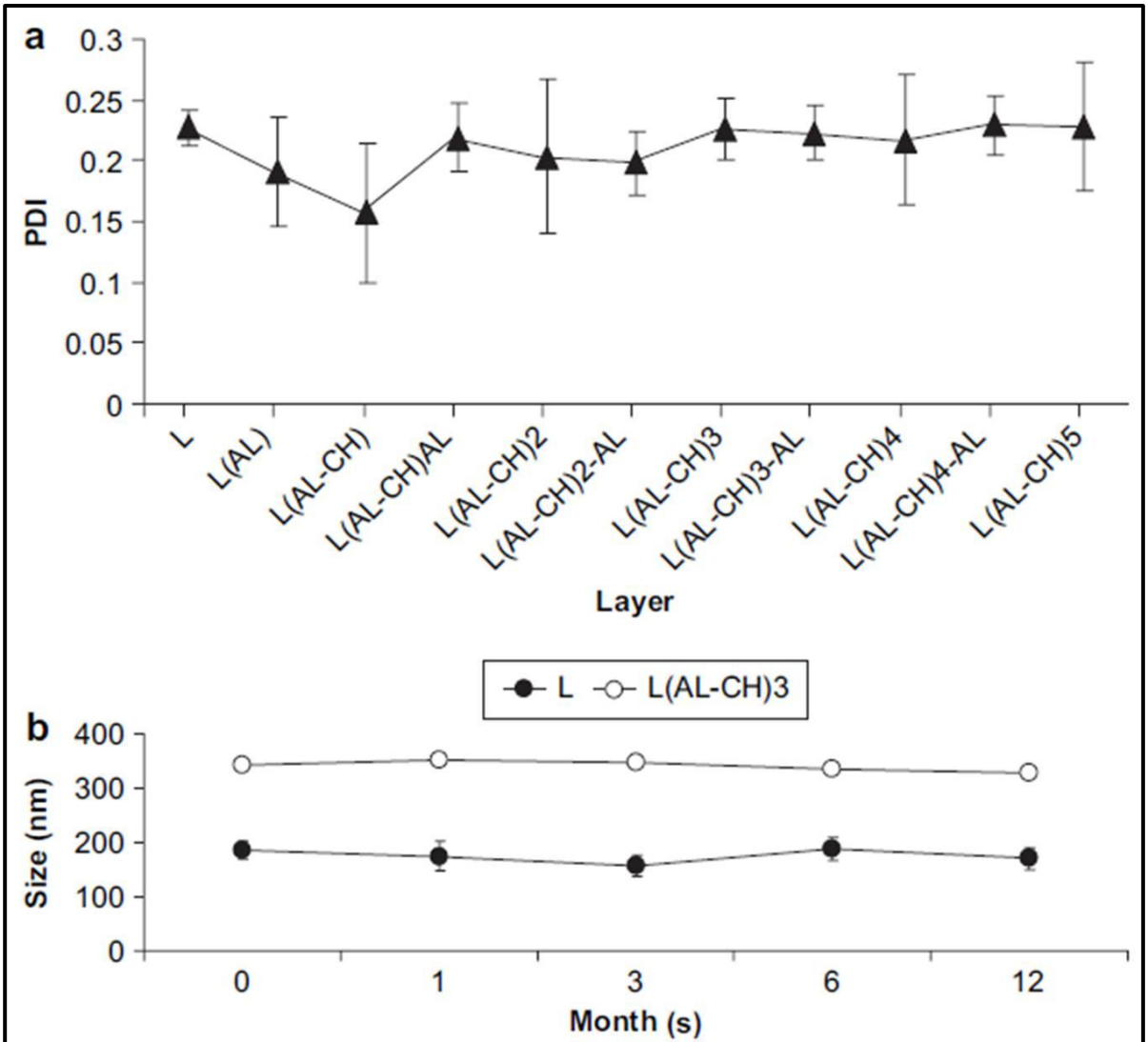


**FIG 6.2. (a)** Polydispersity index (PI) distribution accompanying the build-up of the nanoparticles. **(b)** Particle size change over time at room temperature. Values are reported as mean ± standard error of the mean. No significant differences detected.

### 6.4.2. Surface Charge and Physical Stability

The step-wise adsorption of alginate and chitosan was also monitored by measuring the ζ-potential upon addition of each polyelectrolyte layer. Besides confirming the presence and coverage of the polymer coating, ζ-potential is an important index for the stability of nanoparticulate suspensions. ζ-potential values above +30 mV or below -30 mV are generally considered to be an indication of stability and enhanced uniformity through

causing strong repulsion forces among particles to prevent aggregation (Shiqu et al. 2005). As evidenced in Figure 6.3, the adsorption of each monolayer of charged polymer induced a charge inversion on the surface with ζ-potentials in the order of 36.6 ± 2.9 mV after the addition of six layers of polyelectrolytes; L(AL-CH)3, indicating that the system is stable.

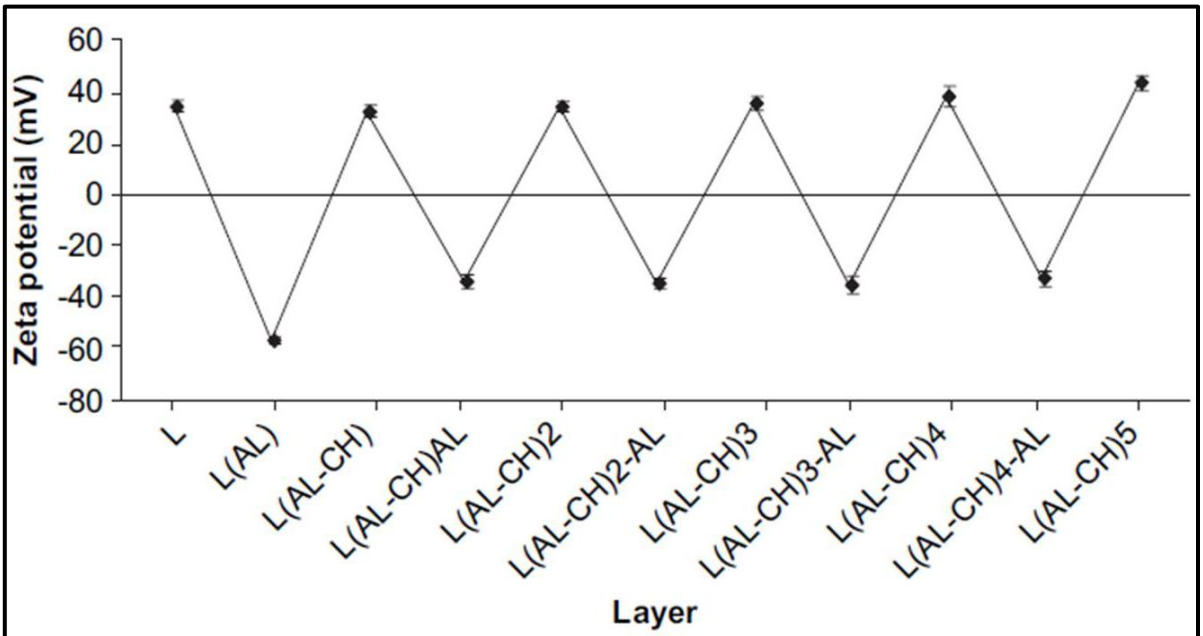


**FIG 6.3.** Zeta (ζ) potential surface charge alternation with the adsorption of each polyelectrolyte layer. The first values are for bare liposomes and continue up to the fifth bi-layer; L(AL-CH)5. Values are reported as mean ± standard error of the mean.

Furthermore, lyophilization (Bridges and Taylor 2001) in the presence of small amounts of sucrose (cryoprotectant) was carried out for this delivery system. Rationale behind freeze-drying is two-fold: (a) additional stability evaluation in terms of particle size and surface charge before and after lyophilization; and (b) loading the nanoparticles with BSA to evaluate their loading capacity, encapsulation efficiency and release profile.

Figure 6.4 demonstrates that the re-hydration of the lyophilized particles could be attained in HPW with no significant difference in particle size or ζ-potential for the coated liposomes. Sucrose seems to prevent fusion or aggregation by acting as a spacer between particles (Womersley et al. 1986). Results show that the freeze-drying/rehydration procedure works as well for polysaccharide-coated liposomes as it does for bare liposomes.

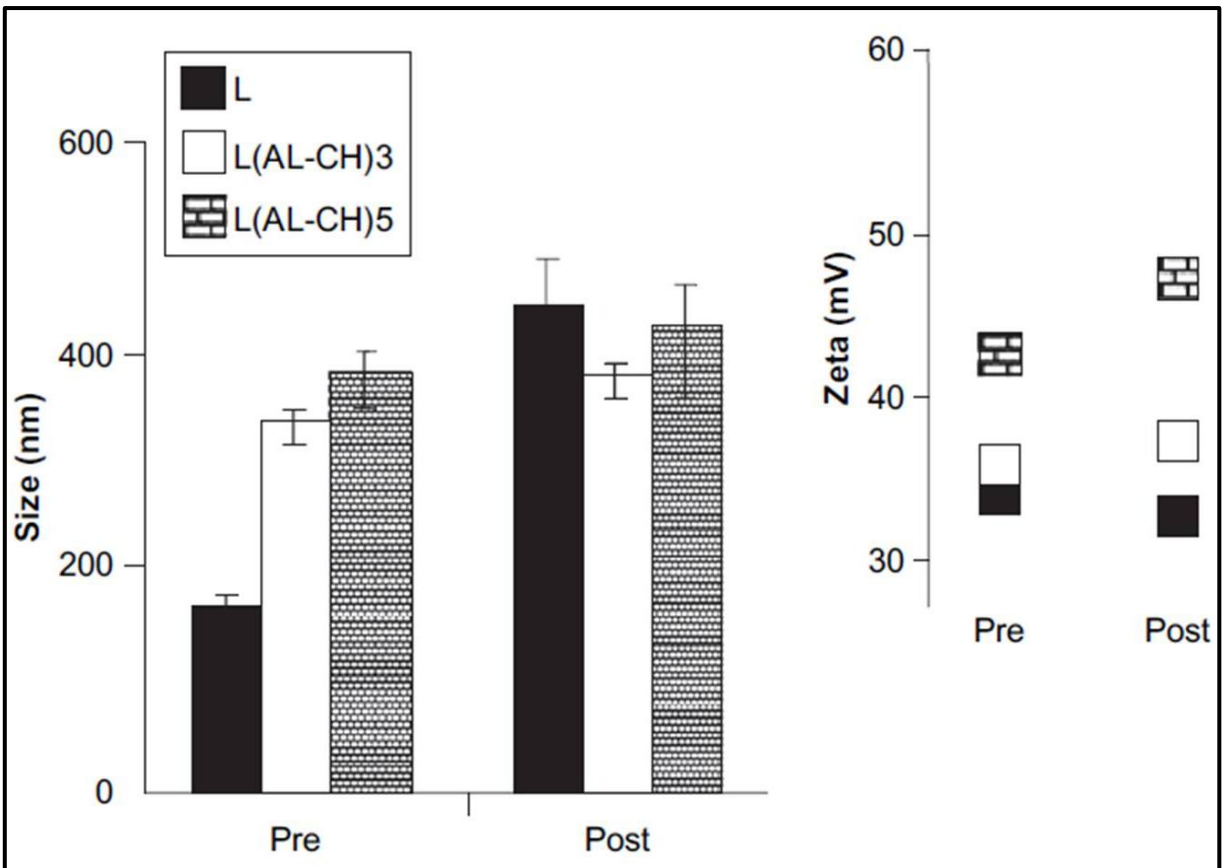


**FIG 6.4.** Stability study comparing the nanoparticle size change pre- and post-lyophilization. Values are reported as mean ± standard error of the mean. **Insert:** the ζ-potential surface charge is compared. No significant differences detected.

### 6.4.3. Morphology

AFM scanning is illustrated in Figure 6.5. Figure 6.5a shows spherical liposomes with an average size of 200 nm and Figure 6.5b illustrates 3-bilayerd nanoparticles; L(AL-CH)3 with an average diameter of 350 nm confirming HPPS readings. The height profile of un-coated

liposomes (L) amplified as an average vertical height was estimated at about 1.005 nm compared to L(AL-CH)3 with 5.042 nm as shown in Figures 6.5c and 6.5d respectively. The observed contraction in thickness is probably owing to the scanning force acting on the surface of the particles, as reported by Lulevich et al. (Lulevich et al.2003).

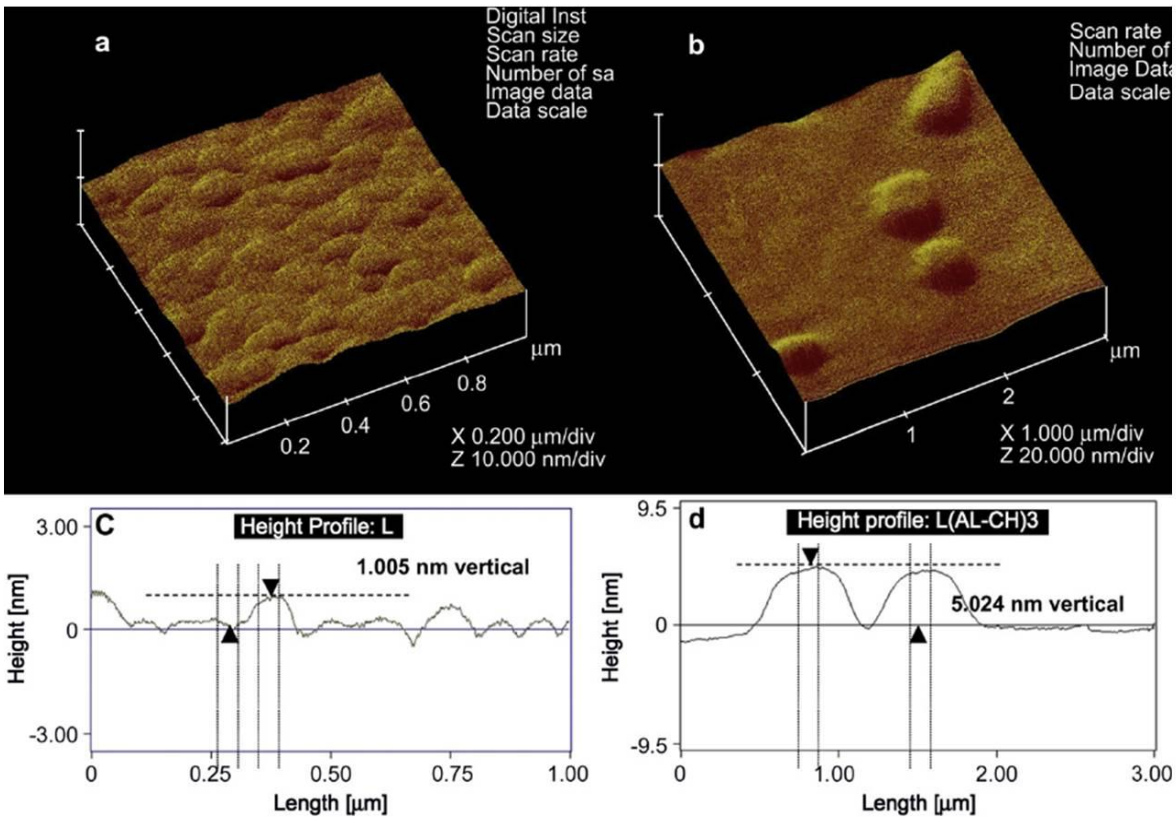


**FIG 6.5.** AFM micrographs illustrating the nanoparticle morphology of **(a)** liposomes with an average size of 200 nm and **(b)** 3-bilayered polyelectrolyte-coated liposomes with an average size of 350 nm. **(c)** and **(d)** display their relevant height profiles in nm.

### 6.4.4. Protein Entrapment Efficiency (EE) and Loading Capacity (LC)

Results of the LC and EE of our delivery system are displayed in Figures 6.6a and 6.6b. Bare liposomes (L); liposomes coated with a single layer of alginate L(AL); liposomes coated with 6 layers of alginate and chitosan L(AL-CH)3; and liposomes coated with 10 layers of

alginate and chitosan L(AL-CH)5 were loaded with different concentrations of BSA (ranging from 0 to 2.0 mg/ml). Results showed that the protein LC in all liposomes, whether coated or un-coated is directly proportional to the BSA concentration used. Generally, the LC was enhanced by increasing the initial BSA concentration, reaching a maximum of ~ 70 mg of BSA entrapped in 100 mg of nanoparticles [L(AL-CH)3 and L(AL-CH)5 for 2.0 mg/ml BSA concentration] after which a plateau seems to attain. Similarly, EE was also affected by the initial BSA concentration where the lower the concentration, the higher the EE (with a range from 0 to 0.5 mg/ml BSA). Yet, the EE tends to decrease afterwards with higher BSA concentrations. This might indicate that the optimum EE was reached; however no significant differences were detected.

Nevertheless, results demonstrate a significant difference between the EE of un-coated liposomes and coated liposomes with 3- and 5-bilayers of polymers ($\rho$<0.05). Coated liposomes can efficiently encapsulate more than double the amount than un-coated liposomes. Hence, higher LCs and EEs are achieved with the addition of the alginate and chitosan layers, enabling the system to entrap additional amounts of protein. Liposomes coated with ten layers of polyelectrolytes were able to encapsulate more than 80% of the loaded protein.

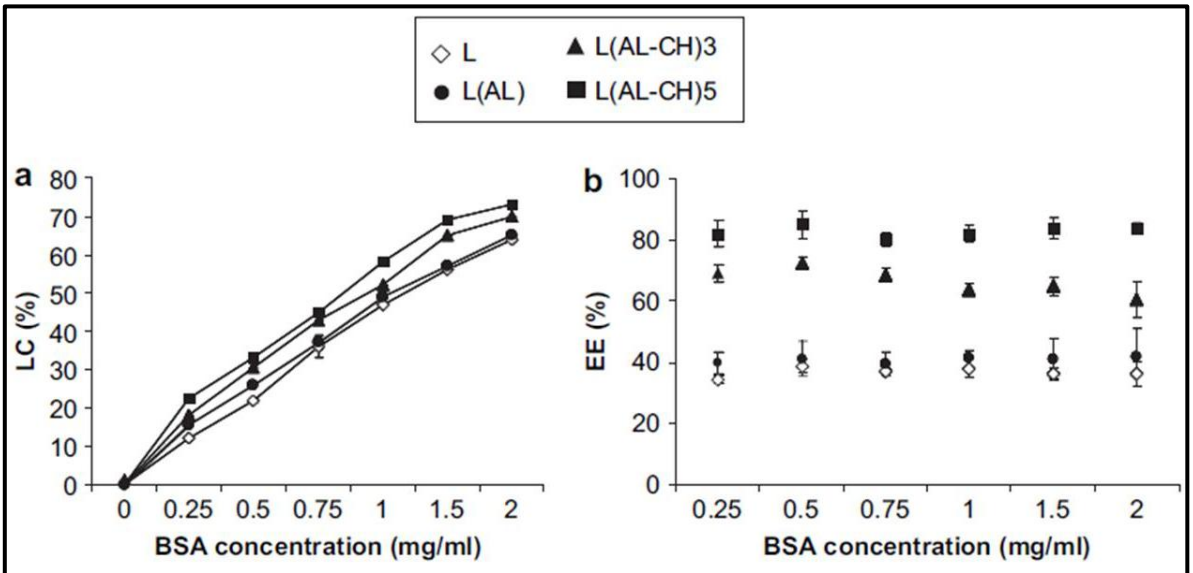


**FIG 6.6. (a)** Loading capacities (LC) and **(b)** encapsulation efficiencies (EE) per layer growth of un-coated and coated liposomes encapsulating different concentrations of BSA (mg/ml). Significant differences detected between L, L(AL-CH)3 and L(AL-CH)5 with $\rho$<0.05.

### 6.4.5. Protein Release Profile

Figure 6.7 illustrates the BSA release profiles plotted as a function of time over a period of 30 days. Figures 6.7a and 6.7b display the cumulative percentage release and the absolute release profiles at every time point, respectively. Un-coated liposomes exhibited a typical initial rapid burst effect of 60% in the first 3 days while coated liposomes displayed an elimination of this burst effect along with a slowed release of albumin (< 50%) over the extended period of 30 days. Controlled, linear and sustained release of BSA was observed throughout the study with up to 88% of BSA released over 4 weeks before reaching a plateau. According to Kim et al. (Kim et al. 2003) the molecular weight of polymers

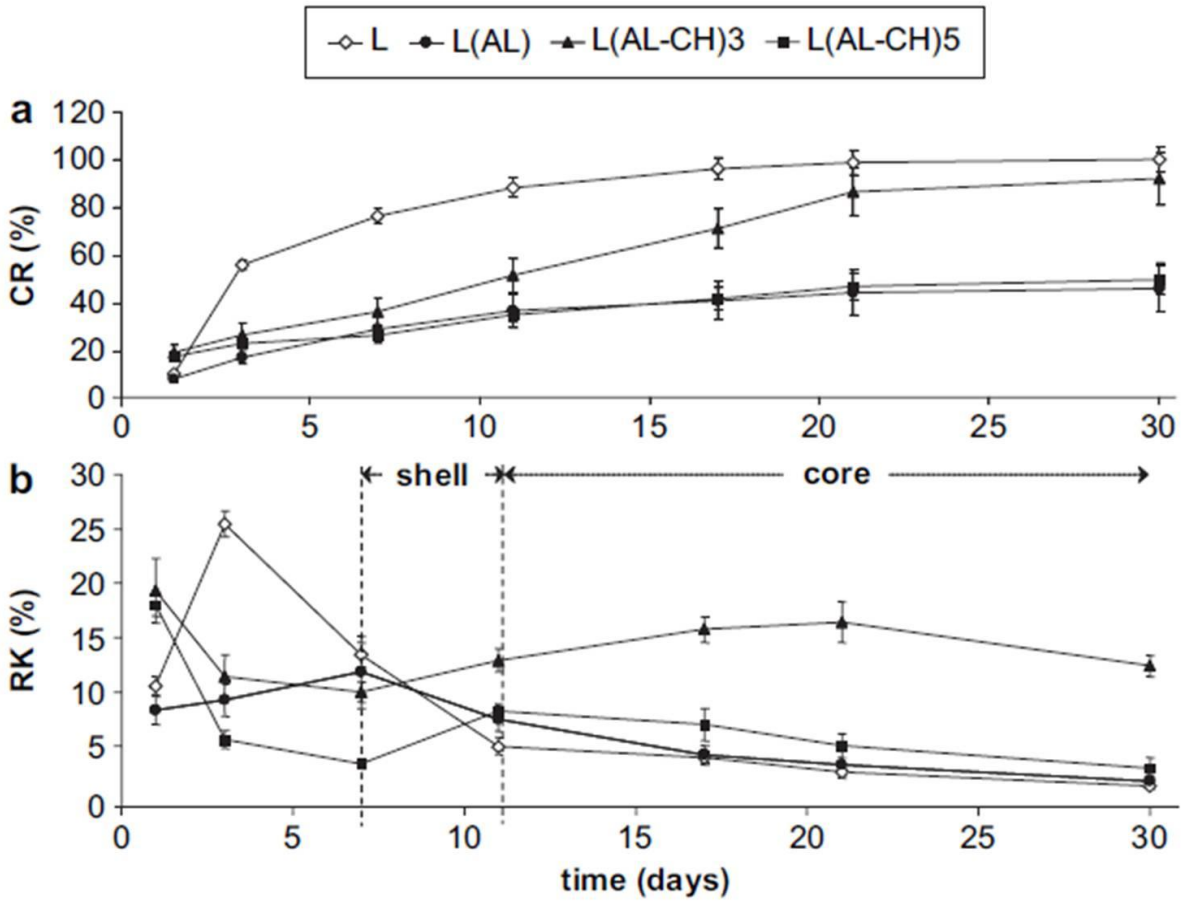


**FIG 6.7. (a)** Cumulative percentage *in vitro* release profile (CR) of BSA-loaded un-coated and coated liposomes. **(b)** Absolute percentage *in vitro* release (RK) of BSA-loaded un-coated and coated liposomes at each time point in UPW. Data represent mean ± standard error of the mean.

incorporated might have an effect on the slower release of albumin as stronger outer coating membrane forms from higher molecular weights of polymers. Conformational changes to

produce a more dense shell might have transpired with adding additional layers, mainly noticeable with the L(AL-CH)5 nanoparticles.

Figure 6.7b demonstrates the release values at each time point. Following the initial burst, BSA release from L and L(AL) starts to decrease dramatically (day 7 onwards). It seems that the effect of the single alginate layer limits itself mainly to reducing the initial BSA burst. On the contrary, BSA release from coated liposomes with 6 or more layers of polyelectrolytes displays higher release percentages in the first 2 days than L and L(AL). The fraction released during the first hours could correspond to the fraction of the free BSA that is released without control from the carrier. This represents the albumin that is physically adsorbed on the surface of the liposomes/nanoparticles. Release starts to increase again on day 7. Almost 35% of the loaded albumin in L(AL-CH)3 was released primarily from the shell followed by an increase in the release profile afterwards.

This would be from the core, decreasing again in the third week of the experiment. The release profile for L(AL-CH)5 provides evidence of the effect of polymer coating and additional compartments on exhibiting slower release profiles. Chellat et al. (Chellat et al. 2000) have previously demonstrated that the complexation of two polymers (one of which was CH) provided a protective effect for shell degradation in simulated gastric and intestinal fluids starting after 15 days. Similarly here in, the ionic interactions between the amine groups of CH and the carboxyl groups of AL seem to control the biodegradation of the delivery system, thus the delayed and longer release of protein from the core.

### 6.4.6. Release Kinetics

We have obtained a 30-day BSA release profile from multi-layered nanocapsules plotted as a function of square root of time (in days) in Figure 6.8. The data obtained has been fitted for the ideal Higuchi model based on calculation of area under the curve using the trapezoidal rule (Gohel et al. 2000). The method is exemplified for 3 experimental formulations [L, L(AL-CH)3 and L(AL-CH)5] allowing for where drug release is complete (100%) or

incomplete (< 100%) at the last sampling time. The literature provides evidence that for such systems, the Higuchi model based on the goodness-of-fit test continues to be the most appropriate model to describe the kinetics of drug release, when compared to zero-order, first-order, Hixson-Crowell's, and Weibull's models (Gohel et al. 2000).

Furthermore, it enables an understanding of the quantitative deviation of the proposed formulation from the diffusion-controlled ideal Higuchi model. The plot showed good linearity for the coated liposomes. The insert in Figure 6.8 displays the slope *K*, axis intercept *a* and squared coefficient of correlation $r^2$ from equation (5) for the release of incorporated BSA out of un-coated and coated liposomes. Diffusion seems to be the main factor controlling the release of the encapsulated BSA from this delivery system over the 30 days. The increase in coating thickness appears to decrease the rate of protein release where

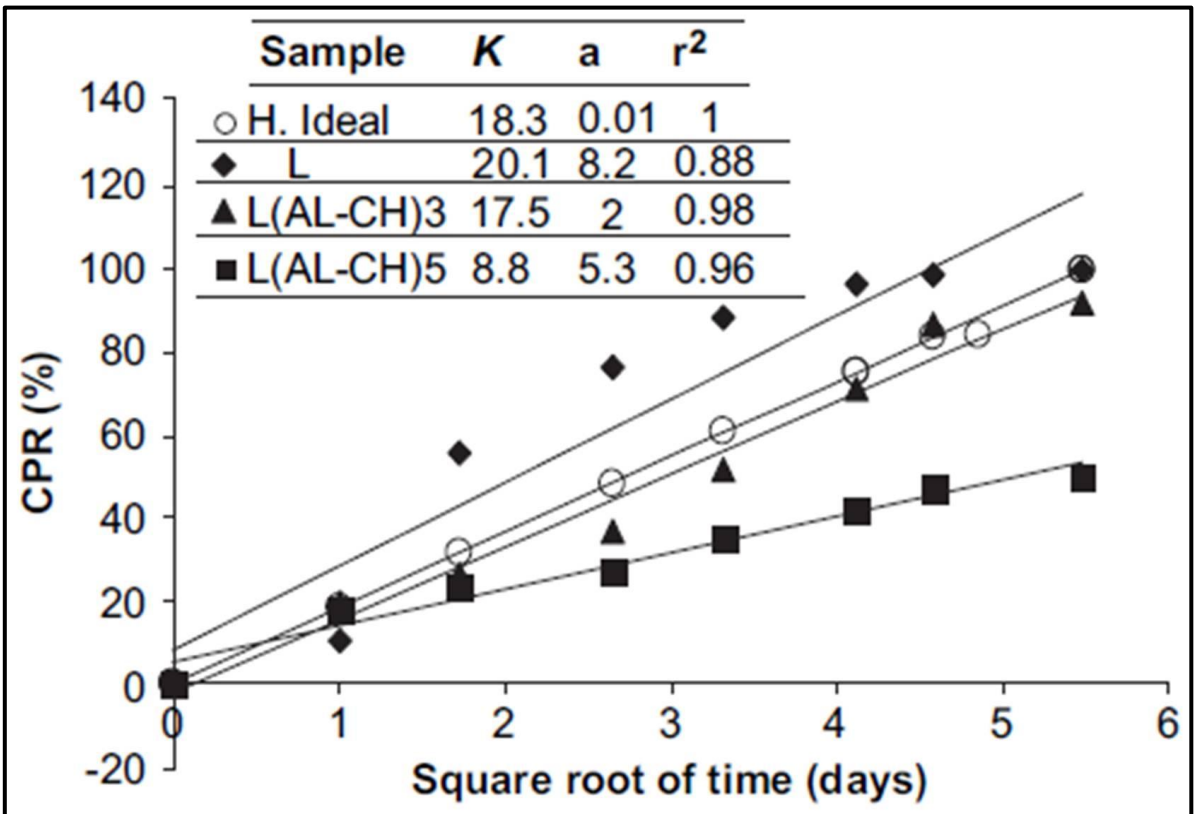


**FIG 6.8.** Release kinetics of un-coated and coated liposomes represented as cumulative protein release percentage (CPR). Release data was fitted in the Higuchi mathematical model to obtain a plot of percentage albumin release as a function of square root of time. Insert displays the release rate slope (*K*), axis intercept (*a*) and correlation coefficient ($r^2$) of albumin from the samples studies in comparison to the ideal Higuchi (H. ideal) which takes into consideration 100% release over the monitored period of time.

BSA release from un-coated liposomes is clearly faster than from coated liposomes. This might be attributed to the presence of albumin on the surface of liposomes.

**TABLE 6.2.** Release rate constants and correlation coefficients of albumin release from bare and coated liposomes showing the initial (shell) phase and the terminal (core) phase of protein release (obtained from the Higuchi plot).

| Model employed | L | | L(AL−CH)3 | | L(AL−CH)5 | |
|---|---|---|---|---|---|---|
| Higuchi | Initial | Terminal | Shell | Core | Shell | Core |
| $K$ | 10.1 ± 0.05 | 3.7 ± 0.85 | 2.84 ± 0.72 | 7.7 ± 0.49 | 1.4 ± 0.77 | 5.0 ± 0.32 |
| $r^2$ | 0.84 | 0.85 | 0.99 | 0.95 | 0.89 | 0.97 |

Finally, the rate of release was divided into an initial phase (shell release; 0-7 days) and a terminal phase (core release; 11-30 days) and fitted to the Higuchi mathematical model as well. Release rate constants (mean ± standard deviation) and correlation coefficients of BSA release from un-coated and coated liposomes are displayed in Table 6.2. The initial burst effect and rapid release of albumin is clearly noted from un-coated liposomes. On the contrary, controlled release initial and terminal phases (via L-b-L build-up) of the coated nanocapsules is demonstrated and would have a functional therapeutic use in maintaining sustained drug/protein delivery over extended periods of time diminishing lag periods.

## 6.5. Conclusion

This paper introduces a novel hydrophilic controlled-release protein delivery system consisting of a suspension of core-shell nanoparticles. Small and stable, monodisperse cationic particles (< 400 nm; PI < 0.3) were obtained by the L-b-L deposition of alternating polyelectrolytes on cationic liposomes. The system demonstrated a good capacity for the encapsulation and loading of albumin. The *in vitro* release profile suggested that albumin has been entrapped in both, the aqueous liposomal core and within the polyelectrolyte shell. These core-shell nanoparticles have the following features: (i) formulated spontaneously and rapidly under mild conditions; (ii) are nanosized and stable; (iii) have a surface charge that can be modulated; (iv) possess a high loading capacity that can be altered by the number of polyelectrolyte layers and (v) provide sustained release of the entrapped protein for extended periods of time. The system tolerates extended shelf storage and drug loading via simple

rehydration immediately preceding administration, thus preventing degradation or loss of the drug. Hence, it seems promising for the *in situ* administration of therapeutic proteins.

## 6.6. Acknowledgments

This work was supported by research grants from the Natural Sciences and Engineering Research Council (NSERC) and the Centre for Biorecognition and Biosensors (CBB). Dr. Ziyad Haidar acknowledges a post-graduate scholarship from the Canadian Institutes for Health Research (CIHR) Skeletal Health Training Program and Center for Bone and Periodontal Research in Montréal. The authors thank Dr. Julien Fatisson for his assistance in characterization, Mrs. L. Mongeon and Dr. L. Marcotte for their assistance in microscopy and Dr. F. Azari for her assistance in the protein loading and release study.

# CHAPTER 7
# Core-Shell NPs – Cytocompatibility and rhOP-1 Release

It has been often reported that most protein-loaded biodegradable *microspheres* exhibit an unpredictable tri-phasic release kinetics beginning with a considerable 'initial burst' effect at the onset, followed by a lengthy lag phase and then culminate with incomplete release despite significant polymer degradation by erosion. This so-called "initial burst" phenomenon poses a serious toxicity risk and consequently is a major hurdle for the development of drug delivery systems with marketing potential. The 'lag' phase is the period during which a very slow (close to zero) release occurs after the rapid initial burst period and usually lasts from days to weeks. During this lag phase, a patient may not be effectively treated due to the lack of sufficient drug release and delivery adding to the dilemma. For nano-sized systems, bioactivity preservation during preparation and following release is one of the most challenging issues in the field today. Commonly, drugs can be entrapped in the polymer matrix, encapsulated in a liquid core, surrounded by a shell-like polymer membrane or bound to the particle surface by adsorption. No studies have reported on a combination of these and/or within liposomes. Also, biocompatibility (safety in vivo) non-toxicity (cytocompatibility, in vitro) is without doubt vital for any drug delivery system, in general.

Following the successful application of the L-b-L self-assembly technique in formulating a suspension of hybrid core-shell nanoparticles with good encapsulation properties and sustained linear release profiles for albumin as a model drug, the second phase of the project was initiated. The main aim was to evaluate the ability of the nanoparticles to serve as an injectable release-controlled delivery system specific for bioactive BMP-7/OP-1 over longer periods of time (for later evaluation in DO) than what was accomplished previously with albumin.

Hence, in the present study representing the second set of in vitro experiments, the physical stability of the nanoparticles was further assessed in simulated physiological media and post-lyophilization/rehydration with OP-1. The potential cytotoxicity/cytocompatibility of the system was evaluated by means of monitoring the viability of preosteoblasts in culture using

MTT colorimetry (in vivo biocompatibility and safety is presented later on in Chapter 8 of Section IV). The effect of the core-shell design and the encapsulation process on maintaining the bioavailability of the immobilized protein was then examined by measuring the alkaline phosphatase activity of preosteoblasts using a micro-BCA assay.

The results of this study were reported in a manuscript published in the peer-reviewed *Journal of Biomedical Materials Research / A* and are reproduced herein. A reprint is included in Appendix C. Likewise, relevant information regarding some of the materials and analytical methods used in this work to evaluate cytocompatibility and rhOP-1 release kinetics in UPW for instance are present in Appendix A.

# Modulated release of OP-1 and enhanced preosteoblast differentiation using a core-shell nanoparticulate system

**ZS Haidar**[1, 2, 4, 5], **F Azari**[2, 3], **RC Hamdy**[2, 4], **M Tabrizian**[1, 2, 5]

[1]*Faculty of Dentistry, McGill University, Montréal (QC) Canada*
[2]*Center for Biorecognition and Biosensors, McGill University, Montréal (QC) Canada*
[3]*Department of Anatomy and Cell Biology, McGill University, Montréal (QC) Canada*
[4]*Shriners Hospital for Children and Division of Orthopaedics, McGill University, Montréal (QC) Canada*
[5]*Department of Biomedical Engineering, Faculty of Medicine, McGill University, Montréal (QC) Canada*

Received 13 March 2008; Revised 5 June 2008; Accepted 11 July 2008

## 7.1. ABSTRACT

A release-controlled OP-1 delivery system consisting of a suspension of core-shell nanoparticles was prepared. The nanoparticles were composed of a core of positively-charged large unilamellar liposomes and a shell constructed through the L-b-L assembly of alternating layers of negatively-charged sodium alginate and positively-charged chitosan. Cytotoxicity was assayed with MC3T3-E1.4 mouse preosteoblast cells and cell viability was determined by colorimetry (CellQuanti-MTT$^{TM}$ kit). The system was loaded with a range of OP-1 concentrations and the release profiles were obtained and fitted into the Higuchi model to determine release kinetics. Alkaline phosphatase (ALP) activity of preosteoblasts was evaluated using a micro-BCA assay. The resulting monodisperse and nontoxic spherical nanoparticles exhibited high physical stability in simulated physiological media as well as an extended shelf-life allowing for immediate protein loading before future administration. ALP activity increased over time with the OP-1 loaded delivery system when compared with control, protein alone, and nanoparticles alone ($\rho < 0.05$). The system offers copious compartments for protein entrapment including the aqueous core and within the polyelectrolyte layers in the shell and demonstrates a sustained triphasic linear release of OP-1 over a prolonged period of 45 days, *in vitro*. This system might offer a great advantage for optimum growth factor performance when applied in different anatomical sites of varying defect sizes and vascularity.

**Key words:** *alginate; alkaline phosphatase; bone morphogenetic protein(s); cell viability; chitosan; controlled drug release; core-shell nanoparticles; liposomes; self-assembly*

## 7.2. Introduction

Bone morphogenetic proteins (BMPs/OPs) are multifunctional osteoinductive cytokines that belong to the transforming growth factor β (TGF- β) superfamily (Ripamonti et al. 2001). BMPs exert diverse biological processes and are able to elicit osteogenesis during both, embryological bone formation and fracture repair (Ripamonti et al. 2001; Sykaras and Opperman 2003). Among the 20 BMPs identified and characterized to date, BMP-2, -4, -5, -6, -7 and -9 have shown the greatest *de novo* osteogenic capacity *in vitro* as well as *in vivo* (Xiao et al. 2007). They have stimulated bone regeneration and repair both orthotopically and heterotopically in several experimental animal models (Termaat et al. 2005). Thus, recombinant BMPs are now recognized as key factors in the arena of bone tissue engineering (Sykaras and Opperman 2003; Saito et al. 2003). They hold great potential for healing bone fractures and large osseous defects, bridging bone nonunions, preventing osteoporosis, and treating periodontal defects, in humans (Giannobile et al. 1998; Termaat et al. 2005).

For example, BMP-7 (osteogenic protein 1, OP-1) induced bone formation into muscle and between bone fragments when implanted subcutaneously (Sampath et al. 1992). Since its production by recombinant DNA technology in 1992, OP-1 has been extensively investigated for bone and cartilage regeneration in preclinical and clinical research (Vukicevic et al. 1995; Cook and Rueger 1996; Cook 1999). OP-1 has been shown to be effective in promoting bone healing in long bone nonunions, open tibial fractures as well as in spinal fusion, providing a full alternative for conventional bone grafts (Giannobile et al. 1998; Friedlaender et al. 2001; Pecine et al. 2001). Furthermore, ossification was accelerated during distraction osteogenesis following a single injection of OP-1 for correcting numerous craniofacial and orthopedic conditions (Mizumoto et al. 2003; Hamdy et al. 2003; Mandu-Hrit et al. 2006; Buxton and Cobourne 2007; Mitsukawa et al. 2007).

However, the clinical efficacy of OP-1 would depend on the carrier system used to ensure a sustained, multistep, and prolonged delivery of adequate protein concentrations to the desired site of tissue repair or restoration (Giannobile et al. 1998; Seeherman et al. 2002; Saito et al. 2003; Hamdy et al. 2003; Luginbuehl et al. 2004; Termaat et al. 2005; Seeherman

and Wozney 2005; Mandu-Hrit et al. 2006). The foremost limitations include the rapid diffusion of OP-1 away from the site of application and the loss of its bioactivity, resulting in suboptimal local induction and thus incomplete or failure of bone regeneration. Researchers over the years have investigated numerous types of carriers to deliver bone growth factors (Winn et al. 1999; Kirker-Head 2000; Li and Wozney 2001; Chen and Mooney 2003). Animal-derived collagens, while successful in many preclinical and human clinical trials (Cook et al. 1995; Geesink et al. 1999) are limited by their immunogenicity and risk of disease transmission due to their xenogenic nature (DeLustro et al. 1990; Bach et al. 1998; Butler et al. 1998). Other materials that were proposed as safer and more effective than collagen in recent years include porous inorganic hydroxyapatite (HAP)(Boden et al. 1999) and synthetic biodegradable polymers such as poly L-lactic acid (PLLA), poly D, L-lactic-glycolic acid (PLGA), and poly ε-caprolactone (PCL)(Boyan et al. 1999; Saito et al. 2003; Sung et al. 2004). However, acid degradation products resulting in aseptic inflammation and further ectopic bone formation have transpired consistently and thus far none of them have gained acceptance for human clinical investigation (Vukicevic et al. 1995; Giannobile et al. 1998). Natural, negatively-charged polymers such as hyaluronic acid and alginate have been used in gel and sponge formats yet are limited due to rapid resorption. This can be surpassed through chemical modification to decrease the intrinsic hydrophilicity of these polymers, minimizing degradation and enhancing ionic bond formation with the positively-charged BMPs (Li and Wozney 2001; Seeherman and Wozney 2005). As a result, the controlled release properties of synthetic polymers have been combined with the biocompatibility of natural polymers in recent years. Examples include PLGA-gelatin composites, collagen-PLG-alginate composites, and hyaluronan-impregnated PLA sponges (Kenley et al. 1994; Brekke 1996; Higuchi et al. 1999).

Nano- and microparticles are other dosage forms that have consummated much attention for delivery of growth factors due to their attractive tendency to amass in sites of inflammation. They can be prepared from either synthetic polymers (PLA and PLGA) or from natural polymers (gelatin and chitosan) (Lee and Shin 2007). Weber et al. (Weber et al. 2002) and Park et al. (Park et al. 2005) reported on enhanced tissue regeneration *in vivo* using PLGA and gelatin microparticles for growth factor release. When compared with microparticles,

nanoparticle delivery systems have demonstrated superiority in terms of longer residencies in general circulation, consequently extending the biological activity of the entrapped molecule (RaviKumar 2000). PLGA nanospheres immobilized onto prefabricated nanofibrous PLLA scaffolds were used to load OP-1 and to promote *in vivo* bone regeneration (Wei et al. 2007). However, significant failure of bone induction was observed due to loss of the bioactivity of the loaded protein and rapid release from the scaffolds once implanted subcutaneously in rats.

Hence, the design of a safe and effective delivery system that immobilizes biologically active growth factors, controls their release at therapeutic levels over the proper periods of time for bone induction, has release kinetics calibrated to local requirements, and ultimately degrades without soliciting unexpected side effects remains a challenge (Hollinger 1993; Cai et al. 2002). Consequently, we focused on two biodegradable natural polymeric carrier materials combined together via the layer-by-layer (L-b-L) self-assembly technique over nanoscaled liposomes to formulate core-shell nanoparticles. In a previous *in vitro* study, we have successfully encapsulated a model protein, bovine serum albumin in this core-shell controlled release system. The nanoparticles constitute a core of positively-charged large unilamellar liposomes and a shell constructed through the L-b-L assembly of alternating layers of negatively-charged sodium alginate and positively-charged chitosan (Haidar et al. 2008 a). The system had a cumulative size of 383 ± 11.5 nm and a zeta potential surface charge of 44.61 ± 3.31 mV for a five bilayered shell onto liposomes. The spherical nanoparticles tolerated extended shelf storage (up to 12 months) and had a capacity for protein loading over a concentration range of 0–2.0 mg/mL BSA. The release profile observed was characterized by an initial burst followed by sustained protein release. This release profile is highly desirable for delivering growth factors; particularly in large bony defects (Li and Wozney 2001; Seeherman and Wozney 2005).

In the present work, we investigate the ability of our core-shell nanoparticulate system to encapsulate OP-1 and its physical stability in serum as well as post-lyophilization. The release kinetics of OP-1 over an extended period of 45 days is determined. The *in vitro*

cytotoxicity of the nanoparticles and the effect of the controlled release of OP-1 from the nanoparticles on mouse MC3T3 preosteoblast cells differentiation were assessed.

## 7.3. Materials and Methods

### 7.3.1. Materials

For the preparation of liposomes, 1,2-Dipalmitoyl-sn-glycero-3-phosphocholine was purchased from Genzyme Pharmaceuticals, Switzerland; cholesterol and dimethyldioctadecyl-ammonium bromide (DDAB) were obtained from Sigma-Aldrich Chemical. The extrusion apparatus was purchased from Avanti® Polar Lipids, and the 19 mm polycarbonate filters (200 nm pore size) were obtained from GE Osmonics. For the L-b-L coating, alginic acid (sodium salt; viscosity of 2% in water) and chitosan (85% deacetylated with molecular weight of 91.11 kDa) were obtained from Sigma-Aldrich Chemical. For the cytotoxicity assay, mouse preosteoblast MC3T3-E1 subclone 14 (American Type Culture Collection, Manassas, VA) were cultured. Recombinant human OP-1 (15.7 kDa molecular weight; lyophilized) was purchased from bio-WORLD, OH. Fetal calf serum was obtained from Invitrogen™ Canada, ON. For the alkaline phosphatase (ALP) activity assay, $\rho$-nitrophenylphosphate substrate was purchased from Pierce Chemical, IL.

### 7.3.2. Preparation of Nanoparticles

Core-shell nanoparticles were prepared through the electrostatic interaction of positively-charged liposomes (L) with alternating layers of negatively-charged alginate (AL) and positively-charged chitosan (CH) according to the method described previously (Haidar et al. 2008 a). Briefly, liposomes (4% and 9%DDAB w/w) were formulated via the thin-film hydration technique, followed by extrusion through double 200 nm polycarbonate filters. For the L-b-L build-up, fresh AL and CH solutions (1 mg/mL) were prepared in highly-pure water (HPW: 18.2 MΩ $cm^{-1}$). CH solution was prepared in 1% (v/v) acetic acid aqueous solution and the final pH adjusted with 1M NaOH to 5.5. The cationic liposomes were coated with alternating layers of AL and CH until the desired number of polyelectrolyte layers was achieved (6 layers: L(AL-CH)3 and 10 layers: L(AL-CH)5). With the deposition

of each polymeric layer, the solution was incubated at room temperature for 60 min and centrifuged at 1600g for 15 min for washing.

### 7.3.3. Characterization of Nanoparticles

#### 7.3.3.1. Particle Size, Surface Charge and Physical Stability

Average hydrodynamic diameter (size) and the net surface charge (zeta potential) of all uncoated and coated 4% and 9% DDAB liposomes were assessed at 25$^{o}$C using low-angle laser light-scattering (DLS-HPPS, Malvern Instruments, UK) and laser Doppler anemometry (Zeta-Plus, Brookhaven Instruments, NY), respectively. Aliquots of particle suspensions were freeze-dried using sucrose as a cryoprotectant at -54$^{o}$C for 48 h (Modulyo D-115, Thermo Savant, MA) and the physical stability upon rehydration of lyophilized powders with OP-1 to the original volume was evaluated. Furthermore, stability over time (stored in solution at room temperature) was assessed by DLS over a period of 12 months.

#### 7.3.3.2. Cell Culture

Mouse preosteoblast MC3T3-E1.14 cells were seeded in a-minimum essential medium supplemented with 10% (v/v) fetal bovine serum and 1% (v/v) penicillin/streptomycin. Cells were allowed to attach to the plates in a humidified atmosphere of 5% $CO_2$ and 95% air incubator at 37$^{o}$C for 24 h and the media changed every 48 h. Cells were sub-cultured after reaching confluence using trypsin-EDTA. Controlled experiments were conducted on conventional well plates for each set of experiments.

#### 7.3.3.3. Cytotoxicity Assay

Cells were seeded in a 96-well plate at an initial density of 1.0 x $10^4$ viable cells/well. The following day, medium was removed and cells were treated with 200 µL of medium containing several concentrations of both uncoated and coated liposomes. Cells were incubated in treatment medium for 24 h, after which cell proliferation and viability with a linear detection range of 1,000 to 50,000 cells was performed using a colorimetric method

using 3-(4,5-Dimethylthiazol-2-yl)-2,5-diphenyltetrazolium bromide, a tetrazole (CellQuanti-MTT$^{TM}$ kit) purchased from BioAssay Systems, CA.

Briefly, treatment solutions were replaced with 100 µL fresh medium to which 10 µL of 12 mM MTT solution was added. After 4 h of incubation at 37$^{o}$C, 100 µL of SDS-HCl solution was added to each well, followed by further incubation at 37$^{o}$C. Samples were then read at 570 nm by a plate spectrophotometer (µQuant, Bio-Tek Instruments). As a negative control, 10 µL of the MTT stock solution were added to 100 µL of medium alone. The viability of cells incubated with DMEM alone was taken as 100%.

#### 7.3.3.4. Stability in Fetal Bovine Serum

To evaluate the stability of the system in simulated physiological medium, aliquots of particle suspensions (uncoated and coated liposomes) were diluted 10 times with fetal calf serum and incubated at 37$^{o}$C for 1 h, 6 h, and 24 h. The change in particle diameter was assessed by DLS.

#### 7.3.3.5. Protein Entrapment Efficiency and Loading Capacity

Lyophilized 4% DDAB nanoparticles were rehydrated to the original volume with different concentrations of OP-1 solution (0.0 to 5.0 µg/mL). The un-adsorbed protein was separated from the protein-loaded particles by ultracentrifugation for 30 min at 180,000g and 25$^{o}$C (TL-100 Ultracentrifuge, Beckman Coulter, CA). Quantification was performed using an enzyme-linked immunosorbent assay (ELISA) construction kit specific for human BMP-7 according to the manufacturer's (Antigenix America) protocol, reading the absorbance plate spectrophotometer at 450 nm. Alongside, the average size and zeta potential surface charge of the particles following rehydration with OP-1 were measured.

#### 7.3.3.6. Protein release study

Aliquots of nanoparticle suspensions loaded with OP-1 were maintained at 37$^{o}$C. Suspensions were then ultracentrifuged for 20 min at 180,000g and 25$^{o}$C to separate the nanoparticles from the supernatant containing the released protein for quantitative analysis.

The pellet was re-suspended in 1 mL of HPW and the procedure repeated over a period of 45 days at pre-determined time points. The cumulative amount of released OP-1 was analyzed spectrophotometrically by measuring the protein concentration in the supernatant using ELISA and reading the absorbance at 450 nm.

#### 7.3.3.7. Measurement of Alkaline Phosphatase (ALP) Activity

Osteogenic differentiation was screened by the expression of the activity of ALP measured via the time-dependent formation of *ρ*-nitrophenol from *ρ*-nitrophenylphosphate substrate (Pierce Chemical, IL) at pH 9.8. Cells were incubated at 2 x $10^4$ cells/well in a 24-well plate for 24 h at 37$^o$C. The following day, cells were treated with uncoated and coated liposomes for 2, 4, and 7 days. The cell layers were washed with PBS and scraped off from the surfaces by adding harvest buffer (10 mM Tris pH 7.4, 0.2% IGPAL). After sonication and centrifugation, preosteoblast cell lysate was used for the analysis of the ALP activity and the total protein level. Each reaction was initiated by adding 100 µL of *ρ*-nitrophenylphosphate to the cell lysate. The reaction was stopped after 30 min by adding 50 µL of 2N NaOH. Optical density was measured at 405 nm by a spectrophotometer on every time point to quantify the amount of *ρ*-nitrophennol produced. The values of ALP activity were normalized with respect to the total protein content obtained from the same cell lysate. Total protein content was determined using a micro-BCA Protein Assay kit (Pierce Biotechnologies, IL) following the recommendations of the manufacturer.

#### 7.3.3.8. Modeling Release Kinetics

The OP-1 release rate and characteristics for this delivery system were described as a time-dependent process based on diffusion. The renowned Higuchi model (Higuchi 1961) was applied, as described earlier (Haidar et al. 2008 a). Briefly, the protein release rate is considered proportional to the reciprocal of the square root of time expressed as quantitative deviation from the Higuchi ideal model which takes into consideration complete (100%) or incomplete (< 100%) protein release at the last sampling time.

### 7.3.4. Statistics

Statistical analysis was performed using unpaired or paired *t*-tests to assess for statistical significance at the 95% confidence level, where $\rho$-values of less than 0.05 were deemed statistically significant.

## 7.4. Results and Discussion

### 7.4.1. Preparation and Characterization of Core-Shell Nanoparticles

Spherical core-shell nanoparticles (Haidar et al. 2008 a) were formulated in mild aqueous conditions by the L-b-L self assembly of negatively-charged AL and positively-charged CH on 4% and 9% DDAB cationic liposomes. Driven by electrostatic interactions, we have previously shown how AL and CH spontaneously interact under these conditions to form a shell around the 4% DDAB liposomal core resulting in particles with small size (<400 nm) and narrow distribution (polydispersity index <0.3). DDAB is a cationic surfactant that tailors the surface charge of the particles. An increase of DDAB concentration from 4% and 9% for the preparation of nanoparticles indicated no significant difference in particle size, polydispersity, surface charge, or physical stability over time (up to 12 months) for 4% and 9% DDAB liposomes coated with up to 5 bi-layers of polymer (data not shown). In general, narrow particle size distribution (Heerklotz et al. 2004) and dispersion homogeneity were evident. Zeta potential measurements indicated an overall positive charge of 46.2 ± 0.8 mV, suitable for complex formation with anionic proteins and confirming the complete coverage of the liposomal core with the surrounding polymer shell (Shiqu et al. 2005).

### 7.4.2. Stability in Serum

Stability in fetal bovine serum evaluated by DLS did not show significant changes in the size of coated nanoparticles following incubation over time (Figure 7.1). In contrast, uncoated liposomes exhibited extensive aggregation upon 1 h incubation. Results demonstrate the protective effect of the polyelectrolyte shell in stabilizing the liposomal core and maintaining the integrity of the overall delivery system in simulated physiological media.

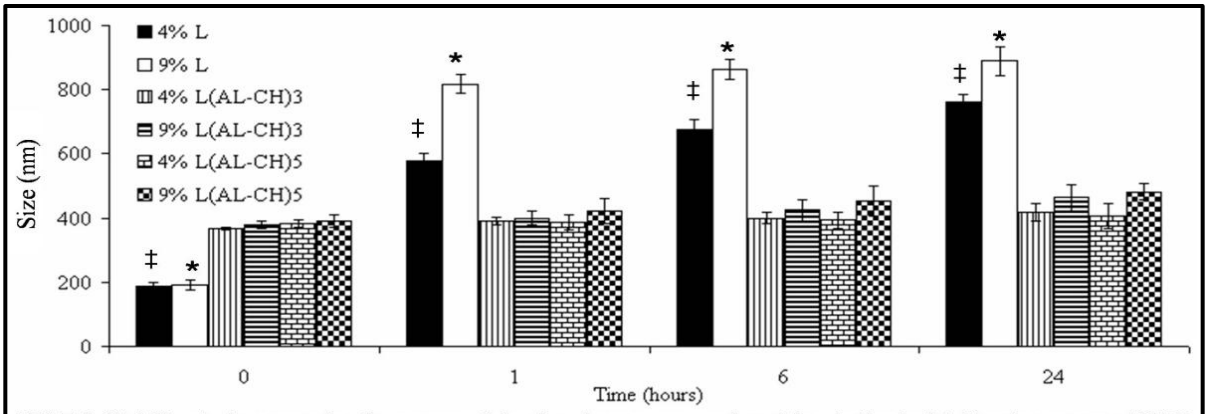


**FIG 7.1.** Stability study comparing the nanoparticle size change pre- and post-incubation in fetal bovine serum at 37°C over an exposure time of 24 h. Values are reported as mean ± standard error of the mean. Statistical significance ($\rho < 0.05$) was detected between uncoated and coated liposomes for 4% (‡) and 9% (*) DDAB concentrations.

### 7.4.3. Cytotoxicity

The viability of MC3T3-E1.4 mouse preosteoblast cells after incubation with varying concentrations of the samples over 24 h exposure time is shown in Figure 7.2. Results show that particulate systems constituting liposome cores with 4% DDAB are not toxic (96% of

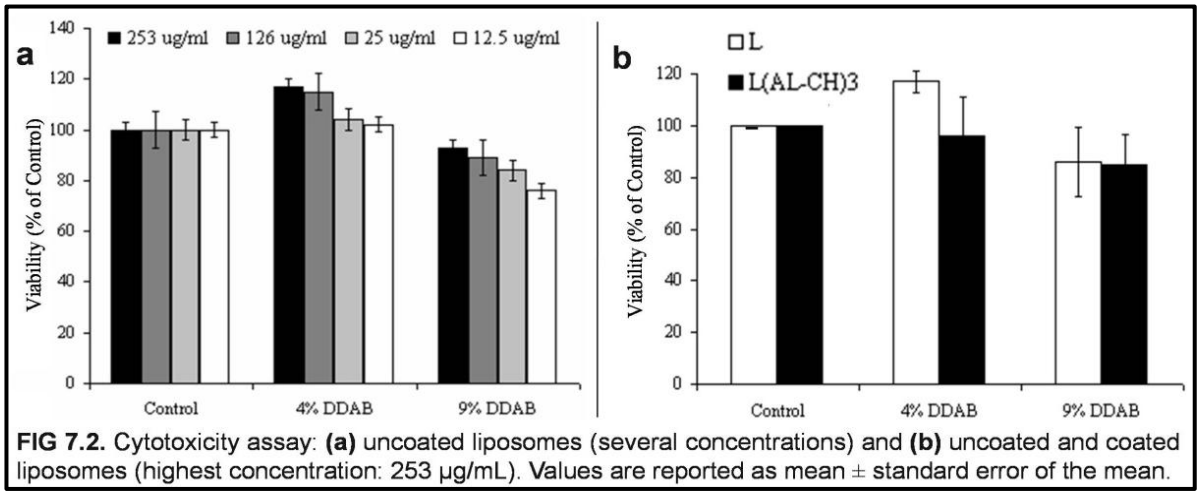


**FIG 7.2.** Cytotoxicity assay: **(a)** uncoated liposomes (several concentrations) and **(b)** uncoated and coated liposomes (highest concentration: 253 µg/mL). Values are reported as mean ± standard error of the mean.

control) to cells (12.5 through 253 µg/mL). Although the nanoparticles made of liposomes containing 9% DDAB were similar in size and surface charge, they caused a decrease in cell viability (85% of control).

This is in agreement with previous reporting that at certain concentrations of DDAB; liposomes are toxic to cells (Tabatt et al. 2004; Asasutjarit et al. 2007). Consequently, nanoparticles containing 9% DDAB were excluded from further experiments.

### 7.4.4. OP-1 Loading Capacity and Entrapment Efficiency

The loading capacity (LC) and entrapment efficiency (EE) of the nanoparticles are displayed in Figure 7.3(a, b), respectively. Liposome (L), liposome with three alginate-chitosan bilayers [L(AL-CH)3], and liposome with five alginate-chitosan bilayers [L(AL-CH)5] were loaded with different concentrations of OP-1 (15.7 kDa) ranging from 0 to 5000 ng/ mL. Results showed that the protein LC and EE in all lipid delivery systems, whether coated or uncoated, were directly proportional to the protein concentration entrapped as previously observed with bovine serum albumin encapsulation (Haidar et al. 2008 a).

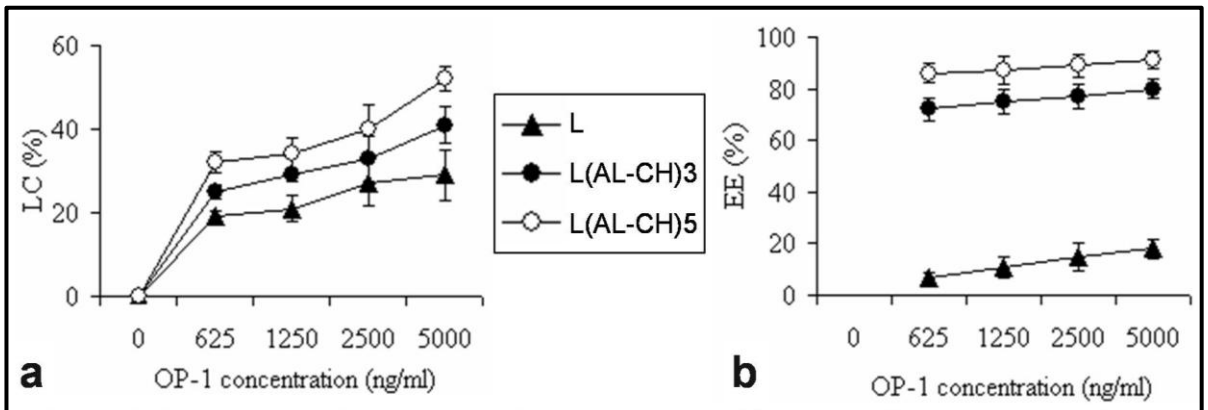


**FIG 7.3. (a)** Loading capacities (LC) and **(b)** encapsulation efficiencies (EE) per layer growth of un-coated and coated liposomes encapsulating different concentrations of OP-1 (ng/ml). Significant differences ($\rho < 0.05$) were detected between un-coated liposomes (L) and those coated with three alginate–chitosan bi-layers [L(AL-CH)3] and five alginate–chitosan bi-layers [L(AL-CH)5].

In general, the LC was enhanced by increasing the initial OP-1 concentration, reaching a maximum of 50% and 40% of OP-1 entrapped in 100 mg of L(AL-CH)3 and L(AL-CH)5 for

5000 ng/mL OP-1 concentration, respectively. The LC of OP-1 was less than that calculated with albumin-loaded nanoparticles. This might be explained by the variation in the concentration and molecular weight of the entrapped proteins. A plateau seems to emerge for loaded liposomes; however not for coated nanoparticles. In fact, they show a potential for a higher LC with elevated concentrations of OP-1. Likewise, the EE was also affected by the initial OP-1 concentration mounting with higher concentrations. Results demonstrated a significant difference between the EE of uncoated liposomes and coated liposomes ($\rho < 0.05$) only. Hence, the addition of the AL and CH layers enhances both, the LC and EE enabling the system to entrap additional amounts of the protein.

Liposomes coated with 10 layers of polyelectrolytes were able to encapsulate more than 80% of the loaded protein. DLS showed no significant changes in particle size following lyophilization and rehydration with the protein (data not shown; reported in Chapter 8) for all coated liposomes indicating the incorporation of OP-1 into the compartments of the core and shell system. This is a very interesting feature for the delivery of recombinant BMPs, because supra-physiologic doses of single growth factors in microgram ranges are essential to induce bone regeneration (Li and Wozney 2001). The required dose depends on the anatomical site being treated in terms of the degree of vascularization and number of resident responding cells in the defect site; thus, the LC and EE of the formulated nanoparticles seem to have the capacity of entrapping BMPs in a range of concentrations and amounts suitable for potential use in an array of bony defects and conditions.

### 7.4.5. OP-1 Release Profile

The ELISA assay constructed to measure the OP-1 release from the delivery system *in vitro* gave a linear absorbance response for OP-1 concentrations from 0 to 5000 ng/mL ($r^2$ = 99.8%). Figure 7.4 illustrates the OP-1 release profiles plotted as a function of time over a period of 45 days for particles loaded with 5000 ng/mL OP-1 concentration. The cumulative percentage release and the absolute release profiles at every time point in HPW are displayed in Figures 7.4(a, b), respectively. A control of the burst effect is revealed by the coated

liposomes followed by a slowed and prolonged release of OP-1. Controlled, linear, and sustained release of OP-1 was observed with up to 85% of OP-1 released over a period of 4 weeks. OP-1 release is faster than what was reported earlier with our albumin-loaded nanoparticles (Haidar et al. 2008 a). This might be attributed again to the variance in the molecular weights of the loaded proteins; 15.7 kDa versus 66 kDa for OP-1 and albumin, respectively. Hence, the smaller the protein, the faster it is to diffuse through the layers of the nanoparticles.

Figure 7.4(b) demonstrates the release values at each time point. Following the initial burst, OP-1 release from L starts to decrease dramatically. On the contrary, biphasic protein release from L(AL-CH) 3 and L(AL-CH)5 is shown where it starts to increase noticeably on day 7 and continues for over a 1 week period. Almost 12% of the loaded OP-1 in L(AL-CH)3 was released primarily from the shell. This was followed by an increase in the release profile afterwards mainly from the core, decreasing again in the third week of the experiment. The release profile for L(AL-CH)5 provides evidence of the effect of polymer coating and additional compartments on exhibiting slower release profiles even with such small proteins. The ionic interaction between the amine groups of CH and the carboxyl groups of AL are known to control biodegradation (Chellat et al. 2000), hence the delayed and longer release of OP-1 from the core. Therefore, low- or high-level sustained protein release profiles with smaller or larger initial protein bursts are feasible with the alteration in the number of polyelectrolyte layers. This is essential for optimum growth factor performance when applied in different anatomical sites of varying defect sizes and vascularity as reported earlier (Kirker-Head 2000; Seeherman et al. 2002; Chen and Mooney 2003; Seeherman and Wozney 2005; Luginbuehl et al. 2004; Li and Wozney 2004). For instance, large or critical-sized defects (Lindholm et al. 2002) that fail to heal spontaneously might require an initial high-level burst release to recruit osteoblasts to defect site, followed by an extended, low-level constant release to differentiate the cells once localized at the repair site (Luginbuehl et al. 2004; Li and Wozney 2004). This triphasic delivery system seems to have the capacity to be tailored and formulated accordingly.

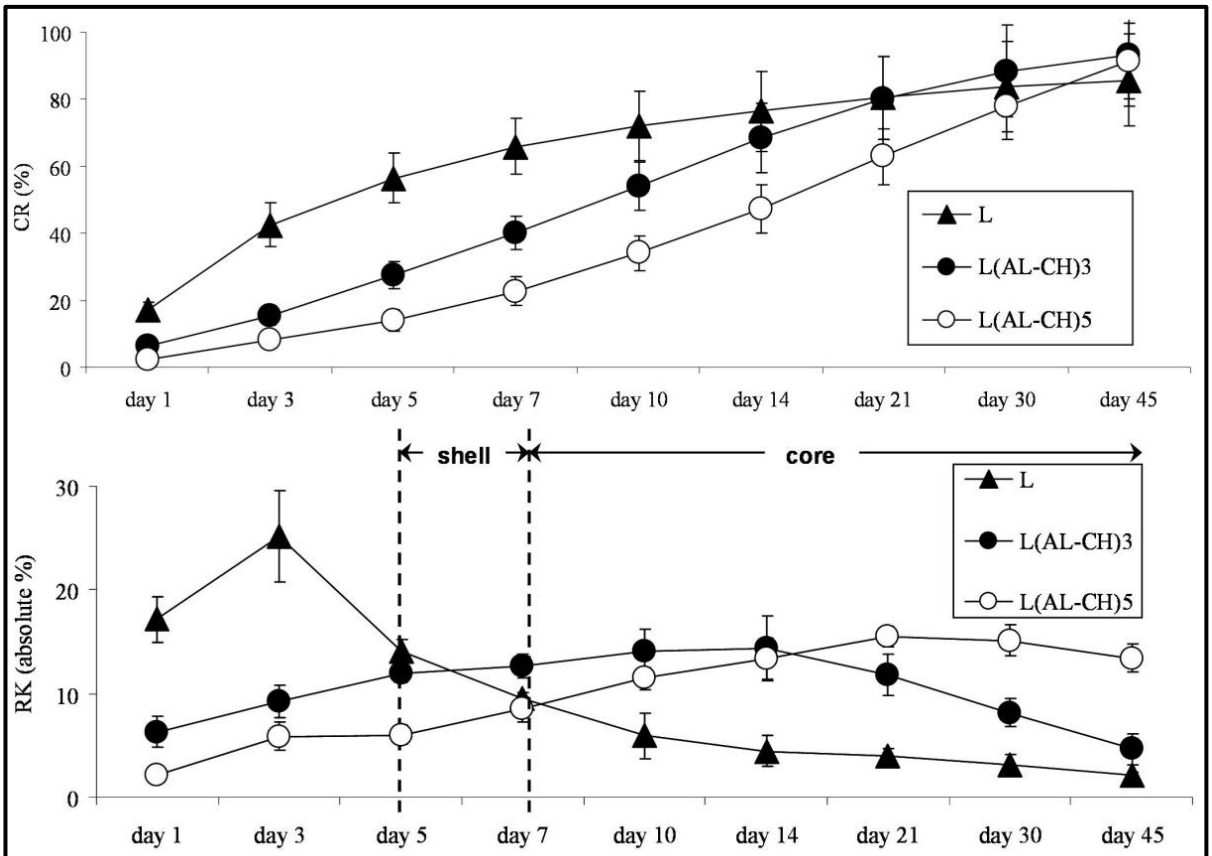


**FIG 7.4. (a)** Cumulative percentage *in vitro* release profile (CR) of OP-1 loaded un-coated and coated liposomes. **(b)** Absolute percentage *in vitro* release (RK) of OP-1 loaded un-coated and coated liposomes at each time point in highly-pure water. Data represent mean ± standard error of the mean. L: un-coated liposomes; [L(AL-CH)3]: liposomes coated with three alginate–chitosan bi-layers; and [L(AL-CH)5]: liposomes coated with five alginate–chitosan bi-layers.

### 7.4.6. ALP Activity

The impact of unloaded and OP-1 (100 ng/mL) loaded nanoparticles on the differentiation of MC3T3-E1.14 preosteoblast cells incubated for 2, 4, and 7 days by measuring the ALP activity is displayed in Figure 7.5. Ascorbic acid and β-glycerophosphate (AA+βGP); medium supplements and nutrients essential for differentiation of preosteoblasts, were present in the assay as positive controls. We have also included OP-1 alone (100 ng/mL) so that to compare its effect with that of OP-1 incorporated into the nanoparticles. Results are expressed relative to untreated cells (control) as µmol *ρ*-nitrophenol (PNP) produced/min/mg protein. High ALP activity is an osteoblastic phenotype (Mizuno and Kuboki 2001). The activity of ALP was significantly increased in cells incubated with OP-1 loaded

nanoparticles, and preosteoblast differentiation was enhanced over the monitored period of 7 days. The stimulatory effect of OP-1 alone was less than when loaded in the delivery system or when compared with both controls. More specifically, it was significantly less when compared with AA+βGP and OP-1 loaded nanoparticles on day 7.

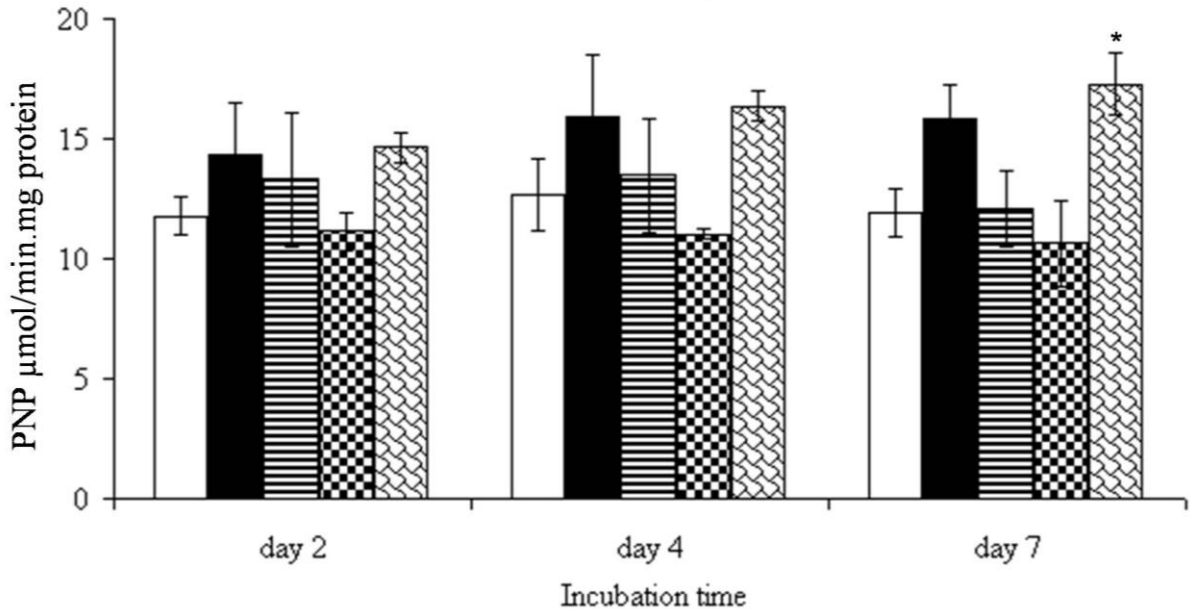


**FIG 7.5.** ALP activity assay. Significant differences ($\rho < 0.05$) were detected for OP-1 loaded nanoparticles [L(AL-CH)3+OP-1] when compared to control, OP-1 alone and unloaded nanoparticles [L(AL-CH)3]. Difference between control and AA+βGP (Ascorbic acid and β-glycerophosphate) was deemed statistically significant as well.

Nonetheless, incubation with a low-level dose of 100 ng/mL OP-1 was sufficient to induce cell differentiation, as assessed by the ALP activity between days 2 and 4. It has been shown recently that OP-1 is mitogenic for MC3T3-E1 cells demonstrating dose-dependant induction of ALP activity and osteocalcin production (Lee et al. 2005). In addition, therapeutic applications are known to require large amounts of recombinant proteins (Wang 1993). Hence, the need for a cost-effective and efficient release-controlled protein delivery system is amplified.

### 7.4.7. In vitro OP-1 Release Kinetics

The 45-day OP-1 release profile from the core-shell delivery system plotted as a function of square root of time (in days) is shown in Figure 7.6. The method is epitomized for L, L(AL-CH)3, and L(AL-CH)5 (Haidar et al. 2008a). A good linearity for coated liposomes is illustrated. The insert displays the slope *K*, axis intercept *a*, and squared coefficient of correlation $r^2$ for the release of incorporated OP-1 from both, uncoated and coated liposomes. The increase in coating thickness appears to decrease the rate of protein release where OP-1 release from uncoated liposomes is clearly faster than from coated liposomes. OP-1 release over the 45 days from this physically dispersed polymeric system may be described by several possible mechanisms: diffusion, polymer degradation, ion complexation, and interactions among the protein and the polymers, although it is primarily governed by a diffusion-based or affinity-based mechanism. Finally, the rate of release was divided into an initial phase (shell release; 0–7 days) and a terminal phase (core release; 8–45 days grouping two release episodes together) and fitted to the Higuchi mathematical model which is based on the calculation of the area under the curve using the trapezoidal rule (Gohel et al. 2000).

Table 7.1 displays the relevant release rate constants and correlation coefficients. This model allows for where drug release is complete (100%) or incomplete (< 100%) at the last sampling time.

The literature provides evidence that for such systems, the Higuchi model based on the goodness-of-fit test continues to be the most appropriate model to describe the kinetics of drug release, when compared with zero-order, first-order, Hixson-Crowell's, and Weibull's models (Gohel et al. 2000). Furthermore, it enables an understanding of the quantitative deviation of the proposed formulation from the diffusion-controlled ideal Higuchi model.

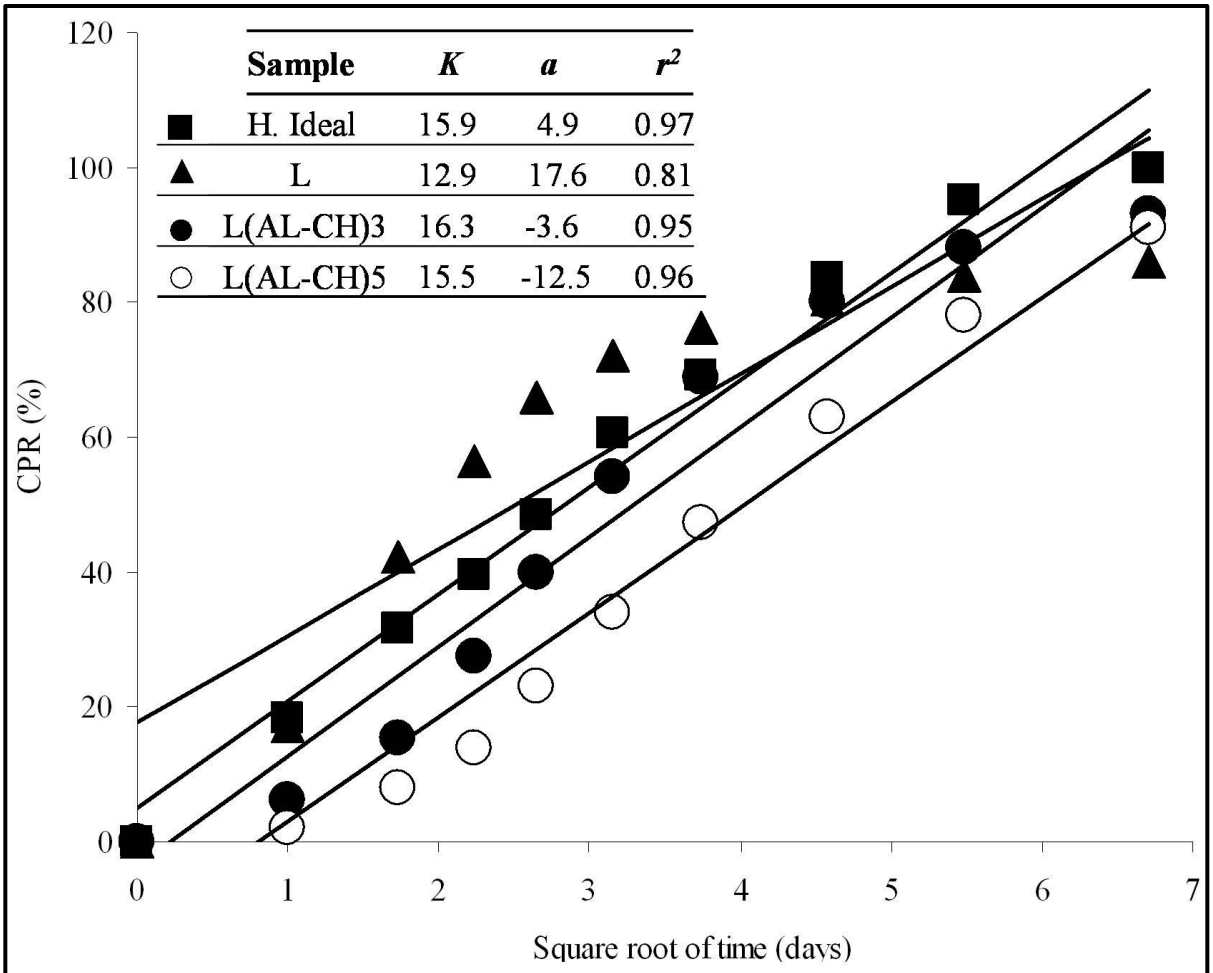


**FIG 7.6.** Release kinetics of un-coated (L) and coated liposomes [L(AL-CH)3 and L(AL-CH)5] represented as cumulative protein release percentage (CPR). Release data was fitted in the Higuchi mathematical model to obtain a plot of percentage protein release as a function of square root of time. Insert displays the release rare slope (*K*), axis intercept (*a*) and correlation coefficient ($r^2$) of OP-1 from the samples studies in comparison to the ideal Higuchi (H. ideal) which takes into consideration 100% release over the monitored period of time. Release was not complete over the studied period of time (< 100%). Slower release rates are shown with coated liposomes than both, uncoated liposomes and the H. ideal, resulting in negative axis intercepts.

The role of the L-b-L build-up of polymers around nanosized liposomes is clearly demonstrated in controlling the release of the entrapped drug or protein over prolonged periods of time. The release patterns of the coated liposomes showed linear profiles with a much lower burst than uncoated liposomes followed by a sustained release of OP-1.

**TABLE 7.1.** Release rate constants (mean ± standard deviation) and correlation coefficients of OP-1 release from bare and coated liposomes showing the initial (shell) phase and the terminal (core) phase of protein release (obtained from the Higuchi plot).

| Model | L | | L(AL-CH)3 | | L(AL-CH)5 | |
|---|---|---|---|---|---|---|
| Higuchi | Initial | Terminal | Shell | Core | Shell | Core |
| $K$ | 16.1 ± 5.4 | 3.5 ± 6.9 | 11.4 ± 6.1 | 9.7 ± 4.7 | 6.7 ± 5.1 | 14.5 ± 1.9 |
| $r^2$ | 0.95 | 0.98 | 0.99 | 0.96 | 0.99 | 0.99 |

## 7.5. Conclusion

The novelty of this work is based on the combination of the polymeric L-b-L self assembly technique and nanoscaled liposomes in formulating a stable and nontoxic release-controlled protein delivery system. It consists of a suspension of monodisperse core-shell nanoparticles suitable for the potential administration of growth factors via a parenteral injection as is preferable for surgeons. The nanoparticles tolerate extended shelf storage and allow for protein loading immediately preceding administration, preventing degradation, or loss of the entrapped growth factor. The system demonstrated a good capacity for the encapsulation and loading of OP-1 which can be altered by the number of polyelectrolyte layers. Sustained and multistep release of OP-1 was evident for an extended period of time with the viability and bioactivity of OP-1 maintained via enhancing preosteoblast differentiation, in vitro. These findings suggest that our core-shell nanoparticulate system could be an effective carrier for morphogens, growth factors, and most likely for other classes of bioactive molecules.

## 7.6. Acknowledgments

The authors wish to the Natural Sciences and Engineering Research Council of Canada (NSERC) and the Centre for Biorecognition and Biosensors (CBB) for making this research possible. Dr. Haidar acknowledges a post-graduate scholarship from the Canadian Institutes for Health Research (CIHR) Skeletal Health Training Program and Center for Bone and Periodontal Research in Montréal, Québec.

# CHAPTER 8
# Core-Shell NPs – Biocompatibility and Safety in Rats

New therapeutically-effective strategies for the treatment of critical bone defects using growth factors that can be used clinically are desirable. Due to the very short half-lives and instability of these morphogens once administered, their incorporation in an appropriate delivery system is thus indispensable. *Collagen* sponges were used as BMP carriers in many experimental and clinical studies. However, it is known that bovine collagen might cause allergic reactions or transmit viral infections. The incorporated growth factor concentrations are relatively high, unsafe and have the risk of ectopic bone formation in the surrounding soft tissue such as muscle or joints leading to dysfunctions further limiting their potential clinical use.

Therefore, other polymers have emerged for use in a wide range of medical and pharmaceutical applications including fabrication/coating of biomedical devices, therapeutic delivery systems and tissue engineering. Of these, **nanoparticles/nanocapsules** composed of biodegradable and biocompatible polymers are good candidates for the design and formulation of nanoparticulate carriers hence the considerable interest in their use as potential alternative peptide drug delivery systems avoiding the drawbacks of collagen and the limitations involved in microparticles/microspheres preparation (frequent need for organic in situ polymer precipitation, for example). Moreover, numerous investigations have suggested that polymeric nanoparticles can not only improve the stability of therapeutic agents against enzymatic degradation, but via different manufacturing methods for modulating and customizing polymer physico-chemical characteristics (size, structure, morphology, surface and composition), they can also achieve the desired therapeutic levels in target tissues and defect sites for the required duration of time optimal for their efficacy. In addition, depending on their composition and projected or intended use, nanoparticulate drug carriers are capable of being administered orally, parenterally or locally. **Injectable systems** have garnered much attention for a variety of applications including tissue engineering, gene therapy and localized drug delivery. Injectability provides several desirable advantages such as ease of application, localization at target site, bypass of various

physiological barriers and improved patient compliance and comfort. A number of synthetic polymer and polyester-based injectable drug delivery systems have been developed. Although considered to have good biocompatibility, such biomaterials lead to a foreign body response hindering drug release. As well, they result in acidic byproducts that could degrade the growth factor. In contrast, **natural polysaccharides** have the potential to circumvent these issues due to their biocompatibility, biodegradability and lack of foreign body response. For example, Chitosan has found applications in the drug delivery field due to its excellent biocompatibility, low toxicity, immune-stimulatory activities, antibacterial and antifungal action, and anticoagulant properties. Furthermore, the degradation products of chitosan have been shown to be nontoxic, non-immunogenic and non-carcinogenic. However, the application of chitosan alone has been limited due to its poor solubility and the acidic compounds normally required to dissolve chitosan, compromise the biocompatibility of the system. It has been reported that favorable interactions (i.e. hydrogen and ionic bonding) exist in when chitosan is blended with other materials such as **alginate** and **phospholipids**.

This amplified use of nanosized biomaterials in the past several years has driven the investigation of any potential hazards of such unique and promising materials, in vitro (cytocompatibility) as well as in vivo (biocompatibility and safety). Animal models are widely used and considered indispensable in order to try and predict the clinical biocompatibility, safety and outcome of such delivery systems and biomaterial blends in humans, although with great caution due to *expected* variability and discrepancy in results.

The **cytocompatibility** of the nanoparticles was demonstrated in Chapter 7 and their performance in rabbits following administration directly into the distraction gap prepared in the tibia had no reported clinical complications or animal body weight changes over the treatment period of around 3-5 weeks as will be demonstrated later on in Chapter 9.

In this first in vivo study, the aim was therefore to further investigate the **biocompatibility and safety** of the nanoparticulate delivery system upon intramuscular (IM) administration in a smaller animal (than rabbits) species that is commonly used in such studies via timely blood and organ function analysis, monitored over a period of 70 days.

This study offers once more an evaluation of the effect of the physico-chemical, localized and release-controlled characteristics of the biomaterials and methods used to formulate the nanoparticles in maintaining the bioactivity of the encapsulated OP-1 in a different environment; muscle tissue. Even so, it is noteworthy that this study when planned and executed, it was **not** aimed to serve as an *ectopic* bone formation model. The immunohistochemical analysis performed at the end was merely exploratory. Yet, supplementary information regarding the *overall* clinical safety of the hybrid delivery system was obtained. The analytical findings from evaluating animal body weight and behavioral changes, a total of 50 blood markers and hematological levels along with the health status of 6 of the major organs suggested that the nanoparticles, the released bioactive load as well as the resulting effects were restricted to the site of administration with no considerable complications or reactions from any degradation by-products. Data from such studies provide pharmacokinetic or biokinetic descriptions essential for the possible extrapolation from animals to humans. This is of crucial significance in designing novel delivery systems especially for BMPs known to be local-acting, dose- and also species-specific.

Findings of this set of experiments were reported in a manuscript just submitted (August 27$^{th}$ of 2009) to the peer-reviewed *Biomaterials*. It is reproduced next.

Manuscript submitted for publication to *Biomaterials* (August 27th of 2009).

# Biocompatibility and Safety of an Injectable Hybrid Nanoparticulate rhOP-1 Delivery System intramuscularly administered in Rats

**Ziyad S. Haidar[a-e], Reggie C. Hamdy[b, d, e], Maryam Tabrizian[a-d]**

[a]*Faculty of Dentistry, McGill University, Montréal (QC) Canada*
[b]*Center for Biorecognition and Biosensors, McGill University, Montréal (QC) Canada*
[c]*Department of Biomedical Engineering, Faculty of Medicine, McGill University, Montréal (QC) Canada*
[d]*Centre for Bone and Periodontal Diseases Research, McGill University, Montréal (QC) Canada*
[e]*Shriners Hospital for Children and Division of Orthopaedics, McGill University, Montréal (QC)Canada*



## 8.1. ABSTRACT

A hybrid, localized and release-controlled bone morphogenetic protein delivery system consisting of a liposomal core incorporated into a shell of alternating layer-by-layer self-assembled natural polyelectrolytes has been formulated. Hydrophilic, monodisperse, spherical and stable cationic nanoparticles (≤ 350 nm) with an extended shelf-life allowing immediate protein loading prior to clinical administration resulted. Cytocompatibility was previously assayed with MC3T3-E1.4 mouse preosteoblasts and cell viability determined by colorimetry showing no adverse effects, in vitro. In this study, the potential in vivo toxicity, biocompatibility and tissue presence of unloaded and loaded nanoparticles with bone morphogenetic porotein-7 (or osteogenic protein-1/OP-1) were investigated. Young male normal Wistar rats (N=22) were injected intramuscularly and monitored over a total period of 10 weeks for any signs of inflammation and/or adverse reactions. Blood samples (600 μL/collection) were withdrawn on days 0 (baseline: pre-injection) and post-injections on days 1, 7, 14, 28, 56 and 70. Hematological and biochemical analysis followed. Body weight changes over the treatment period were noted as well. Finally, upon animal sacrifice, major organs were harvested, weighed and examined histologically for any pathological changes. The muscular injection site was identified and examined histologically and immunohistochemically. Overall, all animals showed no obvious toxic health effects, immune responses and/or change in organ functions. The nanoparticles seem to localize the

release and effect of the bioactive OP-1 within the injection site with no significant tissue distress. Hence, a safe and promising nanosized polymeric carrier for the administration of therapeutic growth factors is presented.

**Keywords:** *Adverse effects; Biocompatibility; BMP; Cytotoxicity; Drug Delivery; Ectopic bone formation; Foreign body response; Haemocompatibility; Morphogens; Nanoparticle; Self-assembly*

## 8.2. Introduction

Bone morphogenetic proteins (BMPs) are cytokines that are able to induce new bone formation in vitro and in vivo (Bessa et al. 2008 a). BMP-7 (also known as osteogenic protein-1 or OP-1) has been shown to accelerate the formation of new bone in numerous preclinical and clinical studies (Mont et al. 2004). Nonetheless, the clinical efficacy of OP-1 still depends on the carrier or delivery system used to ensure a sustained, multi-step, and prolonged delivery of adequate protein concentrations to the desired site of tissue repair or restoration (Termaat et al. 2005; Bessa et al. 2008 b; Haidar et al. 2009 a, b). The foremost limitations include the rapid diffusion of OP-1 away from the site of application and loss of its bioactivity, resulting in orthotopic/heterotopic bone formation or suboptimal local induction and hence failure of bone regeneration. Consequently, supra-physiological, unsafe and expensive dosages of OP-1 in the milligram range for satisfactory bone healing continue to be required (Luginbuehl et al. 2004). Liposomes are the commonly investigated vehicles for delivery of therapeutic compounds, such as enzymes and proteins (Illum and Davis 1991; Chaize et al. 2004) because of their biocompatibility and appealing ability to carry hydrophobic and hydrophilic drugs. Nonetheless, stability in vivo remains a setback, mainly due to their high tendency to degrade or aggregate leading to leakage of the entrapped drug during storage or after administration with considerable toxic effects. Additionally, they are rapidly cleared from circulation via uptake by the reticulo-endothelial system (Takeuchi et al. 2001). To overcome such problems, varying the size of the liposome (Takeuchi et al. 1998; Takeuchi et al. 2000) or modifying the surface by means of coating it with a single layer of hydrophilic polymers have been investigated (Charrois and Allen 2003).

In an initial in vitro study (Haidar et al. 2008 a), we formulated monodisperse nanosized particles constituting a core of cationic liposomes (L) and a shell constructed through the layer-by-layer (l-b-l) self-assembly of alternating layers of naturally-available anionic alginate and cationic chitosan. The system has a cumulative size of 383±11.5 nm and a Zeta ($\zeta$) potential surface charge of 44.61±3.31 mV, suitable for complex formation with anionic proteins such as OP-1. The choice of reducing particle size of biomaterials from the microscale to the nanoscale is mainly to improve the bioavailability of the encapsulated drug once administered in situ and hence allowing for the effective use of much lower and safer

dosages (Kim et al. 2006). In a subsequent work (Haidar et al. 2008 b), the cytobiocompatibility (effect on MC3T3-E1.4 pre-osteoblast cell viability) and capability of the hybrid core-shell nanoparticles to encapsulate a range of concentrations of bioactive OP-1 for their potential administration via a parental injection was investigated. The system exhibited high physical stability in simulated physiological media allowing for immediate protein loading prior to administration, thus preventing degradation or loss of the entrapped growth factor. A sustained tri-phasic linear release of the water-soluble and readily diffusible positively-charged OP-1 was evident for an extended period of 45 days with the bioactivity of the protein maintained via promoting preosteoblast differentiation with no evident cytotoxic effects (96% cell viability), in vitro. In vivo, the localized and release-controlled potential of the delivery system were then demonstrated in rabbits where enhanced de novo bone regeneration in terms of quantity and quality resulted following a single injection of the NPs loaded with doses as low as 1.0 μg OP-1 (Haidar et al. 2009 c). This established the efficiency as well as the potential biocompatibility and safety of the delivery system where no adverse effects or behavioral changes were noted in all animals over a period of ~ 21 days. Besides the known advantages including the size property, longer shelf-life, favorable preparation methods and subsequent ability to entrap more bioactive drugs (Gref et al. 1994), nanosized delivery systems have the advantage of residing longer in circulation when compared to microparticles (Desai et al. 1996), raising safety concerns where acidic by-products, foreign body responses and heterotopic bone formation in undesirable tissues have been reported; especially with injectable nanoparticulate delivery systems (Fabian et al. 2008; De Souza et al. 2009). This has driven the investigation of their pre-clinical safety to compliment the in vitro findings. Hence, animal models are widely used and considered indispensable in the fields of tissue engineering and regenerative medicine to investigate the potency and biocompatibility of such systems in order to investigate any potential hazards and try to predict their clinical outcome in humans, although with great caution due to variability in results (Pearce et al. 2007).

In this study, we further evaluate the biocompatibility and safety of the injectable nanoparticulate delivery system in healthy rats so that to investigate any potential hazards and/or adverse effects not detected in vitro as well as in the larger-sized rabbits. We

considered the commonly-measured blood markers, clinical signs and the major organs (and the site of injection in quadriceps muscle) for any pathological changes.

## 8.3. Materials and Methods

### 8.3.1. Formulation of Hybrid NPs & Evaluation of OP-1 Encapsulation

The formulation and characterization of the hybrid core-shell nanoparticulate protein delivery system has been previously described (Haidar et al. 2008 a, b). Briefly, for the preparation of liposomes, 1,2-Dipalmitoyl-snglycero-3-phosphocholine was purchased from Genzyme Pharmaceuticals, Switzerland; cholesterol and dimethyldioctadecyl-ammonium bromide (DDAB) were obtained from Sigma-Aldrich Chemical. The extrusion apparatus was purchased from Avanti® Polar Lipids, and the 19 mm polycarbonate filters (200 nm pore size) were obtained from GE Osmonics. For the l-b-l coating, alginic acid (AL: sodium salt; viscosity of 2% in water) and chitosan (CH: 85% deacetylated with molecular weight of 91.11 kDa) were obtained from Sigma-Aldrich Chemical. Liposomes were formulated by means of thin-film hydration followed with extrusion through double 200 nm polycarbonate filters. For the l-b-l build-up, fresh AL and CH solutions (1 mg/mL) were prepared in highly-pure water. The cationic liposomes were coated with alternating layers of AL and CH until the desired number of polyelectrolyte layers was achieved; 6 layers: $L(AL\text{-}CH)_3$, herein and after denoted as NPs. With the deposition of each polymeric layer, the solution was incubated at room temperature for 60 min and centrifuged at 1600g for 15 min for washing. Prior to protein loading, aliquots of nanoparticle suspensions were freeze-dried in the presence of sucrose as a cryoprotectant at -54$^{o}$C for 48 h (Modulyo D-115, Thermo Savant, MA). Lyophilized NPs were rehydrated back to the original volume with different concentrations of OP-1 solution (0.0 to 1.0 µg/mL). The recombinant human (rh) osteogenic protein-1/rhOP-1 (15.7 kDa molecular weight, lyophilized) was purchased from bio-WORLD, OH and stored at -20$^{o}$C until use, according to the manufacturer's instructions. Average size and surface charge changes upon loading were then determined using low-angle laser light-scattering (DLS-HPPS, Malvern Instruments, UK) and laser Doppler anemometry (Zeta-Plus, Brookhaven Instruments, NY), respectively.

### 8.3.2. Animals

A total of 22 young and healthy (10-15 weeks old, 350-400 g at the start of the acclimatization period) male normal Wistar rats (Harlan Sprague Dawley®) were included in this study. The animals were housed individually in type III Macrolon cages under conventional hygienic conditions, at 20-24°C and 30-70% relative humidity and with natural day/night light rhythm. Rats were fed a pelleted diet, allowed access to tap water ad libitum and inspected daily by fit animal health care personnel. The housing, care and experimental protocol were approved by the McGill University Animal Care and Ethics Committee.

### 8.3.3. Experimental Study Design and Analyses

#### 8.3.3.1. Study Protocol

The study protocol and timeline is displayed in Figure 8.1. All animals were randomized to each receive a single injection (0.3 mL total volume) in the right quadriceps muscle using latex-free micro-fine® IM syringes (25G½ 0.36 mm x 13 mm, Becton Dickinson and Co.,

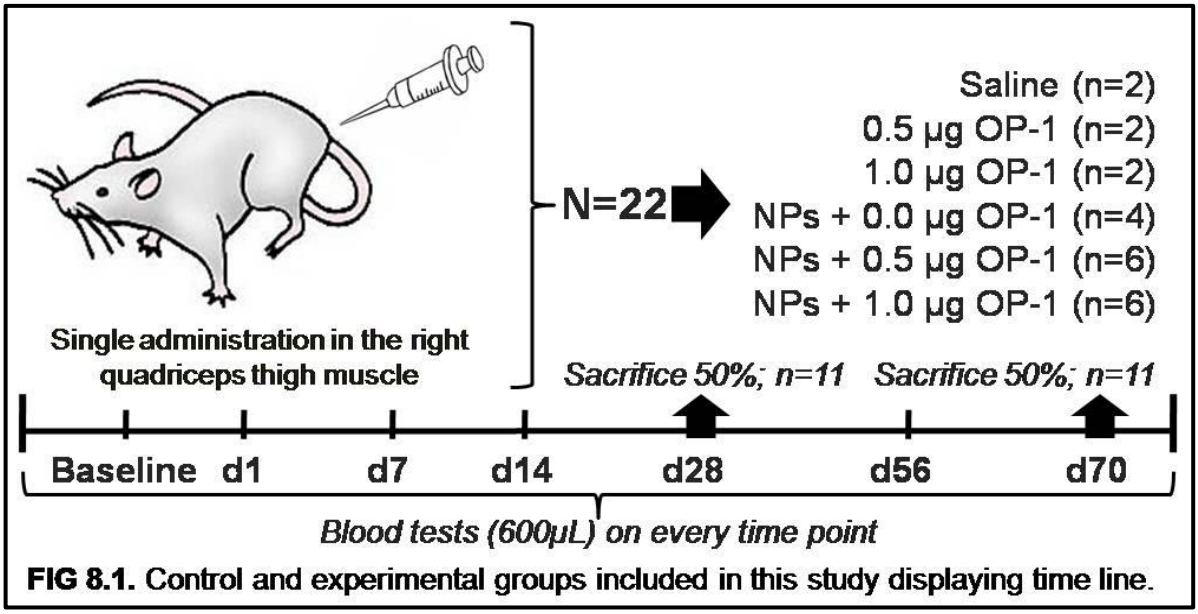


**FIG 8.1.** Control and experimental groups included in this study displaying time line.

NJ) according to the following groups: **A.** Control group 1: saline (n=2); **B.** Control group 2: 0.5 µg OP-1 (n=2); **C.** Control group 3: 1.0 µg OP-1 (n=2) ; **D.** Experimental group 1: blank/unloaded NPs in highly-pure water (n=4); **E.** Experimental group 2: NPs loaded with 0.5 µg OP-1 (n=6); and **F.** Experimental group 3: NPs loaded with 1.0 µg OP-1 (n=6).

No anesthesia was required. Rats were examined daily for signs of infection, inflammation and adverse effects by visual observation. Body weight changes were measured over a period of 10 weeks. All animals were euthanized by carbon dioxide when they have reached their experimental endpoints; d28 (n=11; 50%) and d70 (n=11; 50%). Housing and overall care were at the Animal Resources Center (ARC), Faculty of Medicine, McGill University, Montréal, QC, Canada.

#### 8.3.3.2. Serum Biochemical and Hematological Analysis

Blood samples were collected (6 mL/Kg/3 weeks: 600 µL per collection) on day 0 (baseline: pre-injections) and post-injections on days, 1, 7, 14, 28, 56 and 70. Using a biochemical autoanalyzer (VITALAB, Merck, The Netherlands), serum biochemical analysis was carried out to determine the serum level of total protein, albumin, total bilirubin, aspartate transaminase (AST), alanine transaminase (ALT), alkaline phosphatase (ALP), glucose, cholesterol, triglyceride, bood urea nitrogen (BUN), lactic acid dehydregenase, creatinine, sodium, potassium, chloride, calcium, phosphorus and magnesium. Hematological parameters consisting of erythrocytes, leukocytes, neutrophils, lymphocytes, monocytes, eosinophils, basophils, hemoglobin, hematocrit and platelets were determined using a hematological analyzer (Coulter T540 hematology system, Fullerton., CA). This set of analysis was performed blindly at the pathology laboratories of the Faculty of Medicine, McGill University, Montréal, QC, Canada.

#### 8.3.3.3. Histopathalogical Analysis

The brain, liver, lungs, kidneys, heart, spleen and right quadriceps muscle (site of injection) were removed from each animal at time of euthanasia (50% on d28 and the other 50% on d70), weighed, sectioned and then immersed-fixed in a buffered (0.4 M phosphate buffer, pH 7.61) 4% paraformaldehyde solution for at least 24 - 48 hours. Tissue sections (3µm) were prepared after dehydration and embedded in paraffin. Of these, random samples were stained with hematoxilin and eosin (H&E) and processed for comparative histopathalogical examination under a light microscopy by a qualified veterinary pathologist at the Histology Core facility of the Faculty of Medicine, McGill University, Montréal, QC, Canada.

#### 8.3.3.4. Immunohistochemistry

Those specimens of the right quadriceps muscle assigned for immunohistochemistry were sectioned, fixed in 4% paraformaldehyde overnight, decalcified in 20% ethylenediamine tetraacetic acid for 3 weeks, and embedded in methyl methacrylate or MMA. Seven micrometer sections of a random selection of blocks from every experimental group were then cut. After de-paraffinization and hydration, endogenous peroxidase was blocked with 3% hydrogen peroxide for 10 min. Nonspecific binding was blocked by incubation in phosphate-buffered saline containing 10% normal horse serum and 0.1% Triton for 20 min. For immunostaining, commercially available polyclonal goat antibodies (Santa Cruz Biotechnology Inc., Santa Cruz, CA) were used for the qualitative verification of the presence of genes involved in the BMP signaling pathway during bone formation. Those were categorized according to ligands (BMP-2, -3 and -7/), receptors (BMPR-I, BMPR-IIA, BMPR-IIB), transcription factors (Smads 1-5 and Sox-9), differentiation marker (Collagen-II) and antagonists (BMP-3 or osteogenin and Noggin). Sections were incubated with these primary antibodies at a dilution of 1:100 in phosphate-buffered saline with 1% normal horse serum. Overnight incubation at $4^{o}C$ in a humidified chamber followed. As a secondary antibody, a biotinylated horse anti-goat antibody (Vector Labs, Burlingame, CA) at a dilution of 1:400 was used. Sections were stained using the avidin-biotin complex method along with 3,3'-diaminobenzidine tetrachloride for 30 min, followed by DAB-peroxidase revelation. Finally, the sections were counterstained with Goldner Trichrome, mounted with Permount, imaged and semi-quantified as described below under optical microscopy. Negative controls were prepared similarly however excluding the primary antibody. This was completed at the Shriners Hospital Laboratories, Montréal, QC, Canada.

#### 8.3.3.5. Quantitative Grading of the Immunostained Sections

A semi-quantitative analytical method to describe immunohistochemistry images was previously developed (Hamdy et al. 2003; Haque et al. 2005; Mandu-Hrit et al. 2006; Haque et al. 2008). The number of cells expressing the proteins was assessed by stained cell counting and graded by a blinded observer as follows: – no staining; ┼/– staining in less than 15% of cells; ┼ staining in 15–25% of cells; ┼┼ staining in 25–50% of cells; ┼┼┼

staining in 50–75% of cells; ┼┼┼ staining in more than 75% of cells. Chondrocytes and fibroblastic cells were identified morphologically when detected. It is noteworthy that this set of immunohistochemical preparation and analysis on samples of the harvested muscle was not primarily planned as this study does not aim to evaluate the potential of the nanoparticles in inducing ectopic bone formation; especially given the difficulty in identifying the site of injections in muscle.

#### 8.3.3.6. Statistical Analysis

All results are expressed as means ± standard error (SE) of the mean. For comparisons among treatment groups, a 2-tail Student's *t*-test was used with differences deemed significant at $\rho$-values less than 0.05. Immunohistochemistry data are represented as an average score from blind observations.

## 8.4. Results and Discussion

Combining the advantages of phospholipid vesicles with those of l-b-l nano-assembled systems, we introduced previously in *Biomaterials* a novel hydrophilic protein delivery system consisting of a suspension of core-shell NPs (Haidar et al. 2008 a). Small, stable

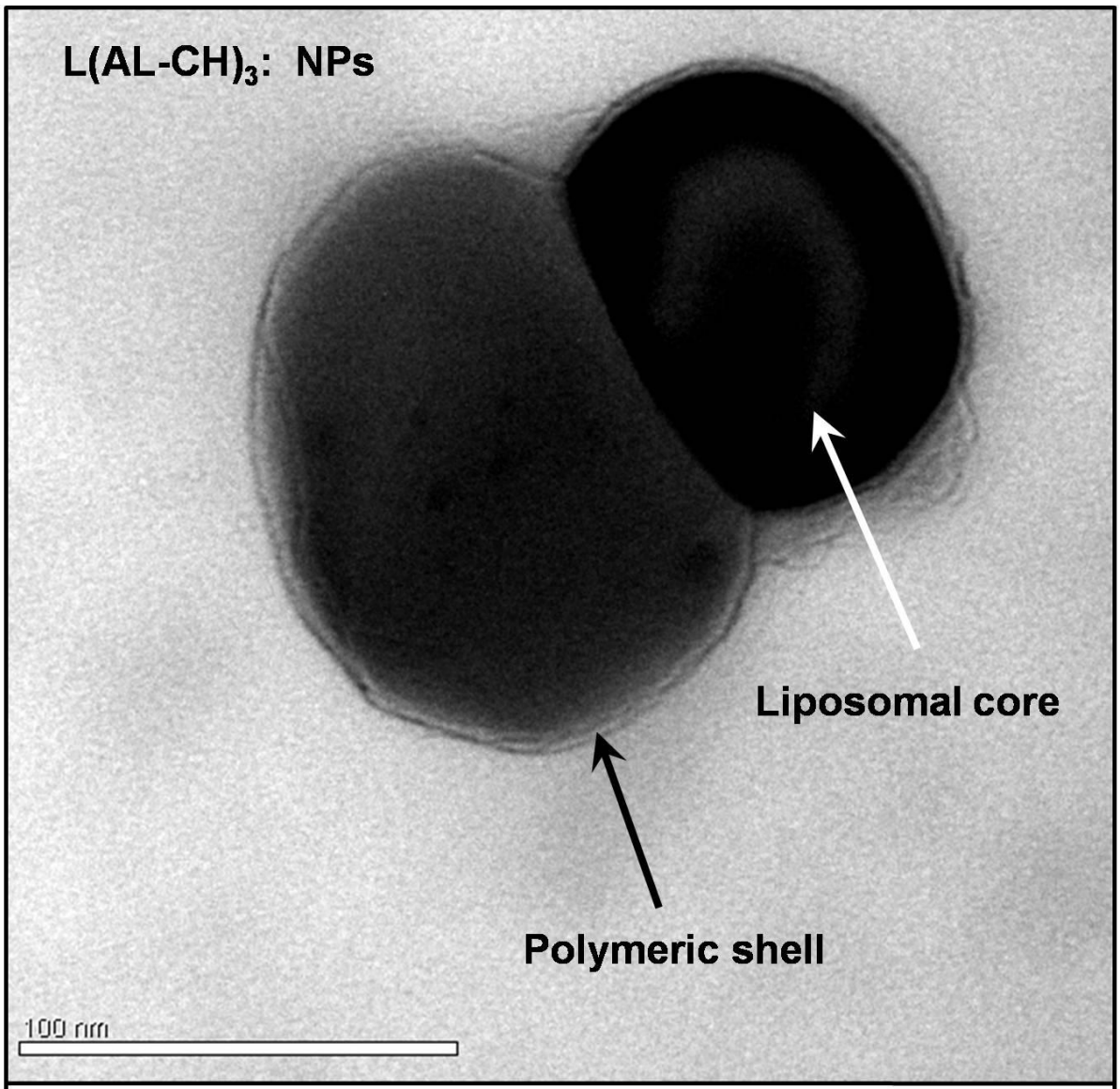


**FIG 8.2.** Cryo-Transmission Electron Microscopy (Cryo-TEM) of coated liposomes forming the nanoparticles. Bar = 100 nm. The polymeric shell coating the liposomal core maintains the spherical morphology and supports the stability of the nanoparticles following the aggressive preparatory steps prior to imaging.

and monodisperse cationic particles (≤ 350 nm with a polydispersity index < 0.3) were obtained by the electrostatic self-assembly of alternating layers of natural polyelectrolytes; anionic alginate and cationic chitosan on cationic liposomes. Figure 8.2 displays a cryo-TEM (cryo-Transmission Electron Microscopy) image of the NPs demonstrating their spherical morphology. We later further investigated the encapsulation efficiency and characterized the release kinetics of the injectable core-shell NPs with favorable results suggesting their potential for the delivery of bioactive growth factors such as osteogenic protein-1 or OP-1 , in vitro (Haidar et al. 2008 b). Using the universal colorimetric method (CellQuanti-MTT$^{TM}$ kit followed by spectrophotometry), the viability of MC3T3-E1.4 preosteoblasts were assessed upon incubation with different concentrations of the NPs. Approximately 96% cell viability was observed at concentrations up to 253µg/mL consistent with other injectable polymer-based hydrogel formulations that employ, for example chitosan with a high degree of deacetylation (Tan et al. 2008).

Table 8.1 summarizes the change in average size and zeta potential surface charge before lyophilizing and after rehydration/loading of the NPs with bioactive OP-1. To further investigate the biocompatibility of the NPs in a smaller and more frequently employed animal species than our rabbits (Haidar et al. 2009 c) in such studies, timely blood and organ function analysis over a period of 70 days were performed to provide supplementary information on the safety of the NPs.

**TABLE 8.1.** Summary of the characterization parametric data measured before and after rehydration and loading the nanoparticles with OP-1. Values are reported as mean (*) and standard error (SE) of the mean for the average hydrodynamic diameter (nm) measured by a particle sizer using a low-angle light scattering device (HPPS, Malvern Instruments, USA) and the Zeta (ζ) potential surface charge (mV) measured by a ZetaPlus analyzer using laser Doppler anemometry (Brookhaven Instruments, USA).

| Pre-loading with OP-1 | | | | Post-loading with OP-1 | | | |
|---|---|---|---|---|---|---|---|
| *Size (nm)** | *SE* | *Zeta (mV)** | *SE* | *Size (nm)** | *SE* | *Zeta (mV)** | *SE* |
| 345 | 10.9 | +37.88 | 1.3 | 386 | 9.4 | +38.77 | 1.5 |

### 8.4.1. Clinical Signs and Body Weight Changes

Throughout the study period, animals showed no apparent signs of dehydration, muscle loss or anorexia; symptoms associated with animal toxicity (Stokes 2002). Body weight loss, particularly when in excess of 10–20% is also indicative of toxicity. All animals irrespective of the injection received did not show any such adverse effects on their growth as evident in their normal body weight gain (Figure 8.3) observed over the experimental time span of 10 weeks with no statistically significant differences ($\rho > 0.05$) detected among groups including control rats. Further, no abnormal physical signs and/or behaviors in any groups were reported by the animal health care technicians supervising the animals.

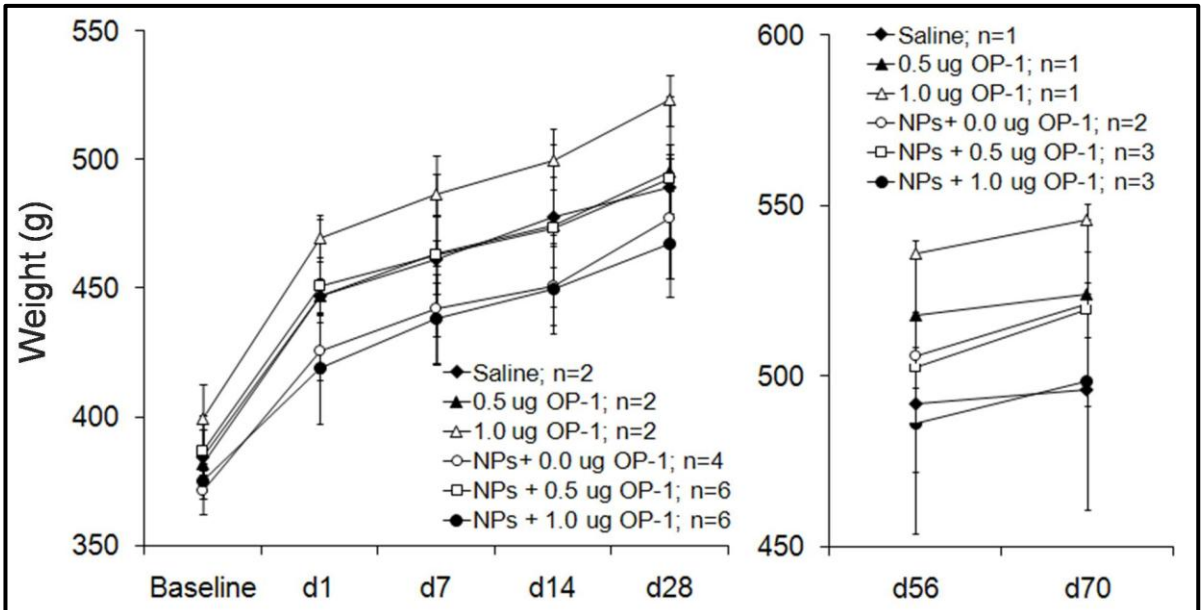


**FIG 8.3.** Average animal body weight changes (in g) pre- and post-IM injections for all animals up to day 70 (where 50% of animals per group were sacrificed on day 28). The data show a consistent body growth with no significant differences among groups. All animals continued in good health with normal food/water consumption and energy intake until time of sacrifice and organ harvest.

### 8.4.2. Serum Biochemical and Hematological Findings

Complete blood count and total panel serum biochemical analysis for various cytokines and enzymes (a total of 50 parameters) were performed for the collected blood samples according to the blood sample withdrawal time line displayed in Figure 8.1 in order to assess any potential inflammatory responses and/or organ injury following the intramuscular

administration of saline (for the cumulative physiological and psychological/behavioral effect of needle insertion), OP-1 solution prepared in ultra-pure water (0.5 and 1.0 µg), unloaded and loaded NPs with 0.5 and 1.0 µg OP-1. None of the measured parameters showed definitive changes by the experimental time points signifying the absence of inflammatory response(s) or organ toxicity and dysfunction post-injections. In addition, hematological analysis demonstrated consistency in the results where no alarming variations in the normal values of any of the evaluated key assessors of biocompatibility such as ALP levels and counts of red blood cells, white blood cells and platelets arose (Figure 8.4). ALT, mostly in red blood cells provides information about the

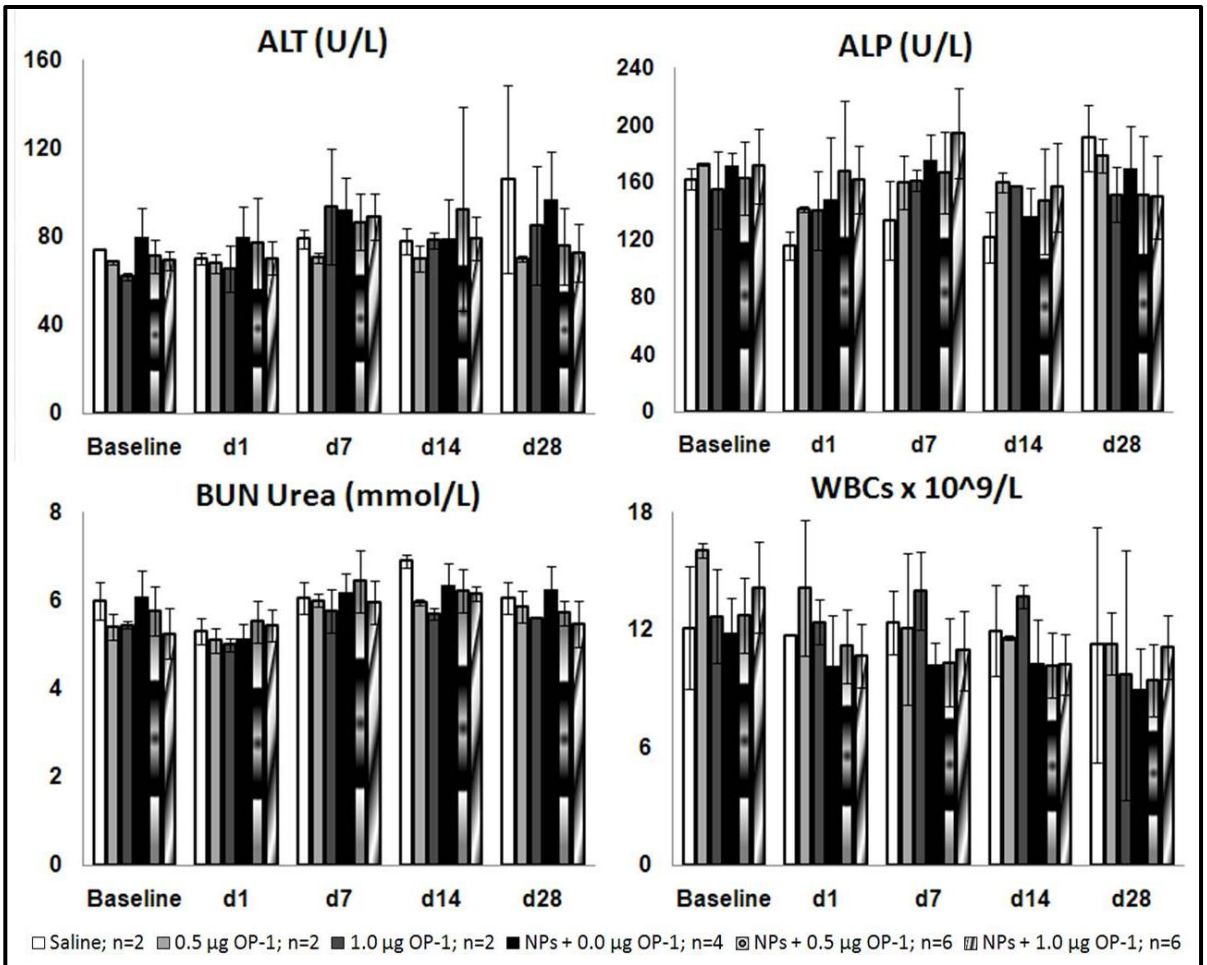


**FIG 8.4.** Selective representation of the most important biochemical and hematological parameters analyzed from the collected blood from the rats demonstrating the safety of the core-shell nanoparticulate system. No significant differences detected. Data is shown up to day 28 so that to include the largest number of animals. No significant differences were noted on days 56 and 70 for the 11 animals that continued to the end of the study.

status of the heart and liver. A level increase or decrease may indicate hepatitis, ischemic cirrhosis or the presence of a liver tumor, for instance. On the other hand, ALP enzymes are normally present regularly in the bile ducts, liver and bone; therefore alterations will often suggest acute liver damage or bone fracture.

Moreover, an elevation in BUN levels indicates kidney and cardiac damage (Wang et al. 2009; Aubert et al. 2009). Blood parameters that are known to indicate an immune response or reflect changes in organs function were also unchanged in the animals receiving the core-shell nanoparticles whether unloaded or loaded with OP-1 ($\rho > 0.05$). Similarly, no trends or indications of change in enzymatic activity reflective of inflammatory response or organ toxicity and failure were noted over the extended period of 70 days. This can be attributed to the localized characteristics of the nanoparticles confining their encapsulant effect to the site of injection, hereby in muscle. Growth factors such as BMPs are known to be dosage-dependent (Wildemann et al. 2004; Bessa et al. 2008 a, b) and large supra-physiological concentrations often in the milligram range continue to be required to obtain an effect (Luginbuehl et al. 2004), as mentioned earlier.

For example, when 'low' dosages (2 μg) of BMP-2 were locally delivered to the dorsum of rats from biphasic calcium phosphate granules, significant molecular changes were not induced while 'higher' (50 μg) dosages did (Oda et al. 1997); mainly due to the bolus and initial burst release, rapid protein dispersal away from intended site and/or loss of the bioactivity (given the short half-lives) especially when administered into more fluid environments requiring slower release rates (Luginbuehl et al. 2004; Termaat et al. 2005; Bessa et al. 2008 a, b). Thus, this can also elucidate why no biochemical or hematological changes were detected in our animals receiving pure OP-1, taking into consideration that the dosages used here in were very low in comparison; 0.1 μg and 0.5μg only. Besides, although host-response to foreign materials was reported to be more intensive in peritoneum-supported organs than in subcutaneous sites (De Souza et al. 2009) for instance, it appears that our core-shell NPs, if reached, were rapidly cleared from the un-targeted tissues and

organs such as the liver and kidney. This might be either due to their small size or more possibly so because of their naturally-biocompatible composition where the rapid degradation of such polymers (and any ensuing by-products are neutralized within the body) was shown to be a contributing factor in numerous in vivo studies (Takeuchi et al. 2001; Yang et al. 2008; De Souza et al. 2009).

### 8.4.3. Organ Weights

Organs were harvested on d56 and d70. Organ weights were consistent among all rats at both endpoints. Table 8.2 summarizes these values (in g) for the organs harvested at day 70.

**TABLE 8.2.** Summary of the measured organ weights on animal sacrifice and harvest (in g) on experimental day 70 (n=11). The range is based on information from the animal supplier and others from the literature. No significant differences were detected among any of the groups indicating no pathological findings.

| Organ | Weight range (g) | Weight mean ± SD (g) | | | | | |
|---|---|---|---|---|---|---|---|
| | | Saline *n=1* | 0.5 µg OP-1 *n=1* | 1.0 µg OP-1 *n=1* | NPs + 0.0 µg OP-1 *n=2* | NPs + 0.5 µg OP-1 *n=3* | NPs + 1.0 µg OP-1 *n=3* |
| Brain | 1.75 - 1.83 | 1.79 | 1.76 | 1.77 | 1.77±0.024 | 1.78±0.026 | 1.80±0.022 |
| Heart | 0.48 - 0.54 | 0.50 | 0.52 | 0.54 | 0.52±0.039 | 0.5±0.049 | 0.49±0.010 |
| Liver | 9.35-11.04 | 9.71 | 10.21 | 10.97 | 9.80±0.452 | 10.79±0.402 | 10.56±0.748 |
| Lung | 0.96-1.99 | 1.21 | 1.34 | 0.99 | 1.40±0.424 | 1.58±0.434 | 1.36±0.397 |
| Spleen | 0.50-0.734 | 0.58 | 0.66 | 0.72 | 0.74±0.212 | 0.79±0.124 | 0.92±0.061 |
| Kidney | 1.851-2.267 | 1.88 | 1.98 | 2.13 | 2.05±0.071 | 2.12±0.141 | 1.99±0.275 |

These results were compared to other works on toxicity of different nanoparticle formulations in similar animal strains (Kim et al. 2006; Fabian et al. 2008) where no trends or indications of any pathological changes were noted.

### 8.4.4. Histopathological Findings

Post-mortem examinations at all time points revealed no visible signs of internal inflammation. The systemic distribution and fate of the different formulations were evaluated via studying the major organs (brain, heart, liver, kidneys, lungs, spleen as well as the injection site in muscle) histologically and histomorphometrically under a light optical microscope. Data from such studies would provide pharmacokinetic and biokinetic descriptions of our nanoparticulate protein delivery system essential for the possible

extrapolation of data from animals to humans for potential applications in bone tissue engineering. The performed comparative pathology in this study (Figure 8.5) focused on identifying any abnormal tissue changes in the organs harvested such as bone metaplasia. Osteoid formation was detected in the lungs of groups 2 through 3 and ranged from rare (5-10%) to moderate (25%-50%). However, in groups 4 through 6, no such observations were evident except in one animal (1/6) from group 5 sacrificed at the 70 days time point and with a diminutive mass. Multifocal inflammation and lymphoid hyperplasia was also observed in the lungs of most animals including controls and therefore are non-specific to one group or another. Similarly, alveolar histiocytosis was observed however seems to be a common finding in this strain of rats, according to Sells et al. 2007 (Sells et al. 2007). In the heart, cardiomyocyte degeneration with mononuclear inflammatory infiltrate was noted

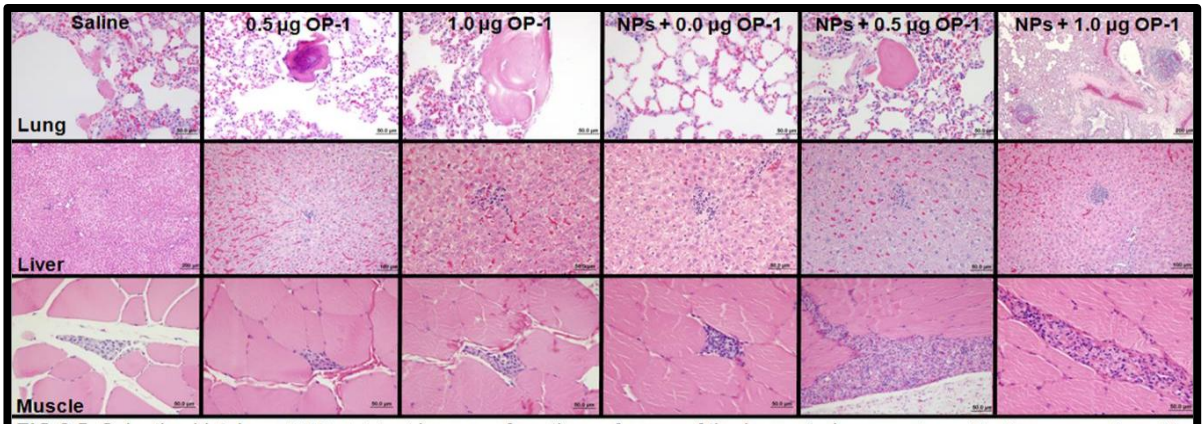


**FIG 8.5.** Selective histology (H&E staining) images of sections of some of the harvested organs (magnification ranges from 20x to 400x). Osteoid formation is more evident in the lungs of groups 1 and 3 than the other groups. Rare inflammation in the liver was noted however is consistent in all animals and has been reported to be normal in this strain of rats given exposure to environmental changes. Site of injection in the right quadriceps muscle can be identified in the displayed images with no clear severe pathologies. The pools of cells shown are endogenous muscular regenerative cells following needle insertion.

as rare (5-10%) to mild (5-20%) as was tubular degeneration and regeneration in the kidneys (no calcifications detected), multifocal mixed inflammatory infiltrate in the liver and lymphoid hyperplasia (white pulp) in the spleen. These observations were common in the control rats and were also reported to be a classic and distinctive-pathological finding in Wistar rats, perhaps environmentally-related (Mohr et al. 1992). In the harvested brains of the animals, no changes or lesions in the studied cerebrums, cerebellums or brain stems were detected whatsoever. Finally, the hematoxilin and eosin (H&E) stained histopathological

analysis performed for the initial collection of random samples of the harvested hind leg muscles of the rats revealed the presence of mixed lymphohistiocytic inflammatory infiltrates associated with skeletal muscle degeneration and regeneration most likely indicating the site of the injections and the associated injury/tear upon needle insertion. This is an expected inflammatory response normally occurring within 2–3 weeks triggered by injured vascularized connective tissue (Anderson 2001; De Souza et al. 2009).

### 8.4.5. Immunohistochemical Findings in Muscle (Site of Injections)

Since the pioneering work of Marshall R. Urist in 1965 introducing the concept of bone formation by auto- or osteoinduction (Urist, 1965; Termaat et al. 2005), several pre-clinical and clinical studies have then continued to report caution when using *local* growth factor application in the treatment of bone-related conditions explicitly as a result of ectopic bone formation in extra skeletal sites and soft tissues such as muscle (Yamamoto et al. 1998; Kurokawa et al. 2000; Okubo et al. 2000; Nakagawa et al. 2001; Kusumoto et al. 2002; Wildemann et al. 2004; Wysocki and Cohen 2007; Nanno et al. 2009). This is highly undesired because it often leads to dysfunction of the normal tissue and therefore should be excluded in safety studies prior to clinical use.

For the proof of ectopic bone formation with BMPs, rat and mice models are the most commonly used (Yamamoto et al. 1998; Nakagawa and Tagawa 2000; Stoeger et al. 2002; Nanno et al. 2009). Previous studies in rats have demonstrated that ectopic bone formation, induced by BMP-2, occurs through an endochondral series of events (Nakagawa et al. 2001). In addition, bone formation has been reported after 21 days in different extra skeletal sites in rats (Yoshida et al. 1998; Okubo et al. 2000). Therefore, we thought of investigating potential ectopic bone formation especially that the animals survived for a period of 70 days. In our preliminary samples of the leg muscle, no bone metaplasia was observed histologically and the injection site could not be always clearly identified; therefore further recuts of blocs at different depths were done and prepared as described earlier for histopathological and immunohistochemical analysis using Goldner Trichrome staining. As shown in the top two rows of Figure 8.6, histologically, signs of bone formation were

evident in groups 5 and 6 represented by the presence of pools of potential bone-forming cells which were absent in any of the other groups and controls. It is known that

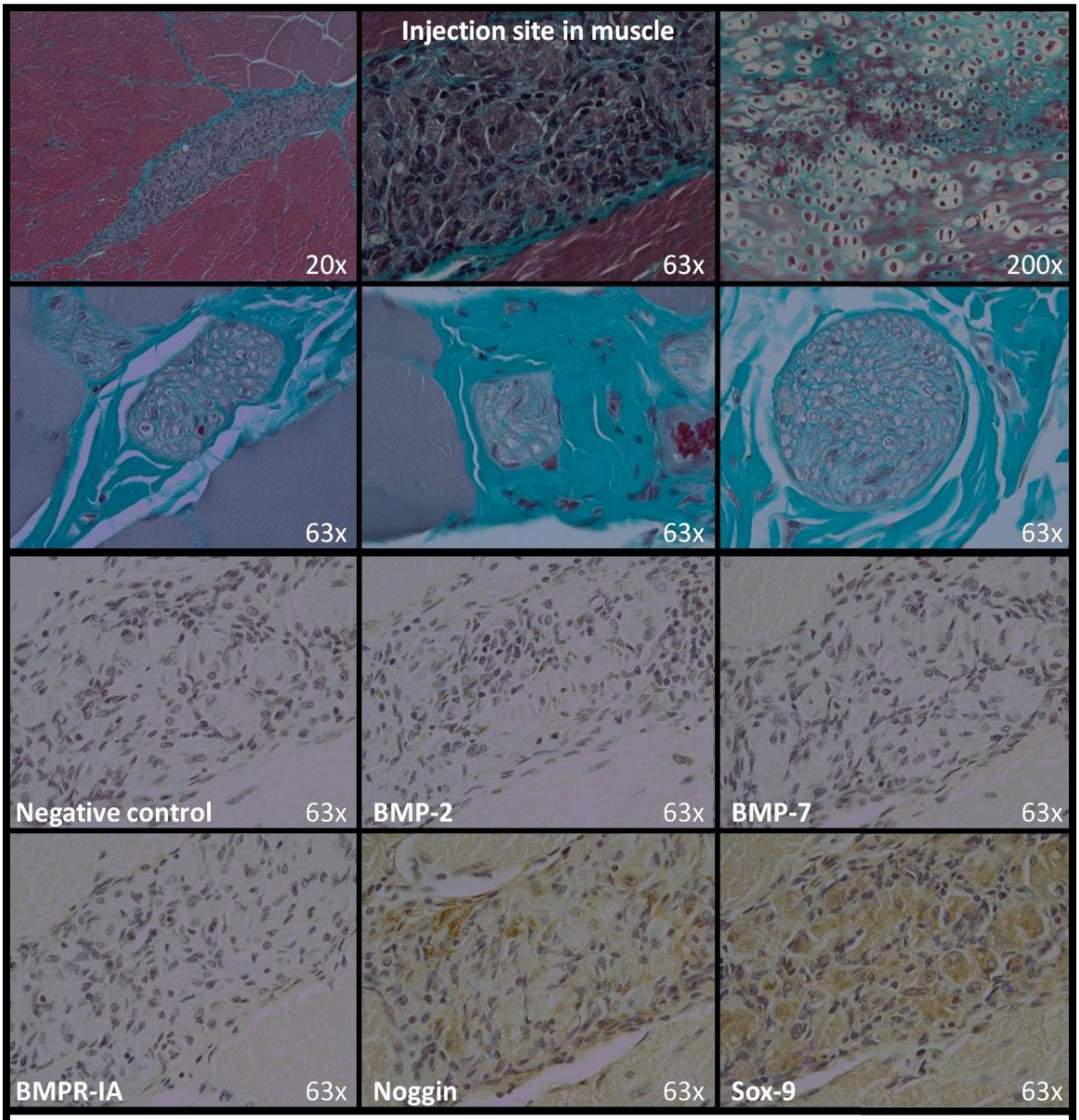


**FIG 8.6.** Selective histology (Goldner Trichrome staining) and immunohistochemistry images for the site of injection in the right quadriceps muscle of a rat injected with NPs loaded with 0.5 µg OP-1 demonstrating the biocompatibility, safety and osteogenic potential of the delivery system. The top 2 rows (histology) show the injection site and pools of osteoblastic cells (top) and healthy transverse sections of nerves and blood vessels (bottom). The bottom 2 rows (immunohistochemistry) shows expression of different ligands, their receptors and transcription factors (brown staining for chondrocytes) indicating the initiation of bone formation.

undifferentiated mesenchymal cells have the potency to differentiate into chondrocytes, fibrocytes and osteocytes (Aubin and Triffitt 2002; Wildemann et al. 2004). Furthermore, it has been suggested that because the effect of growth factors is dosage-dependent, BMPs should be used in dosages high enough to evoke cellular responses, but not ectopic bone formation. Several studies have reported that for osteoinduction to occur, a minimum dosage of 1µg rhBMP-2 (more for other BMPs) would be required (Uludag et al. 2000; Bessho et al. 2002; Yamamoto et al. 2003). Yet, studies continue to require much larger and expensive dosages in part due to the physico-chemical and release characteristics of the carriers used. For example, in one study (Kusumoto et al. 2002) performed in non-human primates, BMP-2 (50, 250 and 1250 µg) in combination with a type I collagen carrier were implanted into pouches prepared in the calf muscle of macaque monkeys. The authors reported osteoinduction in only one third of the animals treated with the highest protein concentration radiographically, while no bone formation was evident in any of the other two animal groups besides slight enlargement of the nuclei of muscle cells that might be indicative of a cellular response (Kusumoto et al. 2002).

In a more recent study (Nanno et al. 2009) using OP-1, synthetic alginate discs were prepared and implanted in the back muscle of mice. Four concentrations were investigated ranging from 3 to 30 µg OP-1. Results once more demonstrated ectopic bone formation only with the use of the highest dosage of OP-1(Nanno et al. 2009). This basically further confirms the role of our core-shell NPs in localizing, confining and restricting the effect of the release-controlled OP-1 within the site of administration. Moreover, the biocompatibility and safety of the delivery system can be recognized where no considerable or irreversible damage was detected in situ; suggested by the clear presence of healthy nerve and blood vessels in the injected area upon examining the histology slides under higher magnification. BMPs have been reported to promote angiogenesis both in vitro and in vivo (Carano and Filvaroff 2003; David et al. 2009; Moreno-Miralles et al. 2009). Angiogenesis precedes bone healing and formation as vasculature supplies the stem cells, nutrients, mineral elements and cytokines vital for osteogenesis. Deckers et al. (Deckers et al. 2002) demonstrated that BMPs stimulate angiogenesis through enhancing the production of vascular endothelial growth factor A (VEGF-A) by osteoblasts and have suggested that low doses of BMPs may be sufficient for initiating angiogenesis but not osteogenesis. This is of crucial significance in

designing drug delivery systems especially for BMPs known to be local-acting and dose-dependant, as described earlier. The capability of the localized and release-controlled hybrid NPs in promoting the bioavailability of the encapsulated growth factor and in very low, safe and cost-effective dosages (0.5 μg OP-1) is thus further demonstrated in rats in the present study as was established formerly in our rabbit tibial distraction osteogenesis model (Haidar et al. 2009 c).

On the other hand, the expression of 15 genes, representing the BMP signaling pathway involved in de novo bone formation (Rosen 2006) was evaluated at the protein level using immunohistochemistry, as displayed in the bottom two rows of Figure 8.6. The obtained data showed that the investigated genes were expressed at various levels in the six animal groups. Cellular localization was more in chondrocytes than in fibroblast-like cells for groups 2 through 6 with no response whatsoever in the control animals of group 1. And so, because the amount of mineralized bone was inconsistent an insufficient, perhaps varying depending on the site and depth of the injections, it was difficult to obtain comparative data from all samples and prepared slides. Generally, most proteins were up-regulated post-injections especially in groups 5 and 6 suggesting that the localized and release-controlled application of exogenous OP-1 most likely did stimulate bone formation processes via increasing the rate of expression of several factors involved in the BMP signaling pathways including receptors such as BMPR-I and BMPR-II, antagonists such as Noggin and BMP-3 and transcription factors such as Smads 1-5. This was not as evident in the animals receiving pure OP-1 injections. However, data could not confirm the presence of formed bone in the muscles of these rats where while group 6 appears to have much more induced activity in the expression of BMP-2, OP-1 and their receptors than the other groups, the expression of the antagonist Noggin well-known to block osteogenesis was also slightly more up-regulated, though with no significant differences detected ($\rho \geq 0.05$). Nonetheless, the observed under-expression of R-Smads1/5/8 herein has been reported earlier to accompany an over-expression of Noggin, in vitro (Tsialogiannis et al. 2009). Table 8.3 summarizes our findings. Although many in vitro studies have been conducted, it is not fully clear yet in the literature how these BMP receptor antagonists regulate in vivo bone formation and therefore the specificity of BMP-receptor signaling is an area that remains to be explored (Rosen 2006). In addition, such analysis has been mainly carried out and limited to fracture healing

and de novo bone regeneration models; further restricting a comparison of findings with other delivery systems and carriers. Finally, the

**TABLE 8.3.** Summary of immunolocalization of some of the investigated ligands and growth factors as well as their receptors and transcription factors in the harvested right quadriceps muscle of the injected rats. Staining for chondrocytes (C) and fibroblasts (F): (–) no positive staining, (+/–) < ¼ of cells stained positive, (+) ¼ of cells stained positive, (++) ¼ - ½ of cells stained positive, (+++) ½ – ¾ of cells stained positive, (++++) more than ¾ of cells stained positive. Groups 2 and 3 yielded the same data and are grouped together.

| | Saline | | 0.5/1.0 µg OP-1 | | NPs + 0.0 µg OP-1 | | NPs + 0.5 µg OP-1 | | NPs + 1.0 µg OP-1 | |
|---|---|---|---|---|---|---|---|---|---|---|
| | C | F | C | F | C | F | C | F | C | F |
| **Ligands** | | | | | | | | | | |
| BMP-2 | - | - | + | + | +/- | + | + | ++ | ++ | + |
| BMP-3 | - | - | +/- | + | +/- | +/- | +/- | + | + | + |
| BMP-7/OP-1 | - | - | +/- | + | +/- | +/- | + | ++ | ++ | ++ |
| **Receptors** | | | | | | | | | | |
| BMPR-I | - | - | +/- | +/- | +/- | + | + | ++ | ++ | + |
| BMPR-IIA | - | - | + | +/- | +/- | +/- | +/- | + | ++ | ++ |
| BMPR-IIB | - | - | +/- | +/- | + | +/- | + | + | + | ++ |
| **Transcription Factors** | | | | | | | | | | |
| SMADS 1-5 | - | - | +/- | +/- | +/- | + | + | ++ | ++ | + |
| Sox-9 | - | - | - | ++ | ++ | +/- | +++ | + | +++ | + |
| **Others** | | | | | | | | | | |
| Collagen-II | - | - | + | + | +/- | + | +++ | +++ | ++++ | ++ |
| Noggin | - | - | ++ | +++ | + | ++ | + | + | ++ | +++ |

effect of BMPs varies with species, gender and age to name a few. For example, when the effects of BMP-2 were evaluated in rats and primates, inconsistent ectopic bone formation resulted in the primate muscle independent on protein dosage whereas this was not the case in the rat muscle showing dose-dependency (Aspenberg and Turek 1996; Wildemann et al. 2004). This discrepancy might be also attributed to differences in the amount of specific BMP receptors present in the muscle sites of animal species (Bessho et al. 2002; Yamamoto et al. 2003) which as well might be consequential to variations in impact of the trauma to tissues and their surroundings from the different modes of application; surgical implantation versus a single injection as is in this study, for instance. Finally, the degree of vascularization will entail the intensity or moderation of cellular responses (Kempen et al. 2009).

## 8.5. Conclusions

Injectable delivery systems for growth factors are in high demand due to ease of application, localization at defect site and improved patient comfort. Besides the previously reported in vitro cytocompatibility, the present study is to the best of our knowledge, the first investigation of the in vivo biocompatibility and safety of an injectable hybrid nanoparticulate rhOP-1 delivery system consisting of a liposomal core and a shell constructed by the layer-by-layer self assembly of two natural polymers; alginate and chitosan, based on electrostatic interactions. The analytical findings from evaluating animal body weight and behavioral changes, a total of 50 blood markers and hematological levels along with the health status of the six major organs suggested that the nanoparticles, the released bioactive load as well as the resulting effects were restricted to the site of administration with no considerable complications or reactions from any degradation by-products. We have previously demonstrated the effect of the physico-chemical, localized and sustained release-controlled characteristics of the nanoparticles in enhancing de novo bone regeneration and consolidation in a long bone distraction osteogenesis model with very low doses of rhOP-1. The results from this study further established the possibilities of (a) maintaining the bioactivity of proteins with short half-lives over the required therapeutic time and consequently (b) alleviating the often need for using precarious and expensive large supra-physiological dosages and (c) overcome the need and issues from the invasive surgical implantation of current scaffolds and carriers for BMP-induced bone regeneration.

## 8.6. Limitations and Future Studies

Losses in the dead volume of the syringe and leakage during injection have been reported previously to result in only ~ 50% of the administered solution initially drawn into the syringe was actually deposited in situ (Ruhe et al. 2003). This might lead to un-uniformity in particle distribution and concentration in the muscle tissue. In addition, the nanoparticles were not administered intravascularly and hence might be argued that their systemic distribution and circulation fate were not fully evaluated. Ongoing studies need to validate

these results in an IV in vivo model where the tissue distribution of the nanoparticles can be monitored/followed in real-time possibly via their combination with quantum dots.

## 8.7. Acknowledgements

The authors would like to thank Mrs. Dominique Lauzier for her assistance in immunohistochemistry, Dr. Fereshteh Azari for her assistance in cryo-TEM imaging and Dr. Marilene Paquet for her comparative pathology analysis. This work was supported by an operating grant from the Shriners of North America, Fonds de la Recherche en Santé du Québec, the National Science and Engineering Research Council (NSERC), the Canadian Institutes of Health Research (CIHR) - Regenerative Medicine/Nanomedicine and the Center for Biorecognition and Biosensors (CBB), McGill University, Montréal, Québec, Canada. Dr. Haidar acknowledges scholarships from the Center for Bone and Periodontal Diseases Research and the Shriners Hospital, Montréal, Québec, Canada.

# CHAPTER 9
# Core-Shell NPs – Evaluation in a Rabbit DO Model

Bone anomalies may be congenital in nature or acquired, resulting from trauma, growth disturbances, neoplastic and/or degenerative processes. Examples include Pierre Robin Sequence (formerly known as Pierre Robin Syndrome), Crouzon Syndrome and Apert Syndrome. In these conditions, severe functional impairments such as upper airway obstruction, obstructive sleep apnea, inability to adequately masticate or persistent speech dysfunction. Although DO is a surgical technique commonly used for bone lengthening and reconstruction of such bone-related defects, it is far from optimum. The foremost limitation is the protracted treatment time required for the newly formed bone to consolidate entailing prolonged external fixation with considerable morbidity. BMP-7/OP-1 has been shown to act on the proliferation and differentiation of osteoprogenitor cells into bone-forming cells and also to stimulate the production of other growth factors such as IGFs and FGFs, thus accelerating the formation of de novo bone in numerous preclinical and clinical studies. For a clinically-beneficial outcome, the application of recombinant human (rh) OP-1 will depend on the delivery strategy and system used to provide a sustained and proper release of adequately bioactive protein concentrations into the distraction gap/callus and its surrounding area. Based on the findings from previous studies aimed at the acceleration of bone regeneration and consolidation in a rabbit model of long bone DO where endogenous OP-1 expression was shown to significantly decline in osteoblasts in the consolidation phase, it was hypothesized that the optimal time for the exogenous administration of OP-1 might be *early* in the distraction period when OP-1 receptors are abundant. Results later agreed where a two-fold increase in bone volume was radiographically apparent in animals receiving **75 µg OP-1 in acetate buffer** at 3 weeks post injection when compared to placebos or control rabbits receiving only the buffer. The difference between the groups then diminished at 5 weeks suggesting that exogenous OP-1 results in an increase in the rate and not necessarily the quantity of bone formed. On the other hand, a dose **as low as 100 ng/mL OP-1** encapsulated in the **core-shell nanoparticulate delivery system** was significantly sufficient to enhance preosteoblast differentiation, in vitro (Chapter 7) where it was also demonstrated how the increase in the shell thickness resulted in a slower rate of protein release. Therefore,

in this second in vivo study, the aim was to further investigate the localized and release-controlled *effect* of the hybrid core-shell (design) nanoparticles loaded with *a much* lower dosages of OP-1 on long bone DO in comparison to the 75 μg of OP-1/acetate buffer from previous studies, similarly administered early in the distraction phase and in the same animal model following an identical protocol (with minor changes). It is noteworthy that ***rabbits***, in part due to ease of handling and size are the one of the most universally used in musculoskeletal research as preclinical models for *bone repair* (Neyt et al. 1998) although are perhaps the least similar in bony structure and properties to humans (please see Appendix A.7).

The results were reported in a manuscript that has been recently accepted for publication (August 15th of 2009) in the peer-reviewed journal of *Growth Factors*: GGRF-2009-0012. It is reproduced with permission 

Manuscript Submitted (June 15th 09); Accepted for publication (August 15th 09) in *Growth Factors.*


# A Hybrid rhOP-1 Delivery System Enhances New Bone Regeneration and Consolidation in a Rabbit Model of Distraction Osteogenesis

**Ziyad S. Haidar[1-5], Maryam Tabrizian[1-4], Reggie C. Hamdy[2, 3, 5]**

[1]*Faculty of Dentistry, McGill University, Montréal (QC) Canada*
[2]*Center for Biorecognition and Biosensors, McGill University, Montréal (QC) Canada*
[3] *Centre for Bone and Periodontal Diseases Research, McGill University, Montréal (QC) Canada*
[4]*Department of Biomedical Engineering, Faculty of Medicine, McGill University, Montréal (QC) Canada*
[5]*Shriners Hospital for Children and Division of Orthopaedics, McGill University, Montréal (QC) Canada*

## 9.1. ABSTRACT

The effect of an early single injection of biodegradable core-shell nanoparticles (NPs) loaded with various low doses of recombinant human bone morphogenetic protein–7 (rhBMP–7/rhOP–1) on new bone regeneration and consolidation in a rabbit model of tibial distraction osteogenesis (DO) was investigated. Regenerate bone was examined using soft radiography, densitometry, micro-computed tomography and histomorphometry. Compared to control, higher bone fill scores and a two-to-three-fold increase in the quantity of mineralized tissue were prominent in the 1.0 µg and 5.0 µg OP-1/NPs groups, 3 weeks post-injections ($\rho$ > 0.05). Histologically, the distraction gap was completely ossified and the osteotomy margins poorly demarcated in those groups, one week into the consolidation phase. An up-regulation of various growth factors, ligands and receptors was observed using immunohistochemistry. This novel hybrid delivery system maintains the bioactivity of the encapsulant; minimizes the therapeutic doses of rhOP-1 and accelerates DO via its localized, release-controlled, osteogenic and naturally-biocompatible polymeric properties.

**Keywords:** *distraction osteogenesis, osteogenic protein-1, nanoparticles, delivery systems, bone densitometry, histomorphometry*

## 9.2. Introduction

Distraction osteogenesis (DO) is a prevailing surgical technique widely used for bone lengthening and includes performing an osteotomy followed by gradually distracting the two bone segments resulting in de novo bone formation within the distracted gap (Ilizarov 1989 a, b). However, a main limitation is the long period of time required for the newly formed bone to consolidate entailing prolonged external fixation with considerable morbidity (Paley 1990). For osteoregeneration to yield proper healing, mechanical stability in the defect site, osteogenic cells and osteoinductive growth factors in combination with a suitable carrier or delivery system, conceptualized as the "Diamond Concept" (Giannoudis et al. 2007) are necessary. Bone morphogenetic proteins (BMPs) are potent cytokines able to induce new bone formation in vitro and in vivo that have been successfully applied in the reconstruction of long bones, spine and the craniofacial skeleton in preclinical (Phillips et al. 2006; Seeherman et al. 2006; Chu et al. 2007) and clinical studies (Li and Wozney 2001; Reddi 2005; Gautschi et al. 2007). BMP-7, also known as osteogenic protein-1 or OP-1 has been shown to act on the proliferation and differentiation of osteoprogenitor cells into bone-forming cells, thus accelerating the formation of new bone in numerous preclinical (Cook and Rueger 1996; Ripamonti et al. 2000; Hamdy et al. 2003) and clinical studies (Cook 1999; Friedlaender et al. 2001; Vaccaro et al. 2008). It was suggested that the clinical efficacy of recombinant human (rh) OP-1 will depend on the carrier system used to ensure a sustained, multi-step, and prolonged delivery of adequate protein concentrations to the desired site of tissue repair (Mont et al. 2004). The foremost limitations include the rapid diffusion of rhOP-1 away from the site and loss of its bioactivity, resulting in ectopic bone formation or suboptimal local induction and hence failure of bone regeneration (Rose et al. 2004). Several materials for the delivery of rhBMP-2 and rhOP-1 have been developed in recent years however with limited clinical use and the ideal delivery system is still to be developed (Mont et al. 2004; Termaat et al. 2005). Thus, supra-physiological and expensive dosages of rhOP-1 in the milligram range for satisfactory bone healing continue to be required (Luginbuehl et al. 2004). Sailhan et al. applied 28.5 mg rhOP-1 with a Type I collagen carrier in a rabbit model of tibial DO, early in the distraction phase. Poor results, in comparison to control animals receiving no treatment were explained by the relatively large

bulk of the solid carrier used therefore mechanically obstructing osteoregeneration (Sailhan et al. 2006). Recently, injectable delivery systems have been gaining interest as a less invasive method for the repair of osseous defects, avoiding extensive/secondary surgery (Einhorn et al. 2003; Bishop and Einhorn 2007).

In an initial *in vitro* study (Haidar et al. 2008 a), we successfully formulated monodisperse and non-toxic nanocapsules constituting a core of cationic liposomes (L) and a shell constructed through the layer-by-layer (L-b-L) self-assembly of alternating layers of anionic alginate (AL) and cationic chitosan (CH). The system has a cumulative size of 383 ± 11.5 nm and a zeta potential surface charge of 44.61 ± 3.31 mV, suitable for complex formation with anionic proteins. In a subsequent work (Haidar et al. 2008 b), the capability of the nanoparticles to encapsulate a range of concentrations of OP-1 was investigated. The system exhibited further high physical stability in simulated physiological media as well as an extended shelf-life (up to 12 months) allowing for immediate protein loading prior to administration, preventing degradation or loss of the encapsulant. The nanoparticles offer copious compartments for protein entrapment including the aqueous core and within the customizable polyelectrolyte layers in the shell which can modulate the release kinetics according to the clinical site of interest. A sustained tri-phasic linear release of the water-soluble and readily diffusible positively-charged OP-1 was evident for an extended period of 45 days with the bioactivity of the protein maintained via enhancing pre-osteoblast differentiation, *in vitro*.

In the present work, we evaluated the effect of a single bolus injection of various low doses of rhBMP-7/rh-OP-1, administered early in the distraction phase in combination with the hybrid core-shell nanoparticulate delivery system (NPs) on the rate, quantity and quality of new bone formation and early consolidation during long bone DO in a rabbit model.

## 9.3. Materials and Methods

### 9.3.1. Animals

A total of 20 skeletally mature male New Zealand White rabbits weighing 3.5–4.5 kg were included in this study. The housing, care and experimental protocol were approved by the McGill University Animal Care and Ethics Committee. All surgeries were performed at the Plastic and Reconstructive Surgery department of the Montréal General Hospital, Montréal, QC, Canada.

### 9.3.2. Operative Protocol

The operative and distraction protocol followed were similar to our earlier studies (Rauch et al. 2000a, b; Hamdy et al. 2003; Haque et al. 2005; Mandu-Hrit et al. 2006) with minor changes. Rabbits were anesthetized via the intramuscular administration of ketamine, xylazine and acepromazine. Anesthesia was further maintained with isoflurane, oxygen and nitric oxide upon intubation. Four half-pins were inserted, two above and two below the osteotomy site (mid-right tibia). The site was then exposed subperiosteally, and the osteotomy performed using an oscillating saw just below the fusion site between the tibia and fibula. An Orthofix uniplanar M-101 external fixator (purchased from Orthofix, Inc., Verona, Italy) was applied under sterile conditions. The periosteum was re-approximated and the wound closed using resorbable sutures. Unrestricted weight bearing and activity were allowed post-operatively. After a delay of 7 days (latency phase), distraction was started at a rate of 0.5 mm every 12 hours for a period of 3 weeks (distraction phase). This was followed by a no manipulation period of 1 week, during which the external fixator was held in place without distraction (consolidation phase) as shown in Figure 9.1.

The rabbits were examined daily for signs of infection, weight loss and pain. All rabbits were sacrificed by intravenous administration of 1 mL/Kg Euthanyl (MTC Pharmaceuticals, Cambridge, ON, Canada) 5 weeks post-osteotomy.

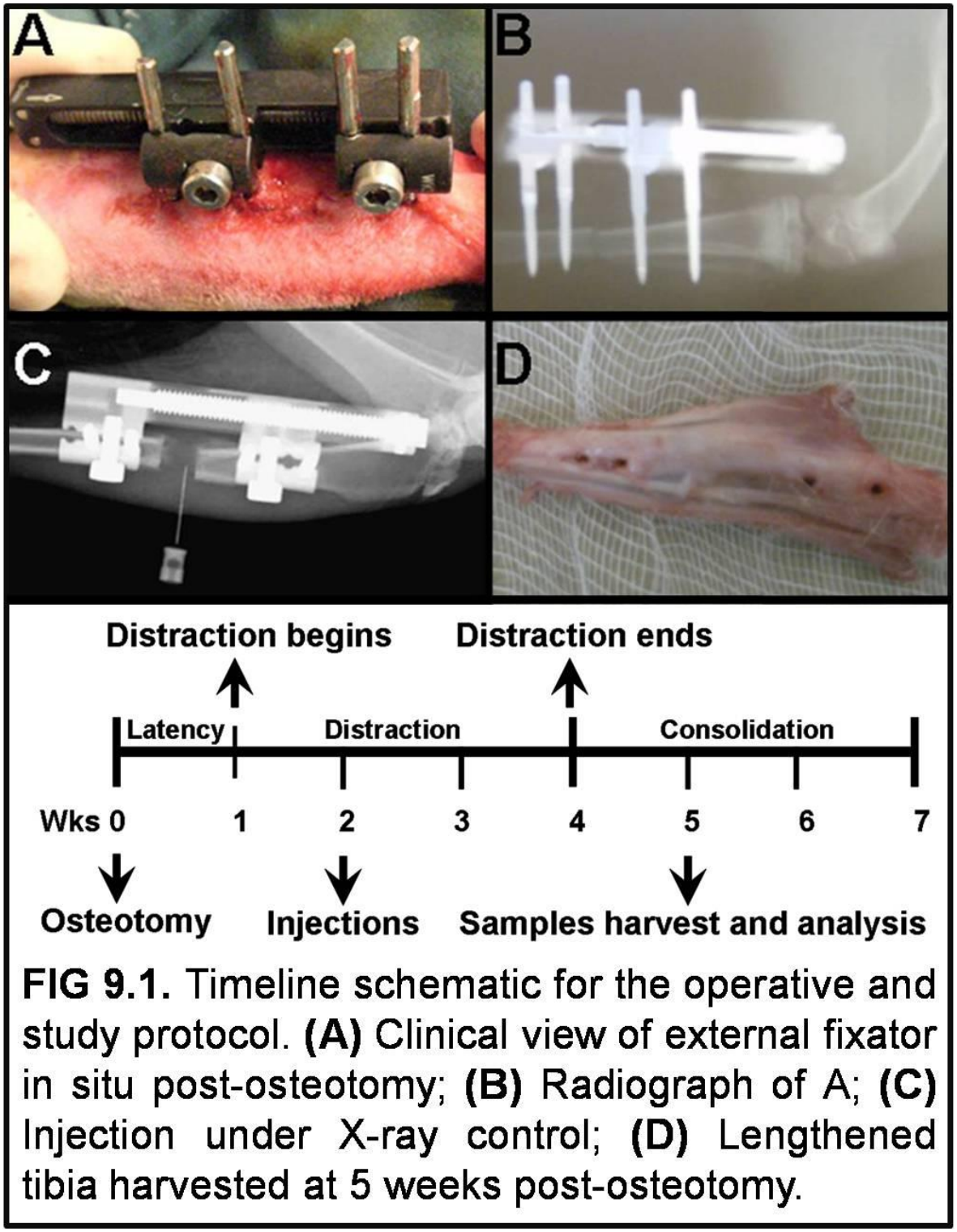


**FIG 9.1.** Timeline schematic for the operative and study protocol. **(A)** Clinical view of external fixator in situ post-osteotomy; **(B)** Radiograph of A; **(C)** Injection under X-ray control; **(D)** Lengthened tibia harvested at 5 weeks post-osteotomy.

### 9.3.3. Formulation of rhOP-1/Core-Shell Nanoparticles

The formulation and characterization of the hybrid core-shell nanoparticulate protein delivery system has been previously described (Haidar et al. 2008a,b). Briefly, for the preparation of liposomes, 1,2-Dipalmitoyl-sn-glycero-3-phosphocholine was purchased from Genzyme Pharmaceuticals, Switzerland; cholesterol and dimethyldioctadecyl-ammonium bromide (DDAB) were obtained from Sigma-Aldrich Chemical. The extrusion apparatus was purchased from Avanti® Polar Lipids, and the 19 mm polycarbonate filters (200 nm pore size) were obtained from GE Osmonics. For the L-b-L coating, alginic acid (AL: sodium salt; viscosity of 2% in water) and chitosan (CH: 85% deacetylated with molecular weight of 91.11 kDa) were obtained from Sigma-Aldrich Chemical. Liposomes were formulated via the thin-film hydration technique followed by extrusion through double 200 nm polycarbonate filters.

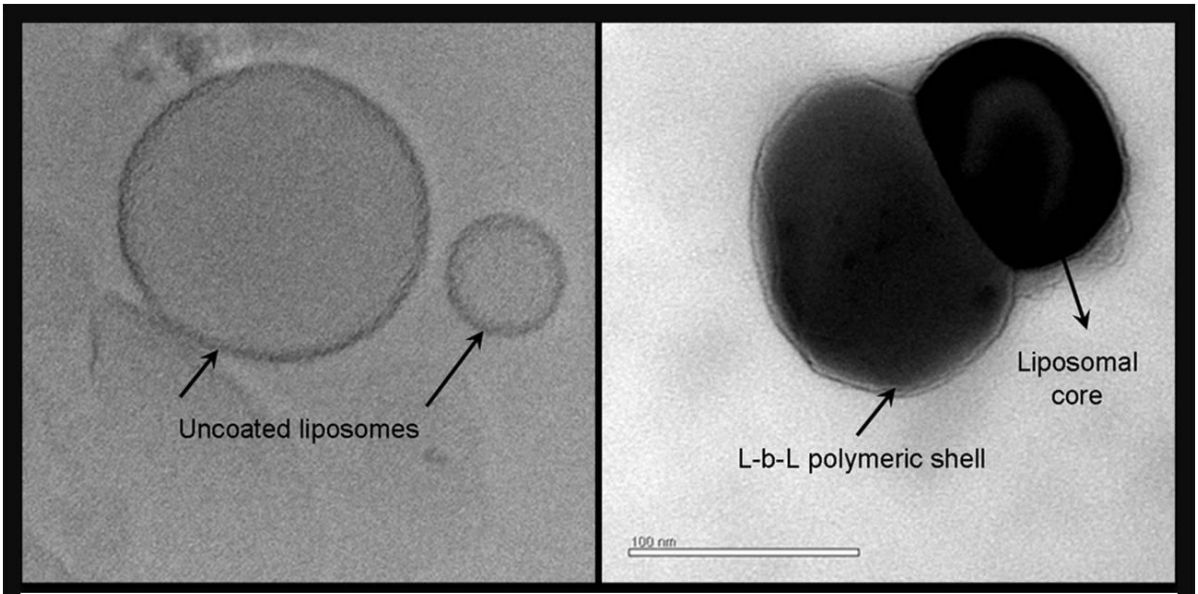


**FIG 9.2.** Cryo-Transmission Electron Microscopy (Cryo-TEM) of uncoated (left) and coated (right) liposomes. Bar = 100 nm. The polymeric shell coating the liposomal core maintains the spherical morphology and supports the stability of the nanoparticles following the aggressive preparatory steps prior to imaging.

For the L-b-L build-up, fresh AL and CH solutions (1 mg/mL) were prepared in highly pure water. The cationic liposomes were coated with alternating layers of AL and CH until the

desired number of polyelectrolyte layers was achieved; 6 layers: L(AL-CH)3, herein. With the deposition of each polymeric layer, the solution was incubated at room temperature for 60 min and centrifuged at 1600g for 15 min for washing.

### 9.3.4. Evaluation of rhOP-1 Encapsulation

Prior to protein loading, aliquots of nanoparticle suspensions were freeze-dried using sucrose as a cryoprotectant at -54$^{o}$C for 48 h (Modulyo D-115, Thermo Savant, MA). Lyophilized nanoparticles were rehydrated to the original volume with different concentrations of OP-1 solution (0.0 to 5.0 µg/mL). rhOP-1 (15.7 kDa molecular weight, lyophilized) was purchased from bio-WORLD, OH and stored at -20$^{o}$C until use. Cryo-Transmission electron microscopy (Cryo-TEM) images of uncoated and coated liposomes are displayed in Figure 9.2. It is evident how the polymeric shell surrounding the liposomal core helps maintain the spherical morphology and stability of the nanoparticles.

### 9.3.5. Study Protocol

Rabbits were randomized into 5 groups to receive a single 0.2 mL injection of either: **A**; distraction with saline (n=4), **B**; distraction with un-loaded or blank NPs (n=4), **C**; distraction with 0.5 µg OP-1/NPs (n=4), **D**; distraction with 1.0 µg OP-1/NPs (n=4) and **E**; distraction with 5.0 µg OP-1/NPs (n=4). All injections were carried out using latex-free micro-fine® IV insulin syringes (28G½ 0.36 mm x 13 mm, Becton Dickinson and Co., NJ, USA). A single bolus was injected in and around the centre of the distracted zone, 1 week after the beginning of distraction. Two sets of experiments were performed. First, the quality and quantity of the regenerate bone tissue 3 weeks after the administration of control and experimental injections was analyzed. After sacrificing, the operated tibia of each animal was disarticulated and wrapped in moist saline dressings. The specimens then underwent radiography, bone densitometry, micro-computed tomography (µCT) and bone histomorphometry. In the second set of analyses, molecular changes at 5 weeks post-osteotomy in the regenerate bone were evaluated using immunohistochemistry. This time

point was chosen as we have previously observed maximal bone formation following the administration of OP-1 (Mandu-Hrit et al. 2006).

### 9.3.6. Radiology

Immediately at time of sacrifice, antero-posterior and/or lateral X-ray views of the operated tibiae were taken. Bone fill scores were determined using a semi-quantitative scale as previously described by Kirkerhead et al. 1995 and Zimmermann et al. 2004. Bone densitometry was performed using a Lunar PixiMUS 1.46 device (GE-Lunar, Madison, WI). Areal bone mineral density (BMD) was determined in the lengthened zone of the right tibia. Samples for μCT were dissected free of soft tissue, fixed overnight in 70% ethanol, and scanned with a SkyScan 1072 microCT instrument (SkyScan, Antwerp, Belgium). A rotation step of 0.9 degrees and an exposition time of 2240 ms were used in order to attain sequential 2D images. The cross-sections along the specimen axis were reconstructed using the available Cone-Beam Reconstruction Software (SkyScan, Antwerp, Belgium), with a distance between each cross-section set at 27.36 μm. CTanalyser and 3Dcreator software (both from SkyScan) were used for image analysis. This set of analysis was carried out at the Genome Québec Innovation Center for Bone and Periodontal Diseases, Montréal, QC, Canada.

### 9.3.7. Bone Histomorphometry

Following radiological analysis, dissected samples assigned for histomorphometry were left un-decalcified, embedded in polymethylmethacrylate and sectioned at 4μm thickness. To distinguish between mineralized and un-mineralized tissue, the sections were stained with toluidine blue and Goldner Trichrome for comparative histology. A Polyvar microscope (Reichert-Jung, Heidelberg, Germany) was then used at an 80 fold magnification and quantification was performed using a digitizing tablet and the Osteomeasure® software (Osteometrics, Atlanta, GA). The defined region of interest (as previously described Figure 5.4 of Chapter 5) was the entire distraction gap and divided into the ‘callus’ region and the

'center' region containing the fibrous inter-zone (Hamdy et al. 2003; Mandu-Hrit et al. 2006). The amount of bone, cartilage, fibro-cartilage and fibrous tissue was calculated as a % of the total volume with bone marrow representing the remainder.

### 9.3.8. Immunohistochemistry

Specimens assigned for immunohistochemistry were prepared as previously described (Mandu-Hrit et al. 2006; Mandu-Hrit et al. 2008). Bone samples were fixed in 4% paraformaldehyde overnight, decalcified in 20% ethylenediamine tetraacetic acid for 3 weeks, and then embedded in paraffin. Seven micrometer sections were then cut. After de-paraffinization and hydration, endogenous peroxidase was blocked with 1% hydrogen peroxide for 10 min. Nonspecific binding was blocked by incubation in phosphate-buffered saline (PBS) containing 1% blocking (normal horse serum) reagent and 0.1% Triton (Boehringer Manhein, QC, Canada) for 30 min.

For immunostaining, commercially available polyclonal goat antibodies (Santa Cruz Biotechnology Inc., Santa Cruz, CA) were used. We have previously published the results of experiments on rabbits using these antibodies, including BMPs, their receptors and Smads for immunohistochemical analysis in DO (Rauch et al. 2000a; Campisi et al. 2003; Haque et al. 2005; Mandu-Hrit et al. 2006) as well as others (Yazawa et al. 2003). Sections were incubated with primary antibodies (25 mg/ml in PBS with 1% blocking reagent and 0.1% Triton) overnight at $4^{o}$C in a humidified chamber. As a secondary antibody, a biotinylated anti-goat antibody was used. Sections were stained using the avidin-biotin complex method (Vector Labs, Burlingame, CA) and 3,3'-diaminobenzidine tetrachloride for 30 min. The sections were then counterstained with Mayer's hematoxyline and mounted. We have previously verified that the antibodies used in this study recognized rabbit proteins (Mandu-Hrit et al. 2006). Bone histomorphometry and immunohistochemistry were done at the Shriners Hospital Laboratories, Montréal, QC, Canada.

### 9.3.9. Qualitative & Quantitative Grading of Immunostained Sections

Based on previously published reports (Tavakoli et al. 1999; Yeung et al. 2001), we have developed and used a semiquantitative analysis in order to evaluate immunohistochemistry images. This technique had been previously described by us (Rauch et al. 2000a; Hamdy et al. 2003; Haque et al. 2005; Mandu-Hrit et al. 2006). The number of cells expressing the various proteins was assessed by cell counting. Sections were graded by a blind observer as follows: - no staining; + staining in less than 25% of cells; ++ staining in 25–50% of cells; +++ staining in 50–75% of cells; ++++ staining in more than 75% of cells. Chondrocytes, osteoblastic and fibroblastic cells were identified morphologically. These analyses were performed separately for the callus and the center regions.

### 8.3.10. Statistical Analysis

*In vivo* bone densitometry, μCT and histomorphometry data are all expressed as mean value ± SD. Differences between treatment groups were tested for significance using a 2-tail student *t*-test where $\rho$-values less than 0.05 were deemed significant throughout. Radiological and immunohistochemistry data are represented as an average score from blind observations.

## 9.4. Results

During the study, no abnormal clinical signs, complications and/or behaviors in any groups occurred post-operatively and all rabbits were fully weight-bearing immediately after surgery. Normal growth over the experimental time span was reported by the animal health care technicians supervising the animals.

### 9.4.1. Cellular Changes following the Administration of Injections

#### 9.4.1.1. Radiology

Radiographs of the harvested tibias were analyzed qualitatively and semi-quantitatively at 3 weeks post-injections (1 week into the consolidation phase where distraction forces ceased). No cortices were identified in the distracted zone and no cyst formation was evident in any of the harvested samples in all groups. Qualitatively, there was more mineralized and calcified bone in the distracted zones of rabbits that had received 1.0 and 5.0 µg of OP-1/NPs than in the negative and positive control groups (saline and blank nanoparticles, respectively) and the 0.5 µg OP-1/NPs group, as is displayed in Figure 9.3.

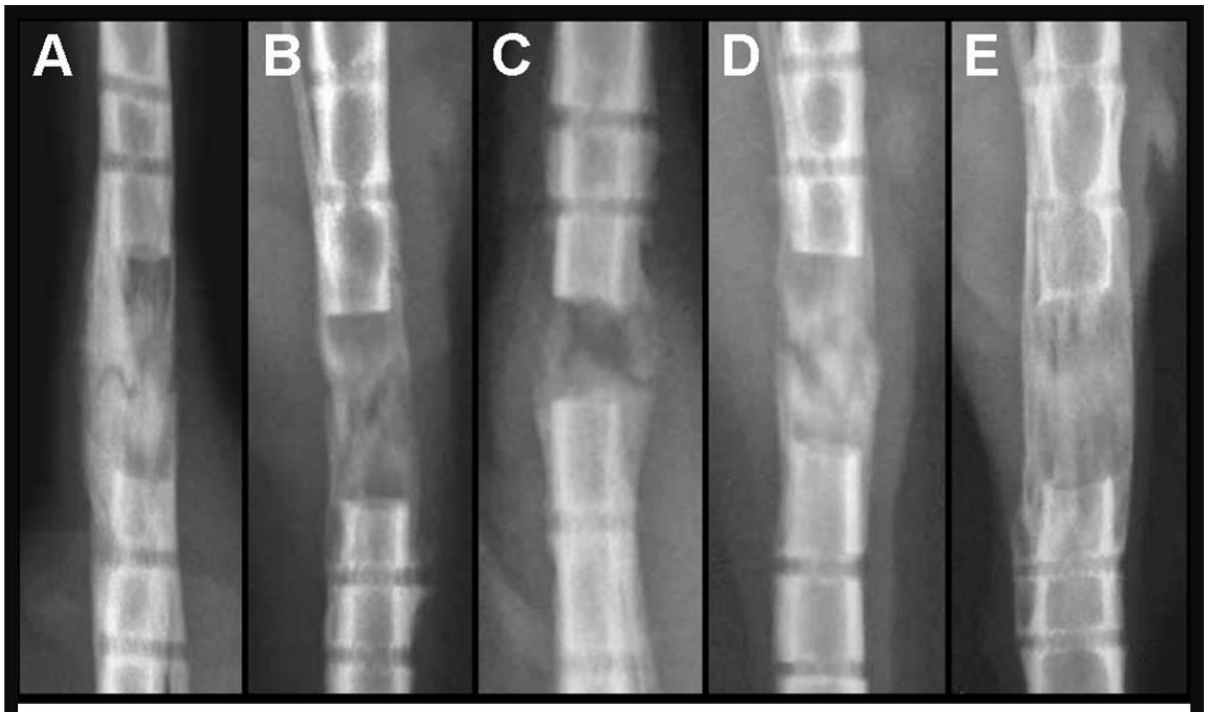


**FIG 9.3.** Radiology images of harvested rabbit tibiae at 3 weeks post-injections of: **(A)** saline; **(B)** unloaded nanoparticles (NPs); **(C)** NPs + 0.5 µg OP-1; **(D)** NPs + 1.0 µg OP-1; **(E)** NPs + 5.0 µg OP-1. A higher radiographic bone fill can be noticed with the increase of the OP-1 concentration.

Semi-quantitative analysis revealed significant differences in radiographic bone fill score (from three independent and blinded raters with radiographic experience) among the groups ($\rho$ = 0.003): 2.7±0.5 (A); 3.9±0.7 (B); 4.33±0.5 (C); 4.78±0.7 (D) and 4.88±0.6 (E). Interestingly, rabbits injected with blank nanoparticles yielded higher radiographic bone fill scores ($\rho$ > 0.05) than what distraction alone showed signifying the osteogenicity of the natural polymers incorporated in the formulation of the nanoparticles.

#### 9.4.1.2. Bone Densitometry

As displayed in Figure 9.4, significantly higher BMD amounts were evident in the distraction zone post-injection in groups D and E ($\rho$ < 0.05) than in the other groups. Groups D and E do not have significant differences in BMD among them. However it is noteworthy that group B or injections of blank nanoparticles in highly-pure water seem to have no negative interference with the bone regeneration process (0.35±0.04 g/cm$^2$, $\rho$ > 0.05).

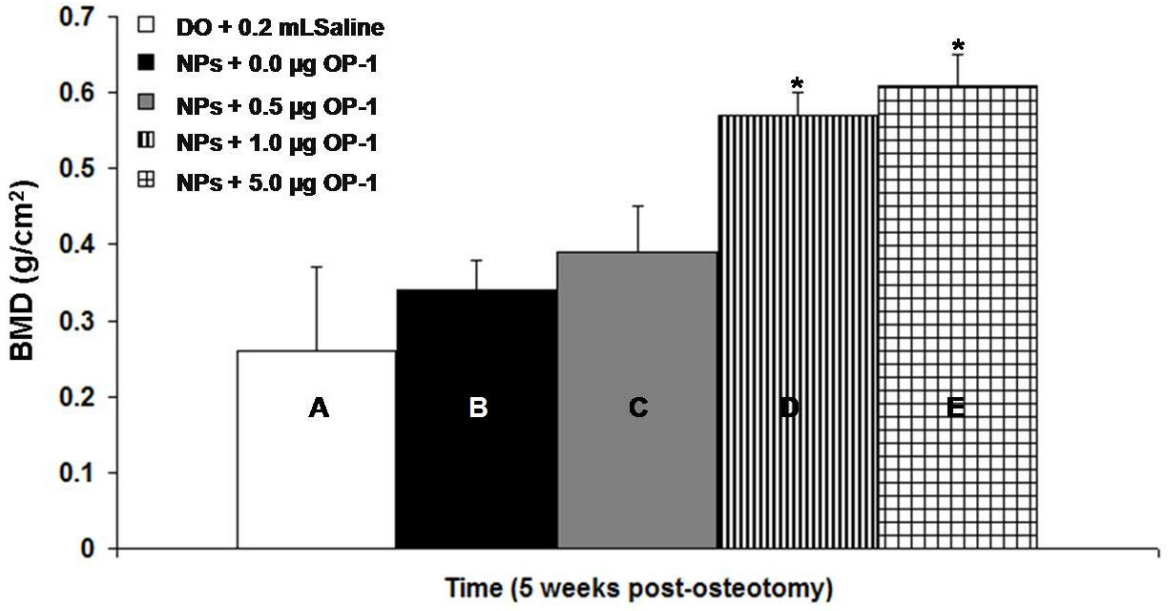


**FIG 9.4.** Bone mineral density (BMD) of the regenerate bone in the distraction gap of the harvested rabbit tibiae at 3 weeks post-injections (0.2 mL) equivalent to 5 weeks post-osteotomy. **(A)** distraction only + saline; **(B)** unloaded nanoparticles in highly pure water (NPs + 0.0 µg OP-1); **(C)** NPs + 0.5 µg OP-1; **(D)** NPs + 1.0 µg OP-1; **(E)** NPs + 5.0 µg OP-1. Significantly higher BMD amounts are evident in groups D and E ($\rho < 0.05$) compared to A-C. Interestingly, group B shows a positive effect on the bone regeneration process compared to group A ($\rho < 0.05$).

#### 9.4.1.3. Bone Architecture

The BMD results above were further confirmed by µCT analysis of the harvested tibias providing quantitative and qualitative information on bone growth and structure in long bone DO.

**TABLE 9.1. Summary of µCT analysis**

| | Distraction only | NPs + 0.0 µg OP-1 | NPs + 0.5 µg OP-1 | NPs + 1.0 µg OP-1 | NPs + 5.0 µg OP-1 |
|---|---|---|---|---|---|
| **Relative bone volume (BV/TV x 100)** | 12.9 ± 4.3 | 17.4 ± 2.7 | 18.2 ± 7.2 | 20.78 ± 12.0 | 22.92 ± 4.2* |
| **Bone surface to volume ratio (BS/BV)** | 17.8 ± 5.4 | 30.53 ± 3.9 | 37.82 ± 8.6 | 48.12 ± 9.0 | 36.5 ± 0.9 |
| **Trabecular thickness (Tb. Th.)** | 0.24 ± 0.07 | 0.22 ± 0.0002 | 0.24 ± 0.1 | 0.25 ± 0.1 | 0.28 ± 0.02 |
| **Trabecular pattern factor (TbPf/mm)** | 12.3 ± 2.4 | 4.3 ± 2.0 | 6.3 ± 8.4 | 8.7 ± 5.1 | 10.9 ± 5.7 |
| **Structural model index (SMI)** | -0.12 ±1.08 | 1.64 ± 0.02 | 1.72 ± 1.004 | 1.904 ± 0.7 | 2.15 ± 0.7* |
| **Bone surface density (BS/TV, mm)** | 1.0 ± 0.09 | 5.5 ± 1.5 | 5.6 ± 2.5 | 3.4 ± 2.4 | 3.91 ± 1.3 |
| **Bone normalization** | 16.1 ± 6.0 | 19.0 ± 9.3 | 19.7 ± 11.1 | 22.4 ± 4.8* | 23.3 ± 6.8* |

Results are expressed as mean ± SD; *$\rho < 0.05$ for statistical difference between groups.

The use of μCT allowed for the evaluation of additional parameters including trabecular thickness (Tb.Th.), structural model index (SMI), relative bone volume (BV) and bone surface (BS) to bone volume (BV) ratio as well as bone surface density. The SMI is a parameter indicating changes in the bone micro-architecture and ranges from 0 to 3 depending on whether the structure is plate-like, rod-like or a combination of both (Haque et al. 2008). These parameters are summarized in Table 9.1. At 3 weeks post-injections, a two-to-three fold increase in the quantity of mineralized tissue (including bone and cartilage) was noted, more markedly in groups D and E.

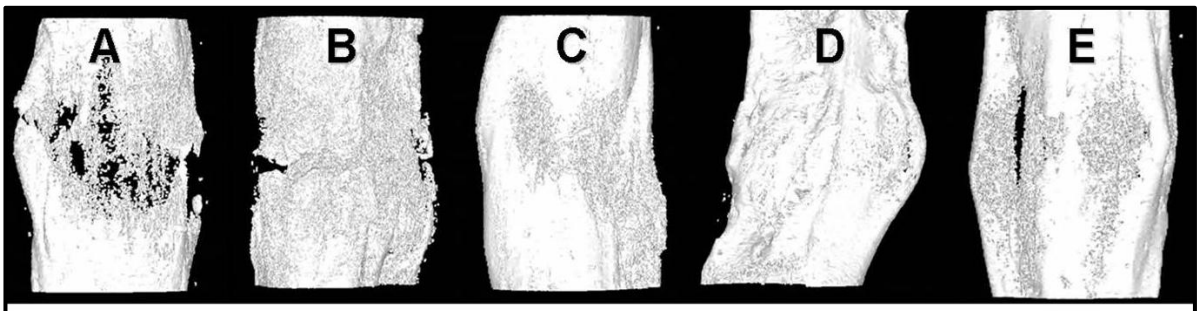


**FIG 9.5.** μCT images of harvested rabbit tibiae at 3 weeks post-injections of: **(A)** distraction only + saline; **(B)** unloaded nanoparticles in highly pure water (NPs + 0.0 μg OP-1); **(C)** NPs + 0.5 μg OP-1; **(D)** NPs + 1.0 μg OP-1; **(E)** NPs + 5.0 μg OP-1. A denser bone structure is present in groups D and E with the mineralized tissue completely filled and consolidated in the distraction gap.

Bone normalization (bone volume/length) for the control groups A (distraction only) and B (distraction and blank nanoparticles injection) was 16.1±6.0 $mm^2$ and 19.0±9.3 $mm^2$, respectively in comparison to 23.3±6.8 $mm^2$ for 5.0 μg OP-1//NPs or group E ($\rho < 0.05$). No significant differences were observed in the Tb.Th. between all groups. Figure 9.5 displays images of the harvested rabbit tibias at 5 weeks post-operatively. It is clear that a denser bone structure is present in groups D and E with the mineralized tissue completely filled and consolidated in the distraction gap.

#### 9.4.1.4. Histology and Histomorphometry of the Newly Formed Bone

Goldner Trichrome stained histological sections were prepared. The mineralized and un-mineralized tissues at the middle of the distraction zone of the harvested rabbit tibiae are shown in Figure 9.6. Table 9.2 displays the findings from the histomorphometric analysis used to determine the percent of bone, cartilage, fibrocartilage and fibrous tissue present.

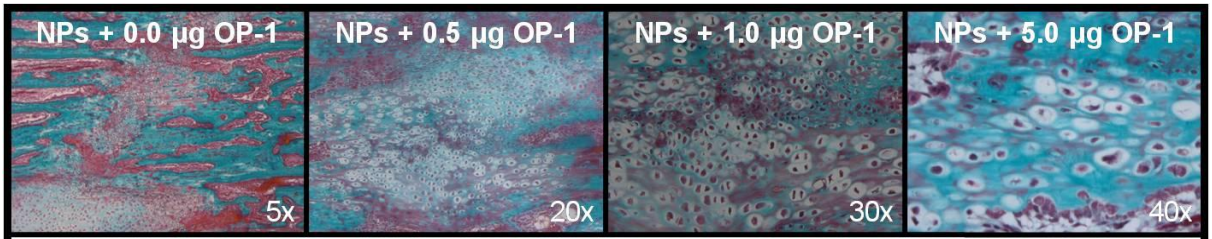


**FIG 9.6.** Several microscopic magnifications of the Goldner Trichrome-stained histological sections of the middle of the distracted zone in the harvested rabbit tibiae at 3 weeks post-injections. High amounts of vascularized connective tissue, osteoblastic and fibroblastic cells are identified throughout the distracted areas of all harvested tibia samples.

Significant amounts of highly vascularized connective tissue, osteoblastic and fibroblastic cells, and cartilaginous areas were identified throughout the distracted areas of all harvested samples. Elongated fibroblastic cells were noticeable in the direction of the distraction strain.

One week into the consolidation phase, the distraction gap was essentially ossified and the osteotomy margins poorly demarcated in groups D and E. Quantitative analysis revealed statistically significant differences with group E for percent of bone, cartilage and fibrocartilage present ($\rho$ = 0.01). Group D showed significance in percent bone and fibrocartilage only ($\rho < 0.05$).

**TABLE 9.2. Summary of histomorphometry analysis**

| | Distraction only | NPs + 0.0 µg OP-1 | NPs + 0.5 µg OP-1 | NPs + 1.0 µg OP-1 | NPs + 5.0 µg OP-1 |
|---|---|---|---|---|---|
| **Bone volume/tissue volume** | 13.3 ± 2.4 | 16.7 ± 2.8 | 19.3 ± 3.3 | 22.7 ± 4.8* | 23.6 ± 3.6* |
| **Cartilage volume/tissue volume** | 2.4 ± 2.0 | 2.5 ± 3.1 | 1.6 ± 0.8 | 1.0 ± 0.4 | 0.8 ± 0.6* |
| **Fibrocartilage volume/tissue volume** | 0.73 ± 0.84 | 0.61 ± 0.82 | 0.2 ± 0.13 | 0.09 ± 0.15 | 0.08 ± 0.18 |
| **Fibrous tissue volume/tissue volume** | 26.1 ± 5.8 | 24.5 ± 6.2 | 18.3 ± 3.7 | 12.7 ± 4.3* | 10.4 ± 3.9* |

Results are expressed as mean ± SD; *$\rho < 0.05$ for statistical difference between groups.

### 9.4.2. Molecular Changes following the Administration of Injections

The mechanical forces applied during distraction stimulate the expression of various genes as verified by our immunohistochemistry results. The expression of 15 genes, representing various pathways leading to de novo bone formation was evaluated at the protein level using immunohistochemistry. Sample images are displayed in Figure 9.7 (supplementary images are represented in Figure 9.8 at the end). The obtained data showed that all investigated proteins were expressed at various levels (up or down-regulation) in all groups. Cellular localization was mostly in chondrocytes and fibroblast-like cells. Their spatial expression was diffuse in the distracted zone.

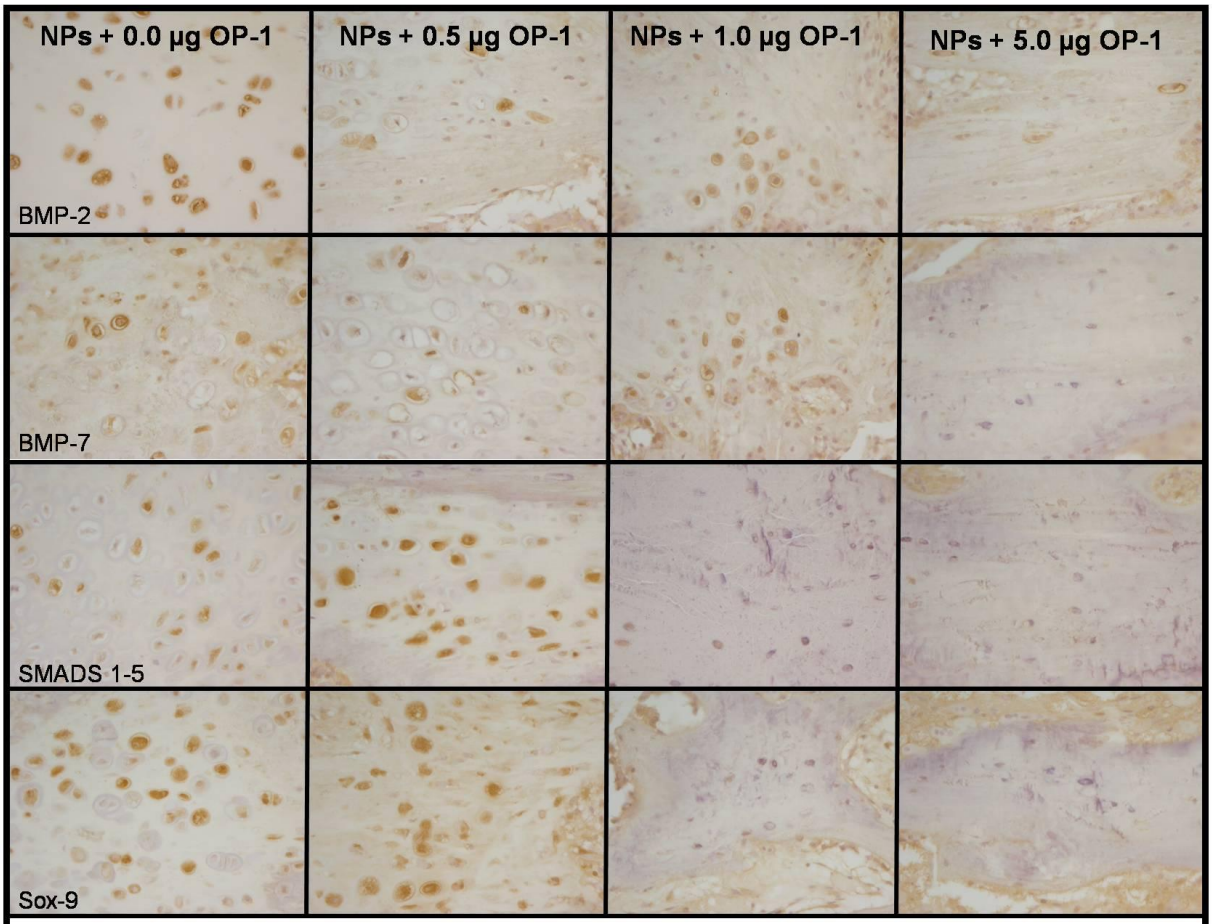


**FIG 9.7.** Selective immunohistochemistry images for the expression of several ligands, growth factors and receptors at 3 weeks post-injections. Cells stained brown indicate expression of the specified protein and pinkish areas indicate consolidated de novo bone.

Tables 9.3 and 9.4 summarize these findings in the center and the callus of the distraction gap, respectively. Generally, all proteins were up-regulated 3 weeks post-injections; especially in groups A, B and C.

**TABLE 9.3. Summary of immunolocalization of the investigated ligands and growth factors as well as their receptors and transcription factors in the center of the DO gap**

| | Distraction only | | NPs + 0.0 µg OP-1 | | NPs + 0.5 µg OP-1 | | NPs + 1.0 µg OP-1 | | NPs + 5.0 µg OP-1 | |
|---|---|---|---|---|---|---|---|---|---|---|
| | Chondrocytes | Fibroblasts | Chondrocytes | Fibroblasts | Chondrocytes | Fibroblasts | Chondrocytes | Fibroblasts | Chondrocytes | Fibroblasts |
| **Ligands** | | | | | | | | | | |
| BMP-2 | ++ | ++ | +++ | ++++ | ++ | ++ | + | - | + | - |
| BMP-3 | ++ | ++ | +++ | ++ | ++++ | +++ | + | - | + | - |
| BMP-7/OP-1 | ++ | ++ | +++ | +++ | ++++ | ++++ | + | - | ++ | - |
| **Receptors** | | | | | | | | | | |
| BMPR-I | +++ | ++ | +++ | +++ | +++ | ++++ | + | - | ++ | ++ |
| BMPR-IIA | +++ | ++ | +++ | +++ | +++ | ++++ | + | - | ++ | ++ |
| BMPR-IIB | +++ | +++ | +++ | +++ | +++ | ++++ | + | - | - | - |
| ACTR-I | +++ | ++ | +++ | +++ | +++ | ++ | + | - | ++ | + |
| ACTR-IIA | +++ | ++ | ++ | +++ | +++ | ++ | + | - | + | + |
| ACTR-IIB | +++ | ++ | ++ | +++ | +++ | +++ | + | - | ++ | + |
| FGFR-III | +++ | ++ | ++ | ++ | ++ | ++ | + | - | + | - |
| **Transcription Factors** | | | | | | | | | | |
| SMADS 1-5 | +++ | ++ | +++ | +++ | +++ | +++ | - | - | + | + |
| Sox-9 | +++ | ++++ | +++ | +++ | +++ | +++ | - | - | + | + |
| **Others** | | | | | | | | | | |
| Collagen-II | +++ | +++ | ++ | ++ | ++++ | ++++ | - | - | + | + |
| Noggin | +++ | ++ | +++ | +++ | +++ | +++ | - | - | + | + |

Staining at the fibrous inter-zone. (–) no positive staining indicating consolidated bone, (+) less than ¼ of cells stained positive, (++) ¼ - ½ of cells stained positive, (+++) ½ – ¾ of cells stained positive, (++++) more than ¾ of cells stained positive.

Results confirm the accelerated bone regeneration and consolidation noted in groups E and D especially in the center of the distraction gap for the earlier and in the callus for the latter. Group D appears to have much more consolidated bone areas than E, however the difference was not significant ($\rho \geq 0.05$).

**TABLE 9.4. Summary of immunolocalization of the investigated ligands and growth factors as well as their receptors and transcription factors in the callus of the DO gap**

| | Distraction only | | NPs + 0.0 µg OP-1 | | NPs + 0.5 µg OP-1 | | NPs + 1.0 µg OP-1 | | NPs + 5.0 µg OP-1 | |
|---|---|---|---|---|---|---|---|---|---|---|
| | Chondrocytes | Fibroblasts | Chondrocytes | Fibroblasts | Chondrocytes | Fibroblasts | Chondrocytes | Fibroblasts | Chondrocytes | Fibroblasts |
| **Ligands** | | | | | | | | | | |
| BMP-2 | + | + | ++++ | ++++ | ++ | ++++ | +++ | + | + | - |
| BMP-3 | + | ++ | +++ | +++ | ++++ | +++ | ++ | ++++ | ++ | + |
| BMP-7/OP-1 | + | ++ | +++ | +++ | +++ | +++ | ++++ | ++++ | + | - |
| **Receptors** | | | | | | | | | | |
| BMPR-I | ++ | + | ++++ | ++++ | ++++ | ++++ | ++++ | ++++ | ++ | - |
| BMPR-IIA | +++ | + | +++ | +++ | ++ | ++++ | ++++ | ++++ | ++ | + |
| BMPR-IIB | +++ | ++ | +++ | +++ | ++ | ++++ | ++++ | ++++ | + | - |
| ACTR-I | ++ | + | +++ | +++ | +++ | +++ | ++ | ++ | - | - |
| ACTR-IIA | ++ | + | +++ | +++ | ++ | +++ | ++++ | +++ | +++ | + |
| ACTR-IIB | +++ | + | ++ | +++ | ++ | +++ | +++ | ++ | ++ | + |
| FGFR-III | + | ++ | ++ | ++ | ++ | ++ | + | - | + | - |
| **Transcription Factors** | | | | | | | | | | |
| SMADS 1-5 | ++ | + | ++ | +++ | +++ | +++ | ++ | ++ | + | ++ |
| Sox-9 | +++ | ++ | ++ | +++ | ++ | +++ | +++ | ++++ | ++ | + |
| **Others** | | | | | | | | | | |
| Collagen-II | ++ | + | +++ | ++++ | +++ | +++ | +++ | ++ | ++++ | ++ |
| Noggin | +++ | + | +++ | +++ | +++ | ++ | ++++ | ++++ | ++ | + |

Staining at the fibrous inter-zone. (–) no positive staining indicating consolidated bone, (+) less than ¼ of cells stained positive, (++) ¼ - ½ of cells stained positive, (+++) ½ – ¾ of cells stained positive, (++++) more than ¾ of cells stained positive.

The simultaneous increase in these genes verifies that exogenous OP-1 induction most likely increases the rate of bone formation in DO via increasing the rate of expression of various factors involved in its signaling pathways. Reduction in staining of activin receptors and antagonists such as Noggin and Chondrin, from group A through E signifies the ossification and consolidation of the distracted gap.

## 9.5. Discussion

Our previous in vitro work with rhOP-1 encapsulated in the core-shell nanoparticulate delivery system showed that a dose as low as 100 ng/ml was significantly sufficient to enhance preosteoblast differentiation noted by an increased alkaline phosphatase activity over 7 days. We have demonstrated how the increase in shell thickness slowed the rate of protein release where OP-1 release from uncoated liposomes was clearly faster than from coated liposomes. OP-1 release from this physically dispersed polymeric system may be described by several possible mechanisms: diffusion, polymer degradation, ion complexation, and interactions among the protein and the polymers, although it is primarily governed by a diffusion-based or affinity-based mechanism (Haidar et al. 2008 a, b).

In vivo, we have previously shown that using 75 μg of OP-1 in acetate buffer early during DO in rabbits accelerated bone formation (Mandu-Hrit et al. 2006). Three weeks following OP-1 injections, radiology, densitometry and μCT data revealed an increase in the quantity of bone for treated groups in comparison to the placebo (acetate buffer only).

Therefore, in this study, we aimed to investigate the effect of the core-shell nanoparticles loaded with very much lower dosages of OP-1 on long bone DO in comparison to the 75 μg of OP-1 in acetate buffer (Mandu-Hrit et al. 2006), similarly administered early in the distraction phase.

Qualitative and quantitative evaluation of the distracted zone suggested that at 3 weeks post-injection there was more mineralized bone in rabbits that had received OP-1 (0.5, 1.0 and 5.0 μg loaded in the nanoparticles) than in the control groups (distraction alone and with unloaded nanoparticles). Bone densitometry revealed that the treated groups had a higher

amount of bone in the distraction gap at 5 weeks post-osteotomy as well. The quantity of mineralized bone was almost double for groups that had received only 1.0 μg of OP-1 treatment in comparison to the control (22.7±4.8 and 13.3±2.4, respectively) and even our results from the previous assays with 75 μg OP-1 (11.3±1.8) as confirmed by μCT analysis. A denser bone structure was clear in the 3-D images with the distraction gap almost completely filled with mineralized tissue.

This demonstrated accelerated osteogenesis and consolidation via a single injection of the core-shell delivery system loaded with a dose of no more than 1.0 μg rhOP-1 in comparison to earlier results from a single injection of rhOP-1 (75 μg in acetate buffer) and to others in the literature, emphasizes the role of our localized and release-controlled nanocapsules. BMPs act locally and therefore, the concentration of BMPs at the site of interest is more crucial than the total dose of the protein (Reddi 2005; Termaat et al. 2005).

Nanoparticulate systems seem therefore to play a major role in the localization and confinement of the released encapsulant to the area of interest, hence, we have not seen the discrepancy in results observed between the histomorphometry and μCT analysis in our previous studies (Mandu-Hrit et al. 2006).

Favorably, in the control group, the unloaded nanoparticles did not interfere with the osteoregenerative process mainly due to their biocompatibility and biodegradability nature. The natural polymers used to formulate the nanoparticles, especially chitosan has been shown to promote osteogenesis and enhance the bioactivity of the encapsulated protein via controlling the release profile (Prabaharan 2008).

We chose in this study to analyze some of the most prominent genes in the BMP signaling pathway which included its receptors, antagonists and transcription factors. Results suggested that the whole BMP signaling pathway seems to be up-regulated during the distraction phase of the lengthening process perhaps due to the mechanical forces exerted (Haque et al. 2005; Haque et al. 2008). Osteogenesis in the BMP pathway (Abe 2006) occurs via the activation of either the Smad pathway or the MAPK pathway (Chapter 5.5.3). Even though BMPs are members of the TGF-β pathway, we did not analyze TGF-β and its related

Smads in this study because we have previously shown that the local application of TGF-β in a rabbit model stimulated only fibrogenesis and not osteogenesis (Rauch et al. 2000b). Yet, Smads 1-5 induction was up-regulated in the center and callus of all distracted tibias in all animals as a direct result of BMP activation. This upstream activation whether by the Smad or MAPK pathway is predominantly regulated by BMP receptors and antagonists. It has been previously reported that BMP-7 uses ACTRII (or ActR2) as its type II receptor and bind to ACTRI (or ActR1) as its type I receptor (Haque et al. 2008) as was also demonstrated here in. On the other hand, considerable down-regulation of antagonists such as Noggin, BMP-3 (or osteogenin) and Chondrin were noted mostly in the center of the distraction gap following the administration of the core-shell nanoparticles loaded with 1.0 and 5.0 μg rhOP-1. Of those well-documented antagonists in their role in blocking BMP-BMPR interactions, osteogenin is the most abundant BMP in adult long bone and has been reported to be a negative regulator of bone formation and a potent antagonist to osteogenic BMPs (Rosen 2006). Therefore, the observed under-regulation might have contributed to the improved function of the administered OP-1 in promoting bone growth in DO.

In **conclusio**n, we have shown that our injectable and non-toxic hybrid core-shell nanoparticles loaded with very low doses of rhBMP-7/rhOP-1 accelerates de novo bone regeneration and consolidation in a rabbit model of long bone DO. To the best of our knowledge, this present study is the first investigation of the combined use of injectable hybrid liposome and polymer-based nanoparticles and rhOP-1 in DO. In addition, we have not found any published studies with such low doses of rhOP-1.

A limitation in the present study is that the OP-1 distribution into the tissue was not evaluated. Inadequate distribution would reduce OP-1 bioactivity and function. Nonetheless, our findings demonstrated that this novel hybrid delivery system is able to maintain the bioactivity of the encapsulated protein. As a result, in a clinical setting, one could expect it to shorten the treatment period of DO and improve the functional outcome in patients via the earlier removal of the fixator. Our ongoing studies aim at validating these results in various animal models with different bone pathologies associated with poor bone formation for the

use of this therapeutic- and cost-effective approach in far reaching clinical applications beyond DO.

## 9.6. Acknowledgments

The authors would like to thank Dr. Fereshteh Azari for her assistance with the cryo-TEM and Mrs. Maria Kotsiopriftis and Mrs. Dominique Lauzier for their assistance in histomorphometry and immunohistochemistry. This work was supported by an operating grant from the Shriners of North America, Fonds de la Recherche en Santé du Québec, the National Science and Engineering Research Council (NSERC), the Canadian Institutes of Health Research (CIHR) - Regenerative Medicine/Nanomedicine and the Center for Biorecognition and Biosensors (CBB), McGill University, Montréal, Québec, Canada. Dr. Haidar acknowledges scholarships from the Center for Bone and Periodontal Diseases Research and the Shriners Hospital, Montréal, Québec, Canada.

## 9.7. Supplementary Data

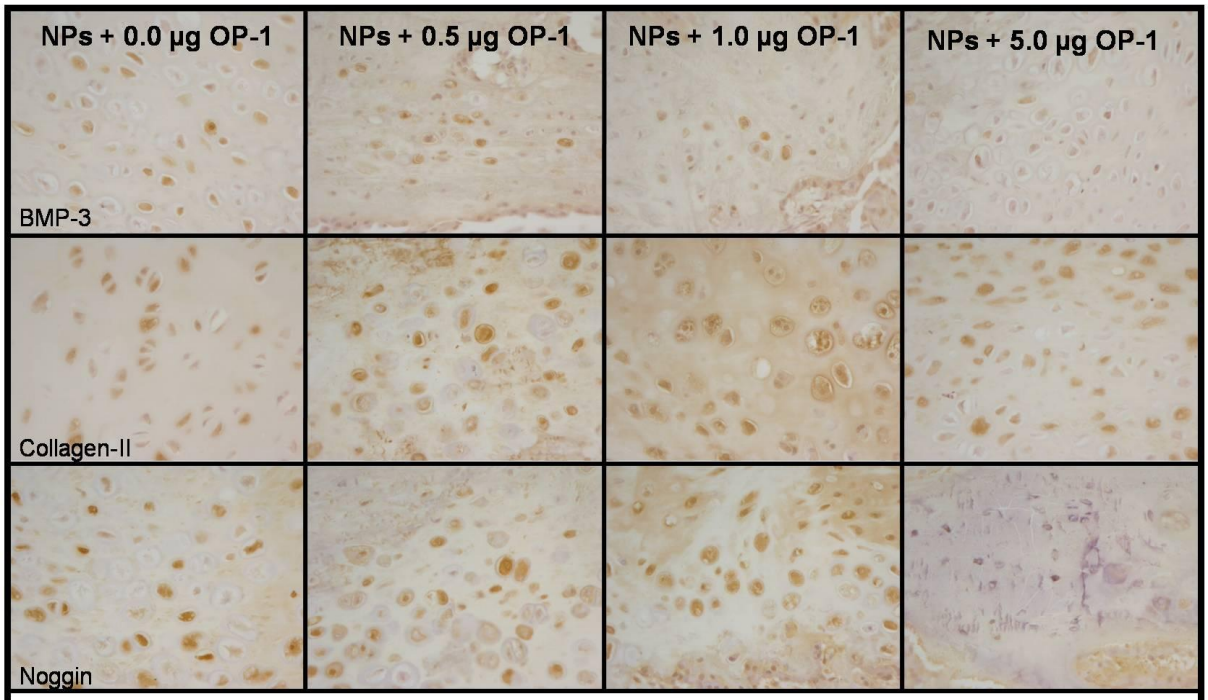


**FIG 9.8.** Supplementary immunohistochemistry images for the expression of BMP-3, Collagen-II and the BMP antagonist Noggin at 3 weeks post-injections. Cells stained brown indicate expression of the specified protein and pinkish areas are consolidated new bone. Evident in the animals receiving an injection of NPs + 5.0 µg OP-1 that the expression of antagonists is under-regulated in cells mainly at the center of the regenerated gap.

**General Note:** In this pilot (rabbit) study, NPs+1.0µg OP-1 seem to be a more suitable combination than NPs+5.0µg OP-1 where pre-mature consolidation often requiring a repeat osteotomy should be avoided.

# CHAPTER 10
# General Discussion of Conclusions and Future Perspectives

## 10.1. Thesis Conclusions

This dissertation embarked on with an introduction addressing the ongoing call for an increased awareness and research to develop novel alternative solutions for bone tissue engineering that would replace the conventional grafting procedures; the ultimate goal being to regenerate native bone to completely fill bone defects, not only in terms of quantity but quality as well and in an accelerated, safe, user-friendly and cost-effective fashion, if possible. And so, the universal inspiration for this project was instigated by the promising strategy known as protein- or BMP-therapy; a biomedical methodology which enables specific cells to enhance the proliferation and differentiation, resulting in natural promotion of tissue regeneration largely based on the innate healing potential of human patients themselves. This lead to identifying the current need for developing a new biocompatible, proficient, predictable, localized and release-controlled injectable delivery system at the nano-scale in order to facilitate and enhance guided tissue regeneration using low and safe dosages of the encapsulated morphogen(s), thus preventing the un-desirable rapid dispersal of the often required large and supra-physiological protein dosages (mostly due to short half-lives and stability issues) from currently-available and surgically-implantable carriers into sites of regeneration and repair. Although the main aim for designing and developing this delivery system was rationalized specifically for cases of long bone distraction osteogenesis, applications might extend beyond.

Below is a summary of the accomplishments of this project thus far (presented chronologically as carried out). While the requirements and characteristics of the 'ideal' protein delivery system might have not been fulfilled yet, the developed nanoparticulate hybrid delivery system has been shown to meet the basic criteria for drug delivery systems, at the least. Further evaluation, characterization and development are without doubt possible. Likewise for the application and/or model tested here in (long bone distraction osteogenesis in rabbits), although findings might have contributed to the current state-of-knowledge

regarding the cellular and molecular processes involved, where for example results confirmed the role of the mechanical forces of distraction in up-regulating the whole BMP signaling pathway which is also detrimental to the functions of endogenous and/or exogenous BMPs and the type(s) of bone formed; a complete understanding is still an area of constant hypothesis, predictions and interest of many researchers.

Therefore, following the summary of accomplishments and contributions from the works offered in this thesis, an outline of the future perspectives for the *field* is presented. Finally, a look into some of our ongoing studies is provided to end this dissertation with a proposed direction for the further advancement of the project.

## 10.2. Summary of Accomplishments *(as related to Objectives in Chapter 2.4)*

***Objective 1:*** **Prepare cationic, stable and monodisperse submicron liposomes with reproducibility.**

The method known as the *thin-film hydration* for the preparation of large multi-lamellar phospholipid vesicles followed by another technique referred to as *extrusion* for the filtration of these vesicles resulting in monodisperse and stable large uni-lamellar vesicles were used and optimized to reproducibly, reliably and efficiently prepare cationic liposomes at the nano-scale in solution. These liposomes had an average size of ~180 nm suitable to decrease their likelihood of uptake by the reticulo-endothelial system and adsorption by the mononuclear phagocystic system, a surface charge of +35 mV beneficial for the entrapment of fragile negatively-charged biomolecules and were prepared in ultra-pure water under mild conditions in order to decrease their potential cytotoxicity from any by-products of the 'evaporated' chloroform:methanol solvent used. Cholesterol was added to enhance the phospholipid bi-layer, proper for their further incorporation in a polymeric shell and the subsequent freeze-drying for rehydration and loading of drugs or proteins.

***Objective 2:*** **Develop discrete and well-defined cationic core-shell hybrid particles at the nano-scale.**

The layer-by-layer self-assembly technique was used to electrostatically coat/deposit alternating layers of alginate and chitosan on liposomes. The polymers were prepared in ultra-pure water and their pH and concentrations determined. The step-wise build-up was characterized with the application of each layer to ensure full coverage while maintaining the desired average size, surface charge, dispersion uniformity and stability in solution. Incubation times and washing were optimized. Hybrid nanoparticles/nanocapsules resulted with an average size of ~345 nm and a surface charge of +37 mV for liposomal cores coated with six polyelectrolyte layers; ~383 nm and 45 mV for those with ten layers. The technique yielded well-defined, uniform and stable suspension of nanoparticles with a shelf-life of a minimum period of 1 year. Freeze-drying was attained whilst preserving their spherical morphology (AFM and cryo-TEM) and physico-chemical characteristics after determining the proper cryoprotectant concentration (presented in Appendix B).

***Objective 3:*** **Evaluate the drug delivery potential of the nanoparticles for initial proof of concept.**

Using bovine serum albumin (BSA) as a model protein, lyophilized nanoparticles were re-hydrated and loaded with a range of concentrations of BSA (66 kDa MW) solution (0.0 to 2.0 mg/mL). The loading capacity, encapsulation efficiency and BSA release profile(s) of the nanoparticles were quantified using spectrophotometry. For these assays, 3-bilayered and 5-bilayered nanocapsules were used, for comparison and biokinetic characterization. Testing established the advantage of the core-shell design in accomplishing a high loading capacity that can be altered by the number of compartments determined by the number polyelectrolyte layers; with an encapsulation efficiency of 70-80% of BSA, more than two-fold of un-coated liposomes. A sustained release of BSA was also demonstrated over 30 days with a controlled initial burst effect and a diminished lag phase. Also, the release rate from the nanoparticles can be modulated (slower/faster) via modifying the number of layers present in the polymeric shell. Finally, the nanoparticles revealed the possibility of drug loading via simple

rehydration immediately preceding use, thus preventing degradation or loss of the load deemed necessary for the administration of therapeutic proteins. Therefore, verifying the potential of the hybrid nanoparticulate delivery system, in vitro.

***Objective 4:*** **Evaluate the cytocompatibility, stability in serum and bioactivity of released rhOP-1.**

The physical stability and uniformity of the hybrid nanoparticles (protective effect of the shell) were demonstrated in simulated physiological media in comparison to the un-coated liposomes displaying clear aggregation. Likewise, the potential cytocompatibility and safety of the system were established, in vitro. The ability of the spherical core-shell nanoparticles to entrap and release a range of rhOP-1 (15.7 kDa MW) concentrations (0.0 to 5000 ng/mL) over an extended period of 45 days was also evaluated. Following freeze-drying and rehydration with the anionic protein solution(s); the loaded particles had an average size of ~386 nm and a surface charge of +39 mV indicating the incorporation of the rhOP-1 within the compartments of the core and shell system. The loading capacity, encapsulation efficiency and rhOP-1 release profile(s) were quantified using an enzyme-linked immunosorbent assay as it was not feasible using the micro-BCA technique used previously with BSA. The system showed a high capacity for loading elevated concentrations of growth factors with an ability to efficiently encapsulate more than 80% of the initial load. Controlled, linear, and sustained tri-phasic release of rhOP-1 was observed with up to 85% of the load released over a period of 4 weeks. A control of the burst effect was also demonstrated in comparison to un-coated liposomes revealing the possibility of tailoring low- or high-level sustained and prolonged protein delivery with smaller or larger initial protein bursts feasible with the alteration in the number of polyelectrolyte layers. This feature is essential for optimum growth factor performance when applied in different anatomical sites or defect sizes with varying vascularity and number of resident responding cells. Finally, the delivery system revealed its potential in maintaining and enhancing the biological activity of the encapsulated growth factor via promoting alkaline phosphatase activity and preosteoblast differentiation with a very low dose; no more than 100 ng/mL rhOP-1, in vitro. Because large, critical and expensive supra-physiologic dosages of growth

factors continue to be required for osteoinduction, this release-controlled hybrid nanoparticulate system suitable for administration parenterally could be a clinically-effective alternative for a range of orthopaedic and craniofacial skeletal applications if not as well for other bioactive molecules and indications beyond bone. Nonetheless for this project, the system was aimed to be evaluated in a long bone distraction osteogenesis model; a pilot in vivo study in white NZW ♂ rabbits.

***Objective 5:*** **Evaluate the rhOP-1 hybrid delivery system in a rabbit tibial distraction osteogenesis model.**

The effect of a single bolus injection of 3-bilayered nanoparticles loaded with low doses of rhOP-1 (0.0 to 5000 ng/mL) administered early in the distraction phase on the rate, quantity and quality of de novo bone formation during long bone distraction osteogenesis was evaluated in a rabbit model. Given that BMPs are known to act locally, the concentration of BMPs at the site of interest is consequently more crucial than the total dose of the loaded protein. The aim was therefore to evaluate the in vivo potential of the localized and release-controlled characteristics of the hybrid core-shell design in (*a*) enhancing the bioavailability of the encapsulant and (*b*) possibly decreasing the required dosage of bioactive growth factors while maintaining a favorable therapeutic effect or outcome. Furthermore, accelerating the distraction osteogenesis procedure and having the fixator perhaps removed at an earlier time via a single, safe, efficient and cost-effective injection would be convenient, attractive and highly-desired by surgeons and patients alike. In this pilot study, qualitative and quantitative evaluation of the regenerate in the distracted tibias suggested that when a dose of no more than 1.0 μg rhOP-1 is delivered via the nanoparticles, it was sufficient to accelerate osteogenesis and consolidation while maintaining a denser and more mineralized (almost two-fold) bony structure than controls (distraction only) or even when compared to 75 μg rhOP-1 delivered in an acetate buffer from previous studies in the same animal model. These findings further establish the favorable (necessary and achievable) role of localized and release-controlled kinetic delivery of bioactive morphogens from injectable nano-sized biomaterials (that was proposed previously in the literature reviews presented in Chapters 3, 4 and 5 of Section II). Finally, the choice of materials constructing this drug

delivery system was proven to be safe and proper where the injected un-loaded nanoparticulate formulations did not interfere negatively with the osteoregenerative process mainly due to their well-known biocompatibility and biodegradability nature. Nonetheless, another in vivo study was designed and executed for further verification.

***Objective 6:*** **Evaluate the biocompatibility and safety of the rhOP-1 hybrid delivery system in vivo.**

Even though the cytocompatibility of the nanoparticles was demonstrated in vitro and their safety and performance in rabbits following administration directly into the distraction gap prepared in the tibia with no complications, body responses or side effects over the treatment period of around 3-5 weeks, the biocompatibility and safety of the delivery system upon intramuscular administration in a smaller animal species commonly used in such studies was further demonstrated via timely blood and organ function analysis, monitored over a total period of 70 days in young and healthy rats. All animals showed no obvious toxic health effects, immune responses and/or change in organ functions, further confirming that the nanoparticles do confine any effects there are of their material composition as well as of the released bioactive load within the site of administration with no acidic by-products or significant tissue distress. Given access and existence of the harvested tissues and prepared specimens for histopathalogical examination under light microscopy, a separate endeavor not initially planned in this study, was attempted concurrently. In the preliminary samples of the leg muscle, no bone metaplasia was observed histologically and the injection site could not be always clearly identified; therefore further recuts of blocs at different depths were prepared with the hope of identifying ectopic bone formation. Indeed, analysis suggested the presence of pools of potential bone-forming cells and signs of promoted angiogenesis in the rats that have been injected with nanoparticles loaded with 0.1 and 0.5 μg rhOP-1 (note: even much lower dosages than those investigated in rabbits). These observations were absent in any of the other animal groups and controls including those receiving pure rhOP-1 injections in water; perhaps confirming the role of the hybrid delivery system once more as well as its biocompatibility and safety where BMPs have been previously reported to promote angiogenesis prior to initiating bone repair and regeneration, in vivo.

## 10.3. Future Perspectives

Over 2000 years elapsed since Hippocrates first considered the enormous healing potential of the human skeleton and formulated the possibility of responsible endogenous substances; bone morphogenetic proteins. Since then, over a ton of bone was needed to be able to figure out the amino acid sequence which led to the cloning of recombinant human BMP-2 and -3 (Wozney et al. 1988; Reddi 1998) and subsequently the possibility to produce BMPs by recombinant DNA techniques using Chinese hamster ovary cell lines (Wang et al. 1990). The past decade witnessed series of in vitro, in vivo and clinical trials demonstrating the enormous therapeutic potential of these morphogens. Results from these studies clearly show that different BMPs play different roles in skeletal development, patterning, and repair. Certain BMPs may be essential to specific biological processes while others may be supportive. Today, bone regeneration and repair with rhBMPs are ushering in a new era in orthopaedic, cranio-maxillofacial as well as dental and periodontal surgery. This should bring a better understanding of the variables that, despite extensive pre-clinical research they lead thus far to the approval of 'restricted' use of BMPs in human indications. Of these variables requiring further investigation are refining the optimal BMP dose, time-course, route of application/administration, release dynamics, interaction mechanism of BMP and Wnt signaling pathways, the role of BMP agonists and inhibitors (Rosen 2006, Abe 2006), potential immunogenicity of BMPs (Hwang et al. 2009) and antibody formation. In addition, while no one species fulfills the requirements of an ideal animal model, an understanding of the differences in bone macroscopic, microscopic and remodeling attributes will likely improve the choice of animal species (and understand any underlying gender differences) and subsequent interpretation of results. Alongside, researchers might finally figure out why the impressive results of animal models are difficult to replicate in humans. On the other hand, advancements in surgical and imaging techniques, biomaterials and nanotechnology with the development of new tissue-engineering delivery systems will possibly uncover a wide range of clinical applications using rhBMPs. For example, combining a localized and release-controlled nanoparticulate delivery system that increases the efficiency of the encapsulant with bioactive rhBMPs (in much lower dosages) in addition to a BMP antagonist blocker (to manipulate the endogenous BMP pathway, up-regulate BMP

expression and enhance osteogenesis) using RNA interference/silencing (Pushparaj et al. 2008) might be of huge benefit in cases of protracted distraction osteogenesis. Also, angiogenic factors which prompt the recruitment and distribution of blood vessel precursor cells vital for the formation of mature bone might be incorporated in guided tissue-engineering delivery systems. Other novel strategies will possibly involve the specific targeting of rhBMPs and stimulus-responsive injectable systems, both of which allow restricted and site-specific (via attaching targeting ligands to the surface of particles, for instance) BMP delivery in addition to BMP-mediated ex-vivo gene therapy (Engel et al. 2008; Bessa et al. 2008 b). Surely though, before any of these can be applied in humans, it will be necessary to carry out comprehensive studies to ensure their safety. Nonetheless, decades to come will see a growing in options for the biomedical incorporation of rhBMPs in the next generation of 'smart' or 'intelligent' delivery systems and use in clinical regenerative medicine (for virtually every type of tissue and organ within the human body) and particularly in bone applications, offering novel and superior therapeutics; and in view of that, a brighter future to millions of patients.

## 10.4. Ongoing Studies

Considering the understanding gained from previous studies and the outcome of the two in vivo investigations presented earlier in Chapters 8 and 9 of Section IV, additional studies were designed and executed. Two of these are included briefly herein to shed light on some of the ongoing studies and future directions of the project; given that the finalized results and manuscripts were not ready by the time of writing this dissertation. The general aim goes in parallel: to develop a method (or combinations thereof) that may enhance and accelerate the consolidation of newly-formed bone in long bone DO and hence improve the functional outcome of this technique via removing the fixator at an earlier time. And so, those studies intend to obtain a better understanding of the role and effect of (**a**) exogenous rhOP-1 and (**b**) the nanoparticulate rhOP-1 delivery system.

For these studies, a tibial bone lengthening protocol was designed, approved and performed in adult wild type mice using the custom-made external ring fixator shown below in Figure

10.1 which would offer more stability to the osteotomized bone segments than the Orthofix uniplanar M-101 external fixator used earlier in the rabbits. The move from rabbits to a smaller animal species is mainly attributed to (*i*) the aspects of the DO regenerate to be examined such as biomechanical testing, (*ii*) feasibility in terms of the available animal housing and care facility, ease of the surgical procedure, post-operative care and possibility of including a larger sample size and (*iii*) cost and time. More importantly, the limited knowledge of the biological and molecular events that regulate tissue response to gradual lengthening restricts optimizing current treatment protocols and so was taken into account. Additionally, animal species, gender and handling post-operatively will influence the outcome of in vivo studies and contribute more to the discrepancies observed in other animal species and humans. This will have implications for the translation of data from pre-clinical studies to clinically-effective applications, as highlighted earlier. Rabbits were found to be the least similar in bone macro- and microstructure, composition and remodeling properties to humans and while no one species fulfills the requirements of an ideal animal model, mice were recommended for studies involving BMP bone-engineering products. Perhaps this was due to the high degree of homology between mouse and man (99% of genes encoding protein in mouse have a sequence match in humans) and therefore, the obtained data should be directly be applicable to human distraction osteogenesis biology (Tay et al. 1998). Furthermore, the small size of the mouse facilitates histological, biochemical, and molecular analyses (Tay et al. 1998; Fang et al. 2004). The developed mouse long bone DO protocol carried out in this continuing group of investigations as well as some of the preliminary findings to date are summarized next.

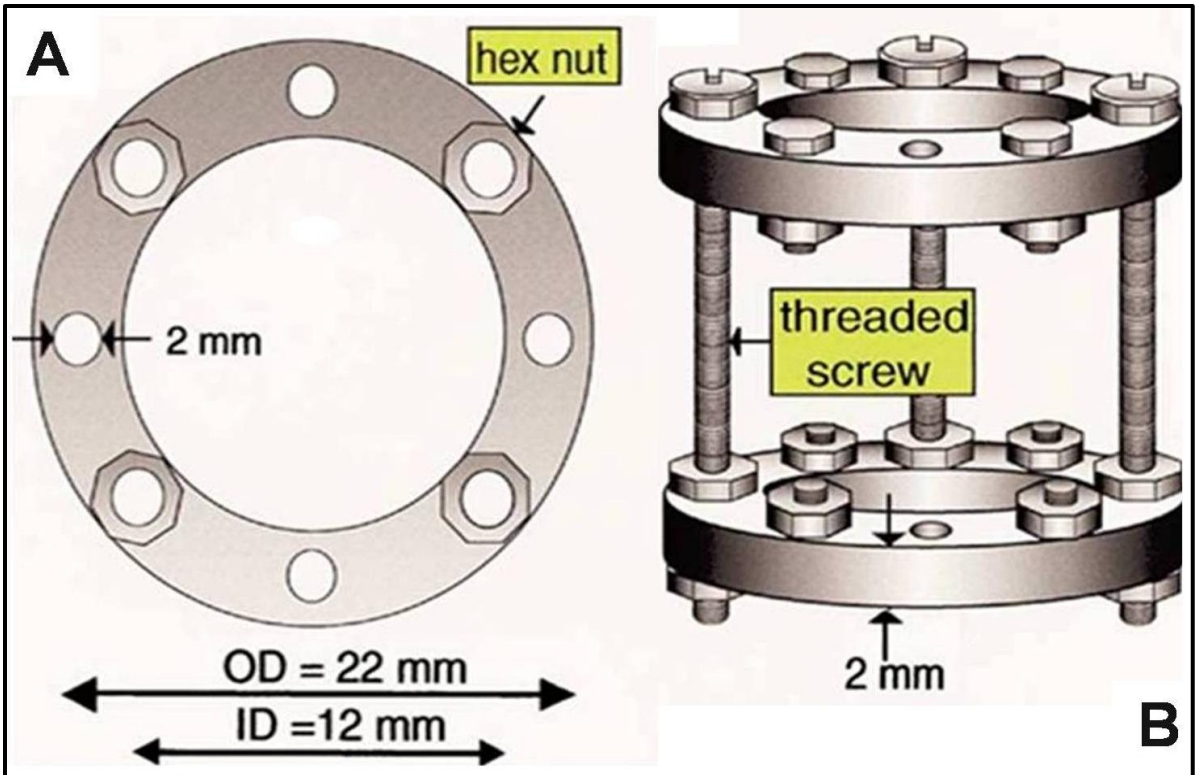


**FIG 10.1.** Schematic diagram of the custom-made aluminum mini-circular external fixator. (**A** )Top view and (**B**) side view. **ID**: inside diameter and **OD**: outside diameter. The threaded screw rods allow precise and quantifiable gradual lengthening along their axis. Hexagonal bolts are used for fixator assembly. The total weight of the apparatus is ~ 7g.

### 10.4.1. Wild-Type Mouse Model of Long Bone DO – *Protocol*

For both studies, the DO procedure was applied to the right tibia of a total of 160 adult male wild type mice (strain C57BL/6, aged 2-3 months and weighing around 25 grams) as summarized in Figure 10.2. The surgery involved percutaneously transfixing four 0.25mm pins, 90° apart in the distal and proximal end of the tibia using a hand-held variable-speed drill. Two 22 mm metal rings (Figure 10.1A) were fixed to the pins using screws and the distractor device assembled (Figure 10.1B). A transverse osteotomy followed, at the centre of the tibia using a scalpel. The bony margins were then aligned prior to suturing the incision. The mice were kept under anesthesia using isoflurane throughout the entire duration of the surgery. They were permitted to weight-bear immediately and were monitored three times daily during the first 3 days post-operatively, then once daily until the

experimental end point(s) and tibia harvest. Following a 5 day latency period, distraction started at a rate of 0.2 mm/12 h. When mice reached their assigned experimental end-points, they were sedated then euthanized by $CO_2$ asphyxiation, the fixator carefully disassembled and the right tibia dissected and processed for analysis.

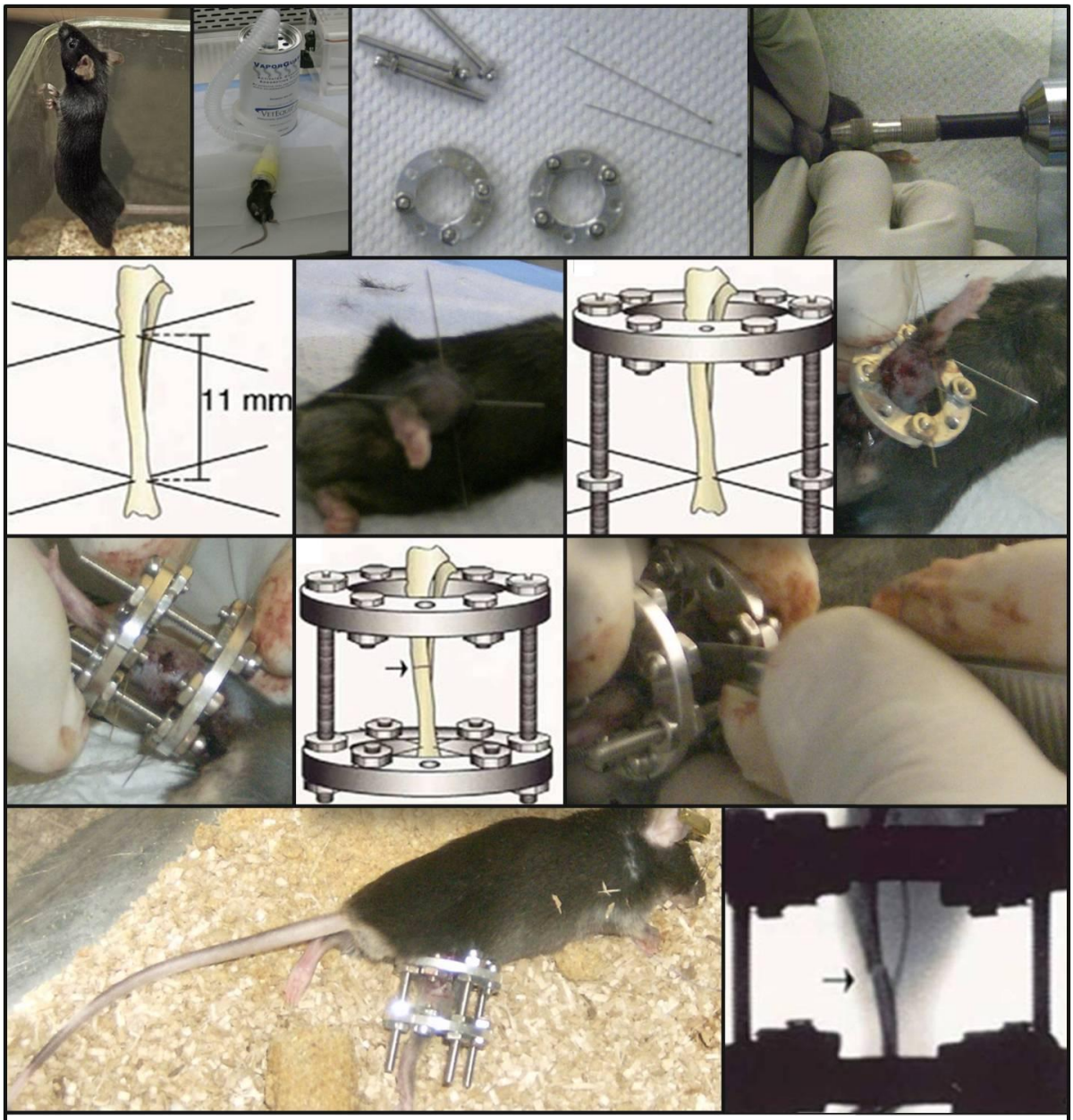


**FIG 10.2.** Summary of the performed DO procedure in mice. The average operative time is ~ 20 – 30 min.

### 10.4.2. Developing a Dose-Response Curve for BMP-7/OP-1 during DO

By: A Izadpanah*, **ZS Haidar***, L Al-Salmi, L Lessard, M Tabrizian and RC Hamdy [*Equal Contribution]

Given that BMPs act locally and are known to be dose-dependant, this study was designed to evaluate the effect of different concentrations of exogenous rhBMP-7/rhOP-1 administered early during the distraction period in order to develop an OP-1 dose-response curve as this was never done before especially in a long bone DO in vivo model. The aim is to further characterize and understand the expression patterns involved during distraction, especially with dosages much lower than the commonly used in the microgram range. In addition, findings from this investigation would serve as a basis for future studies in terms of the minimum rhOP-1 dosage required to induce osteogenesis. The DO procedure was applied to the right tibia of 80 adult male wild type mice as summarized in the earlier paragraph and Figure 10.2. Following the latency period, distraction (0.2 mm/12 h) continued for 2 weeks. On the first day of distraction, animals received a single 0.15 mL injection of rhBMP-7/rhOP-1 prepared from lyophilized powder in ultra-pure water according to the manufacturer's recommendations. Three rhOP-1 dosages were investigated; 0.05 µg (n=20), 0.10 µg (n=20) and 0.50 µg (n=20). A control group (n=20) received single 0.15 mL injections of sterile saline administered into the distraction gap to compensate for any needle insertion-associated effects, as previously done with the rabbits in Chapter 9. Mice were euthanized at day 34 (mid-consolidation; 10 mice per group) and day 51 (end-consolidation; 10 mice per group) and the tibia dissected and processed for analysis. Thus far, all animals have reached their experimental endpoints and their tibias were harvested. Specimens are currently undergoing examination using Faxitron radiology, µCT, biomechanical testing, histomorphometry and immunohistochemistry. Briefly, the harvested lengthened tibias assigned for antero-posterior and lateral Faxitron X-rays and µCT were fixed overnight in 4% paraformaldehyde. For biomechanical testing, the samples were wrapped in Kimwipes, soaked in PBS and stored at -20°C fridge before undergoing evaluation by a three-point bending test (at a rate of 50 µm/s until fracture). For histomorphometry and comparative histological analysis, samples were embedded in 4.5% methylmethacrylate and then 6 µm

sections were de-plastified and stained by Trichrome Goldner for examination under light microscopy.

Preliminary data from the mice sacrificed on day 34 (mid-consolidation) are presented in Figure 10.3. Faxitron and µCT views are shown on the top portion. Selective quantitative histomorphometric data from µCT analysis are displayed in A and B of the lower portion. C shows one of the parameters evaluated biomechanically; regenerate stiffness. Thus far, a significant increase in the ratio of bone volume to tissue volume (BV/TV) between the control group and 2µg/kg at mid-consolidation is noted (A).

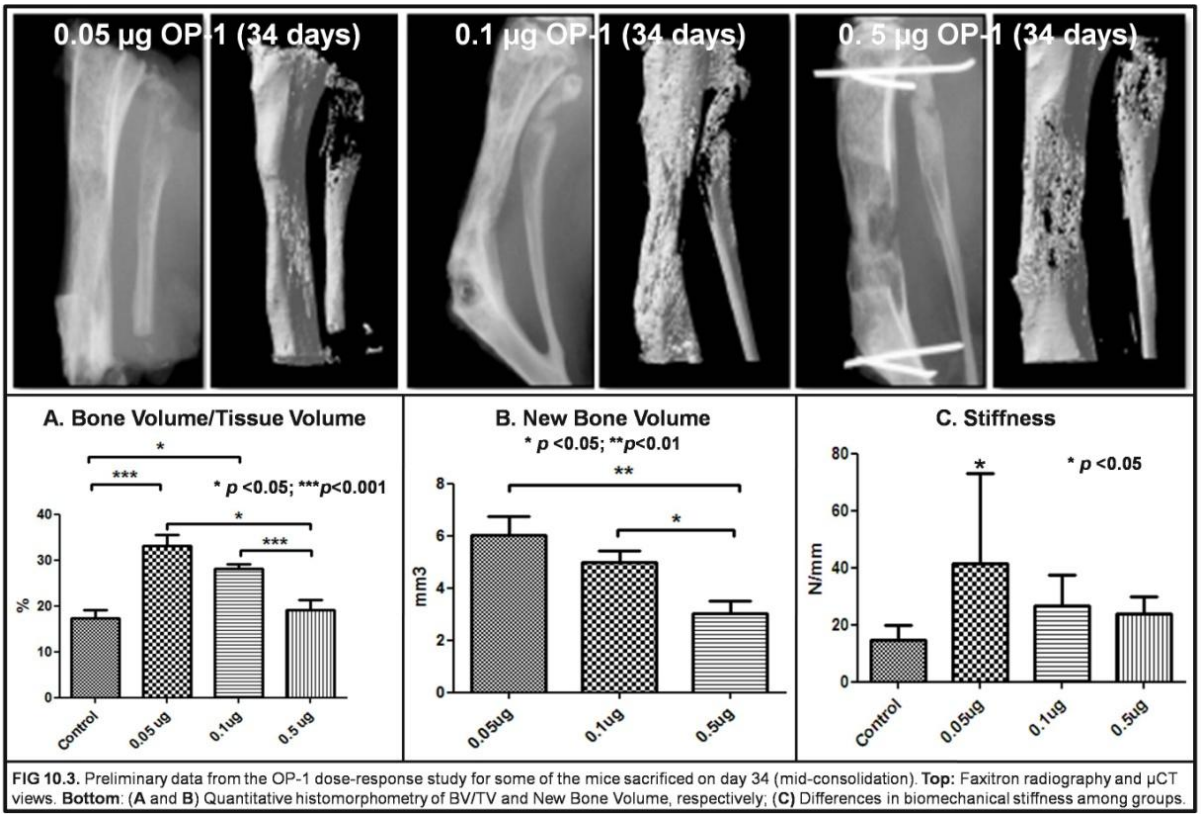


**FIG 10.3.** Preliminary data from the OP-1 dose-response study for some of the mice sacrificed on day 34 (mid-consolidation). **Top:** Faxitron radiography and µCT views. **Bottom**: (**A** and **B**) Quantitative histomorphometry of BV/TV and New Bone Volume, respectively; (**C**) Differences in biomechanical stiffness among groups.

This decreases significantly as the dosage of exogenous rhOP-1 increases to 4µg/kg and 20µg/kg. Looking at only the new bone volume formed in the distraction gap, interestingly, this pattern seems reproducible at the lowest dose of the protein. Regenerate bone formation is accelerated by 78.1% at mid-consolidation post-injection of only 0.05 µg rhOP-1.

Biomechanical evaluation also reveals that a single injection of rhOP-1 significantly enhances bone formation when compared with control (saline). Higher doses seem to have an inhibitory effect on bone formation during distraction osteogenesis in this model.

The analyzed tibias to date had a 0.7 - 1.4 cm length with a distraction length of ~ 0.48 cm. All analysis and results are expected to be finalized, a manuscript submitted for publication consideration very shortly.

### 10.4.3. Evaluating the Nanoparticulate rhOP-1 Delivery System during DO

By: **Ziyad Haidar**, Loai Al-Salmi, Maryam Tabrizian & Reggie Hamdy

In this study, the same procedure was performed on an additional group of mice (N=80). The aim herein is to evaluate the effect of the core-shell nanoparticulate delivery system loaded with the same three concentrations of exogenous rhBMP-7/rhOP-1 and similarly administered early during the distraction period. To date, the DO procedure was applied to the right tibia of all mice. Distractions began after a latency period of 5 days at a rate of 0.2 mm/12 h/2 weeks. On the first day of distraction, animals received a single 0.15 mL injection of rhBMP-7/rhOP-1 loaded in nanoparticles prepared in the three dosages examined above; 2 µg/kg, 4 µg/kg and 20 µg/kg. The control group received a single 0.15 mL injection of blank nanoparticles in ultra pure water. Mice will be sacrificed at day 34 (mid-consolidation) and day 51 (end-consolidation) and their tibias harvested, as well. Specimens will be then prepared to be examined using Faxitron radiology, µCT, biomechanical testing, histomorphometry and immunohistochemistry.

### 10.4.4. Future Directions for this part of the Overall Project

In this last investigation similarly to the earlier studies in rats (Chapter 8) and rabbits (Chapter 9), 3 bi-layered nanoparticles were used. It would be of great interest to evaluate the effect of the previously demonstrated *slower* in vitro release from the 5 bi-layered nanoparticles (Chapters 6 and 7) in another in vivo study. Perhaps prior to that, the release kinetics from the system can be characterized in a different *more* physiologically-relevant media than ultra-pure water, PBS or even in a further cell culture media; ALP and/or osteocalcin activity (osteoblastic phenotype markers) assay(s) over longer periods of time than the presented 7 days, for example. Furthermore, evaluating the degradation of the nanoparticles in vitro and in vivo as well as their systemic fate would provide crucial information regarding the biocompatibility and safety of the delivery system. Exploring the potential of the nanoparticles to encapsulate and deliver (simultaneous or sequential) other BMPs, a cocktail of different BMPs or a combination of the angiogenic vascular endothelial growth factor (VEGF) and osteogenic proteins such as rhOP-1 or rhBMP-2 for instance might be beneficial for the enhancement of bone regeneration and repair. Moreover, this should be accompanied by a look into the distribution, residence time(s) and pharmacokinetics of the locally released morphogen(s) within the application site, perhaps via $^{125}$I-radio-labeling the encapsulant(s) followed by liquid scintillation counting to analyze radioactivity in the blood and excreta in addition to assessing the radioactivity of injection site as well as the full animal body using quantitative whole-body autoradioluminography. Finally, a future direction for this project would be to investigate the effect of the injectable, localized and release-controlled delivery of low bioactive dosages of rhOP-1 and/or rhBMP-2 on models of intra-membranous ossification possibly through in vivo cases of mandibular and alveolar distraction osteogenesis as well as on the regeneration of surgically-created periodontal defects and fenestrations.

# CHAPTER 11
# Cumulative Bibliography List


Abe E (2006) Function of BMPs and BMP antagonists in adult bone. Ann NY Acad Sci 1068; 41–53.

Alsalmi LA, Haidar ZS, Izadpanah A, Lessard LM, Tabrizian M, Hamdy RC (2009) Wnt Signaling increases during Distraction Osteogenesis in Mice. Abstract presented at the American Society of Plastic Surgeons, Seattle, CA – October 2009.

Anderson JM (2001) Biological responses to materials. Annu Rev Mater Res 31; 81–110.

Aronson J, Shen XC, Skinner RA, Hogue WR, Badger TM, Lumpkin CK Jr (1997) Rat model of distraction osteogenesis. J Orthop Res 15: 221–6.

Arosarena OA, Collins WL (2005) Bone regeneration in the rat mandible with bone morphogenetic protein-2: a comparison of two carriers. Otol Head Neck Surg 132: 592–7.

Asasutjarit R, Lorenzen SI, Sirivichayakul S, Ruxrungtham K, Ruktanonchai U, Ritthidej GC (2007) Effect of Solid Lipid Nanoparticles Formulation Compositions on Their Size, Zeta Potential and Potential for In Vitro pHIS-HIV-Hugag Transfection. Pharm Res 24: 1098–107.

Aspenberg P, Turek T (1996) BMP-2 for intramuscular bone induction: effect in squirrel monkeys is dependent on implantation site. Acta Orthop Scand 67: 3–6.

Aubert AE, Vandeput S, Beckers F, Liu J, Verheyden B, Van Huffel S (2009) Complexity of cardiovascular regulation in small animals. Phil Trans A Mat Phy En Sci 367: 1239–50.

Aubin JE, Triffitt JT (2002) Mesenchymal stem cells and osteoblast differentiation, in: J.P. Bilezikan, L.G. Raisz, G.A. Rodan (Eds.) Principles of Bone Biology, Academic Press, San Diego, pp. 59–81.

Bach FH, Fishman JA, Daniels N, Proimo J, Anderson B, Carpenter CB, et al. (1998) Uncertainty in xenotransplantation: individual benefit versus collective risk. Nature Med 4: 141–4.

Barboza EP, Duarte ME, Geolás L, et al. (2000) Ridge augmentation following implantation of recombinant human bone morphogenetic protein-2 in the dog. J Periodontol 71: 488–96.

Barnes B, Boden SD, Louis-Ugbo J (2005) Lower dose of rhBMP-2 achieves spine fusion when combined with an osteoconductive bulking agent in non-human primates. Spine 30: 1127–33.

Barzegar-Jalali M, Adibkia K, Valizadeh H, Shadbad MRS, Nokhodchi A, et al. (2008) Kinetic Analysis of Drug Release From Nanoparticles. J Pharm Pharmac Sci 11: 167–77.

Baskin DS, Ryan P, Sonntag V, Westmark R, Widmayer MA (2003) A prospective, randomized, controlled cervical fusion study using recombinant human bone morphogenetic protein-2 with the CORNERSTONE-SR allograft ring and the ATLANTIS anterior cervical plate. Spine 28: 1219–24.

Basmanav FB, Kose GT, Hasirci V (2008) Sequential growth factor delivery from complexed microspheres for bone tissue engineering. Biomaterials 29: 4195–204.

Batra P, Ryan FS, Witherow H, Calvert ML (2006) Long term results of mandibular distraction. J Indian Soc Pedod Prev Dent 24: 30–9.

Bessa PC, Casal M, Reis RL (2008a) Bone morphogenetic proteins in tissue engineering: the road from the laboratory to the clinic, part I (basic concepts). J Tis Eng Reg M 2:1–13.

Bessa PC, Casal M, Reis RL (2008b) Bone morphogenetic proteins in tissue engineering: the road from laboratory to clinic, part II (BMP delivery). J Tis Eng Reg M 2: 81-96.

Bessho K, Carnes DL, Cavin R, Ong JL (2002) Experimental studies on bone induction using low-molecular-weight poly(DL-lactide-co-glycolide) as a carrier for recombinant human bone morphogenetic protein-2. J Biomed Mater Res 61: 62–5.

Bishop GB, Einhorn TA (2007) Current and future clinical applications of bone morphogenetic proteins in orthopaedic trauma surgery. Int Orthop 31:721–7.

Blattert TR, Delling G, Dalal PS, Toth CA, Balling H, Weckbach A (2002) Successful transpedicular lumbar interbody fusion by means of a composite of osteogenic protein-1 (rhBMP-7) and hydroxyapatite carrier: a comparison with autograft and hydroxyapatite in the sheep spine. Spine 27: 2697–705.

Boden S, Kang J, Sandhu H, Heller J (2002) Use of rhBMP2 to achieve posterolateral lumbar spine fusion in humans: a prospective randomized clinical trial. Spine 27: 2662–7.

Boden SD, Maertin GJ, Morone MA, Ugbo JL, Moskovitz PA (1999) Posterolateral lumbar intertransverse process spine arthodesis with rh bone morphogenetic protein 2/hydroxyapatite-tricalcium phosphate after laminectomy in the nonhuman primate. Spine 24: 1179–85.

Bogdanovic G, Sennerfors T, Zhmud B, Tiberg F (2002) Formation and structure of polyelectrolyte and nanoparticle multilayers: effect of particle characteristics. J Colloid Interface Sci 255: 44–51.

Bohner M, Baroud G (2005) Injectability of calcium phosphate pastes. Biomaterials 26: 1553–63.

Boyan BD, Lohmann CH, Somers A, Niederauer GG, Wozney JM, Dean DD, Carnes DL, Schwartz Z (1999) Potential of porous poly-d,lactide-co-glycolide particles as a carrier for recombinant human bone morphogenetic protein-2 during osteoinducation in vivo. J Biomed Mater Res 46: 51–9.

Boyne PJ (2001) Application of bone morphogenetic proteins in the treatment of clinical oral and maxillofacial osseous defects. J Bone Joint Surg Am 83-A Suppl 1: S146–50.

Boyne PJ, Lilly LC, Marx RE et al. (2005) De novo bone induction by recombinant human bone morphogenetic protein-2 (rhBMP-2) in maxillary sinus floor augmentation. J Oral Maxillofac Surg 63: 1693–707.

Bregni C, Degrossi J, Garcia R, Lamas MC, Firenstein R, y D'aquino M (2000) Alginate microspheres of Bacillus subtilis. Ars Pharmaceutica 41: 245–8.

Brekke JH (1996) A rationale for delivery of osteoinductive proteins. Tiss Eng 2: 97–114.

Bridges PA, Taylor KM (2001) The effects of freeze-drying on the stability of liposomes to jet nebulization. J Pharm Pharmacol 53: 393–8.

Burkus JK, Gornet MF, Dickman CA, Zdeblick TA (2002b) Anterior lumbar interbody fusion using rhBMP-2 with tapered interbody cages. J Spinal Disord Tech 15: 337–49.

Burkus JK, Sandhu HS, Gornet MF, Longley MC (2005) Use of rhBMP-2 in combination with structural cortical allografts: clinical and radiographic outcomes in anterior lumbar spinal surgery. J Bone Joint Surg Am 87: 1205–12.

Burkus JK, Transfeldt EE, Kitchel SH, Watkins RG, Balderston RA (2002a) Clinical and radiographic outcomes of anterior lumbar interbody fusion using recombinant human bone morphogenetic protein-2. Spine 27: 2396–408.

Butler D, Wadman M, Lehrman S, Schiermeier Q (1998) Last chance to stop and think on risks of xenotransplants. Nature 391: 320–4.

Buxton PG, Cobourne MT (2007) Regenerative approaches in the craniofacial region: manipulating cellular progenitors for oro-facial repair. Oral Dis 13: 452–60.

Cadigan K, Liu YI (2006) Wnt signaling: complexity at the surface. J Cell Sci 1: 395–402.

Cai Q, Yang J, Bei JZ, Wang SG (2002) A novel porous cells scaffold made of polylactide–dextran blend by combining phase-separation and particle-leaching techniques. Biomaterials 23: 4483–92.

Calvo P, Remunan-lopez C, Villa-Jato JL, Alonso ML (1997) Novel hydrophilic chitosan-polyethylene oxide nanoparticles as protein carriers. J Appl Polym Sci 63: 125–32.

Campisi P, Hamdy RC, Lauzier D, Amako M, Rauch F, Lessard ML (2003) Expression of BMPs during mandibular distraction osteogenesis. Plast Reconstr Surg 111(1): 201–8.

Campisi P, Hamdy RC, Lauzier D, Amako M, Schloss MD, Lessard ML (2002) Overview of the radiology, histology, and bone morphogenetic protein expression during distraction osteogenesis of the mandible. J Otolaryngol 31(5): 281–6.

Carano RAD, Filvaroff EH (2003) Angiogenesis and bone repair. Drug Discv T 8: 980–9.

Cascone P, Gennaro P, Spuntarelli G, Iannetti G (2005) Mandibular distraction: evolution of treatment protocols in hemifacial microsomy. J Craniofac Surg 16: 563–71.

Chaize B, Colletier JP, Winterhalter M, Fournier D (2004) Encapsulation of enzymes in liposomes: high encapsulation efficiency and control of substrate permeability. Artif Cells Blood Substit Immobil Biotechnol 32: 67–75.

Chan CW, Qin L, Lee KM, Cheung WH, Cheng JC, Leung KS (2006) Dose-dependent effect of low-intensity pulsed ultrasound on callus formation during rapid distraction osteogenesis. J Orthop Res 24: 2072–9.

Chang PC, Liu BY, Liu CM, Chou HH, Ho MH, Liu HC, Wang DM, Hou LT (2007) Bone tissue engineering with novel rhBMP2-PLLA composite scaffolds. J Biomed Mater Res A 81: 771–80.

Charrois GJ. Allen TM (2003) Rate of biodistribution of STEALTH® liposomes to tumor and skin: influence of liposome diameter and implications for toxicity and therapeutic activity 4. Biochim Biophys Acta 1609: 102–8.

Chellat F, Tabrizian M, Dumitriu S, Chornet E, Magny P, Rivard CH, Yahia L (2000) Study of biodegradation behaviour of chitosan-xanthan microspheres in simulated physiological media. J Biomed Mater Res 53: 592–9.

Chen D, Zhao M, Mundy G (2004) Bone morphogenetic proteins. Grwth Fac 22: 233–41.

Chen FM, Zhao YM et al. (2007) Periodontal regeneration using novel glycidyl methacrylated dextran (Dex-GMA)/gelatin scaffolds containing microspheres loaded with bone morphogenetic proteins. J Control Release 121: 81–90.

Chen FM, Zhao YM, Wu H, Deng ZH, Wang QT, Zhou W, Liu Q, Dong GY, Li K, Wu ZF, Jin Y (2006) Enhancement of periodontal tissue regeneration by locally controlled delivery of insulin-like growth factor-I from dextran-co-gelatin microspheres. J Control Release 28: 209–22.

Chen RR, Mooney DJ (2003) Polymeric growth factor delivery strategies for tissue engineering. Pharm Res 20: 1103–12.

Chen Y and Alman BA (2009) Wnt Pathway, an Essential Role in Bone Regeneration. Journal of Cellular Biochemistry 106: 353–62.

Chiapasco M, Zaniboni M, Boisco M (2006) Augmentation procedures for the rehabilitation of deficient edentulous ridges with oral implants. Clin Oral Implants Res 17 Suppl 2: 136–59.

Chin M, Toth BA (1996) Distraction osteogenesis in maxillofacial surgery using internal devices: review of five cases. J Oral Maxillofac Surg 54: 45–53.

Cho CH, Nuttall ME (2002) Emerging techniques for the discovery and validation of therapeutic targets for skeletal diseases. Expert Opin Ther Targets 6: 679–89.

Choi IH, Ahn JH, Chung CY, Cho TJ (2000) Vascular proliferation and blood supply during distraction osteogenesis: a scanning electron microscopic observation. J Orthop Res 18: 698–705.

Chu B, Wang Z, Yu J (1991) Dynamic light scattering study of internal motions of polymer coils in dilute solutions. Macromolecules 24: 6832–8.

Chu TM, Warden SJ, Turner CH, Stewart RL (2007) Segmental bone regeneration using a load-bearing biodegradable carrier of bone morphogenetic protein-2. Biomatr 28: 459–67.

Claes L, Rüter A, Mayr E (2005) Low-intensity ultrasound enhances maturation of callus after segmental transport. Clin Orthop Relat Res 430: 189–94.

Codivilla A (1994) On the means of lengthening, in the lower limbs, the muscles and tissues which are shortened through deformity. 1904. Clin Orthop Relat Res 301: 4–9.

Codvilla A (2008) The classic: On the means of lengthening, in the lower limbs, the muscles and tissues which are shortened through deformity. 1905. Clin Orthop Relat Res 466: 2903–9.

Cook SD (1999) Preclinical and clinical evaluation of osteogenic protein-1 (BMP-7) in bony sites. Orthopedics 22: 669–71.

Cook SD, Rueger DC (1996) Osteogenic protein-1: biology and applications. Clin Orthop Relat Res 324: 29–38.

Cook SD, Wolfe MW, Salkeld SL, Rueger DC (1995) Effect of recombinant human osteogenic protein-1 on healing of segmental defects in non-human primates. J Bone Joint Surg 77: 734–50.

Costantino P, Friedman C, Shindo M, Houston G, Sisson G (1993) Experimental mandibular regrowth by distraction osteogenesis. Long-term results. Arch Otolaryngol Head Neck Surg 119: 511–6.

Crispin RD, Todd LW, Mark AB (2002) Liposomes Containing Dimethyl Dioctadecyl Ammonium Bromide: Formulation, Quality Control, and Lipofection Efficiency. Drug Delivery 9: 11–8.

Crommelin DJ, Storm G, Jiskoot W, Stenekes R, Mastrobattista E, Hennink WE (2003) Nanotechnological approaches for the delivery of macromolecules. J Ctrl Rel 87: 81–8.

Croteau S, Rauch F, Silvestri A, Hamdy RC (1999) Bone morphogenetic proteins in orthopedics: from basic science to clinical practice. Orthopedics 22: 686–95.

Dard M, Sewing A, Meyer J, Verrier S, Roessler S, Scharnweber D (2000) Tools for tissue engineering of mineralized oral structures. Clin Oral Investig 4: 126–9.

David L, Feige JJ, Bailly S (2009) Emerging role of bone morphogenetic proteins in angiogenesis. Cytokine Growth Factor Rev 20: 203–12.

Davis SS, Illum L (1998) Drug delivery systems for challenging molecules. Int J Pharm 176: 1–8.

De Long WG Jr, Einhorn TA et al. (2007) Bone grafts and bone graft substitutes in orthopaedic trauma surgery. A critical analysis. J Bone Joint Surg Am 89: 649–58.

De Souza R, Zahedi P, Allen CJ, Piquette-Miller M (2009) Biocompatibility of injectable chitosan-phospholipid implant systems. Biomaterials 30: 3818–24.

Decher G (1997) Fuzzy Nanoassemblies: Toward Layered Polymeric Multicomposites. Science 277: 1232–7.

Deckers MML, van Bezooijen RL, van der Horst G, Hoogendam J, van der Bent C, Papapoulos SE, Lowik CWGM (2002) Bone morphogenetic proteins stimulate angiogenesis through osteoblast-derived vascular endothelial growth factor A. Endocrinology 143: 1545–53.

DeLustro F, Dasch J, Keefe J, Ellingsworth L (1990) Immune responses to allogeneic and xenogeneic implants of collagen and collagen derivatives. Clin Orthop 260: 263–79.

Demers C, Hamdy RC (1999) Bone Morphogenetic Proteins. Sci Am Sci & Med 6: 8–17.

Demers CN, Tabrizian M, Petit A, Hamdy RC, Yahia L (2002) Effect of experimental parameters on the in vitro release kinetics of transforming growth factor beta1 from coral particles. J Biomed Mater Res 59: 403–10.

Deregowski V, Gazzerro E, Priest L, Rydziel S, Canalis E (2006) Notch 1 overexpression inhibits osteoblastogenesis by suppressing Wnt/beta-catenin but not bone morphogenetic protein signaling. J Biol Chem 281: 6203–10.

Desai MP, Labhasetwar V, Amidon GL, Levy RJ (1996) Gastrointestinal uptake of biodegradable microparticles: Effect of particle size. Pharm Res 13: 1838–45.

Dhoot NO, Wheatley MA (2003) Microencapsulated Liposomes in Controlled Drug Delivery: Strategies to Modulate Drug Release and Eliminate the Burst Effect. J Pharma Sci 92: 679–89.

Dong YC, Feng SS (2004) Methoxy poly(ethylene glycol)-poly(lactide)(MPEG-PLA) nanoparticles for controlled delivery of anticancer drugs. Biomaterials 25: 2843–9.

Douglas KL, Tabrizian M (2005) Effect of experimental parameters on the formation of alginate-chitosan nanoparticles and evaluation of their potential application as DNA carrier. J Biomater Sci Polym Ed 16: 43–56.

Einhorn TA (1995) Enhancement of fracture-healing. J Bone Joint Surg Am 77: 940–56.

Einhorn TA (2003) Clinical applications of recombinant human BMPs: early experience and future development. J Bone Joint Surg Am 85-A: 82–8.

Einhorn TA, Majeska RJ, Mohaideen A, Bouxsein ML, Turek TJ, Wozney JM (2003) A single percutaneous injection of rhBMP-2 accelerates fracture repair. J Bone Joint Surg Am 85-A: 1425–35.

El-Mowafi H, Mohsen M (2005) The effect of low-intensity pulsed ultrasound on callus maturation in tibial distraction osteogenesis. Int Orthop 29: 121–4.

Engel E, Michiardi A, Navarro M, Lacroix D, Planell JA (2008) Nanotechnology in regenerative medicine: the materials side. Trends Biotechnol 26: 39–47.

Engstrand T, Veltheim R, Arnander C, Docherty-Skogh AC, Westermark A, Ohlsson C, Adolfsson L, Larm O (2008) A novel biodegradable delivery system for bone morphogenetic protein-2. Plast Reconstr Surg 121: 1920–8.

Fabian E, Landsiedel R, Ma-Hock L, Wiench K, Wohlleben W, van Ravenzwaay B (2008) Tissue distribution and toxicity of intravenously administered titanium dioxide nanoparticles in rats. Arch Toxicol 82: 151–7.

Fang TD, Nacamuli RP, Song HM, Fong KD, Warren SM, Salim A, Carano RA, Filvaroff EH, Longaker MT (2004) Creation and characterization of a mouse model of mandibular distraction osteogenesis. Bone 34: 1004–12.

Farhadieh RD, Gianoutsos MP, Dickinson R, Walsh WR (2000) Effect of distraction rate on biomechanical, mineralization, and histologic properties of an ovine mandible model. Plast Reconstr Surg 105: 889–95.

Fei Z, Hu Y, Wu D, Wu H et al. (2008) Preparation and property of a novel bone graft composite consisting of rhBMP-2 loaded PLGA microspheres and calcium phosphate cement. J Mater Sci Mater Med 19: 1109–16.

Finkemeier CG (2002) Bone-grafting and bone-graft substitutes. J Bone Joint Surg Am 84: 454–64.

Friedlaender GE, Perry CR, Cole JD, Cook SD, Cierny G, Muschler GF, Zych GA, Calhoun JH, LaForte AJ, Yin S (2001) Osteogenic protein-1 (bone morphogenetic protein-7) in the treatment of tibial nonunions. J Bone Joint Surg Am 83-A: 151–8.

Fu TS, Chen WJ, Chen LH et al. (2008) Enhancement of posterolateral lumbar spine fusion using low-dose rhBMP-2 and cultured marrow stromal cells. J Orthop Res [Epub].

Galovic RR, Barisic K, Pavelic Z, Zanic GT, Cepelak I, Filipovic-Grcic J (2002) High efficiency entrapment of superoxide dismutase into mucoadhesive chitosan-coated liposomes. Eur J Pharm Sci 15: 441–8.

Gao T, Uludag H (2001) Effect of molecular weight of thermoreversible polymer on in vivo retention of rhBMP-2. J Biomed Mater Res 57: 92–100.

Gaserod O, Smidsrod O, Skjak-Braek G (1998) Microcapsules of alginate-chitosan-I. A quantitative study of the interaction between alginate and chitosan. Biomatr 19: 1815–25.

Gautschi OP, Frey SP, Zellweger R (2007) Bone morphogenetic proteins in clinical applications. ANZ J Surg 77: 626–31.

Gebauer D, Correll J (2005) Pulsed low-intensity ultrasound: a new salvage procedure for delayed unions and nonunions after leg lengthening in children. J Pedo Orthop 25: 750–4.

Geesink RGT, Hoefnagels NHM, Bulstra SK (1999) Osteogenic activity of OP-1 bone morphogenetic protein (BMP-7) in a human fibular defect. J Bone Joint Surg 81: 710–8.

Geiger M, Li RH et al. (2003) Collagen sponges for bone regeneration with rhBMP-2. Adv Drug Deliv Rev 55: 1613–29.

Giannoudis P, Einhorn TA, Marsh D (2007) Fracture healing: the diamond concept. Injury 38 S4: 3–6.

Ginebra MP, Traykova T, Planell JA (2006) Calcium phosphate cements as bone drug delivery systems: a review. J Control Release 113: 102–10.

Gittens SA, Uludag H (2001) Growth factor delivery for bone tissue engineering. J Drug Target 9: 407–29.

Gohel MC, Panchal MK, Jogani VV (2000) Novel Mathematical Method for Quantitative Expression of Deviation from the Higuchi Model. AAPS PharmSciTech 1(4): article 31.

Govender S, Csimma C, Genant HK et al. (2002) BMP-2 Evaluation in Surgery for Tibial Trauma (BESTT) Study Group. Recombinant human bone morphogenetic protein-2 for treatment of open tibial fractures: a prospective, controlled, randomized study of four hundred and fifty patients. J Bone Joint Surg Am 84: 2123–34.

Gref R, Minamitake Y, Perracchia MT, Trubeskoy V, Torchilin V, Langer R (1994) Biodegradable long-circulating polymeric nanospheres. Science 263: 1600–3.

Haddad AJ, Peel SA, Clokie CM, Sándor GK (2006) Closure of rabbit calvarial critical-sized defects using protective composite allogeneic and alloplastic bone substitutes. J Craniofac Surg 17: 926–34.

Hagino T, Hamada Y (1999) Accelerating bone formation and earlier healing after using demineralized bone matrix for limb lengthening in rabbits. J Orthop Res 17: 232–7.

Haidar ZS, Hamdy RC, Tabrizian M (2008a) Protein release kinetics for core-shell hybrid nanoparticles based on the layer-by-layer assembly of alginate and chitosan on liposomes. Biomaterials 29: 1207–15.

Haidar ZS, Azari F, Hamdy RC, Tabrizian M (2008b) Modulated release of OP-1 and enhanced pre-osteoblast differentiation using a core-shell nanoparticulate system. J Biomed Mater Res A. In press.

Haidar ZS, Hamdy RC, Tabrizian M (2009a) Review: Recombinant BMP Delivery for Bone Regeneration and Repair. Part A: Current Challenges in BMP Delivery. Biotechnology Letters [Epub].

Haidar ZS, Hamdy RC, Tabrizian M (2009b) Review: Recombinant BMP Delivery for Bone Regeneration and Repair. Part B: Delivery Systems for BMPs in Orthopaedic and Craniofacial Tissue Engineering. Biotechnology Letters [Epub].

Haidar ZS, Tabrizian M, Hamdy RC (2009c) A hybrid OP-1 delivery system enhances new bone regeneration and consolidation in a rabbit model of distraction osteogenesis. Growth Factors. In press.

Hak DJ, Makino T, Niikura T, Hazelwood SJ, Curtiss S, Reddi AH (2006) Recombinant human BMP-7 effectively prevents non-union in both young and old rats. J Orthop Res 24: 11–20.

Hamanishi C, Kawabata T, Yoshii T, Tanaka S (1995) Bone mineral density changes in distracted callus stimulated by pulsed direct electrical current. Clin Orthop Relat Res 312: 247–52.

Hamanishi C, Yoshii T, Totani Y, Tanaka S (1994) Bone mineral density of lengthened rabbit tibia is enhanced by transplantation of fresh autologous bone marrow cells. An experimental study using dual X-ray absorptiometry. Clin Orthop Relat Res 303: 250–5.

Hamdy RC, Amako M, Beckman L, Kawaguchi M, Rauch F, Lauzier D, Steffen T (2003) Effects of osteogenic protein-1 on distraction osteogenesis in rabbits. Bone 33: 248–55.

Hamdy RC, Silvestri A, Rivard C, Ehrlich M (1997) Histologic evaluation of bone regeneration in cases of limb lengthening by Ilizarov's technique. An experimental study in the dog. Ann Chir 51: 875–83.

Haque T, Amako M, Nakada S, Lauzier D, Hamdy RC (2007) An immunohistochemical analysis of the temporal and spatial expression of growth factors FGF 1, 2 and 18, IGF 1 and 2, and TGFbeta1 during distraction osteogenesis. Histol Histopathol 22: 119–28.

Haque T, Hamade F, Alam N, Kotsiopriftis M, Lauzier D, St-Arnaud R, Hamdy RC (2008) Characterizing the BMP pathway in a wild type mouse model of distraction osteogenesis. Bone 42: 1144–53.

Haque T, Mandu-Hrit M, Rauch F, Lauzier D, Tabrizian M, Hamdy R (2005) Immunohistochemical localization of BMP signaling smads during long-bone distraction osteogenesis. J Histochem Cytochem 54: 407–15.

Heerklotz H, Tsamaloukas A, KitaTokarczyk K, Strunz P, Gutberlet T (2004) Structural, volumetric, and thermodynamic characterization of a micellar sphere-to-rod transition. J Am Chem Soc 126: 16544–52.

Herford AS, Boyne PJ (2008) Reconstruction of mandibular continuity defects with bone morphogenetic protein-2 (rhBMP-2). J Oral Maxillofac Surg 66: 616–624.

Higuchi T (1961) Rate of release of medicaments from ointment bases containing drugs in suspension. J Pharm Sci 50: 874–5.

Higuchi T, Kinoshita A, Takahashi K, Oda S, Ishikawa I (1999) Bone regeneration by recombinant human bone morphogenetic protein-2 in rat mandibular defects. An experimental model of defect filling. J Periodontol 70: 1026–31.

Hillberg AL, Tabrizian M (2006) Biorecognition through Layer-by-Layer Polyelectrolyte Assembly: In-situ Hybridization on Living Cells. Biomacromolecules 7: 2742–50.

Holbein O, Neidlinger-Wilke C, Suger G, Kinzl L, Claes L (1995) Ilizarov callus distraction produces systemic bone cell mitogens. J Orthop Res 13: 629–38.

Hollinger J (1993) Strategies for regenerating bone of the craniofacial complex. Bone 14: 575–80.

Hollinger JO, Schmitt J, Buck D, Shannon R, Joh S, Zegzula H, Wozney J (1998) Recombinant human bone morphogenetic protein-2 and collagen for bone regeneration. J Biomed Mater Res 43: 356–64.

Hosseinkhani H, Hosseinkhani M, Tian F, Kobayashi H, Tabata Y (2007) Bone regeneration on a collagen sponge self-assembled peptide-amphiphile nanofiber hybrid scaffold. Tissue Eng 13: 11–9.

Hou Q, De Bank PA, Shakesheff KM (2004) Injectable scaffolds for tissue regeneration. J Mater Chem 14: 1915–23.

Hu YY, Zhang C, Lu R, Xu JQ, Li D (2003) Repair of radius defect with bone-morphogenetic-protein loaded hydroxyapatite/collagen-poly(L-lactic acid) composite. Chin J Traumatol 6: 67–74.

Hwang CJ, Vaccaro AR, Lawrence JP, Hong J, Schellekens H, Alaoui-Ismaili MH, Falb D (2009) Immunogenicity of bone morphogenetic proteins. J Neurosurg Spine 10: 443–51.

Ilizarov GA (1989a) The tension stress effect on the genesis and growth of tissues. 1. The influence of stability of fixation and soft-tissue preservation. Clin Orthop Relat Res 238: 249–81.

Ilizarov GA (1989b) The tension stress effect on the genesis and growth of tissues. 2. The influence of stability of the rate and frequency of distraction. Clin Orthop Relat Res. 239: 263–285.

Ilizarov GA, Ledyaev VI (1992) The replacement of long tubular bone defects by lengthening distraction osteotomy of one of the fragments. 1969. Clin Orthop Relat Res 280: 7–10.

Illum L, Davis SS (1991) Drug delivery. Curr Opin Biotechnol 2: 254–9.

Iranov YM (1996) Spatial organization of a microcirculatory bed in distraction bone regenerates. Genij Orthopedii 1: 14.

Issa JP, Bentley M, Iyomasa M, Sebald W, De Albuquerque RF (2008c) Sustained release carriers used to delivery bone morphogenetic proteins in the bone healing process. Anat Histol Embryol 37: 181–7.

Issa JP, Nascimento C, Bentley MV et al. (2008a) Bone repair in rat mandible by rhBMP-2 associated with two carriers. Micron 39: 373–9.

Issa JP, Spadaro AC, Bentley MV et al. (2008b) Monoolein and chitosan gels as potential carriers of the rhBMP-2, using decortication surgical technique in Wistar rats as experimental model. Micron 39: 952–9.

Itoh S, Kikuchi M, Takakuda K, Nagaoka K, Koyama Y, Tanaka J, Shinomiya K (2002) Implantation study of a novel hydroxyapatite/collagen (HAp/col) composite into weight-bearing sites of dogs. J Biomed Mater Res 63: 507–15.

Itoh T, Mochizuki M, Nishimura R et al. (1998) Repair of ulnar segmental defect by recombinant human bone morphogenetic protein-2 in dogs. J Vet Med Sci 60: 451–8.

Jain D, Banerjee R (2008) Comparison of Ciprofloxacin Hydrochloride-Loaded Protein, Lipid, and Chitosan Nanoparticles for Drug Delivery. J Biomed Mater Res B Appl Biomater 86: 105–12.

Jeon O, Song SJ, Yang HS, Bhang SH, Kang SW et al. (2008) Long-term delivery enhances in vivo osteogenic efficacy of BMP-2 compared to short-term delivery. Biochem Biophys Res Commun 369: 774–80.

Johnsson R, Strömqvist B, Aspenberg P (2002) Randomized radiostereometric study comparing osteogenic protein-1 (BMP-7) and autograft bone in human noninstrumented posterolateral lumbar fusion: 2002 Volvo Award in clinical studies. Spine 27: 2654–61.

Jung RE, Glauser R, Schärer P, Hämmerle CH, Sailer HF, Weber FE (2003) Effect of rhBMP-2 on guided bone regeneration in humans. Clin Oral Implants Res 14: 556–68.

Kanayama M, Hashimoto T, Shigenobu K (2006) A prospective randomized study of posterolateral lumbar fusion using osteogenic protein-1 (OP-1) versus local autograft with ceramic bone substitute: emphasis of surgical exploration and histologic assessment. Spine 31: 1067–74.

Katoh M (2002) WNT and FGF gene clusters (review). Int J Oncol 21: 1269–73.

Kawakatsu N, Oda S, Kinoshita A et al. (2008) Effect of rhBMP-2 with PLGA/gelatin sponge type (PGS) carrier on alveolar ridge augmentation in dogs. J Or Rehab 35: 647–55.

Kawano Y, Kypta R (2003) Secreted antagonists of Wnt signalling pathway. J Cell Sci 116: 2627–34.

Kempen DH, Lu L, Heijink A, Hefferan TE, Creemers LB, Maran A, Yaszemski MJ, Dhert WJ (2009) Effect of local sequential VEGF and BMP-2 delivery on ectopic and orthotopic bone regeneration. Biomaterials 30: 2816–25.

Kenley R, Marden L, Turek T, Jin L, Ron E, Hollinger JO (1994) Osseous regeneration in the rat calvarium using novel delivery systems for recombinant human bone morphogenetic protein-2 (rhBMP-2). J Biomed Mater Res 28: 1139–47.

Kim HD, Valentini RF (2002) Retention and activity of BMP-2 in hyaluronic acid-based scaffolds in vitro. J Biomed Mater Res 59: 573–84.

Kim JS, Yoon TJ, Yu KN, Kim BG, Park SJ, Kim HW, Lee KH, Park SB, Lee JK, Cho MH (2006) Toxicity and tissue distribution of magnetic nanoparticles in mice. Toxicol Sci 89: 338–47.

Kim SS, Gwak SJ, Kim BS (2008) Orthotopic bone formation by implantation of apatite-coated poly(lactide-co-glycolide)/hydroxyapatite composite particulates and bone morphogenetic protein-2. J Biomed Mater Res A 87: 245–53.

Kim TH, Park YH, Kim KJ, Cho CS (2003) Release of albumin from chitosan-coated pectin beads in vitro. Int J Pharma 250: 371–83.

Kimelman N, Pelled G, Helm GA, Huard J, Schwarz EM, Gazit D (2007) Review: gene- and stem cell-based therapeutics for bone regeneration and repair. Tiss Eng 13: 1135–50.

Kingsley DM (1994) What do BMPs do in mammals? Clues from the mouse short-ear mutation. Trends Genet 10: 16–21.

Kirker-Head CA (2000) Potential applications and delivery strategies for bone morphogenetic proteins. Adv Drug Dliv Rev 43: 65–92.

Kirkerhead CA, Gerhart TN, Schelling SH, Hennig GE, Wang E, Holtrop ME (1995) Long-term healing of bone using recombinant human bone morphogenetic protein-2. Clin Orthop Relat Res 318: 222–30.

Kitoh H, Kitakoji T, Tsuchiya H, Mitsuyama H, Nakamura H, Katoh M, Ishiguro N (2004) Transplantation of marrow-derived mesenchymal stem cells and platelet-rich plasma during distraction osteogenesis - preliminary result of three cases. Bone 35: 892–8.

Kneser U, Schaefer DJ, Polykandriotis E, Horch RE (2006) Tissue engineering of bone: the reconstructive surgeon's point of view. J Cell Mol Med 10: 7–19.

Knight PG, Glister C (2006) TGF-beta superfamily members and ovarian follicle development. Reproduction 132: 191–206.

Komuro Y, Takato T, Harii K, Yonemara Y (1994) The histologic analysis of distraction osteogenesis of the mandible in rabbits. Plast Reconstr Surg 94: 152–9.

Kretlow JD, Klouda L, Mikos AG (2007) Injectable matrices and scaffolds for drug delivery in tissue engineering. Adv Drug Deliv Rev 59: 263–73.

Kumar MN, Muzzarelli RA, Muzzarelli C, Sashiwa H, Domb AJ (2004) Chitosan chemistry and pharmaceutical perspectives. Chem Rev 104: 6017–84.

Kurokawa I, Kusumoto K, Bessho K, Okubo Y, Senzaki H, Tsubura A (2000) Immunohistochemical expression of bone morphogenetic protein-2 in pilomatricoma. Br J Dermatol 143: 754–8.

Kusec V, Jelic M, Borovecki F, Vukicevic S, Korzinek K (2003) Distraction osteogenesis by Ilizarov and unilateral external fixators in a canine model. Int Orthop 27: 47–52.

Kusumoto K, Bessho K, Fujimura K, Akioka J, Okubo Y, Wang Y, Iizuka T, Ogawa Y (2002) Osteoinduction by recombinant human bone morphogenetic protein-2 in muscles of non-human primates. J Int Med Res 30: 251–9.

Kwon B, Jenis LG (2005) Carrier materials for spinal fusion. Spine J 5S: 224–30.

Lacroix P (1945) Recent investigations on the growth of bone. Nature 156: 576.

Lauterburg MT, Exner GU, Jacob HA (2006) Forces involved in lower limb lengthening: an in vivo biomechanical study. J Orthop Res 24: 1815–22.

Lee JY, Nam S, Im SY, Park YJ, Lee YM, Seol YJ, Chung CP, Lee SJ (2002) Enhanced bone formation by controlled growth factor delivery from chitosan-based biomaterials. J Control Release 78: 187–97.

Lee K, Yuk S (2007) Polymeric protein delivery systems. Progress in Polymer Science 32: 669–97.

Lee SH, Shin H (2007) Matrices and scaffolds for delivery of bioactive molecules in bone and cartilage tissue engineering. Adv Drug Deliv Rev 59: 339–59.

Leea DH, Baeka HS, Leeb MH, Park JC (2005) Production of bone morphogenetic protein-7 using pET expression system. Curr App Phys 5: 422–5.

Leung KS, Lee W, Tsui H, Liu PP, Cheung WH (2004) Complex tibial fracture outcomes following treatment with low-intensity pulsed ultrasound. Ultras Med Biol 30: 389–95.

Levander G (1938) A study of bone regeneration. Surgery Gynecology and Obstetrics 67: 705–14.

Li G, Simpson AH, Triffitt JT (1999) The role of chondrocytes in intramembranous and endochondral ossification during distraction osteogenesis in the rabbit. Calcif Tissue Int 64: 310–7.

Li G, Virdi AS, Ashhurst DE, Simpson AH, Triffitt JT (2000) Tissues formed during distraction osteogenesis in the rabbit are determined by the distraction rate: localization of the cells that express the mRNAs and the distribution of types I and II collagens. Cell Biol Int 24: 25–33.

Li RH, Wozney JM (2001) Delivering on the promise of bone morphogenetic proteins. Trend Biotechnol 19: 255–65.

Li Z, Ramay HR, Hauch KD, Xiao D, Zhang M (2005) Chitosan-alginate hybrid scaffolds for bone tissue engineering. Biomaterials 26: 3919–28.

Liew CV, Chan LW, Ching AL, Heng PW (2006) Evaluation of sodium alginate as drug release modifier in matrix tablets. Int J Pharm 309: 25–37.

Lindholm TC, Peel SAF, Sàndor GKB, Clokie CML (2002) Intra-oral bone graft used to acquire viable bone cells to be used for tissue engineering. J Can Dent Assoc 68:699.

Little DG, Smith NC, Williams PR, Briody JN, Bilston LE, Smith EJ, Gardiner EM, Cowell CT (2003) Zoledronic acid prevents osteopenia and increases bone strength in a rabbit model of distraction osteogenesis. J Bone Miner Res 18: 1300–7.

Luginbuehl V, Meinel L, Merkle HP, Gander B (2004) Localized delivery of growth factors for bone repair. Eur J Pharm Biopharm 58: 197–208.

Lulevich VV, Radtchenko IL, Sukhorukov GB, Vinogradova OI (2003) Deformation properties of nonadhesive polyelectrolyte microcapsules studied with the atomic force microscope. J Phys Chem B 107: 2735–40.

Ma PX (2008) Biomimetic materials for tissue engineering. Adv Drg Delv Rv 60: 184–98.

Malgaigne JF (1847) Traite de fractures et des luxations, Paris, France : JB Bailliere.

Mandu-Hrit M, Haque T, Lauzier D, Kotsiopriftis M, Rauch F, Tabrizian M, Henderson JE, Hamdy RC (2006) Early injection of OP-1 during distraction osteogenesis accelerates new bone formation in rabbits. Growth Factors 24: 172–83.

Mandu-Hrit M, Seifert E, Kotsiopriftis M, Lauzier D, Haque T, Rohlicek C, Tabrizian M, Hamdy RC (2008) OP-1 injection increases VEGF expression but not angiogenesis in a rabbit model of distraction osteogenesis. Growth Factors 26: 143–51.

Maniscalco P, Gambera D, Bertone C et al. (2002) Healing of fresh tibial fractures with OP-1. Acta Biomed 73: 27–33.

Mayer M, Hollinger J, Ron E, Wozney J (1996) Maxillary alveolar cleft repair in dogs using recombinant human bone morphogenetic protein-2 and a polymer carrier. Plast Reconstr Surg 98: 247–59.

Mayr E, Laule A, Suger G, Rüter A, Claes L (2001) Radiographic results of callus distraction aided by pulsed low-intensity ultrasound. J Orthop Trauma 15: 407–14.

McCarthy JG, Schreiber J, Karp N, Thorne CH, Grayson BH (1992) Lengthening the human mandible by gradual distraction. Plast Reconstr Surg 89: 1-8; discussion 9-10.

McKibbin B (1989) Biological considerations in osteosynthesis. Chirurgie 115: 683–6.

Meyer U, Meyer T, Wiesmann HP, Kruse-Lösler B, Vollmer D, Stratmann U, Joos U (2001) Mechanical tension in distraction osteogenesis regulates chondrocytic differentiation. Int J Oral Maxillofac Surg 30: 522–30.

Mitsukawa N, Satoh K, Suse T, Hosaka Y (2007) Clinical success of mandibular distraction for obstructive sleep apnea resulting from micrognathia in 10 consecutive Japanese young children. J Craniofac Surg 18: 948–53.

Miyazono K, ten Dijke P, Heldin CH (2000) TGF-beta signaling by Smad proteins. Adv Immunol 75: 115–7.

Mizumoto Y, Moseley T, Drews M, Cooper VN 3rd, Reddi AH (2003) Acceleration of regenerate ossification during distraction osteogenesis with recombinant human bone morphogenetic protein-7. J Bone Joint Surg Am 85-A: 124–30.

Mizuno K, Yamamura K, Yano K, Osada T, Saeki S, Takimoto N, Sakurai T, Nimura Y (2003) Effect of chitosan film containing basic fibroblast growth factor on wound healing in genetically diabetic mice. J Biomed Mater Res A 64: 177–81.

Mizuno M, Kuboki Y (2001) Osteoblast-Related Gene Expression of Bone Marrow Cells during the Osteoblastic Differentiation Induced by Type I Collagen. J Biochm 129: 133–8.

Mohanraj VJ, Chen Y (2006) Nanoparticles – A Review. Trop J Pharm Res 5: 561–73.

Mohr U, Dungworth DL, Capen CC (1992) Pathobiology of the aging rat. ILSI Press: 485.

Moioli EK, Clark PA, Xin X, Lal S, Mao JJ (2007) Matrices and scaffolds for drug delivery in dental, oral and craniofacial tissue engineering. Adv Drg Delv Rev 59: 308–24.

Mont MA, Ragland PS, Biggins B, Friedlaender G, Patel T, Cook S, Etienne G, Shimmim A, Keldey R, Rueger DC, Einhorn TA (2004) Use of bone morphogenetic proteins for musculoskeletal applications. An overview. J Bone Joint Surg 86: 41–55.

Moon RT, Bowerman B, Boutros M, Perrimon N (2002) The promise and perils of Wnt signaling through beta-catenin. Science 296: 1644–6.

Moore WR, Graves SE, Bain GI (2001) Synthetic bone graft substitutes. ANZ J Surg 71: 354–61.

Moreno-Miralles I, Schisler JC, Patterson C (2009) New insights into bone morphogenetic protein signaling: focus on angiogenesis. Curr Opin Hematol 16: 195–201.

Mosekilde L, Bak B (1993) The effects of growth hormone on fracture healing in rats: a histological description. Bone 14: 19–27.

Murray JH, Fitch RD (1996) Distraction Histiogenesis: Principles and Indications. J Am Acad Orthop Surg 4: 317–27.

Mussano F, Ciccone G, Ceccarelli M, Baldi I, Bassi F (2007) Bone morphogenetic proteins and bone defects: a systematic review. Spine 32: 824–30.

Na K, Kim S, Woo DG, Sun BK, Yang HN, Chung HM, Park KH (2007) Synergistic effect of TGFbeta-3 on chondrogenic differentiation of rabbit chondrocytes in thermo-reversible hydrogel constructs blended with hyaluronic acid by in vivo test. J Biotechnol 128: 412–22.

Nair LS, Laurencin CT (2008) Nanofibers and nanoparticles for orthopaedic surgery applications. J Bone Joint Surg Am 90 S1: 128–31.

Nakagawa T, Sugiyama T, Kamei T, Murata T, Tagawa T (2001) An immuno-light- and electron-microscopic study of the expression of bone morphogenetic protein-2 during the process of ectopic bone formation in the rat. Arch Oral Biol 46: 403–11.

Nakagawa T, Tagawa T (2000) Ultrastructural study of direct bone formation induced by BMPs-collagen complex implanted into an ectopic site. Oral Dis 6: 172–9.

Nakashima M, Reddi AH (2003) The application of bone morphogenetic proteins to dental tissue engineering. Nat Biotechnol 21: 1025–32.

Nanno K, Sugiyasu K, Daimon T, Yoshikawa H, Myoui A (2009) Synthetic Alginate is a Carrier of OP-1 for Bone Induction. Clin Orthop Relat Res [Epub ahead of print].

Neyt JG, Buckwalter JA, Carroll NC (1998) Use of animal models in musculoskeletal research. Iowa Orthop J 18: 118–23.

Noshi T, Yoshikawa T, Dohi Y (2001) Recombinant human bone morphogenetic protein-2 potentiates the in vivo osteogenic ability of marrow/hydroxyapatite composites. Artif Organs 25: 201–8.

Nussenbaum B, Krebsbach PH (2006) The role of gene therapy for craniofacial and dental tissue engineering. Adv Drug Deliv Rev 58: 577–91.

Oda S, Kinoshita A, Higuchi T, Shizuya T, Ishikawa I (1997) Ectopic bone formation by biphasic calcium phosphate (BCP) combined with recombinant human bone morphogenetic protein-2 (rhBMP-2). J Med Dent Sci 44: 53–62.

Ohashi S, Ohnishi I, Kageyama T, Imai K, Nakamura K (2007) Distraction osteogenesis promotes angiogenesis in the surrounding muscles. Clin Orthop Relat Res 454: 223–9.

Okazaki H, Kurokawa T, Nakamura K, Matsushita T, Mamada K, Kawaguchi H (1999) Stimulation of bone formation by recombinant fibroblast growth factor-2 in callotasis bone lengthening of rabbits. Calcif Tissue Int 64: 542–6.

Okubo Y, Bessho K, Fujimura K et al. (2000) Osteoinduction by recombinant human bone morphogenetic protein-2 at intramuscular, intermuscular, subcutaneous and intrafatty sites. Int J Oral Maxillofac Surg 29: 62–6.

O'Regan M, Martini I, Crescenzi F, De Luca C, Lansing M (1994) Molecular mechanisms and genetics of hyaluronan biosynthesis. Int J Bio Macromol 16: 283–6.

Paley D (1990) Problems, obstacles, and complications of limb lengthening by the Ilizarov technique. Clin Orthop Relat Res 250: 81–104.

Paramore CG, Lauryssen C, Rauzzino MJ, Wadlington VR et al. (1999) The safety of OP-1 for lumbar fusion with decompression: A canine study. Neurosurgery 44: 1151–6.

Park JH, Ye M, Park K (2005) Biodegradable polymers for microencapsulation of drugs. Molecules 10: 146–61.

Pearce AI, Richards RG, Milz S, Schneider E, Pearce SG (2007) Animal models for implant biomaterial research in bone: a review. Eur Cell Mater 13: 1–10.

Pecine M, Giltaij LR, Vukicevic S (2001) Orthopaedic applications of osteogenic protein -1 (BMP-7). Int Orthop 25: 203–8.

Peltier LF (1968) A brief history of traction. J Bone Joint Surg Am 50: 1603–17.

Peng L, Bian WG, Liang FH, Xu HZ (2008) Implanting hydroxyapatite-coated porous titanium with bone morphogenetic protein-2 and hyaluronic acid into distal femoral metaphysis of rabbits. Chn J Traumatol 11: 179–85.

Phillips FM, Turner AS, Seim HB, MacLeay J, Toth CA, Pierce AR, Wheeler DL (2006) In vivo BMP-7 (OP-1) enhancement of osteoporotic vertebral bodies in an ovine model. Spine 6: 500–6.

Pluhar GE, Turner AS, Pierce AR, Toth CA, Wheeler DL (2006) A comparison of two biomaterial carriers for osteogenic protein-1 (BMP-7) in an ovine critical defect model. J Bone Joint Surg Br 88: 960–6.

Prabaharan M (2008) Chitosan derivatives as promising materials for controlled drug delivery. J Biomater Appl 23: 5–36.

Prunier C, Hocevar BA, Howe PH (2004) Wnt signaling: physiology and pathology. Growth Factors 22: 141–50.

Pushparaj PN, Aarthi JJ, Manikandan J, Kumar SD (2008) siRNA, miRNA, and shRNA: in vivo applications. J Dent Res 87: 992–1003.

Qiu Y, Zhang N, Kang Q, An Y, Wen X (2008) Chemically modified light-curable chitosans with enhanced potential for bone tissue repair. J Biomed Mater Res A [Epub].

Quinn JF, Caruso F (2004) Facile tailoring of film morphology and release properties using layer-by-layer assembly of thermoresponsive materials. Langmuir 20: 20–2.

Raiche T, Puleo A (2004) In vitro effects of combined and sequential delivery of two bone growth factors. Biomaterials 25: 677–85.

Rauch F, Lauzier D, Croteau S, Travers R, Glorieux FH, Hamdy R (2000a) Temporal and spatial expression of bone morphogenetic protein-2,-4, and-7 during distraction osteogenesis in rabbits. Bone 26: 611–7.

Rauch F, Lauzier D, Travers R, Glorieux F, Hamdy R (2000b) Effects of locally applied transforming growth factor-beta 1 on distraction osteogenesis in a rabbit limb-lengthening model. Bone 26: 619–24.

RaviKumar MN (2000) Nano and microparticles as controlled drug delivery devices. J Pharm Pharm Sci 3: 234–58.

Reddi AH (1998) Initiation of fracture repair by bone morphogenetic proteins. Clin Orthop Relat Res 355 Suppl: 66–72.

Reddi AH (2001) Bone morphogenetic proteins: from basic science to clinical applications. J Bone Joint Surg Am 83-A Suppl 1: 1–6.

Reddi AH (2003) Cartilage morphogenetic proteins: role in joint development, homoeostasis, and regeneration. Ann Rheum Dis 62 Suppl 2: 73–8.

Reddi AH (2005) BMPs: from bone morphogenetic proteins to body morphogenetic proteins. Cytokine Growth Factor Rev 16: 249–50.

Reddi AH, Huggins C (1972) Biochemical sequences in the transformation of normal fibroblasts in adolescent rats. Proc Natl Acad Sci USA 69: 1601–5.

Reddi AH, Wientroub S, Muthukumaran N (1987) Biologic principles of bone induction. Orthop Clin North Am 18: 207–12.

Rengachary SS (2007) Bone morphogenetic proteins: basic concepts. Neuros Foc 13: 1–6.

Richards RG, Stiffanic M, Owen GR, Riehle M, Ap Gwynn I, Curtis AS (2001) Immunogold labelling of fibroblast focal adhesion sites visualised in fixed material using scanning electron microscopy, and living, using internal reflection microscopy. Cell Biol Int 25: 1237–49.

Richardson TP, Peters MC, Ennett AB, Mooney DJ (2001) Polymeric system for dual growth factor delivery. Nat Biotechnol 19: 1029–34.

Ripamonti U, Crooks J, Rueger DC (2001) Induction of bone formation by recombinant human osteogenic protein-1 and sintered porous hydroxyapatite in adult primates. Plast Reconstr Surg 107: 977–88.

Ripamonti U, Ramoshebi LN, Matsaba T, Tasker J, Crooks J, Teare J (2001) Bone Induction by BMPs/OPs and Related Family Members in Primates: The Critical Role of Delivery Systems, J Bone Joint Surg Am 83: 116–27.

Ripamonti U, Van Den Heever B, Crooks J, Tucker MM, Sampath TK, Rueger DC, Reddi AH (2000) Long-term evaluation of bone formation by osteogenic protein 1 in the baboon and relative efficacy of bone-derived bone morphogenetic proteins delivered by irradiated xenogeneic collagenous matrices. J Bone Miner Res 15: 1798–1809.

Robinson Y, Heyde CE, Tschöke SK et al. (2008) Evidence supporting the use of bone morphogenetic proteins for spinal fusion surgery. Expert Rev Med Dev 5: 75–84.

Rose FR, Hou Q, Oreffo RO (2004) Delivery systems for bone growth factors - the new players in skeletal regeneration. J Pharm Pharmacol 56: 415–27.

Rosen V (2006) BMP and BMP inhibitors in bone. Ann N Y Acad Sci 1068: 19–25.

Rosen V, Thies RS, Lyons K (1996) Signaling pathways in skeletal formation: a role for BMP receptors. Ann N Y Acad Sci 785: 59–69.

Rosier RN, O'Keefe RJ, Hicks DG (1998) The potential role of transforming growth factor beta in fracture healing. Clin Orthop Relat Res 355 Suppl: S294–300.

Ruhe PQ, Hedberg EL, Padron NT, Spauwen PH, Jansen JA, Mikos AG (2003) rhBMP-2 release from injectable poly(DL-lactic-co-glycolic acid)/calcium-phosphate cement composites. J Bone Joint Surg Am 85-A Suppl: 75–81.

Sailhan F, Chatel F, Chousta A, Viguier E, Boivin G (2006) Unexpected absence of effect of rhBMP-7 on distraction osteogenesis. Clin Orthop Relat Res 457: 227–34.

Saito K, Konishi I, Nishiguchi M, Hoshino T, Fujiwara T (2008) Amelogenin binds to both heparan sulfate and bone morphogenetic protein 2 and pharmacologically suppresses the effect of noggin. Bone 43: 371–6.

Saito N, Murakami N, Takahashi J et al. (2005) Synthetic biodegradable polymers as drug delivery systems for bone morphogenetic proteins. Adv Drug Deliv Rev 57: 1037–48.

Saito N, Okada T, Horiuchi H, Ota H, Takahashi J, Murakami N, Nawata M, Kojima S, Nozaki K, Takaoka K (2003) Local bone formation by injection of recombinant human bone morphogenetic protein-2 contained in polymer carriers. Bone 32: 381–6.

Saito N, Takaoka K (2003) New synthetic biodegradable polymers as BMP carriers for bone tissue engineering. Biomaterials 24: 2287–93.

Salgado AJ, Coutinho OP, Reis RL (2004) Bone tissue engineering: state of the art and future trends. Macromol Biosci 9: 743–65.

Samchukov ML, Cherkashin AM, Cope JB (1998) Distraction Osteogenesis: history and biologic basis of new bone formation. In Lynch SE, Geneco RJ, Marx RE; editors: Tissue Engineering: applications in maxillofacial surgery and periodontics. Carol Stream III, Quintessence.

Samchukov ML, Cope JB, Cherkashin AM (2001) Craniofacial Distraction Osteogenesis. St. Louis, Missouri, Mosby Publishing.

Sampath TK, Maliakal JC, Hauschka PV, Jones WK, Sasak H, Tucker RF, White KH, Coughlin JE, Tucker MM, Pang RH (1992) Recombinant human osteogenic protein-1 (hOP-1) induces new bone formation in vivo with a specific activity comparable with natural bovine osteogenic protein and stimulates osteoblast proliferation and differentiation in vitro. J Biol Chem 267: 20352–62.

Sampath TK, Reddi AH (1981) Dissociative extraction and reconstitution of extracellular matrix components involved in local bone differentiation. Proc Natl Acad Sci USA 78: 7599–603.

Savic R, Luo LB, Eisenberg A, Maysinger D (2003) Micellar nanocontainers distribute to defined cytoplasmic organelles. Science 300: 615–8.

Scheufler C, Sebald W, Hülsmeyer M (1999) Crystal structure of human bone morphogenetic protein-2 at 2.7 A resolution. J Mol Biol 19: 103–15.

Schliephake H, Weich HA, Dullin C, Gruber R, Frahse S (2008) Mandibular bone repair by implantation of rhBMP-2 in a slow release carrier of polylactic acid--an experimental study in rats. Biomaterials 29: 103–10.

Schmidmaier G, Schwabe P, Strobel C, Wildemann B (2008) Carrier systems and application of growth factors in orthopaedics. Injury 39 S2: 37–43.

Schopper C, Moser D, Spassova E et al. (2008) Bone regeneration using a naturally grown HA/TCP carrier loaded with rh BMP-2 is independent of barrier-membrane effects. J Biomed Mater Res A 85: 954–63.

Sciadini MF, Johnson KD (2000) Evaluation of recombinant human bone morphogenetic protein-2 as a bone-graft substitute in a canine segmental defect model. J Orthop Res 18: 289–302.

Seeherman H, Wozney J, Li R (2002) Bone morphogenetic protein delivery systems. Spine 27: 16–23.

Seeherman H, Wozney JM (2005) Delivery of bone morphogenetic proteins for orthopedic tissue regeneration. Cytokine Growth Factor Rev 16: 329–45.

Seeherman HJ, Azari K, Bidic S, Rogers L, Li XJ, Hollinger JO, Wozney JM (2006) rhBMP-2 delivered in a calcium phosphate cement accelerates bridging of critical size defects in rabbit radii. J Bone Joint Surg Am 88: 1553–65.

Sells DM, Brix, AE, Nyska A, Jokinen M P, Orzech D P, Walker N J (2007) Respiratory tract lesions in noninhalation studies. Toxicol Pathol 35: 170–7.

Senn N (1889) On the healing of aseptic bone cavities by implantation of antiseptic decalcified bone. Am J Med Sci 98: 219–43.

Shearer JR, Roach HI, Parsons SW (1992) Histology of a lengthened human tibia. J Bone Joint Surg Br 74: 39–44.

Shenoy DB, Antipov AA, Sukhorukov GB, Mohwald H (2003) Layer-by-layer engineering of biocompatible, decomposable core-shell structures. Biomacroml 4: 265–72.

Shi Y, Massagué J (2003) Mechanisms of TGF-beta signaling from cell membrane to the nucleus. Cell 113: 685–700.

Shimazaki A, Inui K, Azuma Y, Nishimura N, Yamano Y (2000) Low-intensity pulsed ultrasound accelerates bone maturation in distraction osteogenesis in rabbits. J Bone Joint Surg Br 82: 1077–82.

Shiqu YE, Chaoyang W, Xinxing L, Zhen T (2005) Multilayer nanocapsules of polysaccharide chitosan and alginate through layer-by-layer assembly directly on PS nanoparticles for release. J Biomat Sci Polymer Ed 16: 909–23.

Shu XZ, Zhu KJ (2002) The release behavior of brilliant blue from calcium-alginate gel beads coated by chitosan: the preparation method effect. Eur J Ph Biopharm 53: 193–201.

Sigurdsson T, Nygaard L, Tatakis D, Fu E, Turek T, Jin L, Wozney JM, Wikesjö UM (1996) Periodontal repair in dogs: evaluation of rhBMP-2 carriers. Int J Periodontics Restorative Dent 16: 524–37.

Simic P, Vukicevic S (2005) Bone morphogenetic proteins in development and homeostasis of kidney. Cytokine Growth Factor Rev 16: 299–308.

Smith MC, Senders CW (2006) Prognosis of airway obstruction and feeding difficulty in the Robin sequence. Int J Pediatr Otorhinolaryngol 70: 319–24.

Solheim E (1998) Growth factors in bone. Int Orthop 22: 410–6.

Stewart KJ, Weyand B, van't Hof RJ, White SA, Lvoff GO, Maffulli N, Poole MD (1999) A quantitative analysis of the effect of insulin-like growth factor-1 infusion during mandibular distraction osteogenesis in rabbits. Br J Plast Surg 52: 343–50.

Stoeger T, Proetzel GE, Welzel H, Papadimitriou A, Dony C, Balling R, Hofmann C (2002) In situ gene expression analysis during BMP2-induced ectopic bone formation in mice shows simultaneous endochondral and intramembranous ossification. Growth Factors 20: 197–210.

Stokes W (2002) Humane endpoints for laboratory animals used in toxicity testing. ILAR J 43: S31–8.

Sung HJ, Meredith C, Johnson C, Galis ZS (2004) The effect of scaffold degradation rate on three-dimensional cell growth and angiogenesis. Biomaterials 25: 5735–42.

Swennen G, Schliephake H, Dempf R, Schierle H, Malevez C (2001) Craniofacial distraction osteogenesis: a review of the literature: Part 1: clinical studies. Int J Oral Maxillofac Surg 30: 89–103.

Sydow-Plum G, Haidar ZS, Merhi Y, Tabrizian M (2008) Modulating the Release Kinetics of Paclitaxel from Membrane-Covered Stents Using Different Loading Strategies. Materials 1: 25–43.

Sykaras N, Opperman LA (2003) Bone morphogenetic proteins (BMPs): how do they function and what can they offer the clinician? J Oral Sci 45: 57–73.

Tabatt K, Sameti M, Olbrich C, Muller RH, Lehr C (2004) Effect of cationic lipid and matrix lipid composition on solid lipid nanoparticles-mediated gene transfer. Eur J Pharm Biopharm 57: 155–62.

Takaoka K, Koezuka M, Nakahara H (1991) Telopeptide-depleted bovine skin collagen as a carrier for bone morphogenetic protein. J Orthop Res 9: 902–7.

Takeuchi H, Kojima H, Yamamoto H, Kawashima Y (2000) Polymer coating of liposomes with a modified polyvinyl alcohol and their systemic circulation and RES uptake in rats. J Control Release 68: 195–205.

Takeuchi H, Kojima H, Yamamoto H, Kawashima Y (2001) Evaluation of circulation profiles of liposomes coated with hydrophilic polymers having different molecular weights in rats. J Control Release 75: 83–91.

Takeuchi H, Kojima H, Yamamoto H, Toshitada T, Hidekazu T, Tomaoki H, Yoshiaki K (1998) Physical stability of size controlled small unilamellar liposomes coated with a modified polyvinyl alcohol. Int J Pharmaceutics 164: 103–11.

Talwar R, Di Silvio L, Hughes FJ, King GN (2001) Effects of carrier release kinetics on bone morphogenetic protein-2-induced periodontal regeneration in vivo. J Clin Periodontol 28: 340–7.

Tan HT, Dass CR, Dunstan DE (2008) Injectable chitosan hydrogels for localized cancer therapy. J Control Release 126: 205–16.

Tavakoli K, Yu Y, Shahidi S, Bonar F, Walsh W, Poole MD (1999) Expression of growth factors in the mandibular distraction zone: A sheep study. Br J Plastic Surg 52: 434–9.

Tay BK, Le AX, Gould SE, Helms JA (1998) Histochemical and molecular analyses of distraction osteogenesis in a mouse model. J Orthop Res 16: 636–42.

Termaat MF, Den Boer FC, Bakker FC, Patka P, Haarman HJ (2005) Bone morphogenetic proteins. Development and clinical efficacy in the treatment of fractures and bone defects. J Bone Joint Surg Am 87: 1367–78.

Thierry B, Winnik FM, Merhi Y, Silver J, Tabrizian M (2003) Bioactive coatings of endovascular stents based on polyelectrolyte multilayers. Biomacromolecules 4: 1564–71.

Tönnesen HH, Karlsen J (2002) Alginate in drug delivery systems. Drug Dev Ind Pharm 28: 621–30.

Tsialogiannis E, Polyzois I, Oak Tang Q, Pavlou G, Tsiridis E, Heliotis M, Tsiridis E (2009) Targeting bone morphogenetic protein antagonists: in vitro and in vivo evidence of their role in bone metabolism. Expert Opin Ther Targets 13:123–37.

Tsubota S, Tsuchiya H, Shinokawa Y, Tomita K, Minato H (1999) Transplantation of osteoblast-like cells to the distracted callus in rabbits. J Bone Joint Surg Br 81: 125–9.

Ueda H, Hong L, Yamamoto M, Shigeno K, Inoue M et al. (2002) Use of collagen sponge incorporating transforming growth factor-beta1 to promote bone repair in skull defects in rabbits. Biomaterials 23: 1003–10.

Uludag H, D'Augusta D, Golden J, Li J, Timony G, Riedel R, Wozney JM (2000) Implantation of recombinant human bone morphogenetic proteins with biomaterial carriers: A correlation between protein pharmacokinetics and osteoinduction in a rat ectopic model. J Biomed Mater Res 50: 227–38.

Uludag H, Gao T, Porter TJ, Friess W, Wozney JM (2001) Delivery systems for BMPs: factors contributing to protein retention at an application site. J Bone Joint Surg Am 83-A: 128–35.

Urist MR (1965) Bone: formation by autoinduction. Science 150: 893–9.

Vaccaro AR, Anderson DG, Patel T et al. (2005) Comparison of OP-1 Putty (rhBMP-7) to iliac crest autograft for posterolateral lumbar arthrodesis: a minimum 2-year follow-up pilot study. Spine 30: 2709–16.

Vaccaro AR, Whang PG, Patel T, Phillips FM, Anderson DG, Albert TJ, Hilibrand AS, Brower RS, Kurd MF, Appannagari A, Patel M, Fischgrund JS (2008) The safety and efficacy of OP-1 (rhBMP-7) as a replacement for iliac crest autograft for posterolateral lumbar arthrodesis: minimum 4-year follow-up of a pilot study. Spine J 8: 457–65.

Välimäki VV, Aro HT (2006) Molecular basis for action of bioactive glasses as bone graft substitute. Scand J Surg 95:95–102.

van den Bergh JP, ten Bruggenkate CM, Groeneveld HH, Burger EH, Tuinzing DB (2000) Recombinant human bone morphogenetic protein-7 in maxillary sinus floor elevation surgery in 3 patients compared to autogenous bone grafts. A clinical pilot study. J Clin Periodontol 27: 627–36.

Vila A, Sanchez A, Tobio M, Calvo P, Alonso MJ (2002) Design of biodegradable particles for protein delivery. J Control Release 78: 15–24.

Vinogradov SV, Bronich TK, Kabanov AV (2002) Nanosized cationic hydrogels for drug delivery: preparation, properties and interactions with cells. Adv Drug Deliv Rev 54: 135–47.

Vonau RL, Bostrom MP, Aspenberg P, Sams AE (2001) Combination of growth factors inhibits bone ingrowth in the bone harvest chamber. Clin Orthop Relat Res 386: 243–51.

Vukicevic S, Stavljenic A, Pecina M (1995) Discovery and clinical applications of bone morphogenetic proteins. Eur J Clin Chem Clin Biochem 33: 661–71.

Walker HW, Grant SB (1998) Influence of surface charge and particle size on the stabilization of colloidal particles by model polyelectrolytes. Colloids surf, A Physicochem eng asp 135(1-3): 123–33.
Walsh WR, Hamdy RC, Ehrlich MG (1994) Biomechanical and physical properties of lengthened bone in a canine model. Clin Orthop Relat Res 306: 230–8.
Wang EA, Rosen V, D'Alessandro JS, Bauduy M, Cordes P, Harada T, et al. (1990) Recombinant human bone morphogenetic protein induces bone formation. Proc Natl Acad Sci U S A 87: 2220–4.
Wang HP, Liang YJ, Long DX, Chen JX, Hou WY, Wu YJ (2009) Metabolic profiles of serum from rats after subchronic exposure to chlorpyrifos and carbaryl. Chem Res Toxicol 22: 1026–33.
Wang L. Khor E. Wee A. Lim LY (2002) Chitosan-alginate PEC membrane as a wound dressing. Assessment of incisional wound healing. J Biomed Mater Res 63: 610–8.
Wei G, Jin Q, Giannobile WV, Ma PX (2007) The enhancement of osteogenesis by nano-fibrous scaffolds incorporating rhBMP-7 nanospheres. Biomaterials 28: 2087–96.
Weinstein SL (2000) 2000-2010: the bone and joint decade. J Bone Joint Srg Am 82: 1–3.
Welch RD, Birch JG, Makarov MR, Samchukov ML (1998) Histomorphometry of distraction osteogenesis in a caprine tibial lengthening model. J Bone Miner Res 13: 1–9.
Westerhuis RJ, van Bezooijen RL et al. (2005) Use of bone morphogenetic proteins in traumatology. Injury 36:1405–12.
Whang K, Tsai DC, Nam EK, Aitken M, Sprague S, Patel P, Healy KE (2000) Ectopic bone formation via rhBMP-2 delivery from porous bioabsorbable polymer scaffolds. J Biomed Mater Res 42:491–9.
Wildemann B, Kandziora F, Krummrey G, Palasdies N, Haas NP, Raschke M, Schmidmaier G (2004) Local and controlled release of growth factors (combination of IGF-I and TGF-beta I, and BMP-2 alone) from a polylactide coating of titanium implants does not lead to ectopic bone formation in sheep muscle. J Control Release 5: 249–56.
Windhager R, Tsuboyama T, Siegl H, Groszschmidt K, Seidl G, Schneider B, Plenk H Jr (1995) Effect of bone cylinder length on distraction osteogenesis in the rabbit tibia. J Orthop Res 13: 620–8.
Winn SR, Uludag H, Hollinger JO (1999) Carrier systems for bone morphogenetic proteins. Clin Orthop Relat Res 367: 95–106.
Womersley C, Uster PS, Rudolph AS, Crowe JH (1986) Inhibition of dehydration-induced fusion between liposomal membranes by carbohydrates as measured by fluorescence energy transfer. Cryobiology 23: 245–55.
Woo BH, Jiang G, Jo Y, DeLuca P (2001) Preparation and characterization of a composite PLGA and poly(acryloyl hydroxyethyl starch) microsphere system for protein delivery. Pharm Res 18: 1600–6.
Wozney JM (1992) Bone morphogenetic protein family and osteogenesis. Mol Reprd Dv 32: 160–7.

Wozney JM, Rosen V, Celeste AJ, Mitsock LM, Whitters MJ, et al. (1988) Novel regulators of bone formation: molecular clones and activities. Science 16: 1528–34.

Wysocki RW, Cohen MS (2007) Ectopic ossification of the triceps muscle after application of bone morphogenetic protein-7 to the distal humerus for recalcitrant nonunion: a case report. J Hand Surg Am 32: 647–50.

Xiao YT, Xiang LX, Shao JZ (2007) Bone morphogenetic protein. Biochem Biophys Res Commun 362: 550–3.

Yamamoto M, Tabata Y, Ikada Y (1998) Ectopic bone formation induced by biodegradable hydrogels incorporating bone morphogenetic protein. J Biomater Sci Polym Ed 9: 439–58.

Yamamoto M, Takahashi Y, Tabata Y (2003) Controlled release by biodegradable hydrogels enhances the ectopic bone formation of bone morphogenetic protein. Biomaterials 24: 4375–88.

Yamamoto M, Takahashi Y, Tabata Y (2006) Enhanced bone regeneration at a segmental bone defect by controlled release of bone morphogenetic protein-2 from a biodegradable hydrogel. Tissue Eng 12:1305–11.

Yamauchi K, Takahashi T (2006) Maxillary distraction osteogenesis combined with mandibular osteotomy to correct asymmetry of the maxillomandibular complex. Plast Reconstr Sur 118: 39e–45e.

Yang K, Wu C, Lin F, Qi Z, Kuo T, Cheng Y, et al. (2008) Chitosan/gelatin hydrogel as immunoisolative matrix for injectable bioartificial pancreas. Xenotransplt 15: 407–16.

Yap HP, Quinn JF, NG SM, Cho J, Caruso F (2005) Colloid surface engineering via deposition of multilayered thin films from polyelectrolyte blend solutions. Langmuir 21: 4328–33.

Yasui N, Kojimoto H, Sasaki K, Kitada A, Shimizu H, Shimomura Y (1993) Factors affecting callus distraction in limb lengthening. Clin Orthop Relat Res 293: 55–60.

Yasui N, Sato M, Ochi T, Kimura T, Kawahata H, Kitamura Y, Nomura S (1997) Three modes of ossification during distraction osteogenesis in the rat. J Bone Joint Surg Br 79: 824–30.

Yazawa M, Kishi K, Nakajima H, Nakajima T (2003) Expression of bone morphogenetic proteins during mandibular distraction osteogenesis in rabbits. J O Maxf Surg 61: 587–92.

Yeung HY, Lee SKM, Fung KP, Leung KS (2001) Expression of basic fibroblast growth factor during distraction osteogenesis. Clin Orthop Relat Res 385: 219–29.

Yoshida K, Bessho K, Fujimura K, Kusumoto K, Ogawa Y, Tani Y, Iizuka T (1998) Osteoinduction capability of recombinant human bone morphogenetic protein-2 in intramuscular and subcutaneous sites: an experimental study. J Cranmaxf Surg 26: 112–5.

Young S, Wong M, Tabata Y, Mikos AG (2005) Gelatin as a delivery vehicle for the controlled release of bioactive molecules. J Control Rel 109: 256–74.

Yu JC, Fearon J, Havlik RJ, Buchman SR, Polley JW (2004) Distraction Osteogenesis of the Craniofacial Skeleton. Plast Reconstr Surg 4: 1E–20E.

Zakhary K, Motakis D, Hamdy RC, Campisi P, Amar Y, Lessard ML (2005) Effect of recombinant human bone morphogenetic protein 7 on bone density during distraction osteogenesis of the rabbit mandible. J Otolaryngol 34: 407–14.

Zellin G, Linde A (1997) Importance of delivery systems for growth-stimulatory factors in combination with osteopromotive membranes. An experimental study using rhBMP-2 in rat mandibular defects. J Biomed Mater Res 35: 181–90.

Zelzer E, Olsen BR. (2003) The genetic basis for skeletal diseases. Nature 423: 343–8.

Zeng Q, Li X, Beck G, Balian G, Shen FH (2007) Growth and differentiation factor-5 (GDF-5) stimulates osteogenic differentiation and increases vascular endothelial growth factor (VEGF) levels in fat-derived stromal cells in vitro. Bone 40: 374–81.

Zhang Z, Feng SS (2006) The drug encapsulation efficiency, in vitro drug release, cellular uptake and cytotoxicity of paclitaxel-loaded poly(lactide)-tocopheryl polyethylene glycol succinate nanoparticles. Biomaterials 27: 4025–33.

Zimmermann CE, Harris G, Thurmuller P, et al. (2004) Assessment of bone formation in a porcine mandibular distraction wound by computed tomography. Int J Oral Maxillofac Surg 33: 569–74.

# APPENDIX A
## Conventions in Nanoparticle Characterization and Evaluation

### A.1. Average Size Measurement (DLS)

The measurement of particle sizes and size distribution is considered fundamental to the characterization and optimization of drug delivery systems. Nanoparticle formation and particle size will depend on the concentration of the surfactants and stabilizers used. They determine the in vivo distribution, biological fate, toxicity and the targeting ability of nanoparticle systems. Also, they can influence the drug loading, drug release and stability of nanoparticles. For example, smaller particles have a larger surface area and so most of the drug would be at or near the particle surface resulting in drug release faster than from larger particles which often have large cores allowing for more drug encapsulation that slowly diffuses out. Smaller particles have a greater risk of aggregation during storage.

Currently, the most common method used for measurement of particles is dynamic light scattering (DLS). Analysis by DLS, alternatively known as photon correlation spectroscopy (PCS) or quasi-elastic light scattering (QELS) is based on the principle of Brownian motion. In solution, all particles demonstrate random motion as a result of collisions with solvent molecules. A laser light is directed at the sample and scattered by the particles to a photon detector. As the particles move, the intensity of the scattered light fluctuates due to alternating constructive and destructive interference in the scattered light. The Stokes-Einstein equation defines an inversely-proportional relationship between the random motion of a particle and its size and so smaller particles move faster than larger ones. Such fluctuations in the intensity of the scattered light are used to calculate size of particles. In turn, the measurement occurs over a period of time during which a correlation function is generated, which plots the relative change in signal intensity over time. It is from the correlation function that particle size and particle size distributions are then calculated.

One disadvantage of DLS is that larger particles are often over-represented in size distributions of disperse populations, owing to their ability to scatter more light than smaller particles. For relatively monodisperse systems, this is therefore not an issue. A further

consideration in the interpretation of DLS measurements is that the method measures the average hydrodynamic diameter of the particle which includes the associated solvent layer and for this reason an experimental error of ± 4% is usually considered with DLS measurements. Most particle size instruments also generate values for the polydispersity index (PI). PI is a measure of the distribution of particle sizes within the population. This value ranges from 0 to 1, with values above 0.7 indicative of a population with a wide range of sizes and lower values being indicative of monodisperse samples; this value should not generally fall below 0.05.

## A.2. Surface Charge Measurement (Zeta Potential)

Nearly all particles reveal a surface charge when in solution, through ionization of surface groups or adsorption of ions. The charge that develops at the surface of the particles is called the zeta potential. The surface hydrophobicity of nanoparticles would determine the amount of adsorbed blood components, mainly proteins (opsonins) once introduced into the blood stream. This in turn influences the in vivo fate of nanoparticles. Hence, to increase the likelihood nanoparticle success, it is necessary to minimize the opsonization (binding of opsonins onto the surface of nanoparticles and acting as a bridge between nanoparticles and phagocytes) and to prolong the circulation of nanoparticles in vivo. This can be achieved via coating the surface with hydrophilic polymers/surfactants. Zeta (ζ) potential is determined by measuring the movement of particles subjected to an electric field where charged particles move through the solution and this movement is then detected as a Doppler shift in the frequency of laser light scattered by the particles. The direction of motion provides the nature of their charge (cationic or anionic), while the velocity allows the value of their charge to be calculated. It is important to realize that changes in solution conditions, including pH, ionic strength and the presence of additional molecules or reagents can affect the surface charge of the particles and alter the measured ζ potential value. Furthermore, ζ potential is an important index for the stability of nanoparticulate suspensions where values above +/-30 mV are generally considered to be an indication of enhanced uniformity via the presence of strong repulsion forces among particles preventing aggregation, as reported in Section III.

## A.3. MTT Assay

For evaluating in vitro cytotoxicity, quantifying cellular responses to biomaterials is one aspect of biocompatibility and a more appropriate term 'cytocompatibility' was introduced (Richards et al. 2001). The most commonly- used method for evaluating cytocompatibility of materials is a colorimetric assay referred to as MTT. It provides a relative measurement of the viability of treated versus untreated cells. Following exposure to the conditions or materials being assessed, MTT or 3-(4,5-Dimethylthiazol-2-yl)-2,5-diphenyltetrazolium bromide), a yellow solution is added to cells. The cells are incubated in this solution for ~ 4 hours during which mitochondrial enzymes reduce the chemical to insoluble purple formazan crystals. Since cell viability is directly related to the activity of mitochondria, this assay requiring the action of mitochondrial reductase enzymes to function, offers a direct measurement of viable cells. Following the initial incubation, cells are lysed and the formazan crystals are solubilized prior to spectrophotometry at 570 nm wavelength. Viability is generally reported relative to untreated control cells. Different materials will present varying degrees of cytocompatibility and safety, in vitro.

## A.4. Human BMP-7/OP-1 Specific ELISA Construction KIT

Enzyme-linked Immunosorbent Assay (ELISA) is a biochemical technique used mainly for the detection of the presence of certain antibodies or antigens in a given sample. It has been commonly used as a diagnostic tool in medicine as well as for quality control monitoring in various industries. A human BMP-7/OP-1 specific ELISA construction kit was used in this thesis (Chapter 6). The kit provides antigen affinity purified polycolonial capture (coating) and tracer (biotin-labeled) antibodies in addition to the required antigen standard necessary for the development of a 96-well microplate assay. It allows for the quantitative determination of human BMP-7/OP-1 concentrations in supernatants of solutions, in vitro. The assay employs the quantitative sandwich enzyme immunoassay technique. A monoclonal antibody specific for BMP-7/OP-1 is pre-coated by the manufacturer onto the microplate. Standards and samples of the formulated nanoparticles are pipette into the wells where any BMP-7/OP-1 present in the assay is then bound by the immobilized antibody.

After washing away any unbound substances, an enzyme-linked monoclonal antibody specific for BMP-7/OP-1 is added to the wells. Following a wash step to remove any unbound antibody-enzyme reagent, a substrate solution is added to the wells and color develops in proportion to the amount of BMP-7/OP-1 bound in the initial step. The color development stops and its intensity is then measured. A microplate reader capable of measuring absorbance at 450 nm with the correction wavelength set at 540 nm is used. This technique requires around 5 hours to be completed and is highly sensitive where and any variation in standard diluents, pipetting, washing, incubation time, storage temperature, exposure to light during bench-top incubation or cross-contamination might cause variations in binding. Hence, the possibility of interference by soluble receptors, binding proteins and any other variables present in biological systems cannot be excluded when analyzing the reported findings.

### A.5. Higuchi Model: a mathematical method for the quantitative deviation from the *ideal* H

The drug loading and entrapment efficiency of nanoparticulate delivery systems very much depend on the solubility of the encapsulant which in turn is related to several factors of which molecular weight and the strength of the ionic interaction between the drug and the biomaterials are involved. Ideally, controlled drug delivery systems should deliver the drug at a controlled rate over a desired duration. The rate of drug release generally depends on also the solubility of the drug; desorption of the surface bound/adsorbed drug; drug diffusion through the core and shell of the nanoparticles; nanoparticle erosion/degradation (usually occurring at later stages) and a combination of erosion/diffusion process. Release rate is affected by the ionic interaction between the drug and the addition of auxiliary ingredients as well as the release media and its pH. A typical tri-phasic release curve often seen with microparticles is displayed below in Figure A.1. Diffusion includes the rapid ‘initial burst’ release phase followed by the slow ‘lag’ release phase as was described earlier in Chapter 7. The rapid release occurs within 24 hours and can range from 10 to 80% of the total drug content. Microspheres tend to have a very slow (close to zero and can last from days to weeks) release period following the initial burst phase. The initial burst phase is believed to be the result of rapid release of drug from the particle surface and so once depleted, the lag

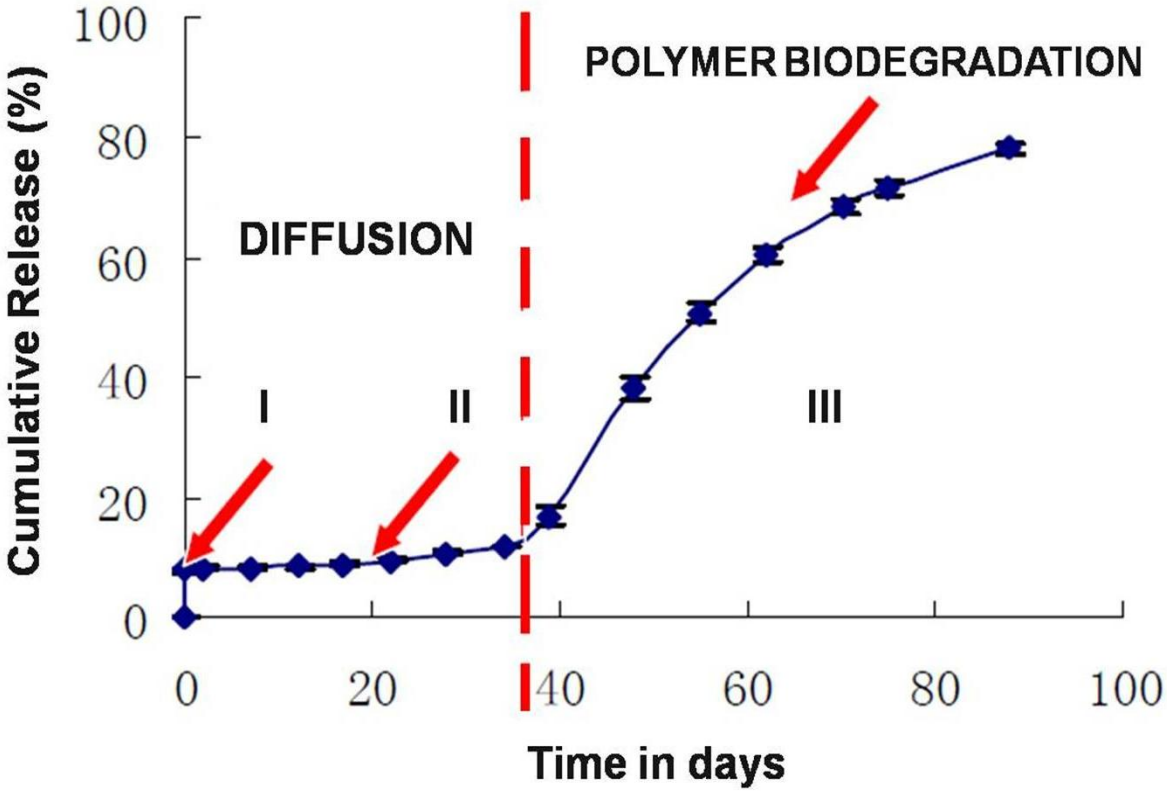


**FIG A.1.** A simulated in vitro tri-phasic release profile displaying phases **I**: rapid 'initial burst' release; **II**: slow 'lag' release and **III**: release by biodegradation. Using mathematical models, elucidating these release kinetics and the underlying mechanism(s) can be represented by several release data with one or two physically meaningful parameters employed for comparative purposes. For example, in our in vitro works, the parameters Slope *K*, axis intercept *a*, squared coefficient of correlation $r^2$ were obtained and plotted to describe the release kinetics of delivery systems and gain a better (comparative) understanding of the (BSA, OP-1 and paclitaxel) release mechanisms from their carriers whether being nanocapsules or microspheres ; where different loading strategies were used. Negative axis intercepts are attributed to a lag effect particularly occurring when hydrophobic drugs are released into an aqueous medium (Sydow-Plum G, Haidar ZS, Merhi Y and Tabrizian M; published in Materials 2008, 1, 25 - 43).

period starts and lasts until extensive degradation of the polymer occurs. Generally, large particles with a large surface area will show a high initial burst. However, drug release remains a complicated process, involving physical and chemical interactions of polymer and drug substances. Efforts to modify the morphology, polymer properties and drug distribution continue in to achieve the desired release profiles; specific for potential clinical indication(s).

The use of mathematical models has been reported to be often helpful in elucidating release kinetics and mechanisms as well as the influence of formulation factors which in turn can be of benefit in controlling and optimizing drug release. Also they can represent several release data with one or two physically meaningful parameters employed for comparative purposes with perhaps important properties such as bioavailability. To the best of knowledge, a kinetic representation of protein release from hybrid nanoparticles or a specific model has not been reported. The percentage of drug released versus time data for controlled-release preparations found in the literature often show a linear apparent first-order rate (depending on the concentration of only one reactant; i.e. a uni-molecular reaction). Other reactants can be present but each will have a zero-order reaction. In 1961, Higuchi tried to relate the drug release rate to the physical constants based on the simple laws of diffusion (Higuchi 1961). And so, he published the probably most renowned and most frequently used mathematical equation to describe the diffusion-controlled release rate of drugs from delivery systems as the square root of a time-dependant process based on Fickian diffusion ($F=kt^{1/2}$; where $F$ is the fraction of drug released at any time $t$ and $k$ is the release rate constant), as described previously in Chapters 6. In that work, a BSA release profile was obtained from the multi-layered nanocapsules and similarly in Chapter 7 for the release of rhOP-1. The data was compared to the ideal (H) model by means of applying the curve-fitting technique which is based on calculation of the area under the curve (AUC) method using the trapezoidal rule. This simplified mathematical approach was developed by Gohel et al. almost 40 years after Higuchi first derived his equation (Gohel et al. 2000). It was aimed to express or in better words “predict” the deviation in zero-order release profiles of a diffused drug from spherical particles (and from the H ideal which considers complete or 100% drug release on the last assayed day, in vitro). And therefore, the precision of this prediction would directly depend on the number of data points. As a result, the analysis provided is a *rough* idea of the

underlying release mechanism (swelling, polymer dissolution and degradation, encapsulant diffusion, presence of drug on the surface of the nanoparticles and/or combinations of these). Furthermore, in the literature first studied (limited to release from tablets), an ideal Higuchi release profile was over a 12-hour period while in Chapters 6 and 7 the mathematics were applied over a prolonged period of time (although it was accounted for by generating an ideal release profile accordingly; $100/\sqrt{720}$ for 30 days and $100/\sqrt{1080}$ for 45 days). Finally, a very recent report was published comparing the accuracy of 13 release kinetic models via applying the release data of 32 drugs from 106 nanoparticle formulations collected from literature by the authors (Barzegar-Jalali et al. 2008). According to their criteria, Higuchi ranked as the $4^{th}$ most accurate model with an overall mean percent error much lower than zero-order, first-order, Hixson-Crowell, square root of mass and linear probability models. All other studied literature stating the linear or non-linear fitting of the in vitro release data performed using the Higuchi square root of time equation have simply mentioned that drug release from nanoparticles followed the Higuchi model (For example, see Ciproflaxacin release from four different nanoparticulate formulation; Jain and Banerjee 2008). Even so, the kinetics information and the generated release equations we reported in Section III should be viewed with caution and treated merely as a theoretical model applicable for drug release via a diffusion and/or diffusion/degradation mechanism(s).

## A.6. Microscopic Imaging: AFM and TEM

In this thesis, 2 main microscopy techniques were employed, atomic force microscopy (AFM) and transmission electron microscopy (TEM). Scanning electron microscopy was used as well however unsuccessfully due to the common associated limitations such as vacuum compatibility, artifacts introduction during sample preparation (dehydration/sputter-coating with Au as conductive material).

**AFM** is a high-resolution type of scanning probe microscopy with demonstrated resolution of fractions of a nanometer, more than a 1000 times better than the optical diffraction limit. Information is gathered by 'feeling' the surface via a mechanical probe (composed typically

of silicone or silicon nitride) that utilizes piezoelectric elements to facilitate its tiny, accurate and precise movements resulting in very precise scans (topographical surface information) of biological samples. The AFM can be operated in a number of modes and conditions. Generally, samples can be scanned either in dry or wet conditions and imaging modes can be either static (contact mode) or dynamic (non-contact mode). In the contact mode, the force between the tip of the probe and the surface is kept constant during scanning by maintaining a constant deflection. On the other hand, the cantilever is externally oscillated at or close to its resonance frequency in the dynamic mode. A dynamic contact (tapping) mode is also feasible when a liquid meniscus layer develops causing the tip to stick to the surface. Thus, the separation distance between the cantilever tip and the sample surface is modulated to prevent damaging soft samples especially when imaged in air. In our work, liposomes were dried in a fume hood and scanned in ambient air under the tapping mode while for the coated nanoparticles, a liquid cell was necessary and scanning was done under the contact mode (to accommodate for the different surface topography and roughness from uncoated liposomes). While AFM provides a true 3-D surface profile, it can only image a maximum height and scanning area on the order of few mm. An incorrect choice of probe or tip and mode can lead to scraping by lateral (shear) forces and image artifacts. The length of scan time required can also lead to a thermal drift or damage to the image.

The **TEM** projects a beam of high voltage electrons (emitted from an electron gun fitted with a tungsten filament cathode) through a very thin slice of a sample to produce a 2-D image in a phosphorescent screen. Hence, the brightness of a particular area of the image is proportional to the number of electrons that are transmitted through the sample or specimen. In preparing specimens, every step of the procedure affects the quality of the final electron micrographs. For our samples, ultra-rapid freezing or plunge-freezing (in ethane then stored in liquid nitrogen) was done to prevent the development of ice crystals. Freeze-fracture/etching followed using a diamond ultra-microtome knife to produce thin slices of the samples, semitransparent to electrons. The etched surface was then shadowed with evaporated platinum at a preset angle of $45^{o}$ while under high vacuum evaporation. A second coat of carbon was applied before being able to obtain the extremely-fragile replica of the fractured surface, carefully placing it on a special copper grid prior to viewing, under

vacuum. Apparently, extensive and time-consuming specimen preparation is involved. Also, the microscope itself requires a well- experienced operator. Hence, our attempts to image several formulations of the nanoparticles failed, perhaps due to conformational changes mainly because of water arranging into a crystalline lettuce of lower density upon freezing. Finally, using a cryo-TEM that allows for studying the samples at cryogenic temperatures with no staining, fixation or etching helped us to obtain the images displayed in Chapters 8 and 9. It is worth mentioning that although this method requires less sample preparation, the measured particle size is still affected. In contrast to TEM measurements, DLS provides a significantly larger size of particles due to the different nature in the working function of the two instruments. DLS measures the hydrodynamic particle diameter in the dispersion medium, as mentioned earlier in A.1. TEM images, on the other hand, show the core particle size without the contribution from the dispersion medium as it evaporates prior to imaging. Hence, the difference in diameter measurements obtained by DLS and those obtained by TEM equals approximately the size of the surrounding layer. Furthermore, the nature of imaging techniques in general makes it difficult to ascertain the particle distribution of a given population.

## A.7. In vivo Models in Bone Tissue Engineering

Numerous animal studies have validated the safety and efficacy of BMP-2 and BMP-7 especially in promoting orthopedic repair. However, the results from human trials were not as impressive. This variability and slower response in humans may be attributed to a smaller population of multipotent cells, which are also less responsive than those in smaller animals (cell size is not directly linked to the size of species). It has been proposed that therapeutic outcomes may be enhanced by carriers capable of (i) delivering BMPs at a rate that matches the responsiveness of the cells or (ii) delivering a suitable cocktail of growth factors to stimulate the cells. Variations in release kinetics are commonly observed due to inherent differences in the affinity of the materials for BMPs and in the carrier/delivery system characteristics and properties. Furthermore, adjustment of BMP release kinetics in order to attain the optimal profile is difficult and has not been accomplished yet as it would vary with animal species, age of host, anatomic site size and vascularity, defect history and other

presence of other complicating factors such as infection, contamination. For example, slower release rates may be required in more fluid environments where BMP clearance may be faster, and in more compromised sites where the healing response is diminished. In DO, many variables are in play and will definitely contribute to discrepancy in generated results. It uses mechanical force to induce and direct bone formation as well as soft-tissue expansion. Yet, unlike the expansion of soft tissues by tissue expanders, the osseous tissue produced does not contract over time after the removal of the distractor device. This is mainly because bone responds to the mechanical demands placed on it although being rigid. It has been reported that bone is the only living tissue that can effectively withstand both tensile and compressive loads (12,000 psi to 15,000 psi). So, these forces and loads will definitely affect the response of bone and the regenerate formation in DO (Yu et al. 2004). Technically, performing a clean osteotomy, mounting the distractor properly, applying the proper distraction rate and rhythm, the type of bone involved (long vs. flat) all play roles in the outcome. Likewise, animal species, age, gender and handling post-operatively would also influence the results of in vivo studies. In a recent review (Pearce et al. 2007) discussing some of the more commonly available and frequently used animal models in medical research such as the dog, sheep and rabbit models, the authors concluded that while non-human primates are often considered the most appropriate model for human bone, there are clear ethical implications for their use as well as cost, disease risk and handling difficulties. Of the species mentioned, the dog was described as perhaps having the most similar bone structure to humans; however, ethical implications of using companion animals subdue also. Species such as sheep and pig are not as ethically emotive however might pose housing, handling and availability issues which are not as critical with rabbits. Yet, rabbits were found to be the least similar in bone structure and properties to humans and while no species fulfills the requirements of an ideal animal model, rabbits remain the most commonly used animals for bone research; ~35% of musculoskeletal research studies. Finally, for testing the biocompatibility and safety of BMP bone-engineering products, rat and mice models were found to be the most commonly used although not much is known about species differences with rabbits and humans (Section IV) and hence will have implications for the translation of data from pre-clinical studies in animals to clinically-effective applications in human cases.

# APPENDIX B
# Supplementary in vitro Experiments

Below, is a presentation of some of the characterization and optimization experiments carried out prior and during the development of the formulated nanoparticles presented in this dissertation. These data were not included in the published manuscripts of Section III. Further development of the nanoparticulate delivery system might want to take a few of these aspects into consideration.

## B.1. Sucrose as a cryoprotectant for freeze-drying (lyophilization)

Incorporating sucrose, aliquots of particulate suspensions were lyophilized (freeze-dried) at -54$^{o}$C for 48 hours resulting in a powder that was then rehydrated with either ultra-pure water (UPW) or different concentrations of bovine serum albumin (BSA) and osteogenic protein-1 (OP-1) to achieve encapsulation and loading within the core and shell of the nanoparticulate formulations, as presented in Chapters 6 and 7. Sucrose has been commonly used as a cryoprotectant or a spacer between particles preventing their fusion and/or aggregation. Also, it has been shown to enhance particle stability as demonstrated in the reported results where no significant differences were found in average particle size or the zeta potential surface charge before and after lyophilization.

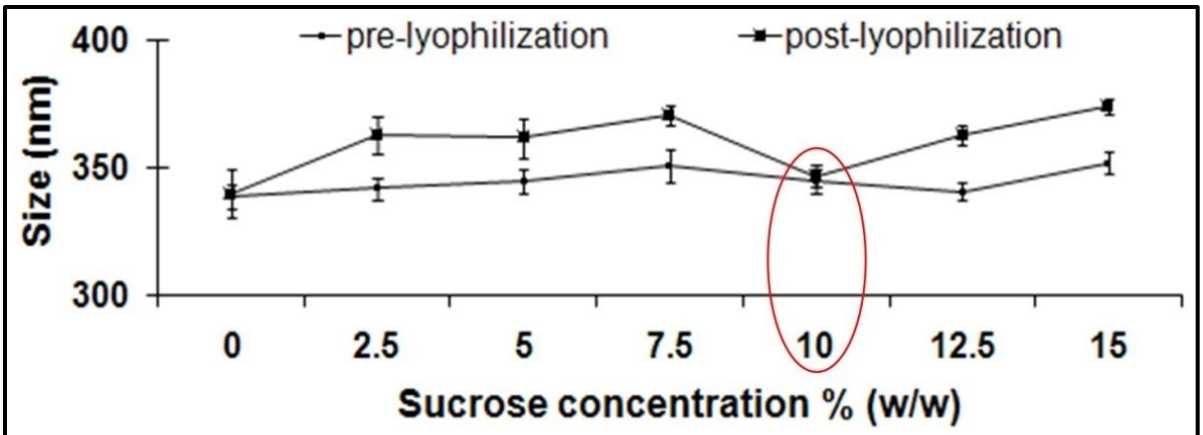


**FIG B.1.** Determining the optimum cryoprotectant (sucrose) concentration (w/w) incubated with 4% DDAB Nanoparticles. Effect on average particle size (in nm) was compared before and after freeze-drying (lyophilization).

Hence, determining the optimum sucrose concentration was necessary as is displayed in Figure B.1 (values as mean ± standard error of the mean). It was not included in the papers for space limitations. This set of experiments was repeated three times. Given no significant differences detected using 10% (w/w) sucrose, it was determined to be the optimum concentration and therefore was incorporated in all of the nanoparticle formulations.

## B.2. Effect of incubation time on NP size and surface charge

To determine the optimum period of time required for the layer-by-layer self-assembly of the polymers and liposomes, an experiment was conducted following the deposition of each polymeric layer and over a time range from 1 to 24 hours. The aim was to be able to produce stable and monodisperse nanoparticles efficiently and in a time-effective manner. Hence, as displayed below in Figure B.2, 60 minutes were deemed sufficient as further or prolonged incubation did not yield any statistically significant differences.

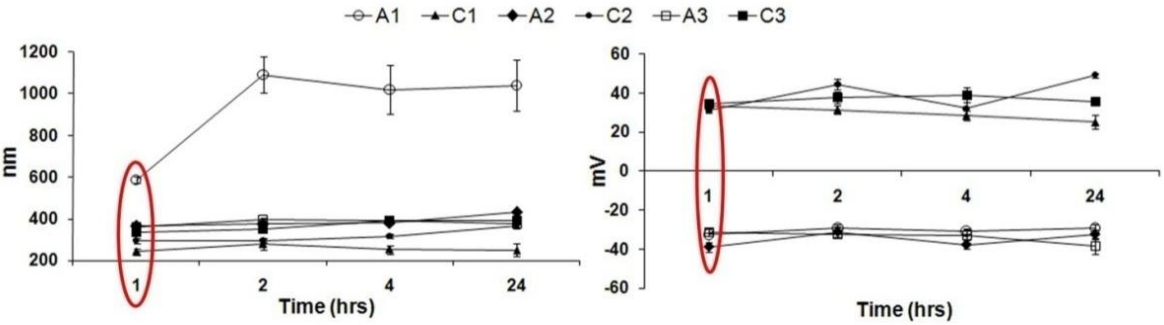


**FIG B.2.** Determining the effect of incubation time on particle average size (in nm) and ζ-potential surface charge (in mV); shown here with the deposition of each polymer layer (up to 3 bi-layers or C3) and over 24 hour cycles.

## B.3. Effect of polymer concentration on surface charge

We also wanted to determine the optimum concentration of the polymer used, alginate and chitosan. As displayed below in Figure B.3, alginate was prepared in concentrations ranging from 0.005 to 2.0 mg/ml. The evaluation of the effect on the average zeta potential surface charge followed. Based on these results and others, alginate and chitosan were prepared in 1 mg/ml concentration prior to coating the liposomes.

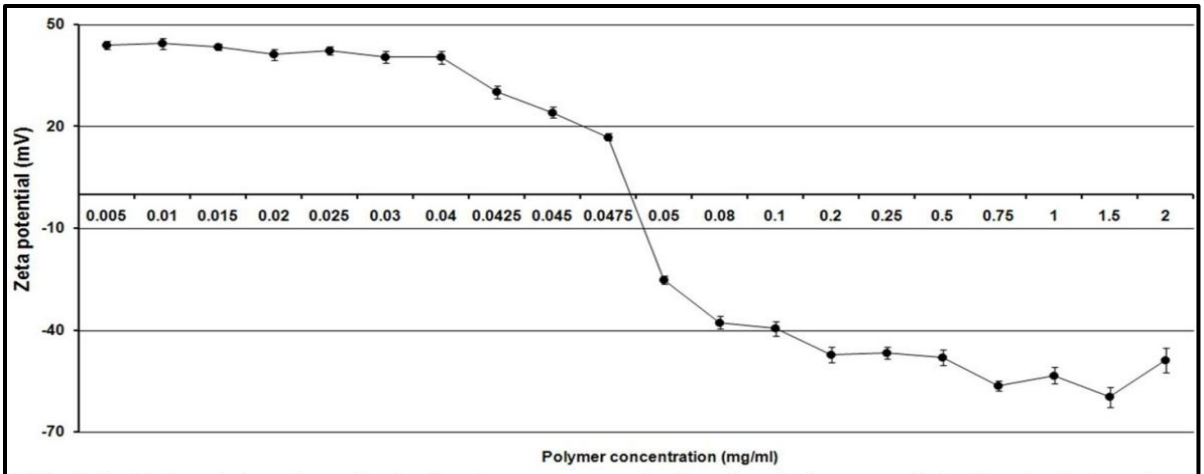


**FIG B.3.** Determining the effect of polymer concentration (mg/ml) on particle ζ-potential surface charge (in mV); shown here with the deposition of a single layer of alginate (1st layer) on liposomes.

## B.4. Effect of PBS on particle size and surface charge

All of the formulations reported in this thesis have been prepared in ultra-pure water (UPW). However, we did investigate formulating the nanoparticles in phosphate-buffered serum (PBS, pH 7.4), as is displayed below in Figure B.4. Overall, larger and un-stable particles resulted. Therefore, we continued all preparations in UPW. Further development should address the effect of pH, as proposed in Chapter 10.

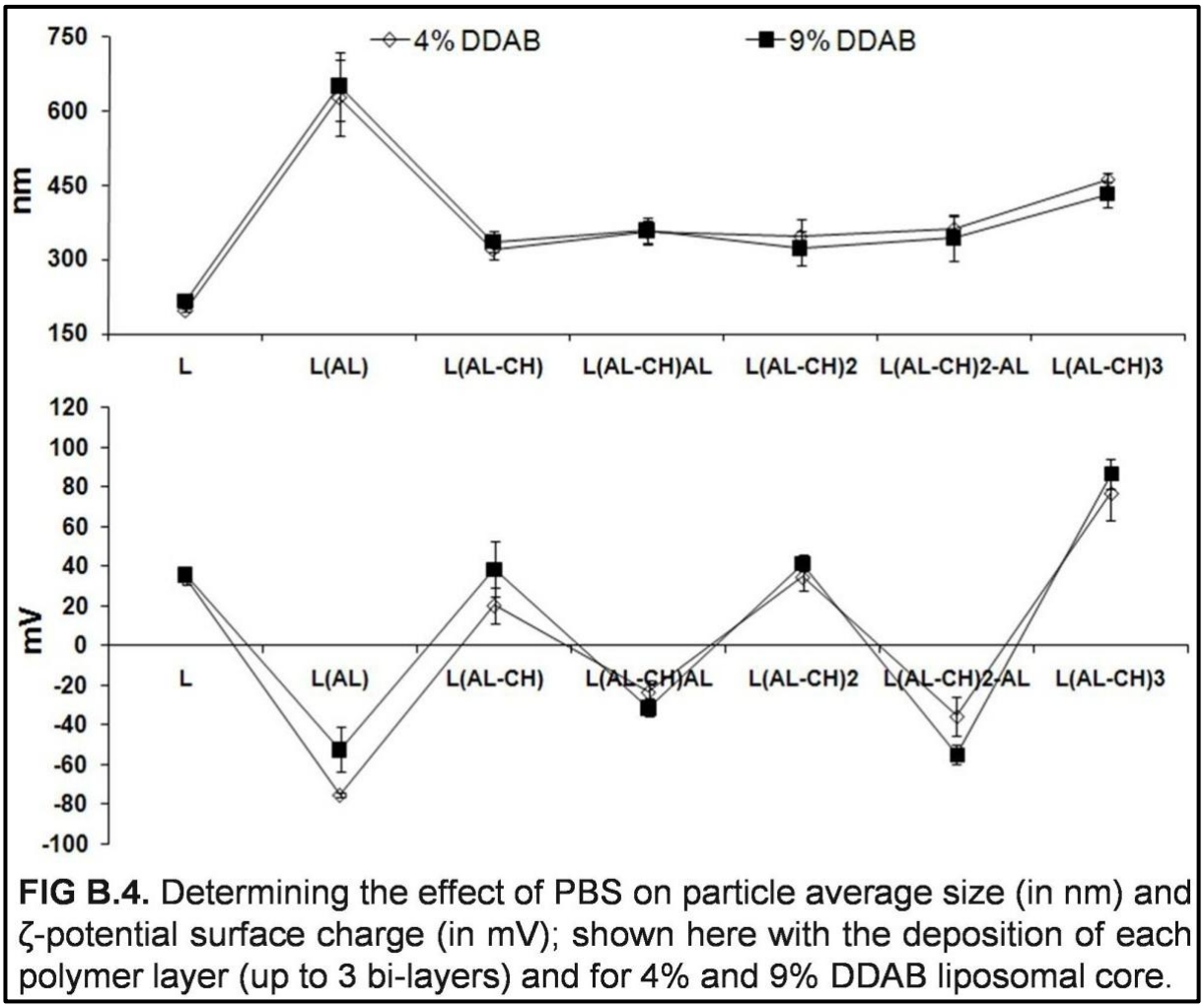


**FIG B.4.** Determining the effect of PBS on particle average size (in nm) and ζ-potential surface charge (in mV); shown here with the deposition of each polymer layer (up to 3 bi-layers) and for 4% and 9% DDAB liposomal core.

## B.5. Effect of centrifugation/washing and MW on size

In a pilot study, the effect of centrifugation/washing after the deposition of polymeric layers was evaluated. Figure B.5 displays the results for the first CH layer (comparing three molecular weights as well) deposited on AL-coated liposomes. Evidently, washing is necessary to remove excess polymer and provide the desirable average particle size. Further development of the system would consider continuing these experiments especially that the molecular weight of CH has been shown to influence the stability of DNA/CH or peptide/CH complexes, transfection efficiency as well as immune-responses. Also, it has been reported that coating thickness of nanoparticles is greatly dependent on both the molecular weight and concentration of CH; dependent on the chain length of CH.

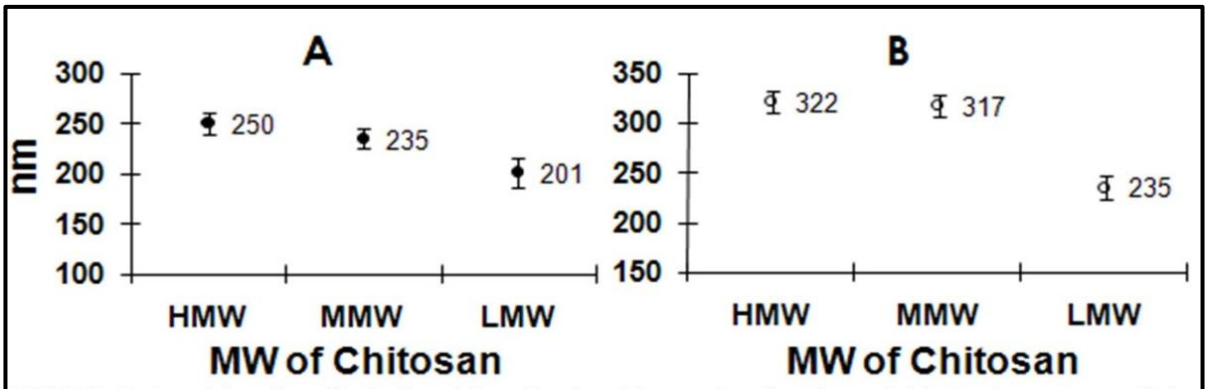


**FIG B.5.** Determining the effect of centrifugation/washing and molecular weight of polymer on particle average size (in nm); shown here with the deposition of the 1st chitosan layer (on alginate-coated liposomes). **A** is the centrifuged group of samples (supernatant) and **B** is the no centrifugation group yielding larger particles where excess and un-reacted polymer were not washed.

## B.6. Effect of extrusion on liposomal average size and PI

Finally, for the preparation of all of the large uni-lamellar vesicles (liposomes) reported throughout this thesis, a filtration step was done using a mini-extruder maintained at 60$^{o}$C. The multi-lameller vesicles resulting upon rehydration of the thin film following rotary evaporation were passed through double 200 nm 19 mm polycarbonate membranes. Solutions were loaded into 1mL glass syringes and pushed 21 times (e*21) back and forth yielding more homogenously distributed vesicles (in size) according to the PI (polydispersity

index). Out initial attempts were done with a single membrane and 15 extrusions (e*15). As shown below in Figure B.6 e*21 with the doubled filters resulted in almost superior liposomes (no significant differences detected, perhaps owing to sample size where only 5 preparations were evaluated). Further experiments might also want to investigate the effect on ζ- potential surface charge and stability.

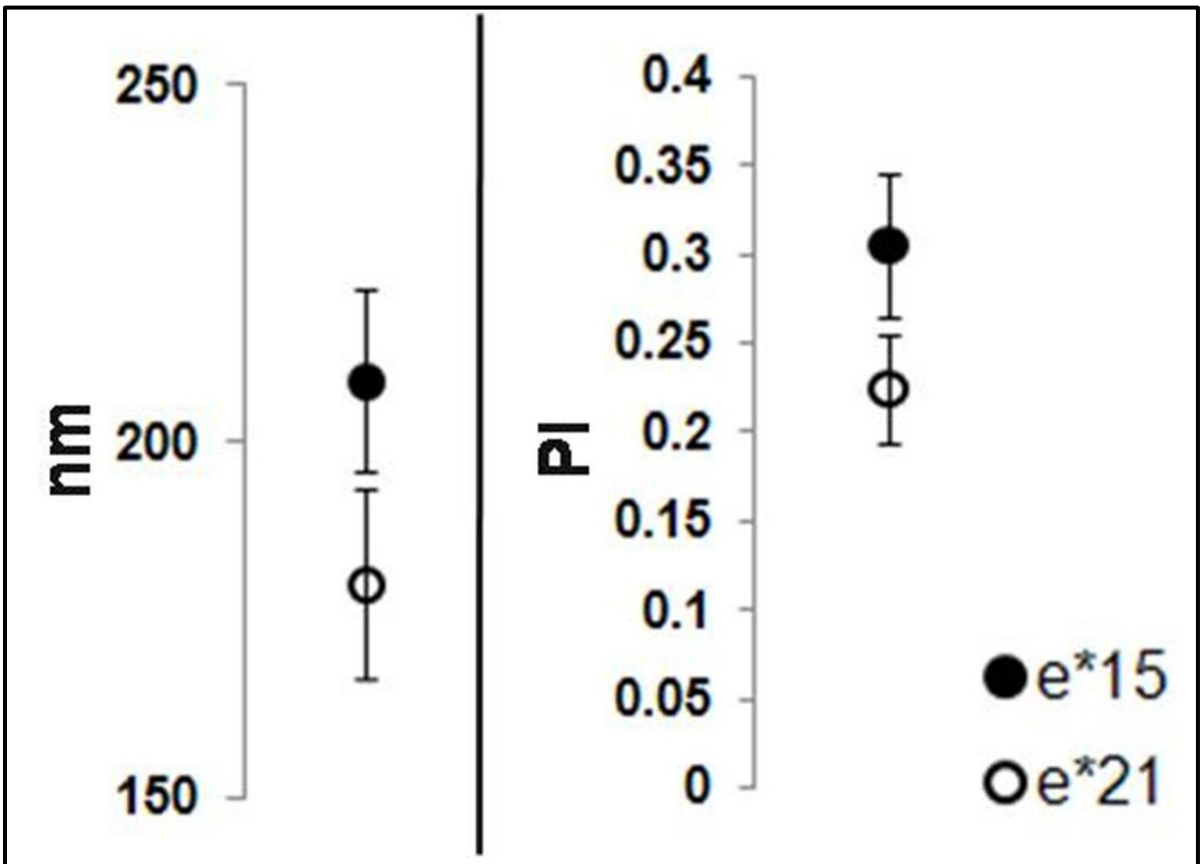


**FIG B.6.** Determining the effect of extrusion/filtration through double 200 nm 19 mm polycarbonate membranes on liposome average size (in nm) and dispersion homogeneity; comparing 15 and 21 extrusion (e) cycles. To prepare 9 ml of liposomes for example, filters were replaced 3 times. Expectedly, increasing the number of extrusion cycles will result in a less final volume.

Available online at www.sciencedirect.com
ScienceDirect
Biomaterials 29 (2008) 1207–1215
Biomaterials
www.elsevier.com/locate/biomaterials

# Protein release kinetics for core–shell hybrid nanoparticles based on the layer-by-layer assembly of alginate and chitosan on liposomes

Ziyad S. Haidar [a,b], Reggie C. Hamdy [b,d], Maryam Tabrizian [a,b,c,*]

[a] Faculty of Dentistry, McGill University, Montréal, Québec, Canada
[b] Center for Biorecognition and Biosensors, McGill University, Montréal, Québec, Canada
[c] Department of Biomedical Engineering, Faculty of Medicine, McGill University, Montréal, Québec, Canada
[d] Shriners Hospital for Children and Division of Orthopaedics, Montreal Children's Hospital, Montréal, Québec, Canada

Received 10 September 2007; accepted 6 November 2007
Available online 10 December 2007

**Abstract**

The present work is focused on the formulation of core–shell nanoparticles via the layer-by-layer (L-b-L) self-assembly technique for delivery of biomacromolecules such as bone growth factors. The drug encapsulation efficiency of liposomes is enhanced with the increased stability of polyelectrolyte systems achieved through the alternate adsorption of several layers of natural polymers: anionic alginate and cationic chitosan on cationic nanosized phospholipid vesicles. The resulting particles were characterized for their size, surface charge, morphology, encapsulation efficiency, loading capacity and release kinetics over an extended period of 30 days. The L-b-L deposition technique succeeded in building a spherical, monodisperse and stable hybrid nanoparticulate protein delivery system with a cumulative size of $383 \pm 11.5$ nm and zeta potential surface charge of $44.61 \pm 3.31$ mV for five bilayered liposomes. The system offers numerous compartments for encapsulation including the aqueous core and within the polyelectrolyte shell demonstrating good entrapment and sustained linear release of a model protein, bovine serum albumin, *in vitro*. Our results demonstrate that this delivery system features an extended shelf life and can be loaded immediately prior to administration, thus preventing any loss of the protein.


*Keywords:* Controlled drug release; Liposome; Polysaccharide; Self-assembly

## 1. Introduction

The recent advancements in the field of biotechnology have led to the development of abundant recombinant protein-based drugs such as vaccines, enzymes and hormones. Yet, since their isolation and purification, optimizing a delivery mechanism continues to be the primary obstacle for the clinical introduction of many protein-based drugs [1,2]. Predominantly due to their short biological half-life, lack of long-term stability, tissue-selectivity, potential toxicity and risk of carcinogenic activity [3]. Hence, repetitive highly dosed injections are often required to obtain the intended therapeutic efficiency, without causing any toxicity or other side effects. The optimal carrier would preserve the biological activity and viability of the protein, prevent its rapid clearance, and, preferably release it in a predictable or metered manner. Accordingly, the development of such new protein-based drugs coincides with the development of custom-made and release-controlled delivery systems [2–6].

Liposomes are the commonly investigated vehicles for delivery of therapeutic compounds, such as enzymes [7,8] because of their biocompatibility and appealing ability to carry hydrophobic and hydrophilic drugs. Nonetheless, stability *in vivo* remains a setback, due to their high tendency to degrade or aggregate and fuse leading to leakage of the entrapped drug during storage or after administration [9]. To overcome those problems, varying the size of the liposome [10,11] or modifying the liposomal surface via coating with a single layer of

* Corresponding author. Faculty of Dentistry, McGill University, 3775 University Street, Montréal, Québec, Canada H3A 2B4.
*E-mail address:* maryam.tabrizian@mcgill.ca (M. Tabrizian).

0142-9612/$ - see front matter © 2007 Elsevier Ltd. All rights reserved.
doi:10.1016/j.biomaterials.2007.11.012

hydrophilic polymers has been investigated [12]. Accordingly, the idea of polyelectrolyte coatings obtained by the alternate deposition of polyanions and polycations emerged as a novel way to functionalize surfaces [13,14]. This was quickly applied to the drug delivery field where the layer-by-layer (L-b-L) technique extended from the build-up of multi-layered polyelectrolytic films on macroscopic flat substrates [15] to the construction of core–shell particles on various spherical templates and colloidal particles [16–18]. However, particle flocculation or aggregation was difficult to overcome and thus far, the adsorption of only a single layer of biopolymer, such as polyvinyl alcohol (PVA) [10] or chitosan [19] on a charged liposomal surface has been reported. In previous work, we have been successful with the L-b-L assembly of polyelectrolytes on 2- and 3-dimensional artificial and biological systems. In addition to being non-toxic, biocompatible, biodegradable and hydrophilic, we have shown that biomolecules could assembled and entrapped within polyelectrolyte layers, hence maintaining their bioactivity [13,20]. We also designed alginate–chitosan nanosized polyionic complexes for gene therapy [21]. Besides the known advantages including the size property, longer shelf life and ability to entrap more drugs [22], nanosized systems reside longer in circulation, and therefore greatly extend the macromolecular biological activity when compared to microparticles [23].

Combining the advantages of liposomes with those of L-b-L assembly systems, we report in this work a novel core–shell release-controlled delivery system. The core is composed of charged large unilamellar liposomes (LUVs) and the shell is constructed through the L-b-L self-assembly of alternating layers of sodium alginate and chitosan. The system was characterized and loaded with a model protein, bovine serum albumin (BSA) to evaluate its encapsulation efficiency, loading capacity and release profile over an extended period. The BSA release kinetics was finally analyzed with the renowned Higuchi model [24].

## 2. Materials and methods

### 2.1. Formulation of liposomes

LUVs were formulated via the thin-film hydration technique [25]. A lipid phase was prepared by dissolving 1,2-dipalmitoyl-sn-glycero-3-phosphocholine (DPPC: Genzyme Pharmaceuticals, Switzerland), cholesterol (Sigma–Aldrich Chemical) and a cationic surfactant; dimethyldioctadecyl-ammonium bromide (DDAB: Sigma–Aldrich Chemical) in a chloroform–methanol (Fisher Scientific) mixture (4:1, v/v). DDAB was used in a 4% molar concentration to tailor the surface charge of the liposomes. The solvent mixture was removed from the lipid phase by rotary evaporation under vacuum resulting in the deposition of a homogenous dry lipid film. The film was hydrated with highly pure water (HPW), vortexed to obtain a suspension of positively charged multilamellar vesicles and transferred into a mini extruder (Avanti® Polar Lipids, Inc.) with two 200-nm pore size 19-mm polycarbonate filters (GE Osmonics).

### 2.2. Preparation of nanoparticles

Fresh alginate (AL) and chitosan (CH) solutions (1 mg/ml) were prepared in HPW (18.2 MΩ cm$^{-1}$). Alginic acid (low viscosity; 12 kDa molecular weight) and chitosan (85% deacetylated; 91.11 kDa molecular weight) were purchased from Sigma–Aldrich Chemical. CH solution was prepared in 1% (v/v) acetic acid aqueous solution and the final pH adjusted with 1 M NaOH to 5.5. Overnight stirring and filtration followed. For the L-b-L build-up, the cationic liposomes were coated with alternating layers of negatively charged AL and positively charged CH (volume ratio of 1:2, respectively) until the desired number of polyelectrolyte layers was achieved. With the deposition of each polymeric layer, the solution was incubated at room temperature for 60 min under gentle stirring. Centrifugation at 1600g for 15 min in order to eliminate aggregates that may form upon the mixture of liposomes and polymeric material (washing) followed.

### 2.3. Characterization of nanoparticles

#### 2.3.1. Particle size, surface charge and physical stability

Average hydrodynamic diameter (size), size distribution (polydispersity index; PI) and mean count rate (MCR) of all un-coated and coated liposomes were assessed at 25 °C by a particle sizer using a low-angle laser light-scattering device (HPPS, Malvern Instruments). The net surface charge was determined by zeta ($\zeta$) potential with a ZetaPlus analyzer using laser Doppler anemometry (Brookhaven Instruments, USA). Using sucrose as a cryoprotectant, aliquots of particle suspensions were freeze-dried at −54 °C for 48 h (Thermo Savant, Modulyo D-115). Physical stability upon rehydration of lyophilized powders in HPW to the original volume was evaluated.

#### 2.3.2. Morphology

Morphological analysis was performed by atomic force microscopy (AFM). Samples were deposited onto alginate-coated silica (Si) wafers. Slides were scanned with a Nanoscope® IIIa Scanning Probe Microscope (Digital Instruments, USA) in a liquid cell at room temperature in contact mode using a silicon nitride ($Si_3N_4$) cantilever at a scan rate of 1.850 Hz.

#### 2.3.3. Protein encapsulation efficiency and loading capacity

Accurately weighed lyophilized nanoparticles were re-hydrated to the original volume with different concentrations of BSA (66 kDa molecular weight, Pierce Biotechnologies) solution (0–2.0 mg/ml). The BSA-loaded particles were separated from the un-adsorbed protein by ultracentrifugation for 30 min at 180,000g and 25 °C (Beckman TL-100 Ultracentrifuge). Un-adsorbed BSA in the supernatant was quantified using a colorimetric method (Micro BCA protein assay, Pierce Biotechnologies) by reading the absorbance at 562 nm (μQuant, Bio-Tek Instruments). The loading capacity (LC) and encapsulation efficiency (EE) of the nanoparticles were calculated using Eqs. (1) and (2) [21,26]:

$$\mathrm{LC} = \frac{\mathrm{BSA_{total}} - \mathrm{BSA_{super}}}{\mathrm{Mass_{part}}} \times 100 \quad (1)$$

$$\mathrm{EE} = \frac{\mathrm{BSA_{total}} - \mathrm{BSA_{super}}}{\mathrm{BSA_{total}}} \times 100 \quad (2)$$

where $\mathrm{BSA_{total}}$ is the initial amount of BSA; $\mathrm{BSA_{super}}$ is the amount of un-adsorbed albumin measured in the supernatant, and $\mathrm{Mass_{part}}$ is the mass of the initial nanoparticles powder lyophilized.

#### 2.3.4. Protein release study

Aliquots of nanoparticle suspensions loaded with albumin were maintained at 37 °C. Suspensions were then ultracentrifuged for 20 min at 180,000g and 25 °C to separate the nanoparticles from the supernatant containing released protein for quantitative analysis. The pellet was re-suspended in 3 ml of HPW and the procedure repeated similarly over a period of 30 days at pre-determined time points. The amount of released BSA was analyzed spectrophotometrically by measuring the protein concentration in the supernatant using the micro-BCA method and reading the absorbance at 562 nm. The cumulative amount of BSA released over the time period was calculated using the following Eq. (3) [27,28]:

$$\text{Cumulative protein released (\%)} = \frac{\mathrm{BSA_{super}}}{\mathrm{BSA_{total}}} \times 100 \quad (3)$$

Table 1
Average size, polydispersity (PI), mean count rate (MCR in kcps) and zeta (ζ) potential surface charge of bare liposomes with 4% DDAB concentration

| Size (nm)* | SE | PI* | SE | MCR* | SE | Zeta (mV)* | SE |
|---|---|---|---|---|---|---|---|
| 180 | 10.5 | 0.227 | 0.015 | 257 | 1.64 | +35.48 | 2.159 |

Values are reported as mean (*) ± standard error (SE) of the mean.

where $BSA_{super}$ is the cumulative amount of protein released at each time point and $BSA_{total}$ is the actual loading of the protein determined earlier.

### 2.3.5. Modeling of release kinetics

To describe the release rate and characteristics of BSA from this delivery system as the square root of a time-dependant process based on diffusion, the Higuchi model [24] was applied. The basic equation is:

$$Q_t = [2DS\varepsilon(A - 0.5S\varepsilon)]^{0.5} \times t^{0.5} = k_H\sqrt{t} \quad (4)$$

where $Q_t$ is the amount of drug released in time $t$, $D$ is the diffusion coefficient, $S$ is the solubility of drug in the dissolution medium, $\varepsilon$ is the porosity, $A$ is the drug content per cubic centimeter of matrix and $k_H$ is the Higuchi constant. Eq. (4) can be expressed as:

$$\frac{M_t}{M_\infty} = k_H \times \sqrt{t} \quad (5)$$

where $M_t$ is the cumulative absolute amount of drug released at time $t$, $M_\infty$ is the absolute cumulative amount of drug released at infinite time (which should be equal to the absolute amount of drug incorporated within the system at time $t = 0$). Thus, the fraction of drug released is proportional to the square root of time. Alternatively, the drug release rate is proportional to the reciprocal of the square root of time.

### 2.4. Statistical analysis

All experiments were done in triplicate. The results are reported as means ± standard deviations. Unpaired or paired $t$-tests were performed for all comparisons to assess for statistical significance at the 95% confidence level.

## 3. Results and discussion

### 3.1. Particle size and size distribution

The relevant size, PI, MCR and ζ-potential surface charge for bare liposomes (L; 4% DDAB) are displayed in Table 1. This concentration was previously investigated proving to yield stable, monodisperse vesicles where DDAB concentrations of less than 4% or more than 19% were reported to alter the colloidal stability of the liposome suspension [29,30]. The build-up of multi-layers on LUVs was accompanied by an increase in particle size, as determined by HPPS. The mean particle diameter of initial LUVs is 180 ± 10.5 nm versus 345 ± 10.9 nm for liposomes coated with six polyelectrolyte layers (Fig. 1). It is noteworthy that the adsorption of the first chitosan layer [L(AL−CH)] on a previously adsorbed alginate layer [L(AL)] causes a decrease of the mean particle size; especially noticeable with the first two layers stabilizing afterwards. This behavior might be explained by the ability of the shorter polymer chains of alginate to easily diffuse between the longer polymer chains of chitosan due to the strong ionic electrostatic interactions and complexation of the polymers forming a denser network [26]. As we reported in a previous work [21], low-molecular weight chitosan favored the creation of smaller chitosan−alginate nanoparticles, as compared to high-molecular weight chitosan. These results are displayed in the insert of Fig. 1. Moreover, the PI is a measure of dispersion homogeneity, ranging from 0 to 1. Values between 0 and 0.3 indicate a relatively homogeneous dispersion [31]. As shown in Fig. 2a, the PI tends to decrease with the addition of polymers nevertheless it remained in the range that indicates dispersion homogeneity (<0.24). The literature provides evidence that particles (<500 nm) cross membranes of epithelial cells through endocytosis while larger particles (>5 μm) would be taken up via lymphatics [32,33]. Dong and Feng

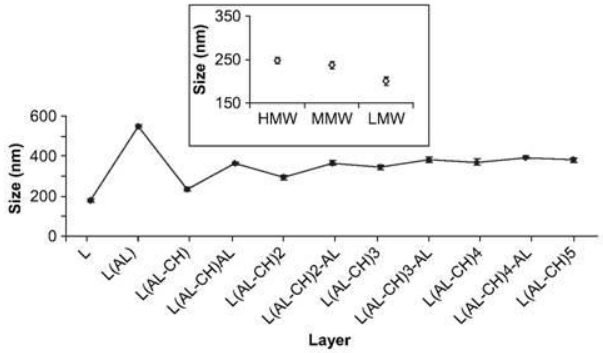


Fig. 1. Average particle size change with the adsorption of each polyelectrolyte layer. The first value is for bare liposomes and continues up to the fifth bi-layer; L(AL−CH)5. Insert: displays change with different molecular masses of chitosan adsorbed to liposomes coated with a single layer of alginate; L(AL). Difference between the HMW (232.6 kDa) and LMW (62.53 kDa) groups is significant with $p < 0.05$. MMW chitosan: 91.11 kDa. Values are reported as mean ± standard error of the mean.

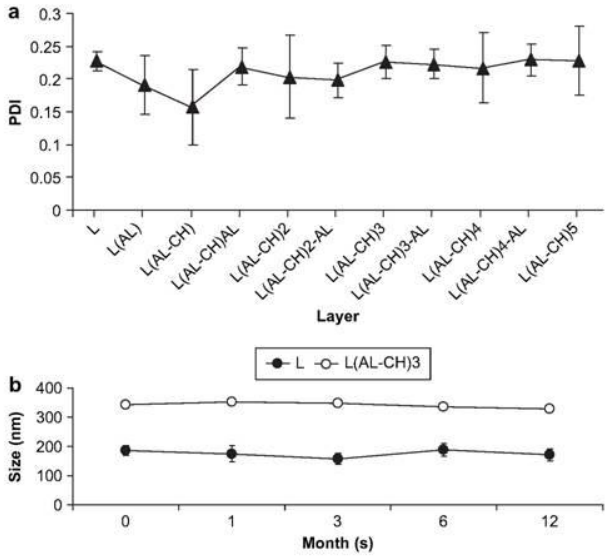


Fig. 2. (a) Polydispersity index (PI) distribution accompanying the build-up of the nanoparticles. (b) Particle size change over time at room temperature. Values are reported as mean ± standard error of the mean. No significant difference detected.

[34] reported that nanoparticles have greater ease of targeting tumors and delivering anti-cancer drugs reason being that they have higher surface area/volume ratio making it easier for the entrapped drug to be released in addition to having the advantage in permeating through the physiological drug barriers. Additionally, we monitored particle size change stored at room temperature over a period of 12 months. Fig. 2b reveals no significant difference indicating the effect of the L-b-L self-assembly in stabilizing these nanoparticles and enhancing their shelf life.

### 3.2. Surface charge and physical stability

The step-wise adsorption of alginate and chitosan was also monitored by measuring the ζ-potential upon addition of each polyelectrolyte layer. Besides confirming the presence and coverage of the polymer coating, ζ-potential is an important index for the stability of nanoparticulate suspensions. ζ-potential values above +30 mV or below −30 mV are generally considered to be an indication of stability and enhanced uniformity through causing strong repulsion forces among particles to prevent aggregation [35]. As evidenced in Fig. 3, the adsorption of each monolayer of charged polymer induced a charge inversion on the surface with ζ-potentials are in the order of 36.6 ± 2.9 mV after the addition of six layers of polyelectrolytes; L(AL−CH)3, indicating that the system is stable. Furthermore, lyophilization [36] in the presence of small amounts of sucrose (cryoprotectant) was carried out for this delivery system. Rationale behind freeze-drying is two-fold: (a) additional stability evaluation in terms of particle size and surface charge before and after lyophilization; and (b) loading the nanoparticles with BSA to evaluate their loading capacity, encapsulation efficiency and release profile. Fig. 4 demonstrates that the rehydration of the lyophilized particles could be attained in HPW with no significant difference in particle size or ζ-potential for the coated liposomes. Sucrose seems to prevent fusion or aggregation by acting as a spacer between particles [37]. Results show that the freeze-drying/rehydration procedure works as well for polysaccharide-coated liposomes as it does for bare liposomes.

### 3.3. Morphology

AFM scanning is illustrated in Fig. 5. Fig. 5a shows spherical liposomes with an average size of 200 nm and Fig. 5b illustrates 3-bilayered nanoparticles; L(AL−CH)3 with an average diameter of 350 nm confirming HPPS readings. The height profile of un-coated liposomes (L) amplified as an average vertical height was estimated at about 1.005 nm compared to L(AL−CH)3 with 5.042 nm as shown in Fig. 5c,d, respectively. The observed contraction in thickness is probably owing to the scanning force acting on the surface of the particles, as reported by Lulevich et al. [38].

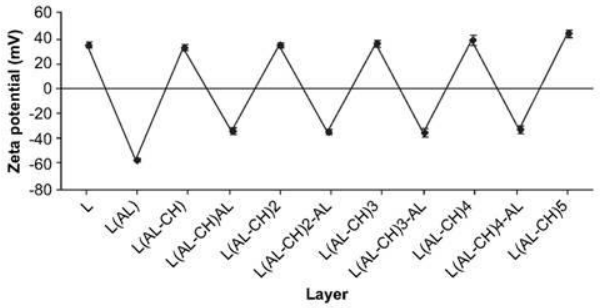


Fig. 3. Zeta (ζ) potential surface charge alternation with the adsorption of each polyelectrolyte layer. The first values are for bare liposomes and continue up to the fifth bi-layer; L(AL–CH)5. Values are reported as mean ± standard error of the mean.

### 3.4. Protein entrapment efficiency (EE) and loading capacity (LC)

Results of the LC and EE of our delivery system are shown in Fig. 6a,b. Bare liposomes (L); liposomes coated with a single layer of alginate L(AL); liposomes coated with six layers of alginate and chitosan L(AL–CH)3; and liposomes coated with 10 layers of alginate and chitosan L(AL–CH)5 were loaded with different concentrations of BSA (ranging from 0 to 2.0 mg/ml). Results showed that the protein LC in all liposomes, whether coated or un-coated is directly proportional to the BSA concentration used. Generally, the LC was enhanced by increasing the initial BSA concentration, reaching a maximum of ~70 mg of BSA entrapped in 100 mg of nanoparticles [L(AL–CH)3 and L(AL–CH)5 for 2.0 mg/ml BSA concentration] after which a plateau seems to attain. Similarly, EE was also affected by the initial BSA concentration where the lower the concentration, the higher the EE (with a range from 0 to 0.5 mg/ml BSA). Yet, the EE tends to decrease afterwards with higher BSA concentrations. This might indicate that the optimum EE was reached; however, no significant differences were detected. Nevertheless, results demonstrate a significant difference between the EE of un-coated liposomes and coated liposomes with 3- and 5-bilayers of polymers ($p < 0.05$). Coated liposomes can efficiently encapsulate more than double the amount than un-coated liposomes. Hence, higher LCs and EEs are achieved with the addition of the alginate and chitosan layers, enabling the system to entrap additional amounts of protein. Liposomes coated with 10 layers of polyelectrolytes were able to encapsulate more than 80% of the loaded protein.

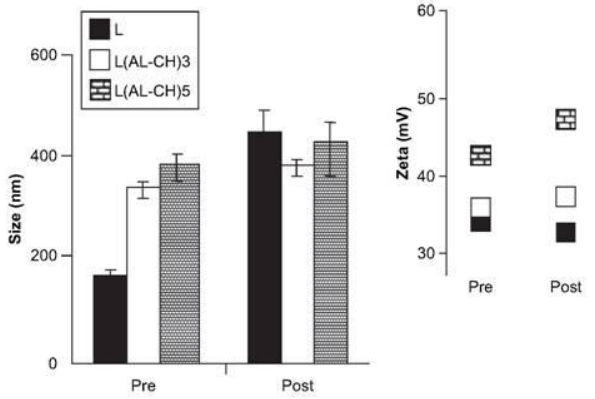


Fig. 4. Stability study comparing the nanoparticle size change pre- and post-lyophilization. Values are reported as mean ± standard error of the mean. Insert: the ζ-potential surface charge is compared. No significant difference detected.

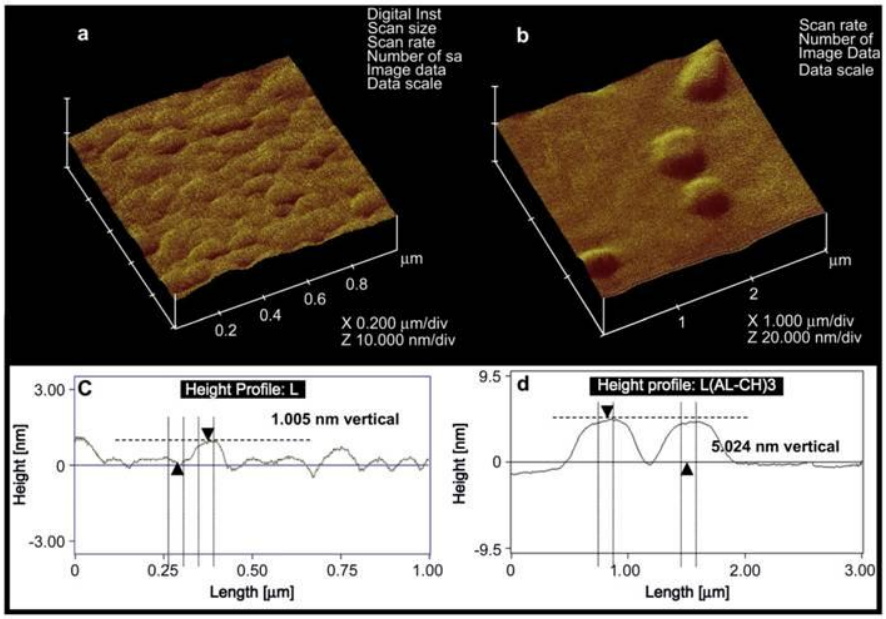


Fig. 5. AFM micrographs illustrating the nanoparticle morphology of (a) liposomes with an average size of 200 nm and (b) 3-bilayered polyelectrolyte-coated liposomes with an average size of 350 nm. Fig. 5c,d displays their relevant height profiles in nm.

### 3.5. Protein release profile

Fig. 7 illustrates the BSA release profiles plotted as a function of time over a period of 30 days. Fig. 7a,b displays the cumulative percentage release and the absolute release profiles at every time point, respectively. Un-coated liposomes exhibited a typical initial rapid burst effect of 60% in the first 3 days while coated liposomes displayed an elimination of

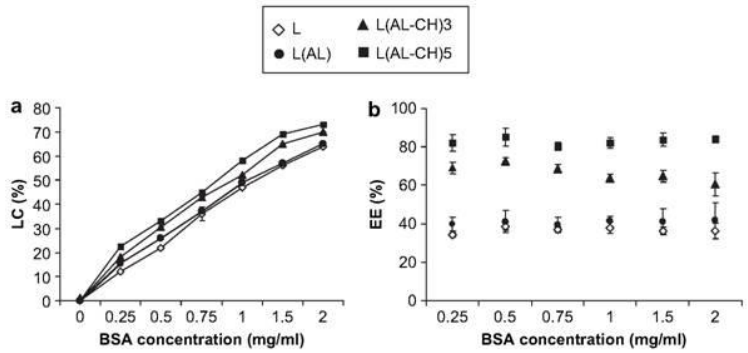


Fig. 6. (a) Loading capacities (LC) and (b) encapsulation efficiencies (EE) per layer growth of un-coated and coated liposomes encapsulating different concentrations of BSA (mg/ml). Significant differences detected between L, L(AL−CH)3 and L(AL−CH)5 with $p < 0.05$.

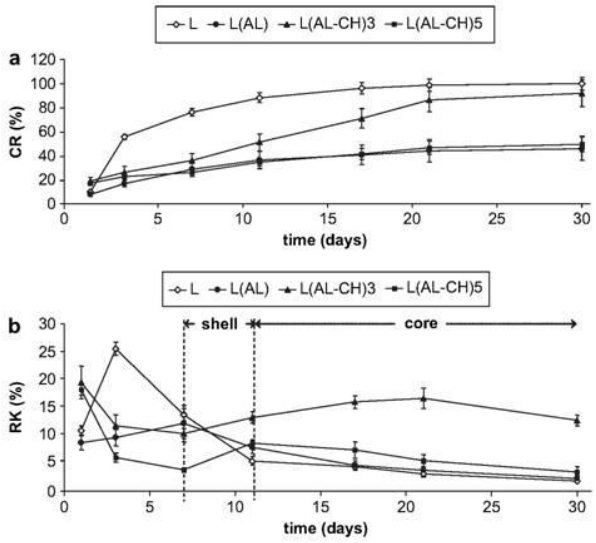


Fig. 7. (a) Cumulative percentage *in vitro* release profile (CR) of BSA-loaded un-coated and coated liposomes. (b) Absolute percentage *in vitro* release (RK) of BSA-loaded un-coated and coated liposomes at each time point in UPW. Data represent mean ± standard error of the mean.

this burst effect along with a slowed release of albumin (<50%) over the extended period of 30 days. Controlled, linear and sustained release of BSA was observed throughout the study with up to 88% of BSA released over 4 weeks before reaching a plateau. According to Kim et al. [28] the molecular weight of polymers incorporated might have an effect on the slower release of albumin as stronger outer coating membrane forms from higher molecular weights of polymers. Conformational changes to produce a more dense shell might have transpired with adding additional layers, mainly noticeable with the L(AL−CH)5 nanoparticles. Fig. 7b demonstrates the release values at each time point. Following the initial burst, BSA release from L and L(AL) starts to decrease dramatically (day 7 onwards). It seems that the effect of the single alginate layer limits itself mainly to reducing the initial BSA burst. On the contrary, BSA release from coated liposomes with six or more layers of polyelectrolytes displays higher release percentages in the first 2 days than L and L(AL). The fraction released during the first hours could correspond to the fraction of the free BSA that is released without control from the carrier. This represents the albumin that is physically adsorbed on the surface of the liposomes/nanoparticles. Release starts to increase again on day 7. Almost 35% of the loaded albumin in L(AL−CH)3 was released primarily from the shell followed by an increase in the release profile afterwards. This would be from the core, decreasing again in the third week of the experiment. The release profile for L(AL−CH)5 provides evidence of the effect of polymer coating and additional compartments on exhibiting slower release profiles. Chellat et al. [39] have previously demonstrated that the complexation of two polymers (one of which was CH) provided a protective effect for shell degradation in simulated gastric and intestinal fluids starting after 15 days. Similarly here in, the ionic interactions between the amine groups of CH and the carboxyl

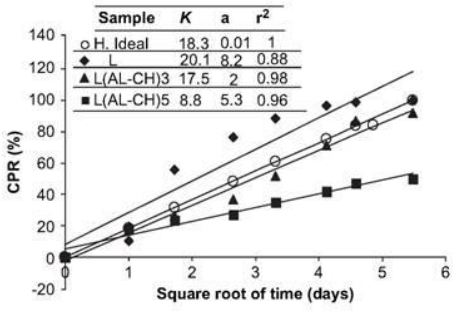


Fig. 8. Release kinetics of un-coated and coated liposomes represented as cumulative protein release percentage (CPR). Release data were fitted in the Higuchi mathematical model to obtain a plot of percentage albumin release as a function of square root of time. Insert displays the release rare slope ($K$), axis intercept ($a$) and correlation coefficient ($r^2$) of albumin from the samples studies in comparison to the ideal Higuchi (H. ideal) which takes into consideration 100% release over the monitored period of time.

Table 2
Release rate constants and correlation coefficients of albumin release from bare and coated liposomes showing the initial (shell) phase and the terminal (core) phase of protein release (obtained from the Higuchi plot)

| Model employed | L | | L(AL–CH)3 | | L(AL–CH)5 | |
|---|---|---|---|---|---|---|
| Higuchi | Initial | Terminal | Shell | Core | Shell | Core |
| $K$ | $10.1 \pm 0.05$ | $3.7 \pm 0.85$ | $2.84 \pm 0.72$ | $7.7 \pm 0.49$ | $1.4 \pm 0.77$ | $5.0 \pm 0.32$ |
| $r^2$ | 0.84 | 0.85 | 0.99 | 0.95 | 0.89 | 0.97 |

groups of AL seem to control and the biodegradation of the delivery system, thus the delayed and longer release of protein from the core.

### 3.6. Release kinetics

We have obtained a 30-day BSA release profile from multilayered nanocapsules plotted as a function of square root of time (in days) in Fig. 8. The data obtained have been fitted for the ideal Higuchi model based on calculation of area under the curve using the trapezoidal rule [40]. The method is exemplified for three experimental formulations [L, L(AL–CH)3 and L(AL–CH)5] allowing for where drug release is complete (100%) or incomplete (<100%) at the last sampling time. The literature provides evidence that for such systems, the Higuchi model based on the goodness-of-fit test continues to be the most appropriate model to describe the kinetics of drug release, when compared to zero-order, first-order, Hixson-Crowell's, and Weibull's models [40]. Furthermore, it enables an understanding of the quantitative deviation of the proposed formulation from the diffusion-controlled ideal Higuchi model. The plot showed good linearity for the coated liposomes. The insert in Fig. 8 displays the slope $K$, axis intercept $a$ and squared coefficient of correlation $r^2$ from Eq. (5) for the release of incorporated BSA out of un-coated and coated liposomes. Diffusion seems to be the main factor controlling the release of the encapsulated BSA from this delivery system over the 30 days. The increase in coating thickness appears to decrease the rate of protein release where BSA release from un-coated liposomes is clearly faster than from coated liposomes. This might be attributed to the presence of albumin on the surface of liposomes. Finally, the rate of release was divided into an initial phase (shell release; 0–7 days) and a terminal phase (core release; 11–30 days) and fitted to the Higuchi mathematical model as well. Release rate constants (mean ± standard deviation) and correlation coefficients of BSA release from uncoated and coated liposomes are displayed in Table 2. The initial burst effect and rapid release of albumin is clearly noted from un-coated liposomes. On the contrary, controlled-release initial and terminal phases (via L-b-L build-up) of the coated nanocapsules is demonstrated and would have a functional therapeutic use in maintaining sustained drug/protein delivery over extended periods of time diminishing lag periods.

## 4. Conclusions

This paper introduces a hydrophilic controlled-release protein delivery system consisting of a suspension of core–shell nanoparticles. Small and stable, monodisperse cationic particles (~400 nm; PI < 0.3) were obtained by the L-b-L deposition of alternating polyelectrolytes on cationic liposomes. The system demonstrated a good capacity for the encapsulation and loading of albumin. The *in vitro* release profile suggested that albumin has been entrapped in both, the aqueous liposomal core and within the polyelectrolyte shell. These core–shell nanoparticles have the following features: (i) formulated spontaneously and rapidly under mild conditions; (ii) are nanosized and stable; (iii) have a surface charge that can be modulated; (iv) possess a high loading capacity that can be altered by the number of polyelectrolyte layers and (v) provide sustained release of the entrapped protein for extended periods of time. The system tolerates extended shelf storage and drug loading via simple rehydration immediately preceding administration, thus preventing degradation or loss of the drug. Hence, it seems promising for the *in situ* administration of therapeutic proteins.

## Acknowledgements

This work was supported by research grants from the Natural Sciences and Engineering Research Council (NSERC) and the Centre for Biorecognition and Biosensors (CBB). Dr. Ziyad Haidar acknowledges a post-graduate scholarship from the Canadian Institutes for Health Research (CIHR) Skeletal Health Training Program and Center for Bone and Periodontal Research in Montréal. The authors thank Dr. Julien Fatisson for his assistance in characterization, Mrs. L. Mongeon and Dr. L. Marcotte for their assistance in microscopy and Dr. F. Azari for her assistance in the protein loading and release study.

## References

[1] Solheim E. Growth factors in bone. Int Orthop 1998;22(6):410–6.
[2] Li RH, Wozney JM. Delivering on the promise of bone morphogenetic proteins. Trends Biotechnol 2001;19(7):255–65.
[3] Luginbuehl V, Meinel L, Merkle HP, Gander B. Localized delivery of growth factors for bone repair. Eur J Pharm Biopharm 2004;58(2):197–208.
[4] Crommelin DJ, Storm G, Jiskoot W, Stenekes R, Mastrobattista E, Hennink WE. Nanotechnological approaches for the delivery of macromolecules. J Control Release 2003;87(1–3):81–8.
[5] Davis SS, Illum L. Drug delivery systems for challenging molecules. Int J Pharm 1998;176(1):1–8.
[6] Richardson TP, Peters MC, Ennett AB, Mooney DJ. Polymeric system for dual growth factor delivery. Nat Biotechnol 2001;19(11):1029–34.
[7] Illum L, Davis SS. Drug delivery. Curr Opin Biotechnol 1991;2:254–9.
[8] Chaize B, Colletier JP, Winterhalter M, Fournier D. Encapsulation of enzymes in liposomes: high encapsulation efficiency and control of

substrate permeability. Artif Cells Blood Substit Immobil Biotechnol 2004;32(1):67–75.
[9] Takeuchi H, Kojima H, Yamamoto H, Kawashima Y. Evaluation of circulation profiles of liposomes coated with hydrophilic polymers having different molecular weights in rats. J Control Release 2001; 75(1):83–91.
[10] Takeuchi H, Kojima H, Yamamoto H, Toyodo Toshitada, Toyobuku Hidekazu, Hino Tomaoki, et al. Physical stability of size controlled small unilamellar liposomes coated with a modified polyvinyl alcohol. Int J Pharm 1998;164(1–2):103–11.
[11] Takeuchi H, Kojima H, Yamamoto H, Kawashima Y. Polymer coating of liposomes with a modified polyvinyl alcohol and their systemic circulation and RES uptake in rats. J Control Release 2000;68(2):195–205.
[12] Charrois GJ, Allen TM. Rate of biodistribution of STEALTH® liposomes to tumor and skin: influence of liposome diameter and implications for toxicity and therapeutic activity. Biochim Biophys Acta 2003;1609(1): 102–8.
[13] Thierry B, Winnik FM, Merhi Y, Silver J, Tabrizian M. Bioactive coatings of endovascular stents based on polyelectrolyte multilayers. Biomacromolecules 2003;4(6):1564–71.
[14] Quinn JF, Caruso F. Facile tailoring of film morphology and release properties using layer-by-layer assembly of thermoresponsive materials. Langmuir 2004;20(1):20–2.
[15] Decher G. Fuzzy nanoassemblies: toward layered polymeric multicomposites. Science 1997;277(5330):1232–7.
[16] Yap HP, Quinn JF, Ng Sok Mian, Cho J, Caruso F. Colloid surface engineering via deposition of multilayered thin films from polyelectrolyte blend solutions. Langmuir 2005;21(10):4328–33.
[17] Bogdanovic G, Sennerfors T, Zhmud B, Tiberg F. Formation and structure of polyelectrolyte and nanoparticle multilayers: effect of particle characteristics. J Colloid Interface Sci 2002;255(1):44–51.
[18] Walker HW, Grant SB. Influence of surface charge and particle size on the stabilization of colloidal particles by model polyelectrolytes. Colloids Surf A-Physicochem Eng Asp 1998;135(1–3):123–33.
[19] Galovic RR, Barisic K, Pavelic Z, Zanic GT, Cepelak I, Filipovic-Grcic J. High efficiency entrapment of superoxide dismutase into mucoadhesive chitosan-coated liposomes. Eur J Pharm Sci 2002;15(5):441–8.
[20] Hillberg AL, Tabrizian M. Biorecognition through layer-by-layer polyelectrolyte assembly: in-situ hybridization on living cells. Biomacromolecules 2006;7(10):2742–50.
[21] Douglas KL, Tabrizian M. Effect of experimental parameters on the formation of alginate–chitosan nanoparticles and evaluation of their potential application as DNA carrier. J Biomater Sci Polym Ed 2005; 16(1):43–56.
[22] Gref R, Minamitake Y, Perracchia MT, Trubeskoy V, Torchilin V, Langer R. Biodegradable long-circulating polymeric nanospheres. Science 1994;263(5153):1600–3.
[23] Desai MP, Labhasetwar V, Amidon GL, Levy RJ. Gastrointestinal uptake of biodegradable microparticles: effect of particle size. Pharm Res 1996;13(12):1838–45.
[24] Higuchi T. Rate of release of medicaments from ointment bases containing drugs in suspension. J Pharm Sci 1961;50:874–5.
[25] New RRC. Liposomes: a practical approach. Oxford: IRC; 1990. p. 256–8.
[26] Calvo P, Remunan-lopez C, Villa-Jato JL, Alonso ML. Novel hydrophilic chitosan–polyethylene oxide nanoparticles as protein carriers. J Appl Polym Sci 1997;63(1):125–32.
[27] Dhoot NO, Wheatley MA. Microencapsulated liposomes in controlled drug delivery: strategies to modulate drug release and eliminate the burst effect. J Pharm Sci 2003;92:679–89.
[28] Kim TH, Park YH, Kim KJ, Cho CS. Release of albumin from chitosan-coated pectin beads in vitro. Int J Pharm 2003;250:371–83.
[29] Crispin RD, Todd LW, Mark AB. Liposomes containing dimethyl dioctadecyl ammonium bromide: formulation, quality control, and lipofection efficiency. Drug Deliv 2002;9:11–8.
[30] Haidar ZS, Azari F, Hamdy RC, Tabrizian M. In vitro characterization and cytotoxic effect of a liposome-based drug delivery system incorporating alternating L-b-L assembly of polyelectrolytes for craniofacial distraction osteogenesis. CBS 2006 [abstract 33].
[31] Chu B, Wang Z, Yu J. Dynamic light scattering study of internal motions of polymer coils in dilute solutions. Macromolecules 1991;24:6832–8.
[32] Savic R, Luo LB, Eisenberg A, Maysinger D. Micellar nanocontainers distribute to defined cytoplasmic organelles. Science 2003;300:615–8.
[33] Zhang Z, Feng SS. The drug encapsulation efficiency, in vitro drug release, cellular uptake and cytotoxicity of paclitaxel-loaded poly (lactide)-tocopheryl polyethylene glycol succinate nanoparticles. Biomaterials 2006;27:4025–33.
[34] Dong YC, Feng SS. Methoxy poly(ethylene glycol)-poly(lactide) (MPEG-PLA) nanoparticles for controlled delivery of anticancer drugs. Biomaterials 2004;25:2843–9.
[35] Shiqu YE, Chaoyang W, Xinxing L, Zhen T. Multilayer nanocapsules of polysaccharide chitosan and alginate through layer-by-layer assembly directly on PS nanoparticles for release. J Biomater Sci Polym Ed 2005;16(7):909–23.
[36] Bridges PA, Taylor KM. The effects of freeze-drying on the stability of liposomes to jet nebulization. J Pharm Pharmacol 2001;53(3):393–8.
[37] Womersley C, Uster PS, Rudolph AS, Crowe JH. Inhibition of dehydration-induced fusion between liposomal membranes by carbohydrates as measured by fluorescence energy transfer. Cryobiology 1986;23(3):245–55.
[38] Lulevich VV, Radtchenko IL, Sukhorukov GB, Vinogradova OI. Deformation properties of nonadhesive polyelectrolyte microcapsules studied with the atomic force microscope. J Phys Chem B 2003; 107(12):2735–40.
[39] Chellat F, Tabrizian M, Dumitriu S, Chornet E, Magny P, Rivard CH, et al. Study of biodegradation behaviour of chitosan–xanthan microspheres in simulated physiological media. J Biomed Mater Res 2000; 53:592–9.
[40] Gohel MC, Panchal MK, Jogani VV. Novel mathematical method for quantitative expression of deviation from the Higuchi model. AAPS PharmSciTech 2000;1(4):31.

J_ID: ZA1 Customer A_ID: 08-0210.R1 Cadmus Art: JBMA32292 Date: 20-SEPTEMBER-08 Stage: I Page: 1

# Modulated release of OP-1 and enhanced preosteoblast differentiation using a core-shell nanoparticulate system

AQ2

**Ziyad S. Haidar,[1,2] Fereshteh Azari,[2,3] Reggie C. Hamdy,[2,4] Maryam Tabrizian[1,2,5]**

[1]*Faculty of Dentistry, McGill University, Montréal (Québec), Canada*
[2]*Center for Biorecognition and Biosensors, McGill University, Montréal (Québec), Canada*
[3]*Department of Anatomy and Cell Biology, McGill University, Montréal (Québec), Canada*
[4]*Shriners Hospital for Children and Division of Orthopaedics, Montreal Children's Hospital, McGill University, Montréal (Québec), Canada*
[5]*Department of Biomedical Engineering, Faculty of Medicine, McGill University, Montréal (Québec), Canada*

Received 13 March 2008; revised 5 June 2008; accepted 11 July 2008
Published online 00 Month 2008 in Wiley InterScience (www.interscience.wiley.com). DOI: 10.1002/jbm.a.32292

**Abstract:** A release-controlled OP-1 delivery system consisting of a suspension of core-shell nanoparticles was prepared. The nanoparticles were composed of a core of positively-charged large unilamellar liposomes and a shell constructed through the L-b-L assembly of alternating layers of negatively-charged sodium alginate and positively-charged chitosan. Cytotoxicity was assayed with MC3T3-E1.4 mouse preosteoblast cells and cell viability was determined by colorimetry (CellQuanti-MTT™ kit). The system was loaded with a range of OP-1 concentrations and the release profiles were obtained and fitted into the Higuchi model to determine release kinetics. Alkaline phosphatase (ALP) activity of preosteoblasts was evaluated using a micro-BCA assay. The resulting monodisperse and nontoxic spherical nanoparticles exhibited high physical stability in simulated physiological media as well as an extended shelf-life allowing for immediate protein loading before future administration. ALP activity increased over time with the OP-1 loaded delivery system when compared with control, protein alone, and nanoparticles alone ($p < 0.05$). The system offers copious compartments for protein entrapment including the aqueous core and within the polyelectrolyte layers in the shell and demonstrates a sustained triphasic linear release of OP-1 over a prolonged period of 45 days, *in vitro*. This system offers a great advantage for optimum growth factor performance when applied in different anatomical sites of varying defect sizes and vascularity. © 2008 Wiley Periodicals, Inc. J Biomed Mater Res 00A: 000–000, 2008

**Key words:** alginate; alkaline phosphatase; bone morphogenetic protein(s); cell viability; chitosan; controlled drug release; core-shell nanoparticles; liposomes; self-assembly



## INTRODUCTION

Bone morphogenetic proteins (BMPs/OPs) are multifunctional osteoinductive cytokines that belong to the transforming growth factor β (TGF-β) superfamily.[1] BMPs exert diverse biological processes and are able to elicit osteogenesis during both, embryological bone formation and fracture repair.[1,2] Among the 20 BMPs identified and characterized to date, BMP-2, -4, -5, -6, -7 and -9 have shown the greatest *de novo* osteogenic capacity *in vitro* as well as *in vivo*.[3] They have stimulated bone regeneration and repair both orthotopically and heterotopically in several experimental animal models.[4] Thus, recombinant BMPs are now recognized as key factors in the arena of bone tissue engineering.[2,5] They hold great potential for healing bone fractures and large osseous defects, bridging bone nonunions, preventing osteoporosis, and treating periodontal defects, in humans.[4,6] For example, BMP-7 (osteogenic protein 1, OP-1) induced bone formation into muscle and between bone fragments when implanted subcutaneously.[7] Because its production by recombinant DNA technology in 1992, OP-1 has been extensively investigated for bone and cartilage regeneration in preclinical and clinical research.[8–10] OP-1 has been shown to be effective in promoting bone healing in long bone nonunions, open tibial fractures as well as in spinal fusion, providing a full alternative for conventional bone grafts.[6,11,12] Furthermore, ossification was accelerated during distraction osteogenesis following a single injection of OP-1 for correcting numerous craniofacial and orthopedic conditions.[13–17]

*Correspondence to*: M. Tabrizian; e-mail: maryam.tabrizian@mcgill.ca



ID: vijayk Date: 20/9/08 Time: 10:14 Path: J:/Production/JBMM/Vol00000/080450/3B2/C2JBMM080450

J_ID: ZA1 Customer A_ID: 08-0210.R1 Cadmus Art: JBMA32292 Date: 20-SEPTEMBER-08 Stage: I Page: 2



However, the clinical efficacy of OP-1 would depend on the carrier system used to ensure a sustained, multistep, and prolonged delivery of adequate protein concentrations to the desired site of tissue repair or restoration.[4–6,14,15,18–20] The foremost limitations include the rapid diffusion of OP-1 away from the site of application and the loss of its bioactivity, resulting in suboptimal local induction and thus incomplete or failure of bone regeneration. Researchers over the years have investigated numerous types of carriers to deliver bone growth factors.[21–24] Animal-derived collagens, while successful in many preclinical and human clinical trials,[25,26] are limited by their immunogenicity and risk of disease transmission due to their xenogenic nature.[27–29] Other materials that were proposed as safer and more effective than collagen in recent years include porous inorganic hydroxyapatite (HAP)[30] and synthetic biodegradable polymers such as poly L-lactic acid (PLLA), poly D, L-lactic-glycolic acid (PLGA), and poly ε-caprolactone (PCL).[5,31,32] However, acid degradation products resulting in aseptic inflammation and further ectopic bone formation have transpired consistently and thus far none of them have gained acceptance for human clinical investigation.[6,8] Natural, negatively-charged polymers such as hyaluronic acid and alginate have been used in gel and sponge formats yet are limited due to rapid resorption. This can be surpassed through chemical modification to decrease the intrinsic hydrophilicity of these polymers, minimizing degradation and enhancing ionic bond formation with the positively-charged BMPs.[20,24] As a result, the controlled release properties of synthetic polymers have been combined with the biocompatibility of natural polymers in recent years. Examples include PLGA-gelatin composites, collagen-PLG-alginate composites, and hyaluronan-impregnated PLA sponges.[33–35] Nano- and microparticles are other dosage forms that have consummated much attention for delivery of growth factors due to their attractive tendency to amass in sites of inflammation. They can be prepared from either synthetic polymers (PLA and PLGA) or from natural polymers (gelatin and chitosan).[36] Weber et al.[37] and Park et al.[38] reported on enhanced tissue regeneration *in vivo* using PLGA and gelatin microparticles for growth factor release. When compared with microparticles, nanoparticle delivery systems have demonstrated superiority in terms of longer residencies in general circulation, consequently extending the biological activity of the entrapped molecule.[39] PLGA nanospheres immobilized onto prefabricated nanofibrous PLLA scaffolds were used to load OP-1 and to promote *in vivo* bone regeneration.[40] However, significant failure of bone induction was observed due to loss of the bioactivity of the loaded protein and rapid release from the scaffolds once implanted subcutaneously in rats. Hence, the design of a safe and effective delivery system that immobilizes biologically active growth factors, controls their release at therapeutic levels over the proper periods of time for bone induction, has release kinetics calibrated to local requirements, and ultimately degrades without soliciting unexpected side effects remains a challenge.[41,42] Consequently, we focused on two biodegradable natural polymeric carrier materials combined together via the layer-by-layer (L-b-L) self-assembly technique over nanoscaled liposomes to formulate core-shell nanoparticles.

In a previous *in vitro* study, we have successfully encapsulated a model protein, bovine serum albumin in this core-shell controlled release system. The nanoparticles constitute a core of positively-charged large unilamellar liposomes and a shell constructed through the L-b-L assembly of alternating layers of negatively-charged sodium alginate and positively-charged chitosan.[43] The system had a cumulative size of 383 ± 11.5 nm and a zeta potential surface charge of 44.61 ± 3.31 mV for a five bilayered shell onto liposomes. The spherical nanoparticles tolerated extended shelf storage (up to 12 months) and had a capacity for protein loading over a concentration range of 0–2.0 mg/mL BSA. The release profile observed was characterized by an initial burst followed by sustained protein release. This release profile is highly desirable for delivering growth factors; particularly in large bony defects.[20,24] In the present work, we investigate the ability of our core-shell nanoparticulate system to encapsulate OP-1 and its physical stability in serum as well as postlyophilization. The release kinetics of OP-1 over an extended period of 45 days is determined. The *in vitro* cytotoxicity of the nanoparticles and the effect of the controlled release of OP-1 from the nanoparticles on mouse MC3T3 preosteoblast cells differentiation were assessed.

## MATERIALS AND METHODS

### Materials

For the preparation of liposomes, 1,2-Dipalmitoyl-sn-glycero-3-phosphocholine was purchased from Genzyme Pharmaceuticals, Switzerland; cholesterol and dimethyldioctadecyl-ammonium bromide (DDAB) were obtained from Sigma-Aldrich Chemical. The extrusion apparatus was purchased from Avanti® Polar Lipids, and the 19 mm polycarbonate filters (200 nm pore size) were obtained from GE Osmonics. For the L-b-L coating, alginic acid (sodium salt; viscosity of 2% in water) and chitosan (85% deacetylated with molecular weight of 91.11 kDa) were



ID: vijayk Date: 20/9/08 Time: 10:14 Path: J:/Production/JBMM/Vol00000/080450/3B2/C2JBMM080450

J_ID: ZA1 Customer A_ID: 08-0210.R1 Cadmus Art: JBMA32292 Date: 20-SEPTEMBER-08 Stage: I Page: 3



obtained from Sigma-Aldrich Chemical. For the cytotoxicity assay, mouse preosteoblast MC3T3-E1 subclone 14 (American Type Culture Collection, Manassas, VA) were cultured. Recombinant human OP-1 (15.7 kDa molecular weight; lyophilized) was purchased from bio-WORLD, OH. Fetal calf serum was obtained from Invitrogen™ Canada, ON. For the alkaline phosphatase (ALP) activity assay, *p*-nitrophenylphosphate substrate was purchased from Pierce Chemical, IL.

### Preparation of nanoparticles

Core-shell nanoparticles were prepared through the electrostatic interaction of positively-charged liposomes (L) with alternating layers of negatively-charged alginate (AL) and positively-charged chitosan (CH) according to the method described previously.[43] Briefly, liposomes (4% and 9%DDAB w/w) were formulated via the thin-film hydration technique,[44] followed by extrusion through double 200 nm polycarbonate filters. For the L-b-L build-up, fresh AL and CH solutions (1 mg/mL) were prepared in highly-pure water (HPW: 18.2 MΩ $cm^{-1}$). CH solution was prepared in 1% (v/v) acetic acid aqueous solution and the final pH adjusted with 1*M* NaOH to 5.5. The cationic liposomes were coated with alternating layers of AL and CH until the desired number of polyelectrolyte layers was achieved (6 layers: L(AL-CH)3 and 10 layers: L(AL-CH)5). With the deposition of each polymeric layer, the solution was incubated at room temperature for 60 min and centrifuged at 1600*g* for 15 min for washing.

### Characterization of nanoparticles

#### Particle size, surface charge and physical stability

Average hydrodynamic diameter (size) and the net surface charge (zeta potential) of all uncoated and coated 4% and 9% DDAB liposomes were assessed at 25°C using low-angle laser light-scattering (DLS-HPPS, Malvern Instruments, UK) and laser Doppler anemometry (Zeta-Plus, Brookhaven Instruments, NY), respectively. Aliquots of particle suspensions were freeze-dried using sucrose as a cryoprotectant at −54°C for 48 h (Modulyo D-115, Thermo Savant, MA) and the physical stability upon rehydration of lyophilized powders with OP-1 to the original volume was evaluated. Furthermore, stability over time (stored in solution at room temperature) was assessed by DLS over a period of 12 months.

#### Cell culture

Mouse preosteoblast MC3T3-E1.14 cells were seeded in α-minimum essential medium supplemented with 10% (v/v) fetal bovine serum and 1% (v/v) penicillin/streptomycin. Cells were allowed to attach to the plates in a humidified atmosphere of 5% $CO_2$ and 95% air incubator at 37°C for 24 h and the media changed every 48 h. Cells were sub-cultured after reaching confluence using trypsin-EDTA. Controlled experiments were conducted on conventional well plates for each set of experiments.

#### Cytotoxicity assay

Cells were seeded in a 96-well plate at an initial density of $1.0 \times 10^4$ viable cells/well. The following day, medium was removed and cells were treated with 200 µL of medium containing several concentrations of both uncoated and coated liposomes. Cells were incubated in treatment medium for 24 h, after which cell proliferation and viability with a linear detection range of 1,000 to 50,000 cells was performed using a colorimetric method using 3-(4,5-Dimethylthiazol-2-yl)-2,5-diphenyltetrazolium bromide, a tetrazole (CellQuanti-MTT™ kit) purchased from BioAssay Systems, CA. Briefly, treatment solutions were replaced with 100-µL fresh medium to which 10 µL of 12 m*M* MTT solution was added. After 4 h of incubation at 37°C, 100 µL of SDS-HCl solution was added to each well, followed by further incubation at 37°C. Samples were then read at 570 nm by a plate spectrophotometer (µQuant, Bio-Tek Instruments). As a negative control, 10 µL of the MTT stock solution were added to 100 µL of medium alone. The viability of cells incubated with DMEM alone was taken as 100%. AQ4

#### Stability in fetal bovine serum

To evaluate the stability of the system in simulated physiological medium, aliquots of particle suspensions (uncoated and coated liposomes) were diluted 10 times with fetal calf serum and incubated at 37°C for 1 h, 6 h, and 24 h. The change in particle diameter was assessed by DLS.

#### Protein entrapment efficiency and loading capacity

Lyophilized 4% DDAB nanoparticles were rehydrated to the original volume with different concentrations of OP-1 solution (0 to 5.0 µg/mL). The unadsorbed protein was separated from the protein-loaded particles by ultracentrifugation for 30 min at 180,000*g* and 25°C (TL-100 Ultracentrifuge, Beckman Coulter, CA). Quantification was performed using an enzyme-linked immunosorbent assay (ELISA) construction kit specific for human BMP-7 according to the manufacturer's (Antigenix America) protocol, reading the absorbance plate spectrophotometer at 450 nm. Alongside, the average size and zeta potential surface charge of the particles following rehydration with OP-1 were measured.

#### Protein release study

Aliquots of nanoparticle suspensions loaded with OP-1 were maintained at 37°C. Suspensions were then ultracentrifuged for 20 min at 180,000*g* and 25°C to separate the nanoparticles from the supernatant containing the released protein for quantitative analysis. The pellet was resuspended in 1 mL of HPW and the procedure repeated over a period of 45 days at predetermined time points. The cu-



ID: vijayk Date: 20/9/08 Time: 10:14 Path: J:/Production/JBMM/Vol00000/080450/3B2/C2JBMM080450

J_ID: ZA1 Customer A_ID: 08-0210.R1 Cadmus Art: JBMA32292 Date: 20-SEPTEMBER-08 Stage: I Page: 4



mulative amount of released OP-1 was analyzed spectrophotometrically by measuring the protein concentration in the supernatant using ELISA and reading the absorbance at 450 nm.

### Measurement of alkaline phosphatase activity

Osteogenic differentiation was screened by the expression of the activity of ALP measured via the time-dependent formation of *p*-nitrophenol from *p*-nitrophenylphosphate substrate (Pierce Chemical, IL) at pH 9.8. Cells were incubated at $2 \times 10^4$ cells/well in a 24-well plate for 24 h at 37°C. The following day, cells were treated with uncoated and coated liposomes for 2, 4, and 7 days. The cell layers were washed with PBS and scraped off from the surfaces by adding harvest buffer (10 m*M* Tris pH 7.4, 0.2% IGPAL). After sonication and centrifugation, preosteoblast cell lysate was used for the analysis of the ALP activity and the total protein level. Each reaction was initiated by adding 100 µL of *p*-nitrophenylphosphate to the cell lysate. The reaction was stopped after 30 min by adding 50 µL of 2*N* NaOH. Optical density was measured at 405 nm by a spectrophotometer on every time point to quantify the amount of *p*-nitrophennol produced. The values of ALP activity were normalized with respect to the total protein content obtained from the same cell lysate. Total protein content was determined using a micro-BCA Protein Assay kit (Pierce Biotechnologies, IL) following the recommendations of the manufacturer.

### Modeling release kinetics

The OP-1 release rate and characteristics for this delivery system were described as a time-dependent process based on diffusion. The renowned Higuchi model[45] was applied, as described earlier.[43] Briefly, the protein release rate is considered proportional to the reciprocal of the square root of time expressed as quantitative deviation from the Higuchi ideal model which takes into consideration complete (100%) or incomplete (<100%) protein release at the last sampling time.

### Statistics

AQ5

Statistical analysis was performed using unpaired or paired *t*-tests to assess for statistical significance at the 95% confidence level, where ρ-values of less than 0.05 were deemed statistically significant.

## RESULTS AND DISCUSSION

### Preparation and characterization of core-shell nanoparticles

Spherical core-shell nanoparticles[43] were formulated in mild aqueous conditions by the L-b-L self assembly of negatively-charged AL and positively-charged CH on 4% and 9% DDAB cationic liposomes. Driven by electrostatic interactions, we have previously shown how AL and CH spontaneously interact under these conditions to form a shell around the 4% DDAB liposomal core resulting in particles with small size (<400 nm) and narrow distribution (polydispersity index <0.3). DDAB is a cationic surfactant that tailors the surface charge of the particles. An increase of DDAB concentration from 4% and 9% for the preparation of nanoparticles indicated no significant difference in particle size, polydispersity, surface charge, or physical stability over time (up to 12 months) for 4% and 9% DDAB liposomes coated with up to 5 bi-layers of polymer (data not shown). In general, narrow particle size distribution[46] and dispersion homogeneity[47] were evident. Zeta potential measurements indicated an overall positive charge of 46.2 ± 0.8 mV, suitable for complex formation with anionic proteins and confirming the complete coverage of the liposomal core with the surrounding polymer shell.[48]

### Stability in serum

Stability in fetal bovine serum evaluated by DLS did not show significant changes in the size of coated nanoparticles following incubation over time (Fig. 1). In contrast, uncoated liposomes exhibited extensive aggregation upon 1 h incubation. Results demonstrate the protective effect of the polyelectrolyte shell in stabilizing the liposomal core and maintaining the integrity of the overall delivery system in simulated physiological media. F1

### Cytotoxicity

The viability of MC3T3-E1.4 mouse preosteoblast cells after incubation with varying concentrations of the samples over 24 h exposure time is shown in Figure 2. Results show that particulate systems constituting liposome cores with 4% DDAB are not toxic (96% of control) to cells (12.5 through 253 µg/mL). Although the nanoparticles made of liposomes containing 9% DDAB were similar in size and surface charge, they caused a decrease in cell viability (85% of control). This is in agreement with previous reporting that at certain concentrations of DDAB; liposomes are toxic to cells.[49,50] Consequently, nanoparticles containing 9% DDAB were excluded from further experiments. F2

### OP-1 loading capacity and entrapment efficiency

The loading capacity (LC) and entrapment efficiency (EE) of the nanoparticles are displayed in Fig-



ID: vijayk Date: 20/9/08 Time: 10:14 Path: J:/Production/JBMM/Vol00000/080450/3B2/C2JBMM080450

J_ID: ZA1 Customer A_ID: 08-0210.R1 Cadmus Art: JBMA32292 Date: 20-SEPTEMBER-08 Stage: I Page: 5



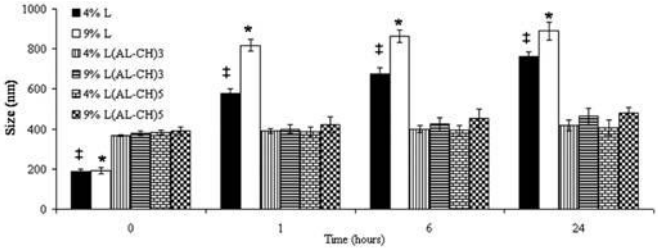


**Figure 1.** Stability study comparing the nanoparticle size change pre- and post-incubation in fetal bovine serum at 37°C over an exposure time of 24 h. Values are reported as mean ± standard error of the mean. Statistical significance ($p < 0.05$) was detected between uncoated and coated liposomes for 4% (‡) and 9% (*) DDAB concentrations. ED1

F3 ures 3(a,b), respectively. Liposome (L), liposome with three alginate-chitosan bilayers [L(AL-CH)3], and liposome with five alginate-chitosan bilayers [L(AL-CH)5] were loaded with different concentrations of OP-1 (15.7 kDa) ranging from 0 to 5000 ng/mL. Results showed that the protein LC and EE in all lipid delivery systems, whether coated or uncoated, were directly proportional to the protein concentration entrapped as previously observed with bovine serum albumin encapsulation.[43] In general, the LC was enhanced by increasing the initial OP-1 concentration, reaching a maximum of 50% and 40% of OP-1 entrapped in 100 mg of L(AL-CH)3 and L(AL-CH)5 for 5000 ng/mL OP-1 concentration, respectively. The LC of OP-1 was less than that calculated with albumin-loaded nanoparticles. This might be explained by the variation in the concentration and molecular weight of the entrapped proteins. A plateau seems to emerge for loaded liposomes; however not for coated nanoparticles. In fact, they show a potential for a higher LC with elevated concentrations of OP-1. Likewise, the EE was also affected by the initial OP-1 concentration mounting with higher concentrations. Results demonstrated a significant difference between the EE of uncoated liposomes and coated liposomes ($p < 0.05$) only. Hence, the addition of the AL and CH layers enhances both, the LC and EE enabling the system to entrap additional amounts of the protein. Liposomes coated with 10 layers of polyelectrolytes were able to encapsulate more than 80% of the loaded protein. DLS showed no significant changes in particle size following lyophilization and rehydration with the protein (data not shown) for all coated liposomes indicating the incorporation of OP-1 into the compartments of the core and shell system. This is a very interesting feature for the delivery of recombinant BMPs, because supra-physiologic doses of single growth factors in microgram ranges are essential to induce bone regeneration.[24] The required dose depends on the anatomical site being treated in terms of the degree of vascularization and number

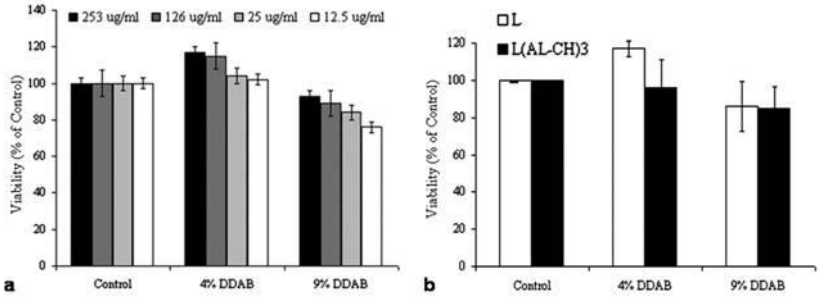


**Figure 2.** Cytotoxicity assay: (a) uncoated liposomes (several concentrations) and (b) uncoated and coated liposomes (highest concentration: 253 μg/mL). Values are reported as mean ± standard error of the mean.



ID: vijayk Date: 20/9/08 Time: 10:14 Path: J:/Production/JBMM/Vol00000/080450/3B2/C2JBMM080450

J_ID: ZA1 Customer A_ID: 08-0210.R1 Cadmus Art: JBMA32292 Date: 20-SEPTEMBER-08 Stage: I Page: 6



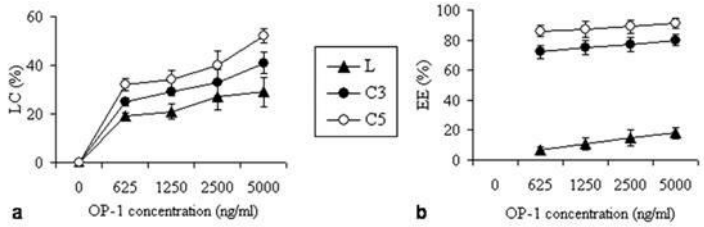


**Figure 3.** (a) Loading capacities (LC) and (b) encapsulation efficiencies (EE) per layer growth of uncoated and coated liposomes encapsulating different concentrations of OP-1 (ng/mL). Significant differences ($p < 0.05$) were detected between uncoated liposomes (L) and those coated with three alginate-chitosan bilayers [L(AL-CH)3] and five alginate-chitosan bilayers [L(AL-CH)5].

of resident responding cells in the defect site; thus, the LC and EE of the formulated nanoparticles seem to have the capacity of entrapping BMPs in a range of concentrations and amounts suitable for potential use in an array of bony defects and conditions.

### OP-1 release profile

The ELISA assay constructed to measure the OP-1 release from the delivery system *in vitro* gave a linear absorbance response for OP-1 concentrations from 0 to 5000 ng/mL ($r^2$ = 99.8%). Figure 4 illustrates the OP-1 release profiles plotted as a function of time over a period of 45 days for particles loaded with 5000 ng/mL OP-1 concentration. The cumulative percentage release and the absolute release profiles at every time point in HPW are displayed in Figures 4(a,b), respectively. A control of the burst effect is revealed by the coated liposomes followed by a slowed and prolonged release of OP-1. Controlled, linear, and sustained release of OP-1 was observed with up to 85% of OP-1 released over a period of 4 weeks. OP-1 release is faster than what was

F4

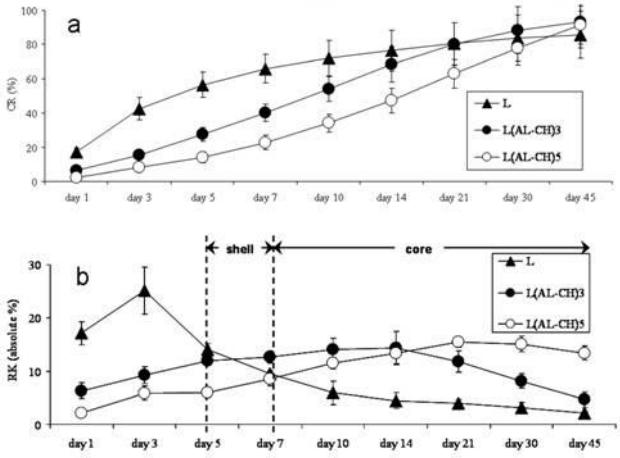


**Figure 4.** (a) Cumulative percentage *in vitro* release profile (CR) of OP-1 loaded uncoated and coated liposomes. (b) Absolute percentage *in vitro* release (RK) of OP-1 loaded uncoated and coated liposomes at each time point in highly-pure water. Data represent mean ± standard error of the mean. L: uncoated liposomes; [L(AL-CH)3]: liposomes coated with three alginate-chitosan bilayers; and [L(AL-CH)5]: liposomes coated with five alginate-chitosan bilayers.



ID: vijayk Date: 20/9/08 Time: 10:14 Path: J:/Production/JBMM/Vol00000/080450/3B2/C2JBMM080450

J_ID: ZA1 Customer A_ID: 08-0210.R1 Cadmus Art: JBMA32292 Date: 20-SEPTEMBER-08 Stage: I Page: 7



reported earlier with our albumin-loaded nanoparticles.[43] This might be attributed again to the variance in the molecular weights of the loaded proteins; 15.7 kDa versus 66 kDa for OP-1 and albumin, respectively. Hence, the smaller the protein, the faster it is to diffuse through the layers of the nanoparticles. Figure 4(b) demonstrates the release values at each time point. Following the initial burst, OP-1 release from L starts to decrease dramatically. On the contrary, biphasic protein release from L(AL-CH)3 and L(AL-CH)5 is shown where it starts to increase noticeably on day 7 and continues for over a 1 week period. Almost 12% of the loaded OP-1 in L(AL-CH)3 was released primarily from the shell. This was followed by an increase in the release profile afterwards mainly from the core, decreasing again in the third week of the experiment. The release profile for L(AL-CH)5 provides evidence of the effect of polymer coating and additional compartments on exhibiting slower release profiles even with such small proteins. The ionic interaction between the amine groups of CH and the carboxyl groups of AL are known to control biodegradation,[51] hence the delayed and longer release of OP-1 from the core. Therefore, low- or high-level sustained protein release profiles with smaller or larger initial protein bursts are feasible with the alteration in the number of polyelectrolyte layers. This is essential for optimum growth factor performance when applied in different anatomical sites of varying defect sizes and vascularity as reported earlier.[18–24] For instance, large or critical-sized defects[52] that fail to heal spontaneously might require an initial high-level burst release to recruit osteoblasts to defect site, followed by an extended, low-level constant release to differentiate the cells once localized at the repair site.[19,24] This triphasic delivery system seems to have the capacity to be tailored and formulated accordingly.

### ALP activity

The impact of unloaded and OP-1 (100 ng/mL) loaded nanoparticles on the differentiation of MC3T3-E1.14 preosteoblast cells incubated for 2, 4, and 7 days by measuring the ALP activity is displayed in Figure 5. Ascorbic acid and β-glycerophosphate (AA+βGP); medium supplements and nutrients essential for differentiation of preosteoblasts, were present in the assay as positive controls. We have also included OP-1 alone (100 ng/mL) so that to compare its effect with that of OP-1 incorporated into the nanoparticles. Results are expressed relative to untreated cells (control) as μmol *p*-nitrophenol (PNP) produced/min/mg protein. High ALP activity is an osteoblastic phenotype.[53] The activity of ALP was significantly increased in cells incubated

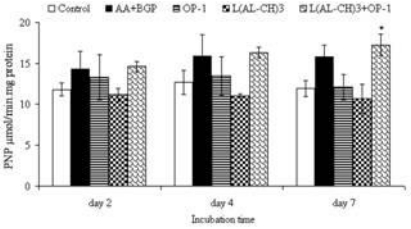


**Figure 5.** ALP activity assay. Significant differences ($p < 0.05$) were detected for OP-1 loaded nanoparticles [L(AL-CH)3+OP-1] when compared with control, OP-1 alone, and unloaded nanoparticles [L(AL-CH)3]. Difference between control and AA+βGP (Ascorbic acid and β-glycerophosphate) was deemed statistically significant as well.

with OP-1 loaded nanoparticles, and preosteoblast differentiation was enhanced over the monitored period of 7 days. The stimulatory effect of OP-1 alone was less than when loaded in the delivery system or when compared with both controls. More specifically, it was significantly less when compared with AA-βGP and OP-1 loaded nanoparticles on day 7. Nonetheless, incubation with a low-level dose of 100 ng/mL OP-1 was sufficient to induce cell differentiation, as assessed by the ALP activity between days 2 and 4. It has been shown recently that OP-1 is mitogenic for MC3T3-E1 cells demonstrating dose-dependant induction of ALP activity and osteocalcin production.[54] In addition, therapeutic applications are known to require large amounts of recombinant proteins.[55] Hence, the need for a cost-effective and efficient release-controlled protein delivery system is amplified.

### *In vitro* OP-1 release kinetics

The 45-day OP-1 release profile from the core-shell delivery system plotted as a function of square root of time (in days) is shown in Figure 6. The method is epitomized for L, L(AL-CH)3, and L(AL-CH)5.[43] A good linearity for coated liposomes is illustrated. The insert displays the slope *K*, axis intercept *a*, and squared coefficient of correlation $r^2$ for the release of incorporated OP-1 from both, uncoated and coated liposomes. The increase in coating thickness appears to decrease the rate of protein release where OP-1 release from uncoated liposomes is clearly faster than from coated liposomes. OP-1 release over the 45 days from this physically dispersed polymeric system may be described by several possible mechanisms: diffusion, polymer degradation, ion complexation, and interactions among the protein and the polymers, although it is primarily governed by a dif-



ID: vijayk Date: 20/9/08 Time: 10:14 Path: J:/Production/JBMM/Vol00000/080450/3B2/C2JBMM080450

J_ID: ZA1 Customer A_ID: 08-0210.R1 Cadmus Art: JBMA32292 Date: 20-SEPTEMBER-08 Stage: I Page: 8



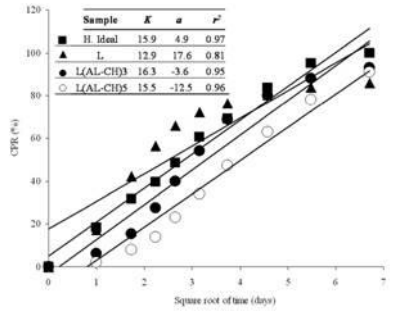


**Figure 6.** Release kinetics of uncoated (L) and coated liposomes [L(AL-CH)3 and L(AL-CH)5] represented as cumulative protein release percentage (CPR). Release data was fitted in the Higuchi mathematical model to obtain a plot of percentage protein release as a function of square root of time. Insert displays the release rare slope ($K$), axis intercept ($a$), and correlation coefficient ($r^2$) of OP-1 from the samples studies in comparison to the ideal Higuchi (H. ideal) which takes into consideration 100% release over the monitored period of time. Release was not complete over the studied period of time (<100%). Slower release rates are shown with coated liposomes than both, uncoated liposomes and the H. ideal, resulting in negative axis intercepts.

fusion-based or affinity-based mechanism. Finally, the rate of release was divided into an initial phase (shell release; 0–7 days) and a terminal phase (core release; 8–45 days grouping two release episodes together) and fitted to the Higuchi mathematical model which is based on the calculation of the area under the curve using the trapezoidal rule.[56] Table I displays the relevant release rate constants and correlation coefficients. This model allows for where drug release is complete (100%) or incomplete (<100%) at the last sampling time. The literature provides evidence that for such systems, the Higuchi model based on the goodness-of-fit test continues to be the most appropriate model to describe the kinetics of drug release, when compared with zero-order, first-order, Hixson-Crowell's, and Weibull's models.[56] Furthermore, it enables an understanding of the quantitative deviation of the proposed formulation from the diffusion-controlled ideal Higuchi model. The role of the L-b-L build-up of polymers around nanosized liposomes is clearly demonstrated in controlling the release of the entrapped drug or protein over prolonged periods of time. The release patterns of the coated liposomes showed linear profiles with a much lower burst than uncoated liposomes followed by a sustained release of OP-1.

## CONCLUSIONS

The novelty of this work is based on the combination of the polymeric L-b-L self assembly technique and nanoscaled liposomes in formulating a stable and nontoxic release-controlled protein delivery system. It consists of a suspension of monodisperse core-shell nanoparticles suitable for the potential administration of growth factors via a parental injection as is preferable for surgeons. The nanoparticles tolerate extended shelf storage and allow for protein loading immediately preceding administration, preventing degradation, or loss of the entrapped growth factor. The system demonstrated a good capacity for the encapsulation and loading of OP-1 which can be altered by the number of polyelectrolyte layers. Sustained and multistep release of OP-1 was evident for an extended period of time with the viability and bioactivity of OP-1 maintained via enhancing preosteoblast differentiation, *in vitro*. These findings suggest that our core-shell nanoparticulate system could be an effective carrier for morphogens, growth factors, and most likely for other classes of bioactive molecules.

The authors wish to the Natural Sciences and Engineering Research Council of Canada (NSERC) and the Centre for Biorecognition and Biosensors (CBB) for making this research possible. Dr. Haidar acknowledges a post-graduate scholarship from the Canadian Institutes for Health Research (CIHR) Skeletal Health Training Program and Center for Bone and Periodontal Research in Montréal, Québec.

**TABLE I**
**Release Rate Constants (Mean ± standard deviation) and Correlation Coefficients of OP-1 Release from Bare and Coated Liposomes Showing the Initial (shell) Phase and the Terminal (core) Phase of Protein Release (Obtained from the Higuchi Plot)**

| Model | L | | L(AL-CH)3 | | L(AL-CH)5 | |
|---|---|---|---|---|---|---|
| Higuchi | Initial | Terminal | Shell | Core | Shell | Core |
| $K$ | 16.1 ± 5.4 | 3.5 ± 6.9 | 11.4 ± 6.1 | 9.7 ± 4.7 | 6.7 ± 5.1 | 14.5 ± 1.9 |
| $r^2$ | 0.95 | 0.98 | 0.99 | 0.96 | 0.99 | 0.99 |



ID: vijayk Date: 20/9/08 Time: 10:14 Path: J:/Production/JBMM/Vol00000/080450/3B2/C2JBMM080450

J_ID: ZA1 Customer A_ID: 08-0210.R1 Cadmus Art: JBMA32292 Date: 20-SEPTEMBER-08 Stage: I Page: 9



## References


1. Ripamonti U, Ramoshebi LN, Matsaba T, Tasker J, Crooks J, Teare J. Bone induction by BMPs/OPs and related family members in primates: The critical role of delivery systems. J Bone Joint Surg Am 2001;83:116–127.
2. Sykaras N, Opperman LA. Bone morphogenetic proteins (BMPs): How do they function and what can they offer the clinician? J Oral Sci 2003;45:57–73.
3. Xiao YT, Xiang LX, Shao JZ. Bone morphogenetic protein. Biochem Biophys Res Commun 2007;362:550–553.
4. Termaat MF, Den Boer FC, Bakker FC, Patka P, Haarman HJThM. Bone morphogenetic proteins. Development and clinical efficacy in the treatment of fractures and bone defects. J Bone Joint Surg Am 2005;87:1367–1378.
5. Saito N, Okada T, Horiuchi H, Ota H, Takahashi J, Murakami N, Nawata M, Kojima S, Nozaki K, Takaoka K. Local bone formation by injection of recombinant human bone morphogenetic protein-2 contained in polymer carriers. Bone 2003;32: 381–386.
6. Giannobile WV, Ryan S, Shih MS, Su DL, Kaplan PL, Chan TC. Recombinant human osteogenic protein-1 (OP-1) stimulates periodontal wound healing in class III furcation defects. J Periodontol 1998;69:129–137.
7. Sampath TK, Maliakal JC, Hauschka PV, Jones WK, Sasak H, Tucker RF, White KH, Coughlin JE, Tucker MM, Pang RH. Recombinant human osteogenic protein-1 (hOP-1) induces new bone formation in vivo with a specific activity comparable with natural bovine osteogenic protein and stimulates osteoblast proliferation and differentiation in vitro. J Biol Chem 1992;267:20352–20362.
8. Vukicevic S, Stavljenic A, Pecina M. Discovery and clinical applications of bone morphogenetic proteins. Eur J Clin Chem Clin Biochem 1995;33:661–671.
9. Cook SD, Rueger DC. Osteogenic protein-1: Biology and applications. Clin Orthop Relat Res 1996;324:29–38.
10. Cook SD. Preclinical and clinical evaluation of osteogenic protein-1 (BMP-7) in bony sites. Orthopedics 1999;22:669–671.
11. Friedlaender GE, Perry CR, Cole JD, Cook SD, Cierny G, Muschler GF, Zych GA, Calhoun JH, LaForte AJ, Yin S. Osteogenic protein-1 (bone morphogenetic protein-7) in the treatment of tibial nonunions. J Bone Joint Surg Am 2001;83: 151–158.
12. Pecine M, Giltaij LR, Vukicevic S. Orthopaedic applications of osteogenic protein -1 (BMP-7). Int Orthop 2001;25:203–208.
13. Mizumoto Y, Moseley T, Drews M, Cooper VN III, Reddi AH. Acceleration of regenerate ossification during distraction osteogenesis with recombinant human bone morphogenetic protein-7. J Bone Joint Surg Am 2003;85:124–130.
14. Hamdy RC, Amako M, Beckman L, Kawaguchi M, Rauch F, Lauzier D, Steffen T. Effects of osteogenic protein-1 on distraction osteogenesis in rabbits. Bone 2003;33:248–255.
15. Mandu-Hrit M, Haque T, Lauzier D, Kotsiopriftis M, Rauch F, Tabrizian M, Henderson JE, Hamdy RC. Early injection of OP-1 during distraction osteogenesis accelerates new bone formation in rabbits. Growth Factors 2006;24:172–183.
16. Buxton PG, Cobourne MT. Regenerative approaches in the craniofacial region: Manipulating cellular progenitors for orofacial repair. Oral Dis 2007;13:452–460.
17. Mitsukawa N, Satoh K, Suse T, Hosaka Y. Clinical success of mandibular distraction for obstructive sleep apnea resulting from micrognathia in 10 consecutive Japanese young children. J Craniofac Surg 2007;18:948–953.
18. Seeherman H, Wozney J, Li R. Bone morphogenetic protein delivery systems. Spine 2002;27:16–23.
19. Luginbuehl V, Meinel L, Merkle HP, Gander B. Localized delivery of growth factors for bone repair. Eur J Pharm Biopharm 2004;58:197–208.
20. Seeherman H, Wozney JM. Delivery of bone morphogenetic proteins for orthopedic tissue regeneration. Cytokine Growth Factor Rev 2005;16:329–345.
21. Chen RR, Mooney DJ. Polymeric growth factor delivery strategies for tissue engineering. Pharm Res 2003;20:1103–1112.
22. Winn SR, Uludag H, Hollinger JO. Carrier systems for bone morphogenetic proteins. Clin Orthop Relat Res 1999;367:95–106.
23. Kirker-Head CA. Potential applications and delivery strategies for bone morphogenetic proteins. Adv Drug Deliv Rev 2000;43:65–92.
24. Li RH, Wozney JM. Delivering on the promise of bone morphogenetic proteins. Trends Biotechnol 2001;19:255–265.
25. Geesink RGT, Hoefnagels NHM, Bulstra SK. Osteogenic activity of OP-1 bone morphogenetic protein (BMP-7) in a human fibular defect. J Bone Joint Surg 1999;81:710–718.
26. Cook SD, Wolfe MW, Salkeld SL, Rueger DC. Effect of recombinant human osteogenic protein-1 on healing of segmental defects in non-human primates. J Bone Joint Surg 1995;77:734–750.
27. Bach FH, Fishman JA, Daniels N, Proimo J, Anderson B, Carpenter CB, Forrow L, Robson SC, Fineberg HV. Uncertainty in xenotransplantation: Individual benefit versus collective risk. Nature Med 1998;4:141–144.
28. Butler D, Wadman M, Lehrman S, Schiermeier Q. Last chance to stop and think on risks of xenotransplants. Nature 1998; 391:320–324.
29. DeLustro F, Dasch J, Keefe J, Ellingsworth L. Immune responses to allogeneic and xenogeneic implants of collagen and collagen derivatives. Clin Orthop 1990;260:263–279.
30. Boden SD, Maertin GJ, Morone MA, Ugbo JL, Moskovitz PA. Posterolateral lumbar intertransverse process spine arthodesis with recombinant human bone morphogenetic protein 2/hydroxyapatite-tricalcium phosphate after laminectomy in the nonhuman primate. Spine 1999;24:1179–1185.
31. Boyan BD, Lohmann CH, Somers A, Niederauer GG, Wozney JM, Dean DD, Carnes DL, Schwartz Z. Potential of porous poly-d,lactide-co-glycolide particles as a carrier for recombinant human bone morphogenetic protein-2 during osteoinduction in vivo. J Biomed Mater Res 1999;46:51–59.
32. Sung HJ, Meredith C, Johnson C, Galis ZS. The effect of scaffold degradation rate on three-dimensional cell growth and angiogenesis. Biomaterials 2004;25:5735–5742.
33. Brekke JH. A rationale for delivery of osteoinductive proteins. Tissue Eng 1996;2:97–114.
34. Kenley R, Marden L, Turek T, Jin L, Ron E, Hollinger JO. Osseous regeneration in the rat calvarium using novel delivery systems for recombinant human bone morphogenetic protein-2 (rhBMP-2). J Biomed Mater Res 1994;28:1139–1147.
35. Higuchi T, Kinoshita A, Takahashi K, Oda S, Ishikawa I. Bone regeneration by recombinant human bone morphogenetic protein-2 in rat mandibular defects. An experimental model of defect filling. J Periodontol 1999;70:1026–1031.
36. Lee SH, Shin H. Matrices and scaffolds for delivery of bioactive molecules in bone and cartilage tissue engineering. Adv Drug Deliv Rev 2007;59:339–359.
37. Weber FE, Eyrich G, Grätz KW, Maly FE, Sailer HF. Slow and continuous application of human recombinant bone morphogenetic protein via biodegradable poly(lactide-co-glycolide) foamspheres. Int J Oral Maxillofac Surg 2002;31:60–65.
38. Park GE, Pattison MA, Park K, Webster TJ. Accelerated chondrocyte functions on NaOH-treated PLGA scaffolds. Biomaterials 2005;26:3075–3082.
39. RaviKumar MN. Nano and microparticles as controlled drug delivery devices. J Pharm Pharm Sci 2000;3:234–258.
40. Wei G, Jin Q, Giannobile WV, Ma PX. The enhancement of osteogenesis by nano-fibrous scaffolds incorporating rhBMP-7 nanospheres. Biomaterials 2007;28:2087–2096.




ID: vijayk Date: 20/9/08 Time: 10:14 Path: J:/Production/JBMM/Vol00000/080450/3B2/C2JBMM080450

J_ID: ZA1 Customer A_ID: 08-0210.R1 Cadmus Art: JBMA32292 Date: 20-SEPTEMBER-08 Stage: I Page: 10



41. Hollinger J. Strategies for regenerating bone of the craniofacial complex. Bone 1993;14:575–580.
42. Cai Q, Yang J, Bei JZ, Wang SG. A novel porous cells scaffold made of polylactide-dextran blend by combining phase-separation and particle-leaching techniques. Biomaterials 2002;23: 4483–4492.
43. Haidar ZS, Hamdy RC, Tabrizian M. Protein release kinetics for core-shell hybrid nanoparticles based on the layer-by-layer assembly of alginate and chitosan on liposomes. Biomaterials 2008;29:1207–1215.
44. New RRC. Liposomes: A Practical Approach. Oxford: IRC; 1990. p 256–258.
45. Higuchi T. Rate of release of medicaments from ointment bases containing drugs in suspension. J Pharm Sci 1961;50: 874–875.
46. Heerklotz H, Tsamaloukas A, Kita-Tokarczyk K, Strunz P, Gutberlet T. Structural, volumetric, and thermodynamic characterization of a micellar sphere-to-rod transition. J Am Chem Soc 2004;126:16544–16552.
47. Haidar ZS, Azari F, Hamdy RC, Tabrizian M. In vitro characterization and cytotoxic effect of a liposome-based drug delivery system incorporating alternating L-b-L assembly of polyelectrolytes for craniofacial distraction osteogenesis. CBS 2006; abstract33.
48. Shiqu YE, Chaoyang W, Xinxing L, Zhen T. Multilayer nanocapsules of polysaccharide chitosan and alginate through layer-by-layer assembly directly on PS nanoparticles for release. J Biomat Sci Polymer Ed 2005;16:909–923.
49. Tabatt K, Sameti M, Olbrich C, Muller RH, Lehr C. Effect of cationic lipid and matrix lipid composition on solid lipid nanoparticles-mediated gene transfer. Eur J Pharm Biopharm 2004;57:155–162.
50. Asasutjarit R, Lorenzen SI, Sirivichayakul S, Ruxrungtham K, Ruktanonchai U, Ritthidej GC. Effect of solid lipid nanoparticles formulation compositions on their size. Zeta potential and potential for in vitro phis-hiv-hugag transfection. Pharm Res 2007;24:1098–1107.
51. Chellat F, Tabrizian M, Dumitriu S, Chornet E, Magny P, Rivard CH, Yahia L. Study of biodegradation behaviour of chitosan-xanthan microspheres in simulated physiological media. J Biomed Mater Res 2000;53:592–599.
52. Lindholm TC, Peel SAF, Sàndor GKB, Clokie CML. Intra-oral bone graft used to acquire viable bone cells to be used for tissue engineering. J Can Dent Assoc 2002;68:699.
53. Mizuno M, Kuboki Y. Osteoblast-related gene expression of bone marrow cells during the osteoblastic differentiation induced by type I collagen. J Biochem 2001;129:133–138.
54. Lee DH, Baek HS, Lee MH, Park JH. Production of bone morphogenetic protein-7 using pET expression system. Curr Appl Phys 2005;5:422–425.
55. Wang EA. Bone morphogenetic proteins (BMPs): Therapeutic potential in healing bony defects. Trend Biotechnol 1993;11: 379–383.
56. Gohel MC, Panchal MK, Jogani VV. Novel mathematical method for quantitative expression of deviation from the Higuchi model. AAPS PharmSciTech 2000;1:31.





ID: vijayk Date: 20/9/08 Time: 10:14 Path: J:/Production/JBMM/Vol00000/080450/3B2/C2JBMM080450

Biotechnol Lett
DOI 10.1007/s10529-009-0099-x

REVIEW

# Delivery of recombinant bone morphogenetic proteins for bone regeneration and repair. Part A: Current challenges in BMP delivery

**Ziyad S. Haidar · Reggie C. Hamdy · Maryam Tabrizian**

Received: 9 June 2009 / Revised: 17 July 2009 / Accepted: 20 July 2009


**Abstract** Recombinant human bone morphogenetic proteins (rhBMPs) have been extensively investigated for developing therapeutic strategies aimed at the restoration and treatment of orthopaedic as well as craniofacial conditions. In this first part of the review, we discuss the rationale for the necessary use of carrier systems to deliver rhBMP-2 and rhBMP-7 to sites of bone tissue regeneration and repair. General requirements for growth factor delivery systems emphasizing the distinction between localized and release-controlled delivery strategies are presented highlighting the current limitations in the development of an effective rhBMP delivery system applicable in clinical bone tissue engineering.

**Keywords** Bone morphogenetic proteins · Bone regeneration · Bone repair · Craniofacial surgery · Delivery systems · Orthopaedics

Z. S. Haidar · M. Tabrizian
Faculty of Dentistry, McGill University, 740 Rue Dr. Penfield Suite # 4300, Montréal, QC H3A 1A4, Canada

Z. S. Haidar · M. Tabrizian
Department of Biomedical Engineering, Faculty of Medicine, McGill University, Montréal, QC, Canada

Z. S. Haidar · R. C. Hamdy · M. Tabrizian (✉)
Center for Biorecognition and Biosensors, McGill University, 3775 University Street, Montréal, QC H3A 2B4, Canada
e-mail: maryam.tabrizian@mcgill.ca

Z. S. Haidar · R. C. Hamdy
Shriners Hospital for Children and Division of Orthopaedics, Montreal Children's Hospital, McGill University, 1529 Cedar Avenue, Montréal, QC H3A 1A6, Canada

Published online: 19 August 2009

## Introduction

Healing of bone fractures and reconstruction of critical-sized bone defects continue to present a significant challenge for orthopedists, traumatologists and maxillofacial surgeons. To address this need, the United Nations and the World Health Organization declared the years 2000–2010 as the Bone and Joint Decade (Weinstein 2000). Although autologous bone grafts are routinely used, limited graft accessibility and donor site morbidity as well as increased costs continue to drive the development of alternative methods for bone regeneration and repair (Geiger et al. 2003; Bishop and Einhorn 2007). Thus far, three new strategies (Rose et al. 2004) are currently undergoing vigorous investigation (Fig. 1): the transduction of genes encoding cytokines with osteogenic capacity into cells at repair sites (gene therapy); the transplantation of cultured osteogenic cells derived from host bone marrow (stem cell therapy) and the application of osteoinductive growth factors (protein therapy). Gene- and stem cell-based therapy will probably represent the next major advance however

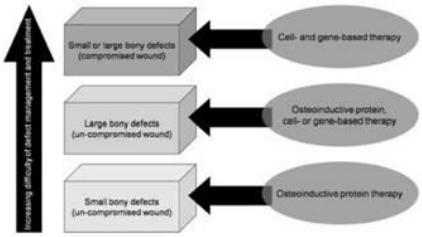


**Fig. 1** Tissue engineering therapeutic approaches and combinations according to defect complexity and difficulty

presently are still in their infancy regarding safety and efficacy in humans (Kimelman et al. 2007). Protein therapy, on the other hand, has demonstrated the most practical promise, mainly incorporating osteoinductive morphogens such as bone morphogenetic proteins (BMPs) even so with some limitations. BMPs are among the most potent cytokines in tissues and organs even beyond bone (Reddi 2005). The role of BMPs in bone development and repair has been extensively reviewed by numerous authors (Termaat et al. 2005; Bessa et al. 2008). BMP-2, -4, -7 and -9 may be the most potent osteoblastic differentiation inducers of mesenchymal progenitor cells into osteoblasts. For example, BMP-7, also known as osteogenic protein-1 or OP-1 has been shown to enhance the formation of new bone in numerous preclinical (Ripamonti et al. 2000; Hamdy et al. 2003) and clinical studies (Friedlaender et al. 2001; Vaccaro et al. 2008). BMPs act locally; yet, the exact cellular and molecular mechanisms are not fully understood (Gautschi et al. 2003). Small amounts induce cellular responses in vitro, however, when administered in vivo, rapid degradation and consequently insufficient and improper tissue regeneration occurred (Engstrand et al. 2008). It was suggested that the clinical efficacy of recombinant human (rh) forms of BMPs will depend on the carrier system used to ensure an effective delivery of adequate protein concentrations to the desired site (Mont et al. 2004). Thus far, several materials for the delivery of rhBMP-2 and rhOP-1 have been developed however with restricted clinical use (Termaat et al. 2005). This review aims at addressing the current challenges in BMP delivery strategies emphasizing the differences between *'localized'* and *'release-controlled'* systems commonly and mistakenly used interchangeably in an attempt to further understand the requirements for an effective protein therapy in clinical bone tissue engineering.

## Challenges in BMP delivery for bone regeneration and repair

For osteoregeneration to yield proper healing, mechanical stability in the defect site, osteogenic cells and osteoinductive growth factors in combination with a suitable carrier or delivery system, conceptualized as the "Diamond Concept" (Giannoudis et al. 2007) are necessary. The main role of the delivery system consequently is to retain the growth factor at the defect site for the bone regeneration and repair pertinent duration of time according to defect anatomical site, size and vascularity in order to allow the regenerative tissue forming cells to migrate to the defect area, proliferate and differentiate (Issa et al. 2008). BMPs are soluble and if delivered in a buffer solution, their clearance is rapid. Less than 5% of the BMP dose remains at the application site whereas combinations of the proteins with gelatin foam or collagen showed increased retention ranging from 15 to 55% (Hollinger et al. 1998). The use of biomaterials that can retain and sequester BMPs at the site of interest have been shown to greatly enhance efficacy and reduce protein dose by localizing the morphogenetic stimulus (Chen and Mooney 2002). Hence, the pharmacokinetics of rhBMP therefore can be influenced by the carrier used. Moreover, other challenges are related to individual proteins—regulation of effects and dose-response ratio. BMPs are currently being used in supra-physiologic concentrations and expensive dosages in the milligram range for satisfactory bone healing (Luginbuehl et al. 2004). The resulting tissue effects are occasionally overwhelming when viewed from a clinical point of view. Soft tissue edema, erythema, local inflammation, heterotopic ossification and immune response are the most remarkable although rarely reported. Osteoclastic activation has been noted in some cases as well where applied in large doses; bone resorption occurred (Gautschi et al. 2003). Additionally, currently used rhBMP-2 and rhBMP-7 are produced lacking a heparin-binding domain, hence probably reducing their clinical bioactivity (Saito et al. 2008). Recently, the osteoinductive effects of rhBMP-2 in combination

with a complex of heparin and chitosan in a gel formulation were shown to be superior when compared to rhBMP-2 implanted with type-I collagen in a rat model (Engstrand et al. 2008). Chemically-modified BMPs with enhanced affinity to their carriers showing altered stability, solubility, surface binding, bioactivity and biospecificity have been reported (Gautschi et al. 2003). Therefore, despite the ample evidence of the benefit of BMPs in bone regeneration and repair from preclinical and clinical studies, conclusive knowledge about BMP dosage, time-course, release dynamics and carriers remains to be determined. It is unclear why the impressive and convincing results seen in vitro and in animal models are difficult to reproduce in humans (Einhorn 2003). Unfavorable release kinetics, insufficient mechanical stability and porosity to allow cell and blood vessel infiltration into the carrier and inflammatory tissue reactions are few reasons. The effects of BMPs must therefore be *localized* as well as *regulated*. BMP delivery will also depend on the anatomic location where the treatment is required, the vitality of the soft tissue envelope and the mechanical strain environment provided by the surgical procedure (Einhorn 2003).

## Delivery systems parameters and requirements

Delivery systems should have the ability to provoke optimal inflammatory responses, be biocompatible and are often required to be bioresorbable. Processing conditions need to prevent protein aggregation or denaturation. Also, they have to be easily and cost-effectively manufactured for large-scale production. Appropriate storage, stability, handling and sterilization conditions are favored as well. Finally, all these processes need to be approved by regulatory agencies for the desired indication and application (Rose et al. 2004; Seeherman and Wozney 2005). There is probably not one single desirable pharmacokinetic profile that is predictive of success (Geiger et al. 2003) where various carrier and delivery materials have been examined *in vitro*, *in vivo* as well as in humans. These include demineralized collagenous bone matrix, collagen products, gelatin hydrogels, natural polymers and combinations of these materials and others (Lee and Shin 2007; Haidar et al. 2008a, b). Table 1 summarizes the desirable qualities of an ideal bone morphogenetic protein delivery system/carrier. Clearly, there is no ideal carrier or delivery system for all growth factors, pathologies, indications or clinical applications. Immediately after administration or implantation, BMPs are subject to the presence of fluid, protein competition, enzymatic activity, temperature, pH influence and salt concentrations (Dard et al. 2000). Each of these factors could lead to the release of a totally denatured growth factor in an uncontrolled manner and thus appends to the limited success of clinical BMP therapies. It is important thereby to emphasize that the enhancement of bone healing by BMPs is predominantly dependant on the parameters of a *combined* localized and release-controlled carrier/delivery system including: protein release kinetics and retention, protein dose size/concentration, mechanism of release and nature of the vehicle used in terms of biomaterial(s) and design/geometry.

### *Release kinetics and retention at defect site*

In physiologic bone repair, some growth factors such as BMP-2 are predominantly expressed during the early inflammatory phase. Others are up-regulated during the chondrogenic and osteogenic phases and have a biphasic expression pattern or are constitutively present. Furthermore, the cell pool present in the defect zone is dynamic by nature and different stimuli can attract different cell types to invade the compromised area (Cho and Nuttall 2002). Therefore, the impact of localized release kinetics for the therapeutic enhancement of skeletal repair becomes evident. Furthermore, recent evidence has suggested that cementogenesis and osteogenesis occur at different

**Table 1** General requirements for BMP delivery systems

| |
|---|
| Biocompatibility |
| Predictable biodegradability |
| Low immunogenicity and antigenicity |
| Enhancement of cellular vascularization and attachment |
| Affinity to BMPs and bone (defect) |
| Maintenance and enhancement of BMP bioactivity |
| Controlled and Metered/tailored protein release at an effective dose for the appropriate period of time according to defect anatomical site, size and vascularity |
| Malleability and ease of manufacture |
| Safety, stability, sterility, availability and cost-effectiveness |
| Regulatory agencies approval for th desired clinical indication and application |

Adopted and updated from Geiger et al. (2003)

rates during BMP-stimulated regeneration (Issa et al. 2008). However, few have investigated the influence of release kinetics on bone regeneration. The effect of BMP-2 release from slow and fast degrading gelatin carriers was not significantly different in a rat model of periodontal defects (Talwar et al. 2001). Higher retention times for BMP-2 were more osteoinductive in a rat ectopic assay (Uludag et al. 2001) and the prolonged delivery of BMP-2 enhanced the in vivo osteogenic efficacy of the protein compared to short-term delivery at equivalent dosage in another recent study (Jeon et al. 2008). Furthermore, retention of BMPs depends on whether the protein is immobilized within the carrier, adsorbed onto the surface or covalently-bonded during its formulation (Luginbuehl et al. 2004). Release should preferably be sustained over time (Haidar et al. 2008a, b). In designing a delivery system for differentiation factor release, it is apparent that the extremes of release (bolus injections or prolonged low level release) are not beneficial to bone induction (Geiger et al. 2003). While timing of the protein release is important, the dynamic nature of the healing zone makes it difficult to assess the state of the defect. It is certainly dependant on the type of defect, its location and appearance, the patient's age, gender, hormone and nutritional status, illness and other parameters (Li and Wozney 2001). Other factors (Kirker-Head 2000) influencing release rates include protein size and conformational changes, solubility, polymer/scaffold composition/geometry and molecular weight. Also, different animal species, ages and sizes may have varying optimum release profiles.

*Dose and concentration*

Maintaining a critical threshold concentration of the rhBMP at the defect site for the necessary period of time (temporal distribution) is crucial. Such supra-physiological dosages range from 0.01 mg/ml in small animal models such as rats to 0.4 mg/ml in rabbits to more than 1.5 mg/ml in non-human primates. Different anatomical sites require different therapeutic doses depending on the degree of vascularization, defect size and the number of resident responding cells. Ranges vary from fusion site to fusion site as well. In humans, for anterior inter-body fusion a total dose of 4.2–12 mg of rhBMP-2 at 1.5 mg/ml is recommended. For inter-transverse arthrodesis, the suggested dose of rhBMP-2 (based on pilot clinical trials) is 20 mg on each side at 2 mg/ml delivered in a 60% hydroxyapatite and 40% tricalcium phosphate (granules) carrier (Boden et al. 2002). The recommended dose of rhBMP-7 for recalcitrant long bone non-unions is 7 mg or 2 vials (each containing 3.5 mg reconstituted with 1 g of type I bovine collagen) and implanted at the non-union site. New delivery systems with optimized and controlled release profiles may decrease or even alleviate the need for excessive and expensive concentrations of BMPs. Our own work with rhBMP-7 encapsulated in a core-shell nanoparticulate delivery system showed that a dose as low as 100 ng/ml was significantly sufficient to enhance preosteoblast differentiation noted by an increased alkaline phosphatase activity over 7 days, *in vitro* (Haidar et al. 2008a, b). The formation of ectopic bone is also a potential concern that is substantially under-investigated. Paramore et al. implanted BMP-7 into the epidural space of dogs after laminectomy and posterolateral fusion. Animals demonstrated bone formation adjacent to their spinal cords causing mild spinal cord compression (Paramore et al. 1999). Novel carriers need to contain the BMP, prevent ectopic and heterotopic bone formation and utilize lower, safe and cost-effective dosages.

*Mechanisms of localized and release-controlled BMP delivery*

Growth factors release from a localized and release-controlled delivery system can either be (i) diffusion-controlled, (ii) chemical and/or enzymatic reaction-controlled, (iii) solvent-controlled, or (iv) controlled by combinations of these mechanisms (Luginbuehl et al. 2004; Haidar et al. 2008a, b). Diffusion-controlled release is governed by the solubility and diffusion coefficient of the protein in the aqueous medium, protein partitioning between the aqueous medium and material of the delivery system, the protein loading and the diffusional distance (Li and Wozney 2001). An example of diffusion-controlled release is BMP-2 release from porous scaffolds that was regulated via adjustment of pore size (Whang et al. 2000). In our own studies, TGF-$\beta$1 release from coral particles was modulated through modification of adsorption conditions and particle size (Demers et al. 2002). BMP-7 release from core-shell nanoparticles (Fig. 2) was controlled via the layer-by-layer build-up of natural polymers on liposomes (Haidar et al. 2008a, b). The

combination of the polymeric electrostatic-based assembly technique and nanoscaled liposomes yielded a stable and non-toxic delivery system consisting of a suspension of monodisperse nanoparticles suitable for the potential administration of growth factors via a parental injection as is preferable by surgeons. The nanoparticles tolerate extended shelf storage and allow for protein loading immediately preceding administration, preventing degradation or loss of the encapsulant. Controlled linear and multistep release of bioactive BMP-7 over an extended period of 45 days was evident. The increase in shell thickness slowed the rate of protein release where BMP-7 release from uncoated liposomes was clearly faster than from coated liposomes. BMP-7 release from this physically dispersed polymeric system may be described by several possible mechanisms: diffusion, polymer degradation, ion complexation, and interactions among the protein and the polymers, although it is primarily governed by a diffusion-based or affinity-based mechanism. Chemical and/or enzymatic reaction-controlled systems include erodible systems, where the protein is physically immobilized in the carrier matrix and released by degradation or dissolution of the carrier, or systems, where the protein is chemically bound to the polymer backbone and released upon hydrolytic or enzymatic cleavage of the bond. TGF-$\beta$1 release from cross-linked collagen sponges depended on the extent of cross-linking, as observed post-subcutaneous implantation into skull defects in rabbits (Ueda et al. 2002), for example. In solvent- or swelling-controlled systems, the protein is embedded in a carrier matrix and diffusional release occurs as a consequence of the rate-controlled penetration of solvent (water) into the system. Hence, to mimic the space- and time-restricted physiologic pattern of growth factor kinetics by the release kinetics of a vehicle, different strategies of controlling growth factor delivery are available (Luginbuehl et al. 2004).

*Injectable and multiple growth factor delivery*

Injectable delivery systems are gaining much interest as they could provide a less invasive method for the regeneration and repair of osseous defects with clinical indications including fresh fractures, non-union or delayed union, large bone defects associated with osseous tumor resection as well as the acceleration of periodontal therapy hence avoiding extensive/secondary surgery (Einhorn et al. 2003; Bishop and Einhorn 2007). A single, local, percutaneous injection of 80 μg rhBMP-2 in 25 μl buffer vehicle was shown to accelerate healing in femoral fracture rat model (Einhorn et al. 2003). Our group demonstrated earlier that a single bolus injection of rhBMP-7 (75 μg in acetate buffer) accelerated bone formation during long bone distraction osteogenesis in rabbits (Hamdy et al. 2003; Mandu-Hrit et al. 2006). Furthermore, preliminary results from our most recent in vivo assays in the same model have demonstrated that osteogenesis and consolidation were accelerated via a single localized injection of the core-shell delivery system loaded with a dose of no more than 1 μg rhBMP-7 (Haidar et al. 2009) accentuating the role of

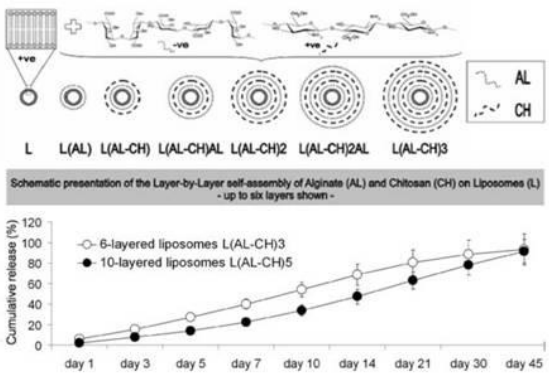


**Fig. 2** Release profile of BMP-7/OP-1 from a core-shell nanoparticulate delivery system

local and release-controlled nanoparticles. Also, we have demonstrated how the injected unloaded delivery system did not interfere with the osteoregenerative process mainly due to its biocompatible and biodegradable nature. Also, the natural polymers used to formulate the nanoparticles especially chitosan has been shown to promote osteogenesis and enhance the bioactivity of the encapsulated protein via controlling the release profile (Prabaharan 2008).

The use of this novel cost-effective delivery system has the potential to shorten the treatment period of long bone distraction osteogenesis and thus could diminish the morbidity and improve the functional outcome in patients via the earlier removal of the external fixator. Injectable scaffolds for bone tissue engineering are consisted of a mixture of bioactive molecules and solidifiable precursors which are injected into the defect site to form a 3-D structure in situ (Hou et al. 2004). Hosseinkhani et al. (2007) fabricated injectable transparent 3-D networks (hydrogel) of self-assembled peptide-amphiphile and BMP-2 and showed significant homogenous ectopic bone formation in the back subcutis of rats. Since growth factors act in a coordinated cascade of events to restore bone, delivering combinations of growth factors may have a great potential. However, the choice of growth factor combinations has to be with great care. The sequential release of BMP-2 in combination with IGF-1 has already been explored by Raiche and Puleo, nevertheless with commercialization-related difficulties (Raiche and Puleo 2004; Westerhuis et al. 2005). In another example, rhBMP-2 and bFGF absorbed to a collagen sponge resulted in decreased bone formation in a rabbit model of tibial fracture (Vonau et al. 2001). In conclusion, the delivery of the appropriate biologically-active growth factor(s) at the proper dose and concentration for the intended application using a biocompatible, biodegradable and bioresorbable delivery vehicle that will stabilize and prevent the rapid diffusion or dispersal of the encapsulant and promote localized osteogenesis at the defect site is essential.

## Future prospects

Bone regeneration and repair with BMPs are leading a new era in orthopaedic and craniofacial reconstruction. Their ability to substantially enhance bone formation and facilitate healing will likely be optimized by the simultaneous use with other growth and differentiation factors and/or with an expanded responsive cell population. The challenge for researchers today remains to deliver these osteoinductive factors in ways that would ensure consistent clinical success in humans. Currently, delivery of BMPs is still attempted through the direct local application of rhBMP to the regeneration or repair site with (primarily with the use of collagen carriers) or without a release-controlled carrier. Future studies will need to focus on the development of customizable, localized and release-controlled delivery materials and systems with the surgical practicality (mainly injectable) and adjustable growth factor(s) release profiles, according to defect site, size and vascularity. Intelligent delivery systems would provide BMPs and other growth factors in response to physiological requirements, having the capacity to sense changes of the bone defect's microenvironment and accordingly, alter protein release. Such systems may represent a step towards individualizing protein release kinetics. Given the complex nature of osseoregeneration, it is possible that multiple growth factor delivery exhibiting both stimulatory and inhibitory responses (for noggin, for instance) on bone formation with different release characteristics be the most desirable approach clinically, with caution to the choice of combinations. Other issues such as biosafety, cost-effectiveness, user-friendliness and optimum delivery time need to be addressed as well. Advances in biotechnology and biomaterials will certainly expand the number of tissue-engineering approaches with the use of BMPs assuring a promising future beyond the present Bone and Joint decade for millions of patients worldwide.

**Acknowledgments** The authors wish to thank grants from the Shriners of North America, Fonds de la Recherche en Santé du Québec, the National Science and Engineering Research Council, the Canadian Institutes of Health Research (CIHR)—Regenerative Medicine/Nanomedicine and the Center for Biorecognition and Biosensors (CBB), McGill University, Montréal, Québec, Canada. Dr. Haidar acknowledges scholarships from the Center for Bone and Periodontal Diseases Research and the Shriners Hospital, Montréal, Québec, Canada.

## References

Bessa PC, Casal M, Reis RL (2008) Bone morphogenetic proteins in tissue engineering: the road from the laboratory to

the clinic, part I (basic concepts). J Tissue Eng Regen Med 2:1–13
Bishop GB, Einhorn TA (2007) Current and future clinical applications of bone morphogenetic proteins in orthopaedic trauma surgery. Int Orthop 31(6):721–727
Boden SD, Kang J, Sandhu HS, Heller JG (2002) Use of rhBMP2 to achieve posterolateral lumbar spine fusion in humans: a prospective randomized clinical trial. Spine 27:2662–2673
Chen RR, Mooney DJ (2002) Polymeric growth factor delivery strategies for tissue engineering. Pharm Res 20: 1103–1112
Cho CH, Nuttall ME (2002) Emerging techniques for the discovery and validation of therapeutic targets for skeletal diseases. Expert Opin Ther Targets 6:679–689
Dard M, Sewing A, Meyer J, Verrier S, Roessler S, Scharnweber D (2000) Tools for tissue engineering of mineralized oral structures. Clin Oral Invest 4:126–129
Demers CN, Tabrizian M, Petit A, Hamdy RC, Yahia L (2002) Effect of experimental parameters on the in vitro release kinetics of transforming growth factor beta1 from coral particles. J Biomed Mater Res 59:403–410
Einhorn TA (2003) Clinical applications of recombinant human BMPs: early experience and future development. J Bone Joint Surg Am 85-A:82–88
Einhorn TA, Majeska RJ, Mohaideen A, Bouxsein ML, Turek TJ, Wozney JM (2003) A single percutaneous injection of rhBMP-2 accelerates fracture repair. J Bone Joint Surg Am 85-A:1425–1435
Engstrand T, Veltheim R, Arnander C, Docherty-Skogh AC, Westermark A, Ohlsson C, Adolfsson L, Larm O (2008) A novel biodegradable delivery system for bone morphogenetic protein-2. Plast Reconstr Surg 121:1920–1928
Friedlaender GE, Perry CR, Cole JD, Cook SD, Cierny G, Muschler GF et al (2001) Osteogenic protein-1 (bone morphogenetic protein-7) in the treatment of tibial nonunions. J Bone Joint Surg Am 83-A:151–158
Gautschi OP, Frey SP, Zellweger R (2003) Bone morphogenetic proteins in clinical applications. ANZ J Surg 77: 626–631
Geiger M, Li RH et al (2003) Collagen sponges for bone regeneration with rhBMP-2. Adv Drug Deliv Rev 55: 1613–1629
Giannoudis PV, Einhorn TA, Marsh D (2007) Fracture healing: the diamond concept. Injury 38(S4):3–6
Haidar ZS, Hamdy RC, Tabrizian M (2008a) Protein release kinetics for core-shell hybrid nanoparticles based on the layer-by-layer assembly of alginate and chitosan on liposomes. Biomaterials 29:1207–1215
Haidar ZS, Azari F, Hamdy RC, Tabrizian M (2008b) Modulated release of OP-1 and enhanced pre-osteoblast differentiation using a core-shell nanoparticulate system. J Biomed Mater Res A (in press)
Haidar ZS, Tabrizian M, Hamdy RC (2009) A hybrid OP-1 delivery system enhances new bone regeneration and consolidation in a rabbit model of distraction osteogenesis. Growth Factors (in press)
Hamdy RC, Amako M, Beckman L, Kawaguchi M, Rauch F, Lauzier D, Steffen T (2003) Effects of osteogenic protein-1 on distraction osteogenesis in rabbits. Bone 33:248–255
Hollinger JO, Schmitt JM, Buck DC, Shannon R, Joh SP, Zegzula HD, Wozney J (1998) Recombinant human bone morphogenetic protein-2 and collagen for bone regeneration. J Biomed Mater Res 43:356–364
Hosseinkhani H, Hosseinkhani M, Tian F, Kobayashi H, Tabata Y (2007) Bone regeneration on a collagen sponge self-assembled peptide-amphiphile nanofiber hybrid scaffold. Tissue Eng 13:11–19
Hou Q, De Bank PA, Shakesheff KM (2004) Injectable scaffolds for tissue regeneration. J Mater Chem 14:1915–1923
Issa JP, Bentley MV, Iyomasa MM, Sebald W, De Albuquerque RF (2008) Sustained release carriers used to delivery bone morphogenetic proteins in the bone healing process. Anat Histol Embryol 37:181–187
Jeon O, Song SJ, Yang HS, Bhang SH, Kang SW et al (2008) Long-term delivery enhances in vivo osteogenic efficacy of BMP-2 compared to short-term delivery. Biochem Biophys Res Commun 369:774–780
Kimelman N, Pelled G, Helm GA, Huard J, Schwarz EM, Gazit D (2007) Review: gene- and stem cell-based therapeutics for bone regeneration and repair. Tissue Eng 13: 1135–1150
Kirker-Head CA (2000) Potential applications and delivery strategies for bone morphogenetic proteins. Adv Drug Deliv Rev 43:65–92
Lee SH, Shin H (2007) Matrices and scaffolds for delivery of bioactive molecules in bone and cartilage tissue engineering. Adv Drug Deliv Rev 59(4–5):339–359
Li RH, Wozney JM (2001) Delivering on the promise of bone morphogenetic proteins. Trend Biotechnol 19:255–265
Luginbuehl V, Meinel L et al (2004) Localized delivery of growth factors for bone repair. Eur J Pharm Biopharm 58:197–208
Mandu-Hrit M, Haque T, Lauzier D, Kotsiopriftis M, Rauch F, Tabrizian M, Henderson JE, Hamdy RC (2006) Early injection of OP-1 during distraction osteogenesis accelerates new bone formation in rabbits. Growth Factors 24:172–183
Mont MA, Ragland PS, Biggins B, Friedlaender G et al (2004) Use of bone morphogenetic proteins for musculoskeletal applications. An overview. J Bone Joint Surg 86:41–55
Paramore CG, Lauryssen C, Rauzzino MJ, Wadlington VR et al (1999) The safety of OP-1 for lumbar fusion with decompression: a canine study. Neurosurgery 44:1151–1156
Prabaharan M (2008) Chitosan derivatives as promising materials for controlled drug delivery. J Biomater Appl 23:5–36
Raiche T, Puleo A (2004) In vitro effects of combined and sequential delivery of two bone growth factors. Biomaterials 25:677–685
Reddi AH (2005) BMPs: from bone morphogenetic proteins to body morphogenetic proteins. Cytokine Growth Fact Rev 16:249–250
Ripamonti U, Van Den Heever B, Crooks J, Tucker MM, Sampath TK, Rueger DC, Reddi AH (2000) Long-term evaluation of bone formation by osteogenic protein 1 in the baboon and the relative efficacy of bone-derived bone morphogenetic proteins delivered by irradiated xenogenic collagenous matrices. J Bone Min Res 15:1798–1809
Rose FR, Hou Q, Oreffo RO (2004) Delivery systems for bone growth factors—the new players in skeletal regeneration. J Pharm Pharmacol 56:415–427

Saito K, Konishi I, Nishiguchi M, Hoshino T, Fujiwara T (2008) Amelogenin binds to both heparan sulfate and bone morphogenetic protein 2 and pharmacologically suppresses the effect of noggin. Bone 43:371–376

Seeherman H, Wozney JM (2005) Delivery of bone morphogenetic proteins for orthopedic tissue regeneration. Cytokine Growth Factor Rev 16:329–345

Talwar R, Di Silvio L, Hughes FJ, King GN (2001) Effects of carrier release kinetics on bone morphogenetic protein-2-induced periodontal regeneration in vivo. J Clin Periodontol 28:340–347

Termaat MF, Den Boer FC, Bakker FC, Patka P, Haarman HJ (2005) Bone morphogenetic proteins. Development and clinical efficacy in the treatment of fractures and bone defects. J Bone Joint Surg Am 87:1367–1378

Ueda H, Hong L, Yamamoto M, Shigeno K, Inoue M et al (2002) Use of collagen sponge incorporating transforming growth factor-beta1 to promote bone repair in skull defects in rabbits. Biomaterials 23:1003–1010

Uludag H, Gao T, Porter TJ, Friess W, Wozney JM (2001) Delivery systems for BMPs: factors contributing to protein retention at an application site. J Bone Joint Surg Am 83-A: 128–135

Vaccaro AR, Whang PG, Patel T, Phillips FM et al (2008) The safety and efficacy of OP-1 (rhBMP-7) as a replacement for iliac crest autograft for posterolateral lumbar arthrodesis: minimum 4-year follow-up of a pilot study. Spine J 8:457–465

Vonau RL, Bostrom MP, Aspenberg P, Sams AE (2001) Combination of growth factors inhibits bone ingrowth in the bone harvest chamber. Clin Orthop Relat Res 386:243–251

Weinstein SL (2000) 2000–2010: the bone and joint decade. J Bone Joint Surg Am 82:1–3

Westerhuis RJ, van Bezooijen RL et al (2005) Use of bone morphogenetic proteins in traumatology. Injury 36: 1405–1412

Whang K, Tsai DC, Nam EK, Aitken M, Sprague SM, Patel PK, Healy KE (2000) Ectopic bone formation via rhBMP-2 delivery from porous bioabsorbable polymer scaffolds. J Biomed Mater Res 42:491–499

Biotechnol Lett
DOI 10.1007/s10529-009-0100-8

REVIEW

# Delivery of recombinant bone morphogenetic proteins for bone regeneration and repair. Part B: Delivery systems for BMPs in orthopaedic and craniofacial tissue engineering

**Ziyad S. Haidar · Reggie C. Hamdy · Maryam Tabrizian**

Received: 9 June 2009 / Revised: 17 July 2009 / Accepted: 20 July 2009


**Abstract** Localized and release-controlled delivery systems for the sustained expression of the biologic potency of rhBMPs are essential. A substantial number of biomaterials have been investigated thus far. Most fail after implantation or administration mainly due to either being too soft, difficult to control and/or stabilize mechanically. In the second part of this review, we review a representative selection of rhBMP-2 and rhBMP-7 carrier materials and delivery systems ranging from simple nano/microparticles to complex 3-D scaffolds in sites of orthopaedic and craniofacial bone regeneration and repair.

Z. S. Haidar · M. Tabrizian
Faculty of Dentistry, McGill University, 740 Rue Dr. Penfield Suite # 4300, Montréal, QC H3A 1A4, Canada

Z. S. Haidar · M. Tabrizian
Department of Biomedical Engineering, Faculty of Medicine, McGill University, Montréal, QC, Canada

Z. S. Haidar · R. C. Hamdy · M. Tabrizian (✉)
Center for Biorecognition and Biosensors, McGill University, 3775 University Street, Montréal, QC H3A 2B4, Canada
e-mail: maryam.tabrizian@mcgill.ca

Z. S. Haidar · R. C. Hamdy
Shriners Hospital for Children and Division of Orthopaedics, Montreal Children's Hospital, McGill University, 1529 Cedar Avenue, Montréal, QC H3A 1A6, Canada

Published online: 19 August 2009

**Keywords** Biomaterials · Bone morphogenetic proteins · Bone regeneration · Controlled-release · Nanoparticles · Synthetic polymers

## Introduction

Attempts to induce *de novo* bone formation for bridging defects using bone grafting procedures, segmental bone transport, distraction osteogenesis or biomaterials have been applied to a great extent (Kneser et al. 2006; Mussano et al. 2007). Several materials for the delivery of recombinant human (rh) forms of bone morphogenetic proteins (BMPs) have been developed in recent years with only specific collagen-based formulations for rhBMP-2 and rhBMP-7/rhOP-1 obtaining FDA approval for their restricted clinical use in humans, namely in orthopaedic and spinal fusion applications (Table 1). The ultimate goal would be to develop safe, proficient, user-friendly and cost-effective rhBMP delivery systems that would completely replace traditional grafting procedures in a number of diverse applications (Moioli et al. 2007; Schmidmaier et al. 2008). In this review, we classify and discuss the carrier biomaterials, particularly natural and synthetic polymers and their combinations in different formats for the delivery of rhBMP-2 and rhBMP-7 to preclinical and clinical sites of bone regeneration and repair.

**Table 1** Overview of FDA-approved rhBMP-2 and rhBMP-7/rhOP-1 devices

| Protein | FDA approval year | Indications | Delivery system | Type of FDA approval |
|---|---|---|---|---|
| rhBMP-2 | 2002 | Single-level anterior lumbar interbody fusion | Medtronic INFUSE® Bone Graft + LT-CAGE® | Full |
| | | Acute, open tibial shall fractures | Medtronic INFUSE® Bone Graft + intramedullary nail | |
| rhBHP-7/rhOP-1 | 2002 | Posterolateral (Intertransverse) lumbar spinal fusion | Stryker® OP-1 putty | HDE program |
| | | Recalcitrant long bone non-unions | Stryker® OP-1 implant | |

*ACS* absorbable collagen sponge; *LT-CAGE®* lumbar tapered fusion device; *HDE* humanitarian device exemption; OP-1 putty; rhOP-1 + Type 1 bovine bone collagen matrix + carboxymethylcellulose as an additive; OP-1 implant rhOP-1 + purified bone-derived collagen particles as a scaffold

## BMP delivery systems

Challenges in BMP delivery have been discussed in Part A of this review (preceding review). It has been for long suggested that to induce osteogenesis, a suitable delivery system is required for new bone to form due to the very short half-life (1–4 h) of these cytokines (Takaoka et al. 1991), thus requiring large single doses or multiple smaller applications (Talwar et al. 2001). Also, given that BMPs are not bony tissue-specific (Okubo et al. 2000), their localized (vs. systemic) and release-controlled (vs. un-controlled) delivery is necessary to prevent any undesired and un-controlled ectopic bone formation in non-bony tissues of the body (Schmidmaier et al. 2008). The FDA of the USA approved bovine collagen-based delivery devices for rhBMP-2 and rhBMP-7 have limited indications in spinal interbody fusion and open tibial non-unions, respectively, mainly due to the large doses required to achieve the desired osteogenic effect where there is more exogenous BMP in a single dose than is present in 1000 humans, hence raising serious concerns regarding safety and cost (Kwon and Jenis 2005). Supra-physiological concentrations resulting from imperfect release kinetics of BMPs where 30% of the encapsulate is lost in the initial bust phase (Geiger et al. 2003) are additionally being related to severe clinical complications including generalized hematomas in soft tissue and para-implant bone resorption (Gautschi et al. 2003; Robinson et al. 2008).

### BMP-specific carrier types and delivery materials

Researchers have commonly explored biomaterials with demonstrated osteoconductive properties. However, an *ideal* BMP carrier material needs to be osteoconductive, osteoinductive and osteogenic (Seeherman and Wozney 2005; De Long et al. 2007; Schmidmaier et al. 2008). Although intensively evaluated in animal studies as well as in clinical trials with satisfactory results, bovine collagen has also demonstrated some safety issues mainly owing to its xenogenic origin. Polymeric matrices have attracted attention over the last years to achieve the localized and controlled release of proteins over long periods of time and overcome limitations in enzymatic susceptibility, stability during storage and efficacy upon administration (Termaat et al. 2005; Moioli et al. 2007; Schmidmaier et al. 2008). Generally, the major categories of carrier materials (Table 2) include: (1) natural-origin polymers such as collagen, hyaluronans, soy- and alga-derived materials, and poly(hydroxyalkanoates); (2) inorganic materials and ceramics/cements such as hydroxyapatite, tri-calcium phosphates and -sulphates as well as bioglasses and metals; (3) synthetic biodegradable polymers such as poly(lactic acid) (PLA), polyglycolide (PLG) and their copolymers, poly L-lactic acid (PLLA), poly D,L-lactide-co-gycolic acid (PLGA) and poly ε-caprolactone (PCL); and (4) *composites* which are combinations that take advantage of each material class as well as other biomolecules (Fei et al. 2008).

**Table 2** Major classes of carrier materials and selective experimental studies of BMP-incorporated delivery systems

| Carrier material | Advantages | Disadvantages | Types | BMP/material type/animal model site | Selected references |
|---|---|---|---|---|---|
| Natural polymers | Biocompatible, biodegradable, soluble in physiologic fluids with natural affinity for BMPs | Immunogenicity, pathogen transmission processing and sterilization difficulties | Collagen (gel, nano fibres, scaffolds and films), fibringlue, alginate and chilosan | BMP-2/getalin hydrogel/rabbit ulna | Yamamoto et al. (2006) |
| | | | | BMP-2/chilosan/ rat mandible | Issa et al. (2008a, b) |
| Inorganic materials | Similar to bone degradable/non-degradable, osteoconductive, self-setting ability in vivo and have affinity for BMPs | Brittle, difficult mold and some calcium phosphate cements (CPC) are exothermic | CPC, bioactive glasses, Hydroxyapatite, hyaluronic acid, tri-calcium phosphates, metals, ceramics and calcium sulfate | BMP-2/ Hyaluronic acid/ in vitro/spine | Kim and Valentini (2002) |
| | | | | BMP-2/CPC in ACS/monkey/ spine | Barnes et al. (2005) |
| | | | | BMP-2/CPC putty/rabbit cranium | Haddad et al. (2005) |
| Synthetic polymers | Excellent chemical and mechanical properties, easy to process and sterilize, flexible to tailor and reproducible | Inflammatory response, localized pH drop due to by-products acidity and limited biological function | Polymers of α-hydroxy esters such as PLA, PGA and copolymers of these two monomers (PLGA) | BMP-2/PLGA micro particle/ rat cranium | Woo et al. (2001) |
| | | | | BMP-2/PLA-DX-PEG | Saito and Takaoka (2003) |
| | | | | Injectable PLA-PEG/mouse/ orthotropic | Saito et al. (2005) |
| Composites | According to combination from different material (and biomolecule) dasses | Complex manufacturing processes | Collagen-HA and titanium-PLLA | BMP-2/collagen PLG-alginate rat calvaria | Kenley et al. (1994) |
| | | | | BMP-7/PLGA-PLLA scaffold/ rat s.c. | Wei et al. (2007) |
| | | | | BMP-7/liposomes coated with alginate and chitosan (layer-by-layer)/rabbit/ libia | Haidar et al. (2008a, b) |
| | | | | | Haidar et al. (2009) |

Modified and updated from Li and Wozney (2001); Lee and Shin (2007)

## Natural-origin polymeric carriers

### *Collagen*

Collagen is the most abundant protein in connective tissues of mammals and the major non-mineral component of bone with a well established role in cellular infiltration and wound healing (Geiger et al. 2003). It has been prepared in powders, membrane films and implantable absorbable sponges as well as in aqueous forms (Geiger et al. 2003; Lee and Yuk 2007). Despite being known for versatility and ease of manipulation, manufacturing collagen carriers is highly sensitive to several factors including mass, soaking time, protein concentrations, sterilization methods, buffer composition as well as pH and ionic strength (between collagen and the encapsulant) that directly affects the binding of rhBMPs (Gao and

**Table 3** rhBMP-2 and rhBMP-7/rhOP-1 use in clinical studies

| Protein | Carrier | Application | Total number of patients | References |
|---|---|---|---|---|
| rhBMP-2 | Absorbable collagen sponge (ACS) | Anterior lumbar interbody arthrodesis | 46 and 279 (2 trials) | Burkus et al. (2002a, b) |
| | Bovine ACS | Open tibial shaft intermedullary fixation | 450 | Govender et al. (2002) |
| | Bovine ACS | Cervical anterior arthrodesis | 33 | Baskin et al. (2003) |
| | Xenogenic bone (Bio-Oss) | Maxillary implant placement | 11 | Jung et al. (2003) |
| | ACS | Anterior lumbar interbody arthrodesis | 131 | Burkus et al. (2005) |
| | ACS | Maxillary sinus floor augmentation | 48 | Boyne et al. (2005) |
| | ACS | Mandibular continuity defects | 14 | Herford and Boyne (2008) |
| rhBMP-7/ rhOP-1 | Type I collagen | Fibular osteotomy (critical-sized defects) | 24 | Geesink et al. (1999) |
| | Type I collagen | Maxillary sinus floor elevation | 3 | van den Bergh et al. (2000) |
| | Type I collagen | Tibial intramedullary fixation (non-union) | 122 | Friedlaender et al. (2001) |
| | Type I collagen | Posterolateral lumbar arthrodesis (non-instrumented) | 20 | Johnsson et al. (2002) |
| | ACS | Fresh tibial fracture (external fixation) | 14 | Maniscalco et al. (2002) |
| | OP-1 putty* | Posterolateral lumbar fusions | 36 | Vaccaro et al. (2005) |
| | OP-1 putty | Posterolateral lumbar arthrodesis (instrumented) | 19 | Kanayama et al. (2006) |
| | OP-1 putty | Posterolateral lumbar arthrodesis | 24 | Vaccaro et al. (2008) |

*OP-1 putty consists of rhOP-1, Type I bovine bone collagen matrix and an additive; carboxymethylcellulose sodium

Uludag 2001; Lee and Yuk 2007). Absorbable collagen sponges (ACS) have been evaluated in numerous in vivo models and clinical trials. In the healing of a critical-sized radial defect stabilized by an external fixator, Sciadini and Johnson compared the efficacy of various dosages of rhBMP-2 delivered in an ACS to autogeneous bone grafts in 27 dogs. Defects treated with rhBMP-2 showed better healing than those treated with the ACS alone or autogeneous bone grafts (Sciadini and Johnson 2000). Paramount evidence, nonetheless, is derived from well-designed clinical trials. Table 3 lists selected examples of randomized clinical trials and clinical case series. The BESTT study investigated low (0.75 mg/ml) and high (1.5 mg/ml) doses of rhBMP-2 impregnated in an ACS. At 12 months, patients in the latter group had statistically significant accelerated healing, fewer invasive interventions and a lower rate of non-union than the control group (Govender et al. 2002). In patients requiring staged maxillary sinus floor augmentation, rhBMP-2/ACS safely induced adequate bone formation for the placement and functional loading of endosseous dental implants (Boyne et al. 2005). The use of rhBMP-2/ACS without concomitant bone grafting materials in critical-sized mandibular defects produced excellent regeneration in a very recent case review of 14 patients (Herford and Boyne 2008). On the other hand, no differences using rhBMP-7 incorporated in a type I collagen carrier over 24 months were detected in a prospective clinical trial (Friedlaender et al. 2001). It was concluded to be similar to autografts in the management of non-unions except for the pain factor associated with the donor site. Although eliminating the need to harvest autologous bone and alleviating the associated pain, animal-derived collagens are limited by their xenogenic nature (mostly bovine and porcine skin) where anti-type I collagen antibodies developed in almost 20% of patients treated with rhBMP-2/ACS (Sciadini and Johnson 2000, Geiger et al. 2003; Bessa et al. 2008). Also, sterilization is usually using ethylene oxide prior to soaking the sponge in the BMP solution; hence, with an effect on the release kinetics or the bioactivity of the protein within (Gittens and Uludag 2001). Furthermore, without delivery in situ, BMPs rapidly diffuse away from defect site (Sciadini and

Johnson 2000) probably explaining some of the discrepancies noted in preclinical and clinical outcomes (Chen and Mooney 2003). Therefore, other sources of collagen (recombinant perhaps) and biomaterials are currently being evaluated for rhBMP delivery, though still at the preclinical stages.

*Alginate and chitosan*

Alginate (AL) is a non-immunogenic polysaccharide found abundantly in the surface of seaweeds used in a wide range of tissue engineering applications due to its gel-forming properties (Tönnesen and Karlsen 2002). Injectable in situ-forming AL gels were prepared then loaded with an osteoinductive growth factor (IGF-I), for example. Significantly accelerated proliferation of osteoblast-like MG-63 cells favorable for the conformal filling of bone defects was demonstrated (Luginbuehl et al. 2004). Furthermore, encapsulant release from AL matrices can be modulated by different parameters such as particle size, viscosity and chemical composition. Liew et al. (2006) in a recent investigation found that particle size affected the extent of burst release and the higher the viscosity the slower the encapsulant release. Chitosan (CH) is a cationic copolymer of *N*-acetyl-D-glucosamine and glucosamine prepared by *N*-deacetylation of chitin well-known for its biological, chelating and adsorbing properties (Kumar et al. 2004; Lee and Yuk 2007). Practical use of CH has been mainly confined to unmodified forms as they have solely demonstrated favorable biodegradation kinetics slower than polymers such as collagen. However, the chemical-modification and graft co-polymerization onto CH further improved controlling the release profile of bioactive molecules and some have been described as osteoinductive materials (Prabaharan 2008). Novel chemically-modified CHs with controllable photo-curability showed enhanced biocompatibility and bone tissue repair in athymic rats (Qiu et al. 2008). Furthermore, rhBMP-2/CH accelerated osteogenesis in a rat critical-sized mandibular defect. CH adapted well to the defect and had favorable release kinetics as revealed by the amount of new bone tissue (Issa et al. 2008a, b).

*Hyaluronic acid*

Hyaluronic acid (HA) is another naturally-occurring biopolymer, which plays a significant role in wound healing. HA and its derivatives have been largely studied in biomedical and tissue engineering applications as gels, sponges and pads and as a viscous gel injected percutaneously in ophthalmic surgery (O'Regan et al. 1994; Bessa et al. 2008). HA also has an osteoinductive action itself where it has been shown to result in improved bone formation in mandibular defects in comparison to collagen sponges when both carriers were used to deliver BMP-2 in rats as well as in a human clinical trial (Arosarena and Collins 2005). That is probably due to that HA-based delivery vehicles might posses the capacity to retain more BMPs than collagen (Kim and Valentini 2002). In addition, hyaluronans seem to stimulate the proliferation of bone marrow stromal cells, expression of osteocalcin, enhance ALP activity and interact positively with BMPs to generate direct and specific cellular effects. This increased affinity is attributed to HA being anionic thus forming ionic bonds with the cationic BMPs significant for potential future clinical applications (Peng et al. 2008). Other less common natural polymers in BMP delivery include gelatin, dextran and fibrin as they are limited by their mechanical strength and fusion with other biomolecules or biomaterials seems necessary, nonetheless with promising applications in angiogenesis (Young et al. 2005).

Inorganic materials

*Hydroxyapatite*

Hydroxyapatite (HAP) is well known for its osteoconductivity and has been widely used as a bone-substitute material clinically since the 1970s due of its ability to bond directly with bone (Li and Wozney 2001). Synthetic HAP comes in ceramic (porous and non-porous) or non-ceramic, cementable form (Moore et al. 2001) with only porous HAP being evaluated as a scaffold and a controlled release carrier (particles, powder, granules, disks or blocks) of BMPs for bone regeneration (Bessa et al. 2008). However, lack of bone induction due to the high affinity between the material and the BMPs in addition to the lack of resorption of the HAP and dependence on the geometry of the substratum was evident (Noshi et al. 2001). Therefore, HAP has often been combined with tri-calcium phosphates, collagen, other natural and synthetic polymers to form a more

rigid, resorbable and porous BMP carrier. Generally, such composites have demonstrated better local BMP delivery and bone formation than HAP alone in various bone defects in vivo (Schopper et al. 2008; Kim et al. 2008).

*Calcium phosphates and bioactive glasses*

Inorganic materials such as calcium phosphate-based cements, ceramics and coatings (CPCs) have proven to be versatile carriers that can be formulated as implantable and injectable cements. They harden in vivo and can be used to deliver bioactive growth factors (in low temperature forms to prevent protein denaturation) with established prominent bone formation (Moore et al. 2001; Ginebra et al. 2006). Ceramics are known to mimic natural bony structure when implanted (Schmidmaier et al. 2008). Furthermore, overall, lower dosages of BMPs are required with the use of CPCs compared to other carriers (Ginebra et al. 2006). However, phase separation during injection, lack of intrinsic macroporosity to allow cell infiltration, intrinsic radiopaque nature and decreased mechanical tensile and shear properties compared to bone and other materials are among the main disadvantages of CPCs (Seeherman and Wozney 2005). Modifications to increase injectability and macroporosity in vivo have been recently reported (Bohner and Baroud 2005). Also, CPCs have been used as a bulking agent to improve the osteogenicity of ACS loaded with rhBMP-2 where it helped lowering the BMP dose (>3-fold) in a spinal fusion model in the non-human primate model (Barnes et al. 2005). Bioactive glasses (BG) are a group of hard and non-porous silica-based bioactive compounds which are known to bond directly to bone due to their good osteointegrative and osteoconductive properties. They have different resorption rates depending on their chemical compositions where solubility is proportional to the sodium oxide content (Välimäki and Aro 2006). BG, such as 45S5 Bioglass, are commonly used as filler material for fractured bone, augmentation of the alveolar ridge and vertebral implants. Recent studies have shown that BG induce a high local bone turnover in vitro and in vivo where they increase the BMP effect, support osteoblast growth and favor osteoblast differentiation by stimulating the synthesis of phenotypic markers like alkaline phosphatase, collagen Type I and osteocalcin (Moore et al. 2001; Välimäki and Aro 2006).

Synthetic biodegradable polymeric carriers

Unlike natural polymers and collagen, synthetic biodegradable polymers pose no danger of immunogenicity or possibility of disease transmission. A number of synthetic biodegradable polymeric delivery systems for BMP-2 were discussed in two recent reviews (Saito and Takaoka 2003, 2005). The most commonly used polymers herein are PLLA and PLGA. Their degradation is primarily via hydrolysis and different proportional combinations of PGA and PLA, for example, demonstrate various material properties which in turn affect biodegradability. Material crystallinity and scaffold morphology (pore size/number) also play an important role in biodegradability where a more porous scaffold degrades faster as will that comprised of low molecular weight polymers. Synthetic polymers can be processed into highly porous 3-D scaffolds, fibers, sheets, blocks or microspheres (Seeherman and Wozney 2005). BMP release is by means of diffusion, polymer swelling followed by fast diffusion-controlled release, and polymer erosion (Engstrand et al. 2008). Bioresorbable PLA/PGA beads were found to be superior to collagen when used to deliver rhBMP-2 to transosseous rat mandibular defects (Zellin and Linde 1997). PLGA was evaluated successfully in several canine defect models such as for BMP-2-induced periodontal regeneration, maxillary alveolar cleft repair, and segmental ulnar long-bone defects (Sigurdsson et al. 1996; Mayer et al. 1996; Itoh et al. 1998). Nonetheless, the main limitation is their acidic breakdown by-products and the associated risk of inflammatory response if not cleared quickly which is detrimental to the stability of the encapsulated BMPs and the overall therapeutic outcome (Saito et al. 2005). As a result, a continuous supply of osteoinductive factors would be crucial to compensate for polymer degradation (Schliephake et al. 2008).

Composites

Combinations of different material classes (Table 2) have been used to optimize the benefits and overcome the limitations of many of the above materials. Examples of recent composites include glycidyl methacrylated dextran (Dex-GMA)/gelatin scaffolds containing microspheres loaded with rhBMP-2 and implanted into the periodontal defects of dogs

(Chen et al. 2007), PLGA-gelatin composites for the delivery of rhBMP-2 to vertical alveolar ridge augmentation in dogs (Kawakatsu et al. 2008), HAP-coated porous titanium/rhBMP-2/HA in the metaphysic of the distal femur of rabbits (Peng et al. 2008) and PEG hydrogel/rhBMP-2/HAP/TCP granules in the rabbit calvarial bones (Jung et al. 2008). A 3-D, highly porous PLA/HAP/collagen scaffold was prepared for use in healing of canine segmental bone defects. The HAP/collagen portion was to mimic the natural extracellular matrix of bone, with the collagen serving as a template for apatite formation. All defects healed satisfactorily (Hu et al. 2003). Fu et al. recently combined rabbit mesenchymal stem cells (MSCs) with AL/BMP-2 and implanted the composite in a posterolateral intertransverse fusion model in 24 rabbits. Results demonstrated that MSCs delivered with rhBMP-2 (2.5 mg) are more osteoinductive than MSCs without rhBMP-2 and that the composite material enhanced bone formation and spine fusion success (Fu et al. 2008).

Nano- and micro-particles from synthetic polymers and natural polymers (Fig. 1) are other dosage forms that have consummated much attention for the localized and release-controlled delivery of growth factors due to their attractive tendency to amass in sites of inflammation (Lee and Shin 2007). Enhanced in vivo tissue regeneration using PLGA and gelatin microparticles for growth factor release was reported (Park et al. 2005). Compared to microparticles, nanoparticle and nanofiber delivery systems have demonstrated superiority in terms of longer residencies in general circulation, consequently extending the bioactivity of the entrapped molecule (Nair and Laurencin 2008). In a recent example of a combined localized and release-controlled delivery system, PLGA nanospheres (NS) immobilized onto prefabricated nanofibrous PLLA scaffolds were used to load and deliver rhBMP-7 (Wei et al. 2007; Ma 2008). BMP-7 delivered from NS-scaffolds induced significant ectopic bone formation while passive adsorption of the protein into the scaffold resulted in failure of bone induction either due to the loss of protein bioactivity or its rapid release from the scaffolds upon implantation in vivo.

We have successfully encapsulated a model protein, bovine serum albumin in monodisperse and non-toxic nanoparticles constituting a core of cationic

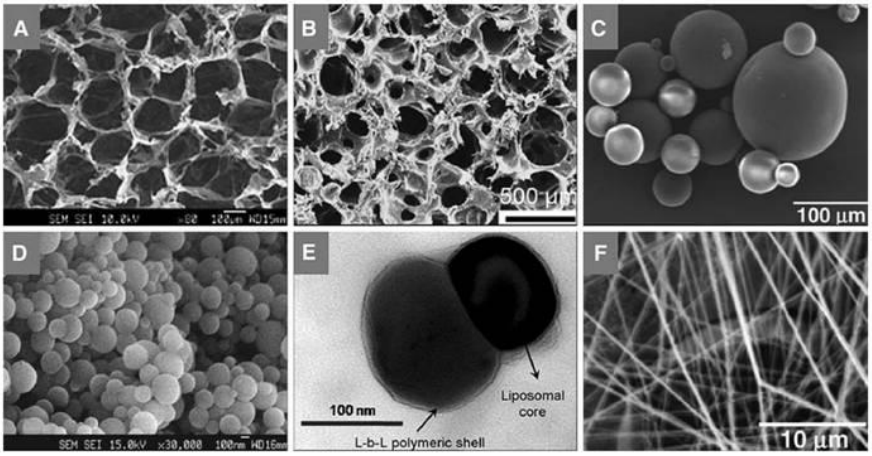


**Fig. 1** Selective electron micrographic images of BMP carriers and delivery systems and carrier biomaterials evaluated for BMPs. **a** Porous collagen sponge, bar = 100 µm **b** PLGA-coated gelatin sponge **c** PLGA microspheres **d** Heparin-conjugated PLGA nanoparticles, bar = 100 µm **e** core-shell nanoparticles constituting liposomes, alginate and chitosan **f** PLGA nanofibres. Adopted from Moioli et al. (2007); Lee and Shin (2007); Kim et al. (2008); Haider et al. (2009)

liposomes and a shell constructed through the layer-by-layer electrostatic-based self-assembly of alternating layers of anionic AL and cationic CH. The release profile was characterized by an initial burst followed by sustained albumin release, highly desirable for growth factor delivery; particularly in large bony defects (Haidar et al. 2008a). In a subsequent work, the ability of the core-shell nanoparticulate delivery system to encapsulate a range of concentrations of BMP-7 was evaluated. The system exhibited high physical stability in simulated physiological media as well as an extended shelf-life allowing for immediate protein loading prior to administration, preventing degradation or loss of the encapsulant. A sustained triphasic linear release of BMP-7 was evident for an extended period of 45 days with the bioactivity of the protein maintained via enhancing pre-osteoblast differentiation (Haidar et al. 2008b). In a rabbit model of tibial distraction osteogenesis, accelerated osteogenesis and consolidation was evident following a single injection of the nanoparticles loaded with a dose of no more than 1 μg rhBMP-7 (Haidar et al. 2009) in comparison to earlier results from a single injection of rhBMP-7 (75 μg in saline), accentuating the role of the injectable localized and release-controlled nanoparticles (Mandu-Hrit et al. 2006). Other groups investigated injectable scaffolds and matrices for drug delivery in bone tissue engineering (Kretlow et al. 2007). A recent example is the work of Hosseinkhani et al. (2007) where an injectable hydrogel of self-assembled peptide-amphiphile and BMP-2 was fabricated. Significant homogenous ectopic bone formation in the back subcutis of rats was demonstrated. A 3-D scaffold for the sequential delivery of BMP-2 and BMP-7 was recently developed (Basmanav et al. 2008). The system consisted of microspheres of polyelectrolyte complexes of poly(4-vinyl pyridine) and AL loaded with both proteins and incorporated in PLGA scaffolds. Neither BMP-2 nor BMP-7 delivery had any direct effect on cellular proliferation; however, their co-administration enhanced osteogenic differentiation to a higher degree than with their single administration. This was suggested to be due to the physical properties (pore size and distribution) of the foams. In conclusion, no single clinically-effective delivery system for rhBMP-2, rhBMP-7 or any other bone growth factors has been developed to date.

## Future prospects

The use of delivery systems is crucial for reliable bone formation and economic application of BMPs. Many carrier materials have been investigated. Collagen matrices have been clinically successful nevertheless with shortcomings including biodegradability, local retention and controlling release kinetics of BMPs. A limited number of other potential delivery systems have been developed and are still at the preclinical stage. Nonetheless, advances in the field will eventually lead to novel customized and optimized BMP-specific carrier materials. Better, safer and more integrated minimally-invasive drug delivery systems that utilize smaller amounts of BMPs effectively are needed. They will be insoluble under physiological conditions in order to retain the BMP yet absorbable by host tissue after implantation/administration so that be replaced by the regenerating bone, preferably following single application. Controlled prospective clinical trials should follow. The use of BMPs and other less understood morphogens will extend into much broader range of orthopaedic as well as craniofacial and orodental indications including bone, cartilage and tendon/ligament (and periodontal) tissue regeneration and repair.

**Acknowledgments** The authors wish to thank grants from the Shriners of North America, Fonds de la Recherche en Santé du Québec, the National Science and Engineering Research Council, the Canadian Institutes of Health Research (CIHR)—Regenerative Medicine/Nanomedicine and the Center for Biorecognition and Biosensors (CBB), McGill University, Montréal, Québec, Canada. Dr. Haidar acknowledges scholarships from the Center for Bone and Periodontal Diseases Research and the Shriners Hospital, Montréal, Québec, Canada.

## References

Arosarena OA, Collins WL (2005) Bone regeneration in the rat mandible with bone morphogenetic protein-2: a comparison of two carriers. Otolaryngol Head Neck Surg 132: 592–597

Barnes B, Boden SD, Louis-Ugbo J (2005) Lower dose of rhBMP-2 achieves spine fusion when combined with an osteoconductive bulking agent in non-human primates. Spine 30:1127–1133

Baskin DS, Ryan P, Sonntag V, Westmark R, Widmayer MA (2003) A prospective, randomized, controlled cervical fusion study using recombinant human bone morphogenetic protein-2 with the CORNERSTONE-SR allograft

ring and the ATLANTIS anterior cervical plate. Spine 28:1219–1224
Basmanav FB, Kose GT, Hasirci V (2008) Sequential growth factor delivery from complexed microspheres for bone tissue engineering. Biomaterials 29:4195–4204
Bessa PC, Casal M, Reis RL (2008) Bone morphogenetic proteins in tissue engineering: the road from laboratory to clinic, part II (BMP delivery). J Tissue Eng Regen Med 2:81–96
Bohner M, Baroud G (2005) Injectability of calcium phosphate pastes. Biomaterials 26:1553–1563
Boyne PJ, Lilly LC, Marx RE et al (2005) De novo bone induction by recombinant human bone morphogenetic protein-2 (rhBMP-2) in maxillary sinus floor augmentation. J Oral Maxillofac Surg 63:1693–1707
Burkus JK, Gornet MF, Dickman CA, Zdeblick TA (2002a) Anterior lumbar interbody fusion using rhBMP-2 with tapered interbody cages. J Spinal Disord Tech 15:337–349
Burkus JK, Transfeldt EE, Kitchel SH, Watkins RG, Balderston RA (2002b) Clinical and radiographic outcomes of anterior lumbar interbody fusion using recombinant human bone morphogenetic protein-2. Spine 27:2396–2408
Burkus JK, Sandhu HS, Gornet MF, Longley MC (2005) Use of rhBMP-2 in combination with structural cortical allografts: clinical and radiographic outcomes in anterior lumbar spinal surgery. J Bone Joint Surg Am 87:1205–1212
Chen RR, Mooney DJ (2003) Polymeric growth factor delivery strategies for tissue engineering. Pharm Res 20:1103–1112
Chen FM, Zhao YM et al (2007) Periodontal regeneration using novel glycidyl methacrylated dextran (Dex-GMA)/gelatin scaffolds containing microspheres loaded with bone morphogenetic proteins. J Control Release 121:81–90
De Long WG, Einhorn TA Jr et al (2007) Bone grafts and bone graft substitutes in orthopaedic trauma surgery. A critical analysis. J Bone Joint Surg Am 89:649–658
Engstrand T, Veltheim R, Arnander C, Docherty-Skogh AC, Westermark A, Ohlsson C, Adolfsson L, Larm O (2008) A novel biodegradable delivery system for bone morphogenetic protein-2. Plast Reconstr Surg 121:1920–1928
Fei Z, Hu Y, Wu D, Wu H et al (2008) Preparation and property of a novel bone graft composite consisting of rhBMP-2 loaded PLGA microspheres and calcium phosphate cement. J Mater Sci Mater Med 19:1109–1116
Friedlaender GE, Perry CR, Cole JD, Cook SD, Cierny G, Muschler GF et al (2001) Osteogenic protein-1 (bone morphogenetic protein-7) in the treatment of tibial nonunions. J Bone Joint Surg Am 83A:151–158
Fu TS, Chen WJ, Chen LH et al (2008) Enhancement of posterolateral lumbar spine fusion using low-dose rhBMP-2 and cultured marrow stromal cells. J Orthop Res (Epub ahead of print)
Gao T, Uludag H (2001) Effect of molecular weight of thermoreversible polymer on in vivo retention of rhBMP-2. J Biomed Mater Res 57:92–100
Gautschi OP, Frey SP, Zellweger R (2003) Bone morphogenetic proteins in clinical applications. ANZ J Surg 77:626–631
Geesink RG, Hoefnagels NH, Bulstra SK (1999) Osteogenic activity of OP-1 bone morphogenetic protein (BMP-7) in a human fibular defect. J Bone Joint Surg Br 81:710–718
Geiger M, Li RH et al (2003) Collagen sponges for bone regeneration with rhBMP-2. Adv Drug Deliv Rev 55:1613–1629
Ginebra MP, Traykova T, Planell JA (2006) Calcium phosphate cements as bone drug delivery systems: a review. J Control Release 113:102–110
Gittens SA, Uludag H (2001) Growth factor delivery for bone tissue engineering. J Drug Target 9:407–429
Govender S, Csimma C, Genant HK et al (2002) BMP-2 Evaluation in Surgery for Tibial Trauma (BESTT) Study Group. Recombinant human bone morphogenetic protein-2 for treatment of open tibial fractures: a prospective, controlled, randomized study of four hundred and fifty patients. J Bone Joint Surg Am 84:2123–2134
Haddad AJ, Peel SA, Clokie CM, Sándor GK (2006) Closure of rabbit calvarial critical-sized defects using protective composite allogeneic and alloplastic bone substitutes. J Craniofac Surg 17:926–934
Haidar ZS, Hamdy RC, Tabrizian M (2008a) Protein release kinetics for core-shell hybrid nanoparticles based on the layer-by-layer assembly of alginate and chitosan on liposomes. Biomaterials 29:1207–1215
Haidar ZS, Azari F, Hamdy RC, Tabrizian M (2008b) Modulated release of OP-1 and enhanced pre-osteoblast differentiation using a core-shell nanoparticulate system J Biomed Mater Res A (in press)
Haidar ZS, Tabrizian M, Hamdy RC (2009) A hybrid OP-1 delivery system enhances new bone regeneration and consolidation in a rabbit model of distraction osteogenesis. Growth Factors (in press)
Herford AS, Boyne PJ (2008) Reconstruction of mandibular continuity defects with bone morphogenetic protein-2 (rhBMP-2). J Oral Maxillofac Surg 66:616–624
Hosseinkhani H, Hosseinkhani M, Tian F, Kobayashi H, Tabata Y (2007) Bone regeneration on a collagen sponge self-assembled peptide-amphiphile nanofiber hybrid scaffold. Tissue Eng 13:11–19
Hu YY, Zhang C, Lu R, Xu JQ, Li D (2003) Repair of radius defect with bone-morphogenetic-protein loaded hydroxyapatite/collagen-poly(L-lactic acid) composite. Chin J Traumatol 6:67–74
Issa JP, Nascimento C, Bentley MV et al (2008a) Bone repair in rat mandible by rhBMP-2 associated with two carriers. Micron 39:373–379
Issa JP, Spadaro AC, Bentley MV et al (2008b) Monoolein and chitosan gels as potential carriers of the rhBMP-2, using decortication surgical technique in Wistar rats as experimental model. Micron 39:952–959
Itoh T, Mochizuki M, Nishimura R et al (1998) Repair of ulnar segmental defect by recombinant human bone morphogenetic protein-2 in dogs. J Vet Med Sci 60:451–458
Johnsson R, Strömqvist B, Aspenberg P (2002) Randomized radiostereometric study comparing osteogenic protein-1 (BMP-7) and autograft bone in human noninstrumented posterolateral lumbar fusion: 2002 Volvo award in clinical studies. Spine 27:2654–2661
Jung RE, Glauser R, Schärer P, Hämmerle CH, Sailer HF, Weber FE (2003) Effect of rhBMP-2 on guided bone regeneration in humans. Clin Oral Implants Res 14:556–568

Jung RE, Weber FE et al (2008) Bone morphogenetic protein-2 enhances bone formation when delivered by a synthetic matrix containing hydroxyapatite/tricalciumphosphate. Clin Oral Implants Res 19:188–195

Kanayama M, Hashimoto T, Shigenobu K (2006) A prospective randomized study of posterolateral lumbar fusion using osteogenic protein-1 (OP-1) versus local autograft with ceramic bone substitute: emphasis of surgical exploration and histologic assessment. Spine 31:1067–1074

Kawakatsu N, Oda S, Kinoshita A et al (2008) Effect of rhBMP-2 with PLGA/gelatin sponge type (PGS) carrier on alveolar ridge augmentation in dogs. J Oral Rehabil 35:647–655

Kenley R, Marden L, Turek T, Jin L, Ron E, Hollinger JO (1994) Osseous regeneration in the rat calvarium using novel delivery systems for recombinant human bone morphogenetic protein-2 (rhBMP-2). J Biomed Mater Res 28:1139–1147

Kim HD, Valentini RF (2002) Retention and activity of BMP-2 in hyaluronic acid-based scaffolds in vitro. J Biomed Mater Res 59:573–584

Kim SS, Gwak SJ, Kim BS (2008) Orthotopic bone formation by implantation of apatite-coated poly(lactide-co-glycolide)/hydroxyapatite composite particulates and bone morphogenetic protein-2. J Biomed Mater Res A 87: 245–253

Kneser U, Schaefer DJ, Polykandriotis E, Horch RE (2006) Tissue engineering of bone: the reconstructive surgeon's point of view. J Cell Mol Med 10:7–19

Kretlow JD, Klouda L, Mikos AG (2007) Injectable matrices and scaffolds for drug delivery in tissue engineering. Adv Drug Deliv Rev 59:263–273

Kumar MN, Muzzarelli RA, Muzzarelli C, Sashiwa H, Domb AJ (2004) Chitosan chemistry and pharmaceutical perspectives. Chem Rev 104:6017–6084

Kwon B, Jenis LG (2005) Carrier materials for spinal fusion. Spine J 5(6):S224–S230

Lee SH, Shin H (2007) Matrices and scaffolds for delivery of bioactive molecules in bone and cartilage tissue engineering. Adv Drug Deliv Rev 59(4–5):339–359

Lee KY, Yuk SH (2007) Polymeric protein delivery systems. Prog Poly Sci 32:669–697

Li RH, Wozney JM (2001) Delivering on the promise of bone morphogenetic proteins. Trend Biotechnol 19:255–265

Liew CV, Chan LW, Ching AL, Heng PW (2006) Evaluation of sodium alginate as drug release modifier in matrix tablets. Int J Pharm 309:25–37

Luginbuehl V, Meinel L et al (2004) Localized delivery of growth factors for bone repair. Eur J Pharm Biopharm 58:197–208

Ma PX (2008) Biomimetic materials for tissue engineering. Adv Drug Deliv Rev 60:184–198

Mandu-Hrit M, Haque T, Lauzier D, Kotsiopriftis M, Rauch F, Tabrizian M, Henderson JE, Hamdy RC (2006) Early injection of OP-1 during distraction osteogenesis accelerates new bone formation in rabbits. Growth Factors 24:172–183

Maniscalco P, Gambera D, Bertone C et al (2002) Healing of fresh tibial fractures with OP-1. Acta Biomed 73:27–33

Mayer M, Hollinger J, Ron E, Wozney J (1996) Maxillary alveolar cleft repair in dogs using recombinant human bone morphogenetic protein-2 and a polymer carrier. Plast Reconstr Surg 98:247–259

Moioli EK, Clark PA, Xin X, Lal S, Mao JJ (2007) Matrices and scaffolds for drug delivery in dental, oral and craniofacial tissue engineering. Adv Drug Deliv Rev 59: 308–324

Moore WR, Graves SE, Bain GI (2001) Synthetic bone graft substitutes. ANZ J Surg 71:354–361

Mussano F, Ciccone G, Ceccarelli M, Baldi I, Bassi F (2007) Bone morphogenetic proteins and bone defects: a systematic review. Spine 32:824–830

Nair LS, Laurencin CT (2008) Nanofibers and nanoparticles for orthopaedic surgery applications. J Bone Joint Surg Am 90(S1):128–131

Noshi T, Yoshikawa T, Dohi Y (2001) Recombinant human bone morphogenetic protein-2 potentiates the in vivo osteogenic ability of marrow/hydroxyapatite composites. Artif Organs 25:201–208

O'Regan M, Martini I, Crescenzi F, De Luca C, Lansing M (1994) Molecular mechanisms and genetics of hyaluronan biosynthesis. Int J Bio Macromol 16:283–286

Okubo Y, Bessho K, Fujimura K et al (2000) Osteoinduction by recombinant human bone morphogenetic protein-2 at intramuscular, intermuscular, subcutaneous and intrafatty sites. Int J Oral Maxillofac Surg 29:62–66

Park JH, Ye M, Park K (2005) Biodegradable polymers for microencapsulation of drugs. Molecules 10:146–161

Peng L, Bian WG, Liang FH, Xu HZ (2008) Implanting hydroxyapatite-coated porous titanium with bone morphogenetic protein-2 and hyaluronic acid into distal femoral metaphysis of rabbits. Chin J Traumatol 11:179–185

Prabaharan M (2008) Chitosan derivatives as promising materials for controlled drug delivery. J Biomater Appl 23:5–36

Qiu Y, Zhang N, Kang Q, An Y, Wen X (2008) Chemically modified light-curable chitosans with enhanced potential for bone tissue repair. J Biomed Mater Res A [Epub ahead of print]

Robinson Y, Heyde CE, Tschöke SK et al (2008) Evidence supporting the use of bone morphogenetic proteins for spinal fusion surgery. Expert Rev Med Dev 5:75–84

Saito N, Takaoka K (2003) New synthetic biodegradable polymers as BMP carriers for bone tissue engineering. Biomaterials 24:2287–2293

Saito N, Murakami N, Takahashi J et al (2005) Synthetic biodegradable polymers as drug delivery systems for bone morphogenetic proteins. Adv Drug Deliv Rev 57:1037–1048

Schliephake H, Weich HA, Dullin C, Gruber R, Frahse S (2008) Mandibular bone repair by implantation of rhBMP-2 in a slow release carrier of polylactic acid–an experimental study in rats. Biomaterials 29:103–110

Schmidmaier G, Schwabe P, Strobel C, Wildemann B (2008) Carrier systems and application of growth factors in orthopaedics. Injury 39(S2):37–43

Schopper C, Moser D, Spassova E et al (2008) Bone regeneration using a naturally grown HA/TCP carrier loaded with rh BMP-2 is independent of barrier-membrane effects. J Biomed Mater Res A 85:954–963

Sciadini MF, Johnson KD (2000) Evaluation of recombinant human bone morphogenetic protein-2 as a bone-graft

substitute in a canine segmental defect model. J Orthop Res 18:289–302
Seeherman H, Wozney JM (2005) Delivery of bone morphogenetic proteins for orthopedic tissue regeneration. Cytokine Growth Factor Rev 16:329–345
Sigurdsson TJ, Nygaard L, Tatakis DN, Fu E, Turek TJ, Jin L, Wozney JM, Wikesjö UM (1996) Periodontal repair in dogs: evaluation of rhBMP-2 carriers. Int J Periodontics Restorative Dent 16:524–537
Takaoka K, Koezuka M, Nakahara H (1991) Telopeptide-depleted bovine skin collagen as a carrier for bone morphogenetic protein. J Orthop Res 9:902–907
Talwar R, Di Silvio L, Hughes FJ, King GN (2001) Effects of carrier release kinetics on bone morphogenetic protein-2-induced periodontal regeneration in vivo. J Clin Periodontol 28:340–347
Termaat MF, Den Boer FC, Bakker FC, Patka P, Haarman HJ (2005) Bone morphogenetic proteins. Development and clinical efficacy in the treatment of fractures and bone defects. J Bone Joint Surg Am 87:1367–1378
Tönnesen HH, Karlsen J (2002) Alginate in drug delivery systems. Drug Dev Ind Pharm 28:621–630
Vaccaro AR, Anderson DG, Patel T et al (2005) Comparison of OP-1 Putty (rhBMP-7) to iliac crest autograft for posterolateral lumbar arthrodesis: a minimum 2-year follow-up pilot study. Spine 30:2709–2716
Vaccaro AR, Whang PG, Patel T (2008) The safety and efficacy of OP-1 (rhBMP-7) as a replacement for iliac crest autograft for posterolateral lumbar arthrodesis: minimum 4-year follow-up of a pilot study. Spine J 8:457–465
Välimäki VV, Aro HT (2006) Molecular basis for action of bioactive glasses as bone graft substitute. Scand J Surg 95:95–102
van den Bergh JP, ten Bruggenkate CM, Groeneveld HH, Burger EH, Tuinzing DB (2000) Recombinant human bone morphogenetic protein-7 in maxillary sinus floor elevation surgery in 3 patients compared to autogenous bone grafts. A clinical pilot study. J Clin Periodontol 27(9):627–636
Wei G, Jin Q, Giannobile WV, Ma PX (2007) The enhancement of osteogenesis by nano-fibrous scaffolds incorporating rhBMP-7 nanospheres. Biomaterials 28:2087–2096
Woo BH, Jiang G, Jo YW, DeLuca PP (2001) Preparation and characterization of a composite PLGA and poly(acryloyl hydroxyethyl starch) microsphere system for protein delivery. Pharm Res 18:1600–1606
Yamamoto M, Takahashi Y, Tabata Y (2006) Enhanced bone regeneration at a segmental bone defect by controlled release of bone morphogenetic protein-2 from a biodegradable hydrogel. Tissue Eng 12:1305–1311
Young S, Wong M, Tabata Y, Mikos AG (2005) Gelatin as a delivery vehicle for the controlled release of bioactive molecules. J Control Rel 109:256–274
Zellin G, Linde A (1997) Importance of delivery systems for growth-stimulatory factors in combination with osteopromotive membranes. An experimental study using rhBMP-2 in rat mandibular defects. J Biomed Mater Res 35:181–190

## SELECTED COMMUNICATIONS (2006 TO DATE)

- **Haidar ZS**, Azari F, Hamdy RC and Tabrizian M. In vitro characterization and cytotoxic effect of a liposome-based drug delivery system incorporating alternating L-b-L assembly of polyelectrolytes for distraction osteogenesis. CBS, Calgary – May 2006.
- **Haidar ZS**, Azari F, Hamdy RC and Tabrizian M. BMP-7 release through a core-shell delivery system enhances pre-osteoblast differentiation. IADR, New Orleans – March 2007.
- **Haidar ZS**, Azari F, Hamdy RC and Tabrizian M. **In vitro Loading and Release Study of Liposome-based Nanoparticles for their potential use in Protein Delivery. SFB, Chicago – April 2007.**
- **Haidar ZS**, Azari F, Hamdy RC and Tabrizian M. **Protein Release from Core-Shell Nanocaspules Assembled via Layer-by-Layer Deposition of Alginate and Chitosan on Liposomes. CBS, London, Ontario – May 2007.**
- **Haidar ZS**, Hamdy RC and Tabrizian M. Core-shell hybrid nanoparticles through layer-by-layer assembly of alginate and chitosan on liposomes for protein delivery: characterization and release kinetics. CIHR Training Program in Skeletal Health Research - 5th Annual Workshop, Royal Victoria Hospital, Montréal – October 2007.
- **Haidar ZS**, Hamdy RC and Tabrizian M. **Novel core-shell nanocaspules for localized growth factor delivery. AADR, Dallas, Texas – April 2008.**
- **Haidar ZS**, Hamdy RC and Tabrizian M. Cytotoxicity, osteogenic activity and release kinetics of OP-1 loaded core-shell nanoparticles. Nano Québec, Montréal – May 2008.
- **Haidar ZS**, Hamdy RC and Tabrizian M. **Novel nanocaspules for sustained protein delivery. Nanoforum, Edmonton, AB – May 2008.**
- **Haidar ZS**, Azari F, Hamdy RC and Tabrizian M. BMP-7 loaded core-shell nanoparticles: cytotoxicity, osteogenic activity and release kinetics. IADR, Toronto, ON – July 2008. *Session Co-Chair.*
- **Haidar ZS**, Hamdy RC and Tabrizian M. **OP-1 release kinetics from an injectable core-shell delivery system. 7th International Conference on BMPs, Lake Tahoe, California** – August 2008.
- **Haidar ZS**, Hamdy RC and Tabrizian M. **A novel core-shell rhOP-1 delivery system for the potential acceleration of regenerate formation and consolidation in tibial bone lengthening.** CIHR Training Program in Skeletal Health Research - 6th Annual Workshop, Royal Victoria Hospital, Montréal – October 2008.
- **Haidar ZS**, Hamdy RC and Tabrizian M. **A novel OP-1 delivery system for the potential acceleration of regenerate formation and consolidation in distraction osteogenesis. International Conference on Osteoporosis and Bone Research/IBMS 2008, Beijing, China and published in Bone 43 (2008) S38-S75: A36.**
- **Haidar ZS**, Hamdy RC and Tabrizian M. Novel localized and release-controlled rhBMP-7/rhOP-1 core-shell nanoparticles accelerate tibial distraction osteogenesis in rabbits. The 2nd Joint Meeting of the International Bone & Mineral Society (IBMS 2009) and the Australian and New Zealand Bone and Mineral Society, Sydney, Australia – March 2009.
- **Haidar ZS**, Hamdy RC and Tabrizian M. In vitro and In vivo Biocompatibility Study of a Hybrid Nanoparticulate BMP-7/OP-1 Delivery System in Rats. 35th Annual Northeast Bioengineering Conference, MIT/Harvard U, Boston, MA – April 2009. IEEE Proceedings 978-1-4244-4364-2/09.

- **Haidar ZS**, Hamdy RC and Tabrizian M. Novel injectable and release-controlled OP-1 hybrid core-shell nanocapsules enhance distraction osteogenesis in rabbits. 25th Southern Biomedical Engineering Conference, FIU, Miami, FL – May 2009. IFBME Proceedings 24 pp: 355–358.
- **Haidar ZS**, Hamdy RC and Tabrizian M. OP-1/Core-shell nanocaspules accelerate distraction osteogenesis in rabbits. CBS, Québec City, QC – May 2009.
- Alsalmi LA, **Haidar ZS**, Izadpanah A, Lessard LM, Tabrizian M and Hamdy RC. Wnt Signaling is up-regulated during long bone distraction osteogenesis in mice. Division of Surgical Research of McGill University: Fraser Gurd Day, Montréal, QC – May 2009.
- Izadpanah A, **Haidar ZS**, Alsalmi LA, Tabrizian M, Hamdy RC and Lessard LM. A Dose-Response Curve of OP-1 for Accelerating Bone Formation in Distraction Osteogenesis. 63rd Annual Meeting of the Canadian Society of Plastic Surgeons, Kelowna, British Columbia – June 2009.
- **Haidar ZS**, Azari F, Hamdy RC and Tabrizian M. A Novel Biocompatible, Localized and Release-controlled BMP-7 Delivery System Enhances Bone Regeneration. Centre for Biorecognition and Biosensors (CBB) Annual Research Day , Montréal, QC – June 2009.
- Alsalmi LA, **Haidar ZS**, Izadpanah A, Lessard LM, Tabrizian M and Hamdy RC. Wnt Signaling increases during Distraction Osteogenesis in Mice. American Society of Plastic Surgeons, Seattle, CA – October 2009.
- **Haidar ZS**, Hamdy RC and Tabrizian M. Biocompatibility and Safety of a Hybrid Nanoparticulate OP-1 Delivery System Intramuscularly administered in Rats. Materials Research Society (MRS) Fall 2009 Meeting, Boston, MA – November 2009.

## PUBLICATIONS (2006 TO DATE)

- **Haidar ZS**, Hamdy RC and Tabrizian M. Protein release kinetics for core-shell hybrid nanoparticles based on the layer-by-layer assembly of alginate and chitosan on liposomes. *Biomaterials* 29 (2008) 1207-1215.
- **Haidar ZS,** Azari F, Hamdy RC, Tabrizian M. Modulated release of OP-1 and enhanced preosteoblast differentiation using a core-shell nanoparticulate system. *JBMR/A*. (2008) Dec 18. [Epub]
- Sydow-Plum G, **Haidar ZS**, Merhi Y and Tabrizian M. Modulating the Release Kinetics of Paclitaxel from Membrane-Covered Stents Using Different Loading Strategies. *Materials 1* (2008) 25-43.
- **Haidar ZS**, Hamdy RC and Tabrizian M. Review: Recombinant BMP Delivery for Bone Regeneration and Repair. Part A: Current Challenges in BMP Delivery. *Biotechnology Letters* (2009) Aug 19. [Epub]
- **Haidar ZS**, Hamdy RC and Tabrizian M. Review: Recombinant BMP Delivery for Bone Regeneration and Repair. Part B: Delivery Systems for BMPs in Orthopaedic and Craniofacial Tissue Engineering. *Biotechnology Letters* (2009) Aug 19. [Epub]
- **Haidar ZS**, Tabrizian M and Hamdy RC. A hybrid OP-1 delivery system enhances new bone regeneration and consolidation in a rabbit model of distraction osteogenesis. *Growth Factors* (2009) In press.
- **Haidar ZS**, Hamdy RC and Tabrizian M. Biocompatibility and Safety of a Hybrid Nanoparticulate OP-1 Delivery System Intramuscularly administered in Rats. *Manuscript submitted to Biomaterials.*
- **Haidar ZS**, Tabrizian M and Hamdy RC. Accelerating De Novo Bone Regeneration In Bone Lengthening Procedures. A Review *submitted to JOSR* (2009).

## AWARDS AND SCHOLARSHIPS

1998 **Dean's Award of Academic Achievement**, FOD – AUST, U.A.E.
1999 **Best Research Project Award**, FOD – AUST, U.A.E.
2002 **Dean's Award of Academic Achievement**, FOD – AUST, U.A.E.
2002 **AUST's President Appreciation Award**, AUST, U.A.E.
2005 **Dean's Honors' list**, FOD – McGill University, Canada
2006 **CIHR** Strategic Skeletal Health Research Training Scholarship
2007 **CIHR** Strategic Skeletal Health Research Training Scholarship
2008 **IADR** conference travel award
2008 **AADR** conference travel award
2009 **IBMS** conference travel award
2009 **Shriners Hospital** Montreal Post-doctoral Research Fellowship

## EDUCATION AND TRAINING

| | |
|---|---|
| 1995 – 2001 | **D.D.S.** Faculty of Dentistry (FOD) AUST – Middle East, U.A.E. with Merit: Very Good; Rank: 2nd/82. |
| 2001 – 2002 | **Clinical Dentistry Externship** (General Dentistry; focus on Oral Surgery) Dubai International Hospital, Dubai, U.A.E. |
| 2002 – 2003 | **Cert. Dent. Implantol.** (Oral Implantology) University of Medicine & Dentistry of New Jersey, Newark, NJ, USA. |
| 2003 – 2005 | **M.Sc.** (Dental Sciences and Research – Implant Prosthetics) FOD, McGill University, Montréal – Canada. |
| 2007 – 2009 | **MBA** (Health Care Organizations Management) John Molson School of Business, Montréal – Canada. |
| 2005 – 2009 | **Ph.D.** (Dental Sciences and Research – Biomedical Engineering) FOD, McGill University, Montréal – Canada. |

## PERSONAL INFORMATION


| | |
|---|---|
| **Full name** | Ziyad Samir Hasan Haidar |
| **Date of birth** | January 30th 1978 |
| **Place of birth** | Dubai, United Arab Emirates |
| **Nationality** | Lebanese Canadian |
| **Home Address** | 1207-1625 Boul. De Maisonneuve O. Montréal H3H 2N4 |
| **Contacts** | (514) 805-8282 ziyad.haidar@mcgill.ca |